Low dimensional dualities

Matrix models, two-dimensional quantum gravity & black holes

Mühlmann, B.

Publication date
2021

Document Version
Final published version

LOW DIMENSIONAL DUALITIES

Beatrix Mühlmann

LOW DIMENSIONAL DUALITIES

Matrix models, two-dimensional quantum gravity
& black holes

Beatrix Mühlmann

Low dimensional dualities

matrix models, two-dimensional quantum gravity & black holes

This work has been accomplished at the Institute for Theoretical Physics (ITFA) of the University of Amsterdam (UvA) and is part of the research program of the former Foundation for Fundamental Research on Matter (now NWO-I), which is part of the Netherlands Organization for Scientific Research (NWO).

Low dimensional dualities

matrix models, two-dimensional quantum gravity & black holes

Academisch Proefschrift

ter verkrijging van de graad van doctor

aan de Universiteit van Amsterdam

op gezag van de Rector Magnificus

prof. dr. ir. K.I.J. Maex

ten overstaan van een door het College voor Promoties

ingestelde commissie,

in het openbaar te verdedigen in de Agnietenkapel

op dinsdag 6 juli 2021, te 12:00 uur

door

Beatrix Mühlmann

geboren te Bozen

Promotiecommissie

Promotor

dr. A. Castro Anich	Universiteit van Amsterdam

Copromotor

prof. dr. E. P. Verlinde	Universiteit van Amsterdam

Overige leden

dr. D. T. Anninos	King's College London
dr. T. M. Anous	Universiteit van Amsterdam
prof. dr. J. de Boer	Universiteit van Amsterdam
prof. dr. C. J. M. Schoutens	Universiteit van Amsterdam
prof. dr. S. J. G. Vandoren	Universiteit van Utrecht

Faculteit der Natuurwetenschappen, Wiskunde en Informatica

Publications

This thesis is based on the following publications:

- D. Anninos and B. Mühlmann, "Notes on matrix models (matrix musings)," J. Stat. Mech. **2008**, 083109 (2020) doi:10.1088/1742-5468/aba499 [arXiv:2004.01171 [hep-th]]

  Presented in Chapter 2

- D. Anninos and B. Mühlmann, "Matrix integrals & finite holography," [arXiv:2012.05224 [hep-th]]

  Presented in Chapter 3

- A. Castro and B. Mühlmann, "Gravitational anomalies in $\mathrm{nAdS}_2/\mathrm{nCFT}_1$," Class. Quant. Grav. **37**, no.14, 145017 (2020) doi:10.1088/1361-6382/ab8bbb [arXiv:1911.11434 [hep-th]]

  Presented in Chapter 4

Other publications by the author:

- A. Belin, A. Castro, C. A. Keller and B. Mühlmann, "The Holographic Landscape of Symmetric Product Orbifolds," JHEP **01**, 111 (2020) [arXiv:1910.05342 [hep-th]]
- A. Belin, A. Castro, C. A. Keller and B. J. Mühlmann, "Siegel Paramodular Forms from Exponential Lifts: Slow versus Fast Growth," [arXiv:1910.05353 [hep-th]]
- C. A. Keller and B. Mühlmann, "The Spectrum of Permutation Orbifolds," Lett. Math. Phys. **109**, no.7, 1559-1572 (2019) [arXiv:1708.01258 [hep-th]]

Contents

1 Introduction

This thesis focuses on low dimensional dualities as tractable models to explore two-dimensional de Sitter space and black holes. The first two chapters review, discuss and explore the framework for a novel attempt to create a connection between de Sitter space and the conjectured duality between matrix models and two-dimensional quantum gravity. The hope is that this could pave a path toward understanding the so far unknown microscopic picture of our Universe. In the last chapter we address fundamental problems about the microscopic picture of black holes through a low dimensional duality dubbed the near-AdS_2/near-CFT_1 correspondence.

1.1 Motivation

We are living in an era in which highly sensitive astronomical tools are granting more and more accurate access to the spacetime we live in. Observations of the cosmic microwave background and the explosions of distant white dwarfs (type Ia supernova) indicate that our Universe is entering a regime of accelerated expansion driven by an incredibly small, yet non-vanishing positive cosmological constant. Over the past couple of years, the LIGO and Virgo detectors observed the gravitational waves emitted by multiple binary black holes, providing new evidence of the existence of black holes [1–3].

A maximally symmetric spacetime with positive cosmological constant is known as a de Sitter space [4]. Because of the accelerated expansion, an observer in a de Sitter spacetime can only see a finite distance and is surrounded by an event horizon. An event horizon also marks the boundary of a black hole where the velocity needed to escape exceeds the speed of light. Both the de Sitter, as well as the black hole horizon, have a finite area, and a finite entropy is conjecturally assigned to both of them [5–7].

Motivated by the finiteness of these entropies my approach to understand the

microscopic picture of a de Sitter spacetime and black holes uses models which are inherently tied to only a finite number of degrees of freedom. These models come in form of low dimensional dualities. A duality is a setup which maps two theories to each other. For every quantity in one theory there is a dual quantity in the other theory. Depending on the problem we are addressing we can choose the formalism which is more appropriate for us. In a low dimensional duality, the theories furthermore live in less than four spacetime dimensions.

In the following two paragraphs we provide a glimpse into the two dualities we focus on in this thesis. The subsequent sections 1.2 and 1.3 provide further details.

Matrix models & **two-dimensional quantum gravity.** To approach the microscopic picture of our expanding Universe we attempt to create a link between a de Sitter spacetime and matrix models. Whereas very little is known about de Sitter space at the quantum level, matrix models are a widely explored theoretical tool. Under certain conditions such as a very large matrix, properties of the matrix model are conjectured to be dual to observables of a specific theory of two-dimensional quantum gravity coupled to a theory of matter. This theory of quantum gravity is known as Liouville theory [8]. Crucially, upon placing the continuum theory (Liouville theory + matter) on a two-sphere topology, and imposing additional conditions such as a large negative central charge of the matter sector and restrictions on the area, the continuum theory admits a semiclassical Euclidean two-dimensional de Sitter saddle. This two-dimensional de Sitter spacetime resembles and moreover shares important features and properties of the higher dimensional theory describing our own Universe. Matrix models could therefore allow for a UV completion of a de Sitter quantum gravity theory and could shed light on the microscopic nature of our own Universe.

Black holes. Black holes are solutions of Einstein's equations of general relativity which have a curvature singularity at the center and an event horizon. Somewhat surprisingly black holes also satisfy thermodynamic properties similar to statistical systems. Even though many features of black holes are well understood, the AdS_2 factor appearing in the near-horizon region of near-extremal black holes still remains a puzzling ingredient. In particular, while the temperature of an extremal black hole vanishes, the entropy assigned to the black hole horizon is finite also in the extremal case. The approach to explore the microscopic origin of this entropy uses what is known as the (near)-AdS_2/(near)-CFT_1 correspondence [9–12]. It relates a theory of two-dimensional gravity with negative curvature (AdS_2) to a one-dimensional conformal quantum mechanics (CFT_1) living at the boundary of the AdS_2 spacetime. The "near" prefix indicates a region close to the pure AdS_2/CFT_1 regime. As explained in the next section, a pure AdS_2 background only allows for ground state configurations [13,14]. Near-AdS_2 is a small deviation

away from AdS_2, and while allowing finite energy excitations is still connected to the AdS_2 background. Finally, since in the near-AdS_2/near-CFT_1 correspondence the boundary theory is a conformal quantum mechanics and not a quantum field theory, this duality also involves a finite number of degrees of freedom.

1.2 Matrix models & two-dimensional quantum gravity

In this section we give a brief overview of matrix models and Liouville theory. We review some of the history and discuss the dictionary between matrix model quantities and quantities of the continuum theory. This section is meant to highlight the main results of chapter 2 and chapter 3 and to connect them to a novel attempt toward obtaining a microscopic picture of de Sitter space.

Matrix models have a long and outstanding history. Two major breakthroughs tied also to my own research are Wigner's energy spectra [21–23] and 't Hooft's diagrams [24].

Wigner's energy spectra. After solving the energy level distribution of the hydrogen atom at the beginning of the last century it took almost 50 years to understand the energy distribution of heavier nuclei. The groundbreaking ansatz was due to Wigner [21–23]. He chose a matrix with entries drawn from a random ensemble as the Hamiltonian (energy) of the system. In an astonishing way, in the limit where the size of this matrix tends to infinity, the system simplifies. The eigenvalue distribution of the random matrix agrees with the energy distribution obtained through experiments. This result is known as Wigner's surmise.

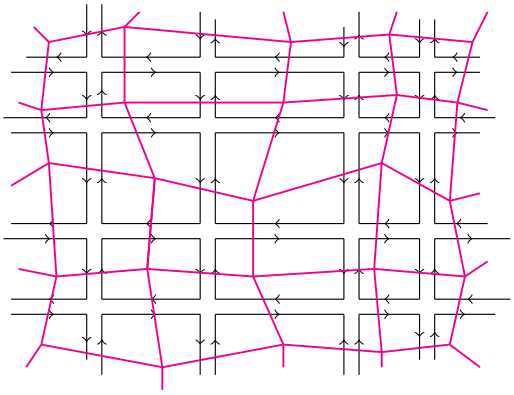

Figure 1.1: *Polygonisation: the black lines are the ribbon diagrams, whereas the magenta lines correspond to the dual lattice.*

't Hooft's diagrams. In the 1970s 't Hooft [24] realised that the Feynman diagrams of matrix integrals triangulate a surface. Building a dual lattice to the Feynman diagrams of matrix integrals, as shown in figure 1.1, resembles this triangulation of Riemann surfaces of arbitrary genus. Pictorially this introduced the conjectured duality between matrix models and two-dimensional quantum gravity. Through 't Hooft's key observations matrix models turned into an arena describing theories of two-dimensional quantum gravity. Even though realistic theories of gravity are four-dimensional, these lower dimensional versions can guide physicists toward understanding features of realistic theories of quantum gravity.

Two-dimensional quantum gravity differs from higher dimensional theories of gravity. In two dimensions the Einstein-Hilbert action is topological. The theory is over-constraint and has no locally propagating degrees of freedom. In fact the Einstein-Hilbert action is proportional to the Euler characteristic of the two-dimensional manifold it is integrated over. The path integral first sums over all geometries of a fixed genus and is then summing over all genera. In two dimensions we can furthermore exploit the two diffeomorphisms to write the metric in terms of a fixed fiducial part $\tilde{g}_{ij}$ and a single degree of freedom appearing in the form of the Weyl factor $\varphi(x)$. It has been postulated that in the Weyl gauge a theory of two-dimensional quantum gravity is given by a path integral over the Weyl factor weighted by the Liouville action [8]

$$S_L[\varphi, \tilde{g}_{ij}] = \frac{1}{4\pi} \int \mathrm{d}^2x \sqrt{\tilde{g}} \left(\tilde{g}^{ij} \partial_i \varphi \partial_j \varphi + \sqrt{\frac{c_L - 1}{6}}\, \tilde{R} \varphi + 4\pi \Lambda\, e^{2b\varphi} \right) . \tag{1.2.1}$$

Here $\tilde{R}$ is the Ricci scalar of the fixed fiducial metric, $\Lambda \geq 0$ is the cosmological constant. Liouville theory is a two-dimensional CFT [33–37] and the parameter b is related to the Liouville central c_L by

$$b = \frac{\sqrt{c_L - 1} - \sqrt{c_L - 25}}{2\sqrt{6}} . \tag{1.2.2}$$

In addition to a theory of pure two-dimensional quantum gravity one can also consider the addition of matter fields. In this thesis we focus on a specific matter theory given by the series $\mathcal{M}_{2,2m-1}$ of minimal models, forming themselves a conformal field theory with known central charge c_m and operator content. Furthermore we fix the fiducial metric to be the round metric on the unit two-sphere. After turning on one of the $(m-1)$ primaries $\mathcal{O}_r$ of the minimal model we find

$$Z[\lambda_r] = \int \frac{[D\varphi]}{\mathrm{vol}\,\mathrm{PSL}(2,\mathbb{C})} [D\Phi][D\mathfrak{bc}]\, e^{-S_L[\varphi,\Lambda=0] - S_{\mathrm{CFT}}[\Phi] - S_{\mathrm{gh}}[\mathfrak{b},\mathfrak{c}] - \lambda_r \int \mathrm{d}^2x \sqrt{\tilde{g}}\, \mathcal{O}_r\, e^{2\sigma_r \varphi}} , \tag{1.2.3}$$

where λ_r is a coupling which for the case where $\mathcal{O}_r$ is the identity operator is equal to the cosmological constant; σ_r replaces b (1.2.2) in such a way to render the dressed operator $\mathcal{O}_r\, e^{2\sigma_r\varphi}$ a marginal operator and $(\mathfrak{b},\mathfrak{c})$ are the Weyl gauge fixing ghosts. Finally $\mathrm{PSL}(2,\mathbb{C})$ denotes the residual symmetry group of the two-sphere.

In the next two section we discuss the dictionary between matrix integrals and two-dimensional quantum gravity.

1.2.1 Matrix integral dictionary

A Hermitian matrix integral is given by [15, 25]

$$\mathcal{M}_N(\boldsymbol{\alpha}) = \int [\mathcal{D}M]\, e^{-N^2 \mathrm{Tr}_{N\times N}\left(\frac{1}{2}M^2+\frac{1}{4}\alpha_2 M^4+\ldots+\frac{1}{2m}\alpha_m M^{2m}\right)}\ , \tag{1.2.4}$$

where M is a Hermitian $N\times N$ matrix. Furthermore $\boldsymbol{\alpha}\equiv(\alpha_2,\ldots,\alpha_m)$ are real couplings and $[\mathcal{D}M]$ denotes the measure in the space of Hermitian matrices. Exploiting the $U(N)$ invariance to rewrite the Hermitian matrix in terms of its N real eigenvalues, in the large N limit we can solve this matrix integral in the leading planar limit using a saddle point approximation [25] and to subleading order using for example orthogonal polynomials [26].

A priori the above integral (1.2.4) only converges for positive couplings, however as an artefact of the large N limit we can push the integral also to negative values of the couplings until at a critical point — known as the multicritical point $(\alpha_{2,c},\ldots,\alpha_{m,c})$ — we encounter a branch cut ambiguity in the large N matrix integral. In particular close to the multicritical point the free energy, $\mathcal{F}_N(\boldsymbol{\alpha})\equiv -\log\mathcal{M}_N(\boldsymbol{\alpha})/\mathcal{M}_N(\mathbf{0})$, cannot be expressed in terms of an ordinary power series in the couplings anymore but shows non-analytic behaviour. The matrix integral (1.2.4) experiences $(m-1)$ distinct non-analyticities in $\mathcal{F}_N(\boldsymbol{\alpha})$, reflecting the $(m-1)$ couplings. In the planar limit we find

$$\lim_{\boldsymbol{\alpha}\to\boldsymbol{\alpha}_c+\epsilon\boldsymbol{s}} \mathcal{F}_N^{(0)}(\boldsymbol{\alpha}) \sim \text{const}\ \times\ \epsilon^{\hat{\Delta}_r}\ ,\quad r=1,\ldots,m\ ,\quad \epsilon\ll 1\ . \tag{1.2.5}$$

In the above expression $\boldsymbol{s}\equiv(s_2,\ldots,s_m)$ parametrise the $(m-1)$ distinct paths in couplings space to approach the multicritical point. More details are provided in chapter 3.

In the large N limit and upon tuning the couplings close to the multicritical point, the matrix integral (1.2.4) leads to the emergence of a two-dimensional theory of quantum gravity. This is conjectured to be Liouville theory coupled to the series $\mathcal{M}_{2,2m-1}$ of non-unitary minimal models [27, 28]. Using original insights by

Distler-Kawai [29] and David [30] , the path integral (1.2.3) with either one of the $(m-1)$ primary operators turned on leads to

$$Z[\lambda_r] \sim \text{const} \times \lambda_r^{\Delta_r} \ , \quad r = 1, \dots, m \ . \tag{1.2.6}$$

The critical exponents Δ_r can be matched to the non-analyticities $\hat{\Delta}_r$ of $\mathcal{F}_N^{(0)}(\boldsymbol{\alpha})$. In the table below (tab. 1.1) we summarise this dictionary

Matrix integrals + $V_m(M, \boldsymbol{\alpha})$	Liouville + $\mathcal{M}_{2,2m-1}$
$(m-1)$ distinct non-analyticities $\hat{\Delta}_r$	$(m-1)$ distinct critical exponents Δ_r
$\vdots$	$\vdots$

Table 1.1: *The dictionary between the matrix integral (1.2.4) and Liouville theory coupled to $\mathcal{M}_{2,2m-1}$.*

The natural question at hand is now: Why did we care so much about identifying the primaries of the minimal model with the paths in coupling space of the multicritical matrix integral?

Upon restricting the area of the physical metric $\upsilon = \int_{S^2} \sqrt{g}$ and turning on the identity operator $\mathcal{O}_1$ the partition function (1.2.3) admits the round two-sphere as a semiclassicle saddle [20]. In other words we do not only have the topology but also the geometry of the two-sphere. The two-sphere however is the Euclidean realisation of two-dimensional de Sitter space. If the conjectured duality between the multicritical matrix integral (1.2.4) and Liouville theory coupled to $\mathcal{M}_{2,2m-1}$ is true, this sphere should also reveal itself in the matrix integral. Our discussion in chapter 3 lead to the identification of the identity operator in the matrix picture. Understanding large m observables as presented in the discussion 5 of this thesis along the identity path could fill the space in tab. 1.1 and might lead to a "Matrix-dS_2" correspondence.

1.2.2 Matrix quantum mechanics dictionary

In addition to integrals over matrices one can also consider quantum mechanical matrices. The model studied is then given by the action

$$S_N[M(t)] = N \text{Tr}_{N\times N} \int \mathrm{d}t \left(\frac{1}{2} \dot{M}(t)^2 - V(M(t)) \right) \ , \tag{1.2.7}$$

where $V(M(t))$ is a polynomial potential, which, as motivated in chapter 2, we assume to be an inverted harmonic oscillator potential. Using as well the $U(N)$ invariance, Hermitian time dependent matrix models can also be expressed in terms of the real eigenvalues of $M(t)$. Promoting the Hamiltonian associated to the Lagrangian of (1.2.7) to its quantum version we can study the wave-functions of this matrix quantum mechanics. In particular the ground state wave-function viewed as a function of the N eigenvalues needs to obey the Pauli exclusion principle. The eigenvalues itself now lead to the emergence of an extra spatial dimension whose ground state configuration in the inverse harmonic oscillator potential (1.2.7) is a filled Fermi sea [25]. The matrix quantum mechanical S-matrix [31, 32] accounts for fluctuations/excitations on top of the filled Fermi sea. In figure 1.2 we depict the setup, whereas in chapter 2 we explicitly calculate the S-matrix for various configuration.

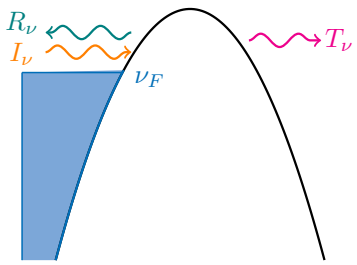

Figure 1.2: *We consider an incoming wave from negative infinity (orange), part of which is reflected (teal), and part of which is transmitted (magenta) from the inverted harmonic oscillator potential. The ground state configuration fills the Fermi sea up to the Fermi level ν_F.*

Remarkably, this S-matrix connects the matrix quantum mechanics via the DOZZ formula [34–37] to Liouville theory coupled to a timelike free boson [31, 32, 38].

Matrix quantum mechanics	Liouville + $c_m = 1$ boson
excitations on top of the filled Fermi sea	correlation functions

Table 1.2: *The dictionary between the matrix quantum mechanics (1.2.7) and Liouville theory coupled to a timelike free boson.*

1.3 Black holes

The goal of this section is to introduce the basic concepts discussed in more detail in chapter 4 of this thesis. Although the subsequent discussion generalises to other black holes for concreteness we restrict to the BTZ black hole [39]. We review the near-extremal BTZ black hole and its thermodynamic properties and explain the connection between the near-horizon, near-extremal BTZ black hole and the near-AdS_2/near-CFT_1 correspondence.

BTZ black hole. The rotating BTZ black hole with metric

$$\begin{aligned} ds_3^2 &= -f(\rho)\mathrm{d}t^2 + \frac{\mathrm{d}\rho^2}{f(\rho)} + \rho^2\left(\mathrm{d}\varphi - \frac{\rho_+\rho_-}{\ell\rho^2}\mathrm{d}t\right)^2 , \\ f(\rho) &\equiv \frac{(\rho^2-\rho_+^2)(\rho^2-\rho_-^2)}{\ell^2\rho^2} . \end{aligned} \tag{1.3.1}$$

is a solution of the three-dimensional Einstein-Hilbert action with negative cosmological constant $\Lambda = -2/\ell^2$. In this metric, $\rho_\pm$ are the position of the outer/inner horizon; without loss of generality, we will pick $\rho_+ > \rho_- > 0$. Further to this $t \in (-\infty, \infty)$, and $\varphi \sim \varphi + 2\pi$ is an angular coordinate. Associated to the black hole we have its mass and angular momemtum

$$m = \frac{\rho_+^2 + \rho_-^2}{8G_3\ell^2} , \qquad j = \frac{\rho_+\rho_-}{4G_3\ell} . \tag{1.3.2}$$

Black hole thermodynamics then relates the change in mass to an entropy

$$\mathrm{d}m = T\mathrm{d}S_{\mathrm{BH}} + \Omega\mathrm{d}j , \tag{1.3.3}$$

where the Hawking temperature and angular velocity are given by

$$T = \frac{\rho_+^2 - \rho_-^2}{2\pi\ell^2\rho_+} , \qquad \Omega = -\frac{\rho_-}{\ell\rho_+} . \tag{1.3.4}$$

Additionally we have the black hole entropy given by the Bekenstein-Hawking formula [6, 7]

$$S_{\mathrm{BH}} = \frac{A}{4G_3} = \frac{\pi\rho_+}{2G_3} . \tag{1.3.5}$$

Depending on the radial coordinate the near-extremal BTZ black hole reaches two different regimes (fig.1.3). For large $\rho \to \infty$ we reach the UV. In this region the metric of the BTZ black hole (1.3.1) reaches an asymptotically AdS_3 form and we can adopt the language common to the AdS/CFT correspondence. In the AdS_3/CFT_2 dictionary the BTZ black hole is a thermal state and we can use the

Cardy formula to determine the entropy of the CFT_2 conjecturally dual to AdS_3

$$S_{\mathrm{CFT}} = 2\pi\left(\sqrt{\frac{c_L h_L}{6}} + \sqrt{\frac{c_R h_R}{6}}\right) \ , \ h_{L/R} = \frac{1}{2}(m\ell \pm j) \ , \ c_{L/R} = \frac{3\ell}{2G_3} \ . \quad (1.3.6)$$

The Cardy formula (1.3.6) matches the Bekenstein-Hawking entropy (1.3.5).

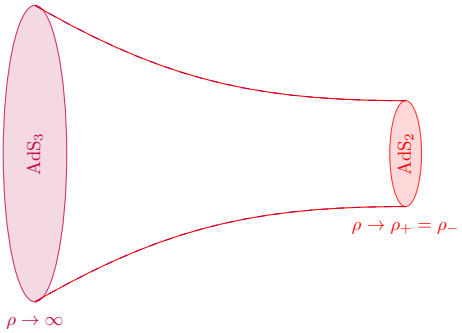

Figure 1.3: *Depending on the radial coordinate the BTZ black hole reaches either asymptotically AdS_3 or an AdS_2 geometry.*

For $\rho \to \rho_+ = \rho_-$ we reach the IR. The metric of the BTZ black hole turns into an S^1 fibration over AdS_2 and we talk about the near-horizon geometry of an extremal BTZ black hole. Its mass and angular momentum (1.3.2) coincide and its temperature (1.3.4) vanishes. On the other side the entropy (1.3.5) still attains a huge value. Now we move a tiny little bit away from extremality and observe the reaction of these thermodynamic quantities upon taking the near-horizon limit of the near-extremal BTZ black hole. Near-extremality is a regime close to $\rho_\pm = \rho_0 \pm \ell^2\pi T/2$, $T \ll 1$ and $\rho_+ = \rho_- \equiv \rho_0$, which we obtain by slightly increasing the temperature while keeping the angular momentum fixed. Both the mass as well as the entropy respond under this deviation quadratically and linearly in temperature respectively [40]

$$E \equiv m - m_{\mathrm{ext}} = \frac{1}{m_{\mathrm{gap}}}T^2 + \dots \ , \quad S = S_{\mathrm{ext}} + \frac{2}{m_{\mathrm{gap}}}T + \dots \ . \quad (1.3.7)$$

The coefficient $m_{\mathrm{gap}} \equiv 8G_3/(\pi\ell^2)$ is known as the mass gap. Below m_{gap} the thermodynamic description of the black hole breaks down as the energy of a Hawking quantum, which is of order $E_{\mathrm{HQ}} \sim T$, emitted in a non-extremal black hole during Hawking radiation has more energy than the black hole itself. This gap is believed to be the gap between the ground state and excited states in the black hole microstates picture [9].

near-AdS$_2$/near-CFT$_1$ correspondence. For many years, states above the ground state were not accessible because the AdS$_2$ factor contained in the geometry of the extremal black hole. In a pure AdS$_2$/CFT$_1$ correspondence imposing conformal invariance the trace of the stress tensor needs to vanish. As in a one dimensional CFT the stress tensor only has one component, tracelessness implies the vanishing of the stress tensor itself. Consequently all states have the same vanishing energy and the only states allowed in a pure AdS$_2$ geometry are the ground states [13, 14].

The near-AdS$_2$/near-CFT$_1$ correspondence overcomes this obstacle by breaking the full reparametrization symmetry of AdS$_2$ not just *spontaneously* but also *explicitly* [10]. Choosing an AdS$_2$ vacuum spontaneously breaks this symmetry down to SL$(2,\mathbb{R})$. This spontaneous breaking is nothing new; in the AdS$_3$/CFT$_2$ correspondence the asymptotic symmetry group of the CFT$_2$ — the Virasoro group — is spontaneously broken down to two copies of SL$(2,\mathbb{R})$ by choosing an AdS$_3$ vacuum [41]. The new ingredient of the near-AdS$_2$/near-CFT$_1$ correspondence is the explicit breaking coupled to the spontaneous symmetry breaking. We now illustrate this on the example of the BTZ black hole.

Einstein-Maxwell-Dilaton theory. One way to capture the near-extremal dynamics of the BTZ black hole is to dimensionally reduce the three-dimensional Einstein-Hilbert action along a circle. Using the Kaluza-Klein ansatz

$$ds_3^2 = g_{\mu\nu}\mathrm{d}x^\mu \mathrm{d}x^\nu + e^{-2\phi}\left(\mathrm{d}z + A_\mu \mathrm{d}x^\mu\right)^2 \ , \quad z \sim z + 2\pi L \ , \tag{1.3.8}$$

where Greek indices run along the two-dimensional directions, we obtain the two-dimensional Einstein-Maxwell-Dilaton theory [42, 43]

$$I_{\mathrm{EMD}} = \frac{L}{8G_3}\int \mathrm{d}^2x\,\sqrt{-g}\,e^{-\phi}\left(R + \frac{2}{\ell^2} - \frac{1}{4}e^{-2\phi}\,F_{\mu\nu}F^{\mu\nu}\right) \ , \tag{1.3.9}$$

where $F_{\mu\nu} = \partial_{[\mu}A_{\nu]}$. From a two-dimensional perspective A_μ can be interpreted as a gauge field and ϕ will be interpreted as the Dilaton field.

The equations of motion of this theory allow for two distinct cases, distinguished by the behaviour of the Dilaton ϕ. Whereas in one case we encounter a radial dependent (running) Dilaton ϕ which will asymptote back the AdS$_3$ region, the Einsten-Maxwell-Dilaton theory is also compatible with a constant Dilaton solution $e^{2\phi} = e^{2\phi_0}$, reflecting the IR in figure 1.3. In chapter 4 of this thesis we discuss both solutions; to relate to the near-extremal behaviour of black holes we will for now only focus on this IR solution. This solution describes a locally AdS$_2$

background. In Fefferman-Graham gauge we find

$$ds^2 = \mathrm{d}r^2 + \gamma_{tt}\mathrm{d}t^2 \ , \quad \gamma_{tt} = -\left(\alpha_{\rm ir}(t)\, e^{2r/\ell} + \beta_{\rm ir}(t)\, e^{-2r/\ell}\right)^2 \ , \tag{1.3.10}$$

where $\alpha_{\rm ir}(t)$ can be seen as the source and $\beta_{\rm ir}(t)$ as the vev of the metric. In particular $\beta_{\rm ir}(t)$ reflects the large diffeomorphisms in AdS_2. To understand the near-horizon region we add a deformation to the Dilaton $e^{-2\phi} = e^{-2\phi_0} + \mathcal{Y}$. Adding $\mathcal{Y}$ we explicitly break AdS_2. Importantly the equations of motion of $\mathcal{Y}$ imply that it is an irrelevant deformation and so it indeed has the effect of slightly moving us away from the IR fixed point. We obtain from the equations of motion of $\mathcal{Y}$

$$\mathcal{Y} = \lambda_{\rm ir}(t)\, e^{2r/\ell} + \sigma_{\rm ir}(t)\, e^{-2r/\ell} \ , \tag{1.3.11}$$

where again $\lambda_{\rm ir}(t)$ and $\sigma_{\rm ir}(t)$ are source and vev respectively. A priori it seems that adding this irrelevant deformation changes the problem, however the source of this irrelevant deformation pushing us away from AdS_2 still talks with the vev $\beta_{\rm ir}(t)$ of the background metric (1.3.10). Denoting by $t \to f(t)$ reparametrizations of the boundary time which preserve the AdS_2 geometry (1.3.10) we obtain

$$\ell^2 \lambda_{\rm ir}(t)''' + 8\lambda_{\rm ir}(t)\beta_{\rm ir}(t)' + 16\beta_{\rm ir}(t)\lambda_{\rm ir}(t)' = 0 \ , \quad \beta_{\rm ir}(t) = \frac{\ell^2}{8}\{f(t), t\} \ , \tag{1.3.12}$$

where $\{f(t), t\}$ denotes the Schwarzian derivative of $f(t)$

$$\{f(t), t\} \equiv \left(\frac{f''}{f'}\right)' - \frac{1}{2}\left(\frac{f''}{f'}\right)^2 \ . \tag{1.3.13}$$

The details leading to (1.3.12) are explained in chapter 4. Evaluating the renormalised on-shell Einstein-Maxwell-Dilaton action (4.3.3) we obtain a boundary effective action

$$I_{\rm bdy} = m_{\rm gap} \int \mathrm{d}t\, e^{\phi_0}\, \lambda_{\rm ir}(t)\, \{f(t), t\} \ , \tag{1.3.14}$$

where the prefactor governing the boundary theory, the near-CFT_1 regime, is nothing else than the mass gap (1.3.7) of the BTZ black hole.

In chapter 4 of this thesis we illuminate the near-AdS_2/near-CFT_1 correspondence after embedding the BTZ black hole into a three-dimensional theory violating parity. This theory is known as topologically massive gravity [44–46] and the dual CFT_2 has distinguishable left and right movers. Consequently we are able to infer where inside the CFT_2 the near-CFT_1 resides.

.

2 Matrix Musings

2.1 Introduction

The Universe is replete with spacetime. Although there is no known complete theory of spacetime at the quantum level, various ideas in modern theoretical physics suggest the radical notion that the classical description of spacetime must somehow be replaced by a microscopic theory whose basic variables are no longer built from a metric field. For general spacetimes, particularly those dominated by a vanishing or positive cosmological constant, little is known about this microscopic theory. Nevertheless, there are important hints that this theory must contain a large number N of building blocks which are strongly interacting amongst each other. In these notes we explore several systems composed of a large number N of constituents and discuss a variety of computational techniques used to solve them in the large N limit. A significant focus will be placed on large N systems whose components are organised in a matrix-like fashion. We will focus on both ordinary integrals over matrices as well as quantum mechanical models whose degrees of freedom and interactions are organised in a matrix-like structure.

The theory of random matrices has a rich history in physics and mathematics. It is not our aim to review this history, but we would like to mention a few examples. Perhaps the earliest application, dating back to the 1950s, was Wigner's proposal [21, 22, 48] that the distribution of adjacent energy level spacings for the spectra of heavy nuclei is well approximated by those of a random real symmetric matrix drawn from a Gaussian ensemble. This remarkable hypothesis constitutes a conceptual leap – a single theory is approximated by an ensemble of theories. This is different to performing averages over an ensemble of configurations within a single theory.[1] Wigner surmised that the distribution of level spacings s of a

[1] A method that is conceptually similar to Wigner's hypothesis is the quenched disorder approximation used in certain condensed matter and statistical systems such as spin glasses [58]. In this context, certain couplings in the theory, rather than the entire Hamiltonian, are chosen to be random.

random $N \times N$ real symmetric matrix whose elements are independently drawn from a Gaussian distribution obeys the following universal form in the large N limit

$$p(s) = \frac{\pi s}{2} e^{-\pi s^2/4} \ .$$

The above formula has been successfully compared to numerous spectra of heavy nuclei such as ^{238}U and ^{166}Er. The precise form of $p(s)$ was obtained by Mehta and Gaudin [49], and is indeed described to good approximation by the above expression. The class of ensembles was broadened to random Hermitian and random symplectic matrices by Dyson [23]. The choice of ensemble is tied to what global symmetries are present in the underlying system. An important characteristic feature of the above distribution is the suppression of $p(s)$ at small values of s. More generally, level repulsion in the eigenvalue spacing is a common litmus of complex systems.

Wigner's hypothesis is that certain properties of systems governed by sufficiently 'complex' Hamiltonians may be well approximated by a random ensemble. There is no reason this hypothesis should be restricted to the spectra of heavy nuclei. Indeed, another context where the ideas of random matrices have been applied is the theory of quantum chaos. At the classical level, a dynamical system can be said to be non-integrable if the number of conserved quantities is less than half the dimension of its phase space. A characteristic feature is exponential sensitivity to variations in the initial conditions, encoded in quantities such as the Lyapunov coefficients, the Kolmogorov-Sinai entropy, and the study of Poincaré sections. Any analogous framework for quantum systems, whose wavefunction obeys a linear equation, is significantly more involved. Nevertheless, it has been observed in numerous systems that the spectra of quantum Hamiltonians stemming from the quantisation of classically chaotic theories also exhibit a level spacing of the type in $p(s)$. This has been postulated by Bohigas-Giannoni-Schmit [52] as a general principle. Although exceptions to the rule have been observed, the BGS postulate is an intriguing tenet.

Matrix integrals, and hence the theory of random matrices, are connected to another class of physical systems. Consider a quantum theory whose degrees of freedom transform in the adjoint representation of an $SU(N)$ symmetry. Such theories include, but are in no sense limited to, Yang-Mills theory with an $SU(N)$ gauge group. If the theories admit a perturbative diagrammatic expansion, we can calculate terms using a path integral over the matrix degrees of freedom. The crucial observation due to 't Hooft [24] is that at large N the Feynman diagrams of such theories can be organised in terms of a genus expansion of triangulated Riemann surfaces Σ_h. The lattice points of Σ_h are the interaction vertices in the Feynman graph. This perturbative expansion resembles the perturbative expan-

sion of a string theory. If it so happens that for certain values of the coupling the number of vertices in Σ_h diverges, one might imagine associating a string theory to the large N limit of a quantum mechanical theory of matrices. Upon quantisation, the spectrum of a string often includes a massless spin-two particle. In such circumstances, the low energy description of the string theory is given by general relativity coupled to matter [53]. As such, assuming the hypothesis that large N matrix models are associated to string theories is indeed valid, one encounters a powerful avenue to explore theories of quantum gravity from an entirely different perspective. There is overwhelming evidence that this hypothesis is indeed correct for certain matrix models. Perhaps the most well known example [47] is maximally supersymmetric $SU(N)$ Yang-Mills theory in four-dimensions which is captured by the type IIB superstring on $\mathrm{AdS}_5 \times S^5$ – an instance of the AdS/CFT correspondence.

Finally, we note that the relation between the diagrammatic expansion of large N matrices and triangulated Riemann surfaces also finds interesting roots in the realm of two-dimensional geometry and quantum gravity. Early and remarkable numerical work on random triangulation motivated by Polyakov's path integral formulation of string theory [8] as well as the ideas of Regge-calculus [50] has been performed in [54–56]. From a more mathematical perspective, Kontsevich has shown that Witten's conjecture [59] on the intersection theory of Riemann surfaces is captured by a particular matrix integral resembling the Airy integral [60]. The beautiful results obtained by Maryam Mirzakhani for volumes of certain hyperbolic moduli spaces (Weil-Petersson volumes) [61] fit nicely into the topological recursion of Eynard and Orantin [62], itself having connections to matrix integrals.

It is natural to suspect that the theory of large N random matrices as well as the scope of Wigner's hypothesis – particularly in the context of string theory and the theory of black holes – will continue to surprise. This is an important motivation for our choice of content. There are many excellent and detailed reviews [64–77] on the subjects we discuss, many of which we have drawn enormous inspiration from. Nevertheless, it seems appropriate to bring together several of the subjects that are often presented in a somewhat disjoint fashion, and to provide a discussion on the relation to more recent developments. We develop our presentation in order of simplicity starting with integrals over vector-like variables, followed by integrals over a single as well as multiple matrices, quantum mechanical matrix theories, and finally the relation to two-dimensional quantum gravity and Liouville theory. We provide a brief overview of the broader scope of the ideas explored and end with a speculative overview. Details of some calculations and further results can be found in the various appendices. Finally, the bibliography is partitioned in terms of the various themes and ideas discussed.

2.2 Large N vector integrals

In this section we provide a brief discussion of the saddle point approximation in its simplest form. We subsequently apply it to a class of integrals over a large number N of variables organised in a vector-like structure.

2.2.1 Saddle point approximation

We begin by considering the following family of integrals

$$\mathcal{I}_N = \int_{\mathbb{R}} \mathrm{d}x\, e^{-Nf(x)} \ , \tag{2.2.1}$$

where N is a positive integer which will eventually be taken to be large, and $f(x)$ is a real valued function. In the limit where N becomes large, the exponential causes the integrand to peak sharply at the minima of the function $f(x)$, while all other values are suppressed. Of all extrema, the integral $\mathcal{I}_N$ will be dominated by the one which minimises $f(x)$ as N becomes large, and we denote this by x_e. Expanding $f(x)$ in a Taylor series around x_e

$$f(x) = f(x_e) + \frac{f''(x_e)}{2!}\,\delta x^2 + \dots \ , \qquad \delta x \equiv x - x_e \ , \tag{2.2.2}$$

one can approximate $\mathcal{I}_N$ as

$$\mathcal{I}_N \approx e^{-Nf(x_e)} \int_{\mathbb{R}} \mathrm{d}\delta x\, e^{-\frac{N}{2}f''(x_e)\delta x^2} \left(1 - \frac{N}{3!} f^{(3)}(x_e)\,\delta x^3 + ...\right) \ . \tag{2.2.3}$$

Upon redefining $\delta x = \delta\xi/\sqrt{N}$, we see that all higher powers of $\delta\xi$ are suppressed at large N, and we can compute the sub-leading correction to $\mathcal{I}_N$ in the large N expansion:

$$\mathcal{I}_N \approx \sqrt{\frac{2\pi}{Nf''(x_e)}} e^{-Nf(x_e)} \left(1 + \mathcal{O}(1/N)\right) \ . \tag{2.2.4}$$

If our function $f(x)$ has multiple minima, we must scan for the global one since the others will give contributions that are exponentially suppressed. If there are degenerate minima, on which $f(x)$ takes the same value, we must include them all to get a good approximation. Finally, if there are an infinite number of minima care must be exercised in our approximation scheme.

Example. As a simple example we consider the integral

$$\mathcal{J}_N = \int_0^\infty \mathrm{d}x\, x^N\, e^{-Nx} = \int_0^\infty \mathrm{d}x\, e^{-N(x - \log x)} \ . \tag{2.2.5}$$

This integral can be solved exactly by performing N partial integrations yielding $(N-1)!/N^N$. Moreover, we note that taking $f(x) = x - \log x$ the integral is of the form (2.2.1). The extremum of $f(x)$ is given by $x_e = 1$, with $f(x_e) = 1$. Expanding $f(x)$ around x_e in a Taylor series up to second order and inserting it into (2.2.1) we get

$$\lim_{N\to\infty} \mathcal{J}_N \approx \sqrt{\frac{2\pi}{N}}\, e^{-N}\,(1+\mathcal{O}(1/N))\ . \tag{2.2.6}$$

The same expression can be obtained by expanding the exact result $\mathcal{J}_N = (N-1)!/N^N$ using the Stirling approximation for the factorial.

Complex saddles & contour deformations

The above discussion captures the basic gist of the saddle point approximation in its simplest form. This dates back to Laplace's work in the eighteenth century. It is worth emphasising, however, that in general it may be the case that some of the extrema do not lie on the original contour of integration. As a very simple example, we might consider $f_c(x) = x^2 + \log\left(x^2+1\right)$ with $x \in \mathbb{R}$. Though this gives rise to a perfectly well defined integral (2.2.1), the extrema lie at $x_\pm = \pm i\sqrt{2}$ and $x_0 = 0$. It is straightforward to check that only one of the three saddles, in this case the one lying on the original contour of integration, contributes. More generally, for a complex function $g(z)$ with $z \in \mathbb{C}$ integrated along some contour $\mathcal{C}$ in the complex plane, the saddle point approximation is implemented by identifying a novel contour $\tilde{\mathcal{C}}$ that crosses through some subset of the critical points of $g(z)$ in such a way that the imaginary part of $g(z)$ remains constant along $\tilde{\mathcal{C}}$. Though we will generally not require such a treatment in what follows, it is important to keep it in mind.

2.2.2 Vector integrals

As a next step we consider the saddle point approximation for integrals with N variables $x_I \in \mathbb{R}$ containing a vector index $I = 1, 2, \ldots, N$. Consider the family of integrals

$$\mathcal{V}_N = \int_{\mathbb{R}^N} \prod_{I=1}^{N} \mathrm{d}x_I\, e^{-N f(x_I x_I/N)}\ , \tag{2.2.7}$$

where we use the double index notation $x_I x_I \equiv \sum_{I=1}^N x_I x_I$ here and throughout. The integrals $\mathcal{V}_N$ are invariant under $O(N)$ rotations of the x_I. By changing to

spherical coordinates

$$x_I = \sqrt{N} R\, \Omega_I \ , \qquad \sum_{I=1}^{N} \Omega_I^2 = 1 \ , \tag{2.2.8}$$

we reduce the integral to the one-dimensional case we already worked out in the previous section. Importantly, this change of variables produces a nontrivial Jacobian leading to the following expression

$$\mathcal{V}_N = \mathrm{vol}\, S^{N-1}\, N^{N/2} \int_0^\infty \mathrm{d}R\, e^{(N-1)\log R - N f(R^2)} \ . \tag{2.2.9}$$

Happily, in the large N limit the Jacobian of the coordinate change competes at the same order with the original integrand in (2.2.7). Thus, we can employ the saddle point approximation in its simplest form to estimate $\mathcal{V}_N$ at large N.

Example. As a straightforward example we can approximate the volume of the N-sphere S^N. To this end, we take $f(x_I x_I) = x_I x_I$ in (2.2.7) and compute the integral

$$\mathcal{V}_N = \int_{\mathbb{R}^N} \prod_{I=1}^{N} \mathrm{d}x_I\, e^{-x_I x_I} \tag{2.2.10}$$

in two different ways. An explicit calculation using Gaussian integrals tells us that the value of (2.2.10) gives $\mathcal{V}_N = \pi^{N/2}$. On the other hand, we can change to spherical coordinates and perform a saddle point approximation. Taking care of the Jacobian we rewrite (2.2.10) as

$$\mathcal{V}_N = \mathrm{vol}\, S^{N-1}\, N^{N/2} \int_0^\infty \mathrm{d}R\, e^{-N F(R)} \ , \tag{2.2.11}$$

with $F(R) \equiv R^2 - (1 - 1/N)\log R$ which at large N can be approximated as $F(R) \approx R^2 - \log R$. The dominant extremum of $F(R)$ is given by $R_e = 1/\sqrt{2}$ and so we obtain for the leading term of the integral

$$\lim_{N\to\infty} \mathcal{V}_N = \mathrm{vol}\, S^{N-1} \sqrt{\frac{\pi}{8N}} \left(\frac{N}{2}\right)^{N/2} e^{-N/2} \ . \tag{2.2.12}$$

Setting this equal to (2.2.10) we find an expression for the volume of S^N in the limit $N \gg 1$

$$\mathrm{vol}\, S^N \approx \sqrt{N} \left(\frac{2\pi e}{N}\right)^{N/2} \ . \tag{2.2.13}$$

This agrees with the large N limit of the volume of an N-sphere with known exact expression $\mathrm{vol}\, S^{N-1} = N\pi^{N/2}/\Gamma(N/2+1)$.

2.2.3 A perturbative expansion: the Cactus diagrams

We would now like to consider the vector-like integrals (2.2.7) from a slightly different perspective that is motivated by perturbative expansions often employed in the context of quantum field theory. We will do so by studying a specific example given by

$$\mathcal{Z}_N(\alpha) = \int_{\mathbb{R}^N} \prod_{I=1}^{N} \mathrm{d}x_I \; e^{-N\left(x_I x_I/N + \alpha (x_I x_I/N)^2\right)} \;, \tag{2.2.14}$$

where $\alpha \in \mathbb{R}$ will be taken to be a small parameter. For $\mathcal{Z}_N(\alpha)$ to be well-defined we should further take α to be positive, but we shall see shortly that in the large N limit, it may be sensible to allow α to also take small negative values. We will first consider the integral (2.2.14) in the small α limit, for which we can Taylor expand the exponential and calculate the correction terms using Wick contractions. To this end, it is convenient to introduce the 'propagator' $\langle x_I x_J \rangle$ given by

$$\langle x_I x_J \rangle = \mathcal{Z}_N^{-1}(0) \int_{\mathbb{R}^N} \prod_{K=1}^{N} \mathrm{d}x_K \, x_I x_J \, e^{-x_I x_I} = \frac{1}{2}\, \delta_{IJ} \;. \tag{2.2.15}$$

The corresponding graphical representation for the propagator and the quartic vertex in the integrand of (2.2.15) are dispayed in the figure below

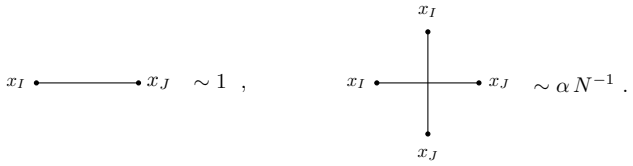

Figure 2.1: *Propagator and quartic vertex.*

Using the propagator and the quartic vertex we can form closed 'bubble' diagrams which compute perturbative contributions to $\mathcal{Z}_N(\alpha)$. The set of connected bubble diagrams is generated by $\mathcal{F}_N(\alpha) \equiv -\log\left(\mathcal{Z}_N(\alpha)/\mathcal{Z}_N(0)\right)$. To leading order, we can approximate $\mathcal{Z}_N(\alpha)$ by

$$\mathcal{Z}_N(\alpha) = \int_{\mathbb{R}^N} \prod_{K=1}^{N} \mathrm{d}x_K \, e^{-x_I x_I} \left(1 - \alpha\, N \left(\frac{x_I x_I}{N}\right)^2 + \cdots\right) \;. \tag{2.2.16}$$

One can evaluate the perturbative terms in the above integral by standard Gaus-

sian integration. The first order correction in the small α expansion yields

$$\alpha\, N \int_{\mathbb{R}^N} \prod_{K=1}^{N} \mathrm{d}x_K\, e^{-x_I x_I} \left(\frac{x_I x_I}{N}\right)^2 = \frac{\alpha}{4N} \sum_{I,J} (\delta_{II}\delta_{JJ} + 2\delta_{IJ}\delta_{IJ}) = \frac{\alpha}{4}(N+2)\ . \tag{2.2.17}$$

Diagrammatically, the above integral corresponds to a bubble diagram where we have closed the propagators emanating from the quartic vertex. Thus, to linear order in α we have

$$\lim_{\alpha\to 0} \mathcal{F}_N(\alpha) = \frac{\alpha}{4}\,(N+2) + \mathcal{O}(\alpha^2)\ . \tag{2.2.18}$$

As we proceed with higher order corrections, we encounter a variety of diagrams. For any given power of α a certain class of diagrams, known as *cactus diagram*, will dominate at large N. In the figure below, we demonstrate several diagrams of which the first three belong to the cactus family

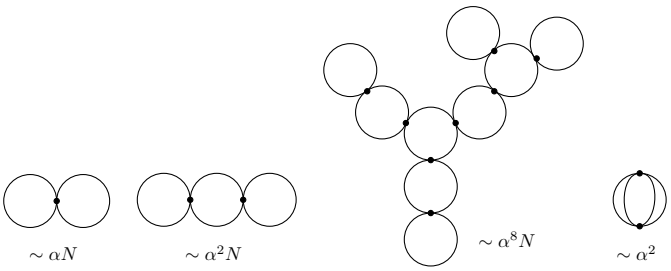

Figure 2.2: *Some bubble diagrams. The first three are cactus diagrams.*

2.2.4 Diagrams resummed

The fact that at large N only a subclass of diagrams survives leads to a dramatic simplification of the theory, and to the hope that a resummation can be performed. This resummation is precisely the saddle-point approximation of $\mathcal{Z}_N(\alpha)$. Let us perform the saddle point analysis to confirm the $\mathcal{O}(\alpha)$ correction we calculated perturbatively. To do so, let us go to spherical coordinates and perform the same steps as in (2.2.9). We find

$$\mathcal{Z}_N(\alpha) = \mathrm{vol}\, S^{N-1}\, N^{N/2} \int_0^\infty \mathrm{d}R\, e^{-NF_\alpha(R)}\ , \tag{2.2.19}$$

where we have defined $F_\alpha(R) \equiv \left(R^2 + \alpha R^4 - (1 - 1/N)\log R\right)$. To leading order in the large N limit, the extrema of $F_\alpha(R)$ are given by

$$R_\pm^2 = \frac{1}{4\alpha}\left(-1 \pm \sqrt{1+4\alpha}\right) \ . \tag{2.2.20}$$

Of the two saddles, only R_+^2 lies on the original contour of integration and has a well-defined limit as α tends to zero. The other saddle R_-^2 goes to infinity in the limit of vanishing α and hence cannot be relevant to compare to the perturbative analysis. Using the saddle point approximation, we are thus led to the leading N approximation of $\mathcal{F}_N(\alpha)$:

$$\begin{aligned}&\lim_{N\to\infty} \mathcal{F}_N(\alpha) \\ &= \frac{N}{8\alpha}\left(-1 + \sqrt{1+4\alpha} - \alpha(2 - 4\log 2) - 4\alpha \log\left(\frac{-1+\sqrt{1+4\alpha}}{\alpha}\right)\right) + \mathcal{O}(1) \ .\end{aligned} \tag{2.2.21}$$

The above result is valid to *all* orders in the small α expansion. Expanding (2.2.21) to leading order in α one can readily recover our perturbative correction (2.2.17). It is remarkable that the resummation of all the diagrams was encoded in the solution of the simple algebraic equation $\partial_R F_N(R) = 0$. Moreover (2.2.21) reveals that the expression gives a sensible result for $\mathrm{Re}\,\alpha \geq -1/4$ which includes a negative interval. To continue beyond the critical value $\alpha_c = -1/4$ one has to specify a branch cut due to the non-analytic behaviour. That negative values of α might be sensible in the large N limit, even though the finite N integral is ill-defined for negative α, comes about precisely because at large N most of the contribution to the integral is localised near the critical value of R_+. Fortuitously, the integral (2.2.19) can be evaluated exactly for any value of N. One finds

$$\exp\left(-\mathcal{F}_N(\alpha)\right) = \left(\frac{N}{4\alpha}\right)^{\frac{N}{4}} U\left(\frac{N}{4}, \frac{1}{2}, \frac{N}{4\alpha}\right) \ , \tag{2.2.22}$$

where $U(a,b,z)$ is Tricomi's confluent hypergeometric function. We have

$$\lim_{N\to\infty}\lim_{\alpha\to 0}\left(\frac{N}{4\alpha}\right)^{\frac{N}{4}} U\left(\frac{N}{4}, \frac{1}{2}, \frac{N}{4\alpha}\right) = 1 - \frac{\alpha}{4}(N+2) + \mathcal{O}\left(\alpha^2\right) \ . \tag{2.2.23}$$

This agrees again with the exponential of (2.2.18). In relation to the critical value R_+, it is worth mentioning a quantity that will become of increasing relevance throughout our discussion. Recall that the generating function of connected bubble

diagrams admits a large N expansion of the form

$$\mathcal{F}_N(\alpha) = N\mathcal{F}^{(0)}(\alpha) + \mathcal{F}^{(1)}(\alpha) + \frac{1}{N}\,\mathcal{F}^{(2)}(\alpha) + \dots \ . \tag{2.2.24}$$

Moreover, each of the functions $\mathcal{F}^{(k)}(\alpha)$ themselves admits a Taylor expansion near $\alpha = 0$. For instance

$$\mathcal{F}^{(0)}(\alpha) = \sum_{n=0}^{\infty} f_n^{(0)} \alpha^n \ . \tag{2.2.25}$$

The power of α counts the number of bubbles in a given cactus diagram. Consequently, we can define the moments of the 'bubble number' as

$$\langle n^L \rangle = \partial^{(L)}_{\log \alpha} \log \mathcal{F}^{(0)}(\alpha) \ . \tag{2.2.26}$$

Near the critical value α_c, and for $L \geq 2$, the above moments will diverge. For instance $\langle n^2 \rangle \sim (\alpha - \alpha_c)^{-1/2}$. This suggests that in the limit $\alpha \to \alpha_c$ the contribution of cacti with arbitrarily large numbers of bubbles becomes increasingly important. Moreover, the behaviour near α_c is somewhat reminiscent of critical phenomena.

Order of limits & analytic continuation

Expanding (2.2.22) at large N gives us expressions for all the $\mathcal{F}^{(n)}(\alpha)$. We can moreover study (2.2.22) for finite values of N. For positive integers N, the function (2.2.22) can be expressed either in terms of Bessel functions (for N odd) or the complementary error function (for N even). At finite N the integral (2.2.19) is defined for $\mathrm{Re}\,\alpha > 0$, though it can be analytically continued to certain regions of complex α-plane depending on whether N is even or odd. On the other hand, the infinite N approximation (2.2.21) can be extended to $\mathrm{Re}\,\alpha > -1/4$, after which we encounter a branch cut. We see that the analytic structure of $\mathcal{F}_N(\alpha)$ across the complex α-plane can depend on whether we first take the $N \to \infty$ limit and then analytically continue α or vice versa. In other words, the infinite N limit can qualitatively affect the analytic structure of a family of functions labelled by $N \in \mathbb{Z}$. We will not explore this aspect of the large N limit and the accompanying theoretical tools in any detail. We felt it important, nevertheless, to give a flavour of what they entail.

2.3 Large N integrals over a single matrix I

Having introduced the saddle point approximation and its application to vector integrals, we will now proceed to discuss matrix integrals, whose variables are organised in the form of an $N \times N$ Hermitian matrix M_{IJ} with $I, J = 1, 2, \dots, N$.

As briefly mentioned in the introduction, such integrals play a role in a remarkably rich set of physical systems ranging from nuclear theory to quantum chaos and string theory. The class of integrals we will study is of the following form

$$\mathcal{M}_N = \int_{\mathbb{R}^{N^2}} [\mathrm{d}M]\, e^{-N \operatorname{Tr} V(M)} \ , \tag{2.3.1}$$

where $V(M)$ is a matrix valued function of M, and the trace is only taken at the end. The measure factor is given by

$$[\mathrm{d}M] \equiv \prod_J \mathrm{d}M_{JJ} \prod_{I<J} \mathrm{dRe}M_{IJ}\, \mathrm{dIm}M_{IJ} \ . \tag{2.3.2}$$

The integrals are invariant under a conjugation of M by an $N \times N$ unitary matrix $U \in U(N)$.

2.3.1 Eigenvalue distribution

Every Hermitian matrix can be diagonalised using a unitary matrix $\mathcal{U}$ as $M = \mathcal{U} D_M \mathcal{U}^\dagger$ with $D_M \equiv \mathrm{diag}(\lambda_1, \lambda_2, \ldots, \lambda_N)$ a real diagonal matrix. Consequently, the exponent of the integrand in (2.3.1) depends purely on the N eigenvalues $\lambda_I \in \mathbb{R}$ of M. Thus, it is natural to consider the problem using a new set of variables given by an $N \times N$ unitary matrix $\mathcal{U} \in U(N)/U(1)^N$, and N real variables λ_I, such that $M = \mathcal{U} D_M \mathcal{U}^\dagger$. Notice that $\mathcal{U}$ resides in the coset space $U(N)/U(1)^N$, rather than the full $U(N)$, because those unitary matrices where each diagonal entry is multiplied by a pure phase are redundant. One must also compute the Jacobian associated to the change of variables $M = \mathcal{U} D_M \mathcal{U}^\dagger$. To this end, it is useful to write $\mathcal{U} = e^{i\mathcal{L}}$, with $\mathcal{L}$ an $N \times N$ Hermitian generator of $U(N)/U(1)^N$. The infinitesimal line element on the space of Hermitian matrices M is

$$\mathrm{d}s^2 = \operatorname{Tr} \mathrm{d}M \mathrm{d}M^\dagger = \sum_I \mathrm{d}\lambda_I^2 + 2 \sum_{I<J} (\lambda_I - \lambda_J)^2 |\mathrm{d}\mathcal{L}_{IJ}|^2 \ . \tag{2.3.3}$$

The Jabobian is the determinant of the above line element. It follows that

$$[\mathrm{d}M] = \frac{1}{\mathrm{vol}\ S_N} \prod_I \mathrm{d}\lambda_I \prod_{I \neq J} |\lambda_I - \lambda_J| [\mathrm{d}\mathcal{L}] \ , \tag{2.3.4}$$

where $[\mathrm{d}\mathcal{L}]$ is the volume element of the coset space $U(N)/U(1)^N$ and we have further divided by the volume of the permutation group S_N to avoid multiple counting of eigenvalue matrices D_M with permuted elements.

Example. As an example, let us consider the case $N = 2$. We can parametrise

the unitary matrix $\mathcal{U}$ as

$$\mathcal{U} = \begin{pmatrix} \sin\frac{\theta}{2} & e^{i\varphi}\cos\frac{\theta}{2} \\ -e^{-i\varphi}\cos\frac{\theta}{2} & \sin\frac{\theta}{2} \end{pmatrix} , \tag{2.3.5}$$

where $\theta \in [0, \pi)$ and $\varphi \in (0, 2\pi]$ are coordinates on the coset space $U(2)/U(1)^2$, whose geometry is the round two-sphere. Using that the relation $\mathcal{U} = e^{i\mathcal{L}}$ implies

$$\mathrm{d}\mathcal{L} = -i\,\mathcal{U}^{-1}\mathrm{d}\mathcal{U} . \tag{2.3.6}$$

The line element (2.3.3) can be written out explicitly:

$$\mathrm{d}s^2 = \mathrm{d}\lambda_1^2 + \mathrm{d}\lambda_2^2 + \frac{(\lambda_1 - \lambda_2)^2}{2}\left(\mathrm{d}\theta^2 + \sin^2\theta\mathrm{d}\varphi^2\right) . \tag{2.3.7}$$

Defining $r = (\lambda_1 - \lambda_2)/\sqrt{2}$ and $z = (\lambda_1 + \lambda_2)/\sqrt{2}$ the above becomes

$$\mathrm{d}s^2 = \mathrm{d}z^2 + \mathrm{d}r^2 + r^2\left(\mathrm{d}\theta^2 + \sin^2\theta\mathrm{d}\varphi^2\right) . \tag{2.3.8}$$

We observe that the above metric is indeed the flat metric on $\mathbb{R}^4$ in cylindrical coordinates up to the fact that $r \in \mathbb{R}$ as opposed to $r \geq 0$. However, the map $r \to -r$ is in fact a permutation of the eigenvalues $\lambda_1 \leftrightarrow \lambda_2$. This is a double counting in our configuration space, since conjugation with respect to $\mathcal{U}$ in (2.3.5) with $\theta = 0$ exchanges λ_1 and λ_2. Thus, after dividing by the volume of the two-dimensional permutation group the volume element becomes

$$[\mathrm{d}M] = r^2\mathrm{d}r\,\mathrm{d}z\,\mathrm{d}\Omega_2 , \qquad r > 0 , \tag{2.3.9}$$

where $\mathrm{d}\Omega_2$ is the standard volume element on the unit sphere S^2. The right hand side is indeed the flat metric on $\mathbb{R}^4$ expressed in cylindrical coordinates.

The Vandermonde contribution

The product appearing in the volume element (2.3.4) is the determinant of the Vandermonde matrix

$$\mathbf{V}_N \equiv \begin{pmatrix} 1 & \lambda_1 & \lambda_1^2 & \cdots & \lambda_1^{N-1} \\ 1 & \lambda_2 & \lambda_2^2 & \cdots & \cdots \\ \vdots & \vdots & \vdots & \ddots & \\ 1 & \lambda_N & \lambda_N^2 & \cdots & \lambda_N^{N-1} \end{pmatrix} . \tag{2.3.10}$$

Since it will appear several times throughout our discussion, we introduce the

following notation for the determinant of the Vandermonde matrix

$$\Delta_N(\lambda) \equiv \prod_{I<J} (\lambda_I - \lambda_J) \ . \tag{2.3.11}$$

We can bring our original integral (2.3.1) to the following form

$$\mathcal{M}_N = \text{vol}\, \frac{U(N)}{U(1)^N \times S_N} \int_{\mathbb{R}^N} \prod_{I=1}^{N} \mathrm{d}\lambda_I \, e^{-N^2 S[\lambda]} \ , \tag{2.3.12}$$

where we have defined the multivariable function

$$S[\lambda] \equiv \frac{1}{N} \sum_{I=1}^{N} V(\lambda_I) - \frac{1}{N^2} \sum_{J \neq I} \log |\lambda_I - \lambda_J| \ . \tag{2.3.13}$$

As for the vector integral case, the change of coordinates adds a nontrivial Jacobian that will compete with the original integrand. Moreover, the Jacobian causes an effective 'repulsive' pressure against the eigenvalues all lying on top of each other. The repulsive effect is the matrix analogue of the logarithmic term encountered in (2.2.9) for the vector integrals.

Before proceeding to solve (2.3.1) in the large N limit, let us summarise what we have achieved so far. By a unitary transformation of the Hermitian matrix M we reduced the matrix integral from a theory with N^2 independent degrees of freedom to a theory described by the N real eigenvalues of the Hemitian matrix M. The Jacobian arising from this change of coordinates gives rise to the square of the Vandermonde determinant $\Delta_N(\lambda)^2$. This contribution competes with $V(\lambda)$ such that the eigenvalues are distributed around the mininum of $V(\lambda)$.

2.3.2 Saddle point approximation & the resolvent

In order to solve the matrix integrals at large N, we will once again employ the saddle point approximation. The saddle point equations for $S[\lambda]$ in (2.3.13) are given by

$$V'(\lambda_I) = \frac{2}{N} \sum_{J \neq I} (\lambda_I - \lambda_J)^{-1} \ . \tag{2.3.14}$$

To solve these equations, it is convenient to introduce the following normalised eigenvalue distribution

$$\rho(\lambda) = \frac{1}{N} \sum_{I=1}^{N} \delta(\lambda - \lambda_I) \ , \qquad \int_{-a}^{a} \mathrm{d}\lambda \, \rho(\lambda) = 1 \ . \tag{2.3.15}$$

In the large N limit, and under the assumption that the range $[-a, a]$ is compact and does not grow with N, we can approximate $\rho(\lambda)$ by a continuous, non-negative function. For simplicity, we further assume that the range of $\rho(\lambda)$ is symmetric about the origin. This is not at great cost since we can always shift all the λ by a constant to accommodate this. We can then rewrite (2.3.14) as the following integral equation

$$V'(\lambda) = 2 \fint_{-a}^{a} \mathrm{d}\mu \, \frac{\rho(\mu)}{\lambda - \mu} \ , \tag{2.3.16}$$

where it is understood that we are taking the principal value for the integral. Our goal is to find the eigenvalue distribution $\rho(\lambda)$ which solves the above equation. To do so, it is instructive to introduce the resolvent [25]

$$\mathrm{R}_N(z) \equiv \frac{1}{N} \mathrm{Tr} \left(z \, \mathbb{I}_N - M \right)^{-1} = \frac{1}{N} \sum_{I=1}^{N} \frac{1}{z - \lambda_I} \ , \qquad z \in \mathbb{C} / \{\lambda_I\} \ . \tag{2.3.17}$$

Sending $N \to \infty$ the sum can be replaced by an integral where each eigenvalue is weighted by its average density

$$\lim_{N \to \infty} \mathrm{R}_N(z) \equiv \mathrm{R}(z) = \int_{-a}^{a} \mathrm{d}\mu \, \frac{\rho(\mu)}{z - \mu} \ . \tag{2.3.18}$$

By evaluating the resolvent close to the real axis $z = x \pm i\epsilon$ we find

$$\mathrm{R}(x + i\epsilon) = \int_{-a}^{a} \mathrm{d}\mu \, \frac{\rho(\mu)}{x - \mu + i\epsilon} = \int_{-a}^{a} \mathrm{d}\mu \, \frac{\rho(\mu)(x - \mu)}{(x - \mu)^2 + \epsilon^2} - i \int_{-a}^{a} \mathrm{d}\mu \, \frac{\rho(\mu)\epsilon}{(x - \mu)^2 + \epsilon^2} \ , \tag{2.3.19}$$

where in the limit $\epsilon \to 0$ the first integral is a principal value integral, while we evaluate the second integral using delta function identities. Finally, we arrive at

$$\mathrm{R}(x \pm i\epsilon) = \fint_{-a}^{a} \mathrm{d}\mu \, \frac{\rho(\mu)}{(x - \mu)} \mp i\pi\rho(x) \ , \tag{2.3.20}$$

where we have employed the Sokhotski-Plemelj theorem. Using (2.3.14) and (2.3.15)

$$\mathrm{R}(x \pm i\epsilon) = \frac{1}{2} V'(x) \mp i\pi\rho(x) \ . \tag{2.3.21}$$

Using (3.2.7) and the above expressions we obtain the following properties the resolvent must satisfy:

$$\text{res}_a \ : \quad \lim_{z\to\infty} \mathrm{R}(z) = \frac{1}{z} \ , \tag{2.3.22}$$

$$\text{res}_b \ : \quad \rho(x) = \frac{1}{2\pi i}\left(\mathrm{R}(x-i\epsilon) - \mathrm{R}(x+i\epsilon)\right) , \quad x \in \text{supp}(\rho) \ , \tag{2.3.23}$$

$$\text{res}_c \ : \quad V'(x) = \mathrm{R}(x+i\epsilon) + \mathrm{R}(x-i\epsilon) \ , \quad x \in \text{supp}(\rho) \ . \tag{2.3.24}$$

The condition res_b specifies the jump of the resolvent across the branch cut $x \in [-a, a]$. Elsewhere, the resolvent is analytic. Finally, res_c fixes the real part of the resolvent to the derivative of the potential. Thus, the class of problems we are trying to solve is a Riemann-Hilbert type problem.

In the large N limit the exponent of our original integral (2.3.12) takes the form

$$S[\rho(\lambda)] = \int_{-a}^{a} \mathrm{d}\lambda\, \rho(\lambda) V(\lambda) - \int_{-a}^{a} \mathrm{d}\lambda\, \rho(\lambda) \int_{-a}^{a} \mathrm{d}\mu\, \rho(\mu) \log|\lambda - \mu| \ . \tag{2.3.25}$$

Using the saddle point equations, we can further simplify

$$S[\rho_{\text{ext}}(\lambda)] = \frac{1}{2}\int_{-a}^{a} \mathrm{d}\lambda\, \rho_{\text{ext}}(\lambda) V(\lambda) - \int_{-a}^{a} \mathrm{d}\lambda\, \rho_{\text{ext}}(\lambda)\, \log|\lambda| \ , \tag{2.3.26}$$

where, for simplicity, we have further assumed that $V(0) = 0$ and $\rho_{\text{ext}}(\lambda)$ is that solution of (2.3.16) which minimises $S[\rho(\lambda)]$ in (2.3.25). Thus, our original integral (2.3.12) is approximated by the expression

$$\mathcal{M}_N \approx \text{vol}\, U(N)\, e^{-N^2 S[\rho_{\text{ext}}(\lambda)]} \ , \tag{2.3.27}$$

where we have dropped the volume of $U(1)^N \times S_N$ since it does not compete with terms that grow exponentially in N^2.

Gaussian example. We now consider the simplest concrete example. Let us take $V(M) = \frac{1}{2}M^2$ such that

$$\mathcal{M}_N = \int_{\mathbb{R}^{N^2}} [\mathrm{d}M]\, e^{-\frac{N}{2}\mathrm{Tr}\, M^2} = \left(\frac{2\pi}{N}\right)^{N^2/2} \ , \tag{2.3.28}$$

where we obtained the exact result using Gaussian integrals. We will now approximate (2.3.28) using the saddle point approximation. As was already outlined, this involves finding the resolvent $\mathrm{R}(z)$. Let us consider the following ansatz

$$\mathrm{R}(z) = \frac{1}{2}V'(z) - P(z)\sqrt{z^2 - a^2} \ , \tag{2.3.29}$$

where $P(z)$ is a polynomial in z. The degree of $P(z)$ must be chosen such that it cancels all positive powers of $\mathrm{R}(z)$ to guarantee res_a. For $V(z) = z^2/2$ we find that $P(z)$ must be constant. Moreover, imposing the remaining conditions $\mathrm{res}_{b,c}$ on the resolvent one obtains

$$\mathrm{R}(z) = \frac{1}{2}z - \frac{1}{2}\sqrt{z^2-4} \qquad \text{and} \qquad \rho_{\mathrm{ext}}(x) = \frac{1}{2\pi}\sqrt{4-x^2}\ , \quad x \in [-2,2]\ . \tag{2.3.30}$$

The eigenvalue distribution (2.3.30) is known as *Wigner's semicircle law* and appears in a wide range of physical and mathematical examples. Notice that it is connected and has compact support. Using the eigenvalue distribution we obtain the large N approximation

$$\mathcal{M}_N \approx \mathrm{vol}\, U(N)\, e^{-\frac{3}{4}N^2}\ . \tag{2.3.31}$$

Setting this expression equal to the exact result in (2.3.28), we can provide an approximation for the volume of the unitary group in the limit of large rank

$$\lim_{N\to\infty} \log\, \mathrm{vol}\, U(N) \approx \frac{N^2}{2}\left(\log\frac{2\pi}{N} + \frac{3}{2}\right) + \mathcal{O}(N)\ . \tag{2.3.32}$$

We can readily verify that the above expression agrees with the large N approximation of the exact expression

$$\mathrm{vol}\, U(N) = \frac{(2\pi)^{N(N+1)/2}}{G(N+1)}\ , \tag{2.3.33}$$

where $G(N+1)$ is Barnes G-function and we recall that at large N

$$\log G(N+1) = -\frac{3N^2}{4} + \frac{N^2}{2}\log N + \frac{N}{2}\log 2\pi - \frac{1}{12}\log N + \dots\ . \tag{2.3.34}$$

Quartic example. Having done the Gaussian case, we now move on to a slightly more involved example. We will consider the integral

$$\mathcal{Z}_N(\alpha) = \int_{\mathbb{R}^{N^2}} [\mathrm{d}M]\, e^{-N\,\mathrm{Tr}V_\alpha(M)}\ , \quad V_\alpha(M) = \frac{1}{2}M^2 + \alpha M^4\ . \tag{2.3.35}$$

Using the ansatz (2.3.29) and following the approach delineated for the Gaussian case, we can write down the resolvent with $P(z)$ a quadratic polynomial

$$\mathrm{R}(z) = \frac{1}{2}z + 2\alpha z^3 - (p_1 + p_2 z + p_3 z^2)\sqrt{z^2-a^2}\ . \tag{2.3.36}$$

The parameters p_1, p_2 and p_3 are fixed by res_a.

$$p_1 = \frac{1}{2} + \alpha\, a^2 \ , \quad p_2 = 0 \ , \quad p_3 = 2\alpha \ . \tag{2.3.37}$$

The parameter a solves the equation

$$3\alpha\, a^4 + a^2 - 4 = 0 \quad \Rightarrow \quad a_\pm^2 = -\frac{1}{6\alpha} \pm \frac{1}{6\alpha}\sqrt{1+48\alpha} \ . \tag{2.3.38}$$

We are interested in the solution that is continuously connected to the Gaussian solution as $\alpha \to 0$, which is a_+. Notice that the saddle point solution (2.3.38) exhibits non-analytic behaviour as α approaches $\alpha_c = -1/48$, somewhat reminiscent of what we saw in our vector integral example (2.2.20). If we wish to continue past $\alpha = \alpha_c$, the argument of the square root becomes negative and we have to specify a branch cut. Our expression for the resolvent and eigenvalue density are given by

$$\mathrm{R}(z) = \frac{1}{2}z + 2\alpha z^3 - \left(\frac{1}{2} + \alpha\, a_+^2 + 2\alpha z^2\right)\sqrt{z^2 - a_+^2} \ , \tag{2.3.39}$$

$$\rho_{\text{ext}}(\lambda) = \frac{1}{\pi}\left(\frac{1}{2} + \alpha\, a_+^2 + 2\alpha\lambda^2\right)\sqrt{a_+^2 - \lambda^2} \ , \tag{2.3.40}$$

with a_+ given by (2.3.38).

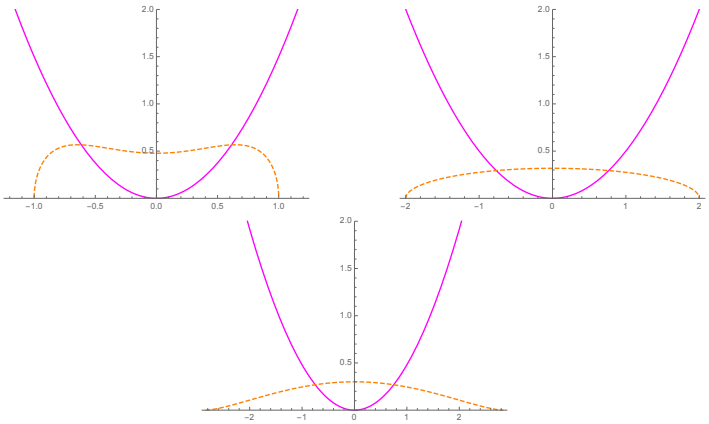

Figure 2.3: *Quartic polynomial $V_\alpha(\lambda)$ (magenta) and corresponding eigenvalue distribution $\rho_{\text{ext}}(\lambda)$ (orange, dashed) for $\alpha = 1$ (left), $\alpha = 0$ (center), and $\alpha = \alpha_c$ (right).*

To approximate our original integral (2.3.35) at large N, we must evaluate

$$S[\rho_{\text{ext}}(\lambda)] = \int_0^{a_+} \mathrm{d}\lambda\, \rho_{\text{ext}}(\lambda) \left(\frac{1}{2}\lambda^2 + \alpha\lambda^4\right) - 2\int_0^{a_+} \mathrm{d}\lambda\, \rho_{\text{ext}}(\lambda) \log|\lambda| \tag{2.3.41}$$

on the saddle point solution $\rho_{\text{ext}}(\lambda)$. In the above expression we also used that our integrands are symmetric around the origin to adjust the boundaries of the integrals. Evaluating this integral at the saddle $\rho_{\text{ext}}(\lambda)$ we find

$$S[\rho_{\text{ext}}(\lambda)] - S[\rho_{\text{ext}}(\lambda)]_{\alpha=0} = -\frac{3}{8} - \frac{1}{384}\left(a_+^2 - 40\right) a_+^2 + \log\frac{2}{a_+}\ , \tag{2.3.42}$$

where we used (2.3.38) to write the above as a function of a_+. Substituting a_+, a small α expansion reveals the following [25, 79, 80]

$$\lim_{N\to\infty} \frac{\mathcal{F}_N(\alpha)}{N^2} = 2\alpha - 18\alpha^2 + 288\alpha^3 - 6048\alpha^4 + \frac{746496}{5}\alpha^5 + \mathcal{O}\left(\alpha^6\right)\ , \tag{2.3.43}$$

where we have defined $\mathcal{F}_N(\alpha) \equiv -\log \mathcal{Z}_N(\alpha)/\mathcal{Z}_N(0)$, analogously to the vector integral case. More generally, and somewhat similar to the vector integral case (2.2.24), the matrix integrals allow for an expansion in large N^2

$$\mathcal{F}_N(\alpha) = N^2\mathcal{F}^{(0)}(\alpha) + \mathcal{F}^{(1)}(\alpha) + \frac{1}{N^2}\mathcal{F}^{(2)}(\alpha) + \cdots\ , \tag{2.3.44}$$

where each of the $\mathcal{F}^{(n)}(\alpha)$ itself admits a power series expansion around $\alpha = 0$. A careful examination of (2.3.42) and (2.3.43) reveals [25]

$$\mathcal{F}^{(0)}(\alpha) = -\sum_{n=1}^{\infty}(-12\alpha)^n \frac{(2n-1)!}{n!(n+2)!} = 2\alpha\, {}_3F_2\left(1, 1, \frac{3}{2}; 2, 4; -48\alpha\right)\ . \tag{2.3.45}$$

We can expand the above near the critical value $\alpha_c = -1/48$ to find the leading non-analytic behaviour (which we denote with a subscript n.a.)

$$\lim_{\alpha\to\alpha_c} \partial_\alpha^{(3)}\, \mathcal{F}^{(0)}_{\text{n.a.}}(\alpha) = 4608\sqrt{3}\,(\alpha - \alpha_c)^{-1/2} + \dots\ . \tag{2.3.46}$$

We will analyse the terms $\mathcal{F}^{(h)}(\alpha)$ in (2.3.44) in the next section. In particular we will provide detailed evidence that near the critical value α_c the leading non-analytic behaviour goes as

$$\lim_{\alpha\to\alpha_c} \mathcal{F}^{(h)}_{\text{n.a.}}(\alpha) \sim (\alpha - \alpha_c)^{5\chi_h/4}\ , \qquad h \in \mathbb{N}\ , \tag{2.3.47}$$

where a logarithmic behaviour is understood for $h = 1$ and $\chi_h = 2 - 2h$.

2.3.3 General polynomial & multicritical models

The planar solution for the eigenvalue distribution stemming from a general $V(\lambda)$ can be written down rather concisely. We discuss here the case for which the eigenvalue distribution is connected and has compact support on a single real interval $\lambda \in [b, a]$. In that case the resolvent is given by [85]

$$\mathrm{R}(z) = \frac{1}{2} \oint_{\mathcal{C}} \frac{\mathrm{d}u}{2\pi i} \frac{V'(u)}{z-u} \sqrt{\frac{(z-a)(z-b)}{(u-a)(u-b)}} \,, \tag{2.3.48}$$

where the contour $\mathcal{C}$ goes around the branch cut $z \in [b, a]$. The end points a and b follow from the conditions (2.3.22) and (2.3.24) imposed on the resolvent. Given $\mathrm{R}(z)$, we can extract the eigenvalue density from (2.3.23).

It is interesting to note that there exist a variety of polynomials which upon tuning the coefficients give rise to non-analytic behaviour different from (2.3.47). These matrix integrals are known as multicritical matrix integrals and were originally introduced in [15]. For $V_m(M, \boldsymbol{\alpha})$ an even polynomial of degree $2m$ we denote the matrix integral

$$V_m(M, \boldsymbol{\alpha}) = \sum_{n=1}^{m} \frac{1}{2n} \alpha_n M^{2n} \tag{2.3.49}$$

as an m^{th} multicritical model. For $(\alpha_2, \ldots, \alpha_m)$ close to the multicritical point

$$\alpha_{n,c}^{(m)} \equiv (-1)^{n+1} \binom{m}{n} \frac{2n}{(4m)^n} B(n, 1/2) \,, \quad 2 \leq n \leq m \,. \tag{2.3.50}$$

this matrix integral experiences $(m-1)$ distinct non-analyticties as we will show in chapter 3. For instance, using the above techniques, the following polynomial [15, 82]

$$V_3(M, \alpha_2, \alpha_3) = \frac{1}{2} M^2 + \frac{1}{4} \alpha_2 M^4 + \frac{1}{6} \alpha_3 M^6 \,. \tag{2.3.51}$$

with the eigenvalues of M distributed in the range $[-a, a]$ has Resolvent and eigenvalue distribution given by

$$\begin{aligned} &\mathrm{R}_3(z, \alpha_2, \alpha_3) \\ &= \frac{1}{2} V_3'(z, \alpha_2, \alpha_3) - \frac{1}{16} \left(8 + 4u\alpha_2 + 3u^2\alpha_3 + z^2(8\alpha_2 + 4u\alpha_3) + 8\alpha_3 z^4\right) \sqrt{z^2 - u} \,, \\ &\rho_{\text{ext}}^{(3)}(z, \alpha_2, \alpha_3) = \frac{1}{16\pi} \left(8 + 4u\alpha_2 + 3u^2\alpha_3 + z^2(8\alpha_2 + 4u\alpha_3) + 8\alpha_3 z^4\right) \sqrt{u - z^2} \,. \end{aligned} \tag{2.3.52}$$

2.3.4 Large N factorisation & loop equations

A natural set of integrals living in the same class as (2.3.1) are the following

$$\mathcal{M}_N^{(k_1,k_2,\ldots,k_n)} \equiv \frac{1}{\mathcal{M}_N}\int_{\mathbb{R}^{N^2}}[\mathrm{d}M]e^{-N\mathrm{Tr}V(M)}\prod_{i=1}^{n}\frac{1}{N}\mathrm{Tr}\,M^{k_i} = \frac{1}{N^n}\Big\langle\prod_{i=1}^{n}\mathrm{Tr}M^{k_i}\Big\rangle\,. \tag{2.3.53}$$

These integrals also preserve the $U(N)$ symmetry. To leading order in the large N limit we can use the eigenvalue density to estimate the $\mathcal{M}_N^{(k_1,k_2,\ldots,k_n)}$. For example

$$\mathcal{M}_N^{(k_1,k_2,\ldots,k_n)} = \prod_{i=1}^{n}\int_{-a}^{a}\mathrm{d}\lambda\,\rho_{\mathrm{ext}}(\lambda)\,\lambda^{k_i} + \mathcal{O}(1/N^2)\,. \tag{2.3.54}$$

So long as neither n nor k_i scale with N we see that to leading order in the large N limit we cannot distinguish $\mathcal{M}_N^{(k_1,\ldots,k_n)}$ from $\mathcal{M}_N^{(k_1)}\mathcal{M}_N^{(k_2)}\ldots\mathcal{M}_N^{(k_n)}$. This is a characteristic property of large N systems known as large N factorisation [81]. From this perspective, $\mathrm{Tr}M^k/N$ can be viewed as a collection of weakly correlated quantities, the correlation strength going as some inverse power of N. The phenomenon of large N factorisation thus provides us with a novel type of perturbative expansion for a certain class of matrix functions.

As an example, let us use large N factorisation to recover the equations governing the resolvent at large N. The starting point is the observation that the integral $\mathcal{M}_N$ should be left unchanged under a change in variables $M \to F(M)$ where F is a matrix-valued function. For instance, we can consider the family of functions $F_\ell(M) = M + g\,e^{\ell M}$ where g is taken to be parametrically small and ℓ is a real number. Invariance of $\mathcal{M}_N$ under these transformations imposes a set of interesting constraints [85]. For parametrically small g one finds

$$\frac{\ell}{N^2}\sum_{k=0}^{\infty}\frac{\ell^k}{k!}\sum_{j=0}^{k}\big\langle\,\mathrm{Tr}\,M^j\mathrm{Tr}\,M^{k-j}\big\rangle = \hat{G}_\ell^{(V)}\,\frac{1}{N}\big\langle\,\mathrm{Tr}\,e^{\ell M}\,\big\rangle\,. \tag{2.3.55}$$

The left hand side stems from the variation of the measure, whereas the right hand side stems from the variation of the exponent. $\hat{G}_\ell^{(V)}$ is a differential operator acting on functions of ℓ. If $V(M)$ admits a power series, $V(M) = \sum_{n=0}^{\infty}\alpha_n M^n$, we have

$$\hat{G}_\ell^{(V)} = \sum_{n=1}^{\infty} n\,\alpha_n\,\partial_\ell^{(n-1)}\,. \tag{2.3.56}$$

To leading order in the large N expansion, we can use large N factorisation to break the left hand side of (2.3.55) into a sum over a product of traces. The leading

large N expression is then given by

$$\int_0^\ell \mathrm{d}u \, \langle W_u \rangle \, \langle W_{\ell-u} \rangle = \hat{G}_\ell^{(V)} \, \langle W_\ell \rangle \ . \tag{2.3.57}$$

The above equation is a type of equation known as a loop equation [83–86], and the object

$$W_\ell \equiv \frac{1}{N} \mathrm{Tr} \, e^{\ell M} \tag{2.3.58}$$

is known as a macroscopic loop operator. The resolvent $\mathrm{R}_N(z)$ defined in (3.2.6) can be obtained from the loop operator by the following Laplace transform

$$\mathrm{R}_N(z) = \int_0^\infty \mathrm{d}\ell \, e^{-\ell z} \, W_\ell \qquad \Longrightarrow \qquad \mathrm{R}(z) = \lim_{N\to\infty} \int_0^\infty \mathrm{d}\ell \, e^{-\ell z} \, \langle W_\ell \rangle \ . \tag{2.3.59}$$

We can take the Laplace transform of (2.3.57) with respect to ℓ and find

$$\mathrm{R}(z)^2 = V'(z)\mathrm{R}(z) - \mathcal{P}(z) \ , \qquad \mathcal{P}(z) = -\int_0^\infty \mathrm{d}\ell \, \hat{G}_\ell^{(V)} \left\langle W_\ell \, e^{-\ell z} \right\rangle \ . \tag{2.3.60}$$

Solving the quadratic equation leads to

$$\mathrm{R}(z) = \frac{1}{2} \, V'(z) - \frac{1}{2} \sqrt{V'(z)^2 - 4\mathcal{P}(z)} \ , \tag{2.3.61}$$

where we choose the negative root to satisfy res_a (2.3.22). Equation (2.3.61) constitutes a derivation of (2.3.48).

Examples. We present the loop operators for the three polynomials discussed in the beginning of this section. For the Gaussian case we can use the density in (2.3.30) to calculate the loop operator

$$\lim_{N\to\infty} \langle W_\ell \rangle = \frac{1}{\ell} \, I_1(2\ell) \ , \tag{2.3.62}$$

where $I_n(z)$ is the modified Bessel function of the first kind. The differential operator is $\hat{G}_\ell^{(V)} = \partial_\ell$ and it confirms (2.3.57). In the large z limit we obtain

$$\mathcal{P}(z) = -\int_0^\infty \mathrm{d}\ell \, \partial_\ell \left(\frac{1}{\ell} \, I_1(2\ell) \, e^{-\ell z} \right) = 1 \ , \tag{2.3.63}$$

such that (2.3.61) agrees perfectly with the resolvent in (2.3.30). For the quartic

polynomial we find $\hat{G}_\ell^{(V_\alpha)} = \partial_\ell + 4\alpha\partial_\ell^3$ and using the density in (2.3.39) we obtain

$$\lim_{N\to\infty} \langle W_\ell \rangle = \frac{a_+(1+6\,a_+^2\alpha)}{2\ell}\, I_1(a_+\,\ell) - \frac{6\,a_+^2\alpha}{\ell^2}\, I_2(a_+\,\ell)\ , \tag{2.3.64}$$

where a_+ has been defined in (2.3.38). Combining W_ℓ with $\hat{G}_\ell^{(V_\alpha)}$ we easily confirm (2.3.57) and combining it with (2.3.61) we confirm the polynomial in (2.3.39).

2.3.5 A perturbative expansion: the Riemann surfaces

We now proceed to study how the perturbative expansion of a matrix type integral is organised in the large N limit. We will uncover a remarkable connection, originally observed by 't Hooft [24], to Riemann surfaces.

Let us focus on matrix integrals with the following structure

$$\mathcal{M}_N = \int_{\mathbb{R}^{N^2}} [\mathrm{d}M]\, e^{-N\,\mathrm{Tr}\,V(M)}\ , \tag{2.3.65}$$

where $V(M)$ is an arbitrary polynomial in M containing parameters α which will be taken to be small. Though the lessons will be general, for the sake of concreteness we will consider again a purely quartic example $V_\alpha(M)$ (2.3.35). Since we will be interested in a perturbative expansion in small α, it is convenient to write down the propagator

$$\langle M_{IK} M_{JL} \rangle = \mathcal{Z}_N^{-1}(0) \int_{\mathbb{R}^{N^2}} [\mathrm{d}M]\, e^{-\frac{N}{2}\mathrm{Tr}\,M^2} M_{IJ} M_{KL} = \frac{1}{N}\delta_{IL}\delta_{KJ}\ . \tag{2.3.66}$$

For small coupling α we expand the exponential (2.3.35) leading to

$$\mathcal{Z}_N(\alpha) = \int_{\mathbb{R}^{N^2}} [\mathrm{d}M]\, e^{-\frac{N}{2}\mathrm{Tr}\,M^2} \sum_{k\in\mathbb{N}} (-1)^k \frac{(N\alpha)^k}{k!}\, (\mathrm{Tr}M^4)^k\ . \tag{2.3.67}$$

The graphical representation of the propagator and the quartic vertex is given in the figure below:

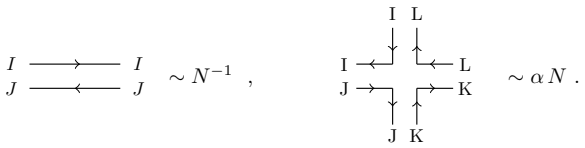

Figure 2.4: *Propagator and quartic vertex.*

Using standard Gaussian integration, we can compute the various terms in the small α expansion. For example, to linear order in α the large N integral (2.3.35) becomes

$$\mathcal{F}_N(\alpha) \equiv -\log \frac{\mathcal{Z}_N(\alpha)}{\mathcal{Z}_N(0)} = (2N^2+1)\alpha + \mathcal{O}(\alpha^2) \ . \tag{2.3.68}$$

Each of the terms in the α expansion has a diagrammatic representation. We give some examples in the figure below. Due to their double line representation, these diagrams are often called ribbon diagrams.

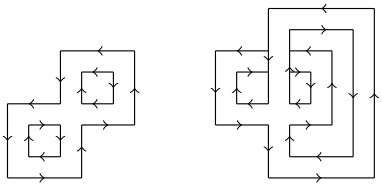

Figure 2.5: *Figure of a planar (left) and a non-planar (right) diagram.*

From the small α expansion it is clear that the diagrams contributing to the perturbative expansion of a matrix integral can scale with different powers of N. In (3.3.7) we observed that the propagator scales with inverse power of N. Moreover, each loop contributes a factor of N, and each vertex adds a factor αN. This implies that a diagram with L loops, V vertices, and P propagators scales as $\alpha^V N^{V+L-P}$. Making the identification [24]

$$\text{loops } L \mathrel{\hat{=}} \text{faces } F \ , \quad \text{propagators } P \mathrel{\hat{=}} \text{edges } E \ , \quad \text{vertices } V \mathrel{\hat{=}} \text{vertices } V \ , \tag{2.3.69}$$

one can identify the power of N associated to a particular ribbon diagram with the Euler characteristic χ_h of the two-dimensional compact surface Σ_h of genus h it can be drawn on. Since $\chi_h = 2-2h$, at least pictorially, there seems to be a natural genus expansion in the large N limit for the perturbative expansion of our matrix integral $\mathcal{Z}_N(\alpha)$. We leave it to the reader to verify that this conclusion will not be affected by allowing $V_\alpha(M)$ to be an arbitrary polynomial, so long as the couplings are scaled appropriately as we take N large.

To recapitulate: the large N organisation of our perturbative expansion can be expressed as

$$\mathcal{F}_N(\alpha) = \sum_{h=0}^{\infty} e^{\chi_h \log N}\, \mathcal{F}^{(h)}(\alpha) \ , \tag{2.3.70}$$

where h labels the genus of the Riemann surface Σ_h, χ_h its Euler characteristic, and each $\mathcal{F}_h(\alpha)$ is a sum of connected diagrams that can be drawn on a surface of

genus h

$$\mathcal{F}^{(h)}(\alpha) = \sum_{V=0}^{\infty} f_V^{(h)} \, \alpha^V \ . \tag{2.3.71}$$

The leading contribution in the large N expansion is known as the *planar* contribution, and sub-leading contributions in the large N expansion are known as non-planar contributions. We argued that there exists a natural map between fat graphs and the polygonisation of Σ_h. For the quartic theory, the surfaces of the graph dual to the polygonisation of Σ_h are squares.

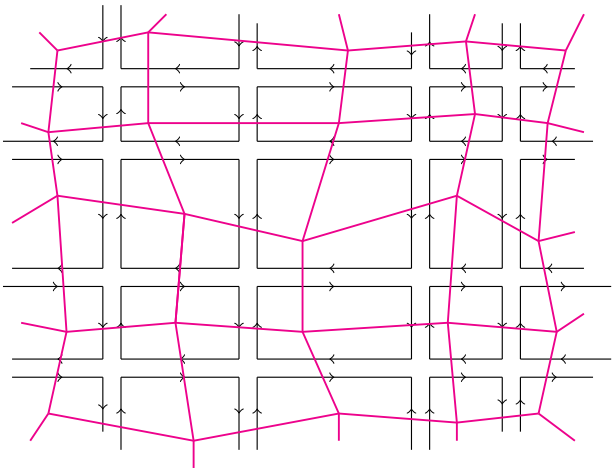

Figure 2.6: *Polygonisation: the black lines are the ribbon diagrams, whereas the magenta lines correspond to the dual lattice.*

Riemann surfaces with boundaries

In addition to ribbon diagrams corresponding to discretised Riemann surfaces without boundary, we can also examine diagrams living on Riemann surfaces with boundaries. We start by coupling N dimensional complex Grassmann valued vectors $\bar{\xi}^{(s)}$ and $\xi^{(s)}$ to the matrix integral (2.3.1)

$$\mathcal{K}_N(\alpha; z) \equiv \frac{1}{\mathcal{M}_N(\alpha)} \int_{\mathbb{R}^{N^2}} [\mathrm{d}M] \int \prod_{s=1}^{N_f} \prod_{I=1}^{N} \mathrm{d}\bar{\xi}_I^{(s)} \mathrm{d}\xi_I^{(s)} \, e^{-N \mathrm{Tr}\, V_\alpha(M) - \bar{\xi}^{(s)}(z\,\mathbb{I}_N - M)\xi^{(s)}} \ , \tag{2.3.72}$$

where $z \in \mathbb{C}$. The index s can be viewed as a flavour index ranging over N_f 'flavours'. For concreteness, although not necessary, we choose the quartic polynomial (2.3.35). The ribbon diagrams in figure 3.3 get enhanced by graphs with a single line.

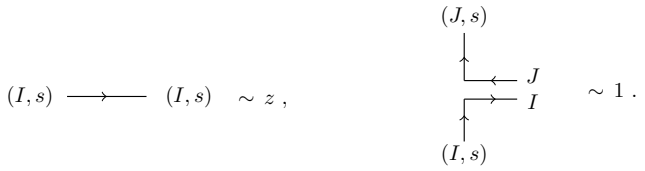

Figure 2.7: *Propagator and vertex.*

Integrating out $\bar{\xi}^{(s)}$ and $\xi^{(s)}$ in (2.3.72) we obtain

$$\begin{aligned}\mathcal{K}_N(\alpha;z) &= \frac{1}{\mathcal{M}_N(\alpha)}\int_{\mathbb{R}^{N^2}}[\mathrm{d}M]\, e^{-N\,\mathrm{Tr}V_\alpha(M)+N_f\,\mathcal{W}(z)} \\ &= 1+\ \big\langle N_f\ \mathcal{W}(z)\big\rangle + \frac{1}{2!}\big\langle N_f^2\ \mathcal{W}(z)^2\big\rangle\ +\cdots\ , \end{aligned} \tag{2.3.73}$$

where we defined

$$\mathcal{W}(z)\equiv \mathrm{Tr}\log(z\,\mathbb{I}_N - M)\ . \tag{2.3.74}$$

It is worth noting that $\partial_z\mathcal{W}(z)$ is equal to the resolvent introduced in (3.2.6). Further defining $\mathcal{B}_N(\alpha;z)\equiv\log\mathcal{K}_N(\alpha;z)$ we obtain the large N expansion

$$\mathcal{B}_N(\alpha;z)=\sum_{h=0}^{\infty}\sum_{b=1}^{\infty} e^{\chi_{h,b}\log N} N_f^b\,\mathcal{B}^{(h,b)}(\alpha;z)\ ,\quad \chi_{h,b}\equiv 2-2h-b\ . \tag{2.3.75}$$

Here, $\mathcal{B}_N(\alpha;z)$ encodes the sum of connected diagrams corresponding to discretised Riemann surfaces with h holes and b boundaries. In the figure below we display an example of a ribbon diagram and its dual lattice for $h=0$ and $b=1$.

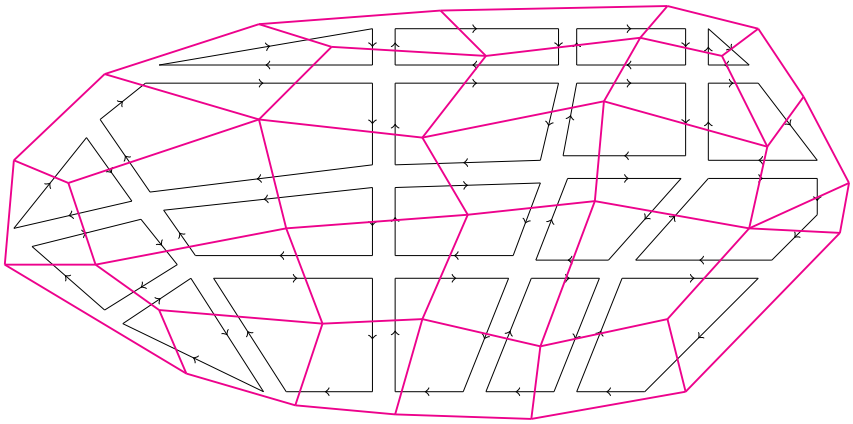

Figure 2.8: *Polygonisation with boundary: the black lines are the ribbon diagrams, whereas the magenta lines correspond to the dual lattice.*

Each term $\mathcal{B}^{(h,b)}(\alpha;z)$ in (2.3.75) is itself a sum of connected diagrams with fixed h and b:

$$\mathcal{B}^{(h,b)}(\alpha;z) = \sum_{V=0}^{\infty}\sum_{B=1}^{\infty} f_{V,B}^{(h,b)}\alpha^V z^B \ . \tag{2.3.76}$$

The parameter z is the boundary analog of α, while N_f is the boundary analog of N. Keeping track of the powers of N_f in (2.3.75) allows one to distinguish Riemann surfaces which would be indistinguishable purely from their power of N.

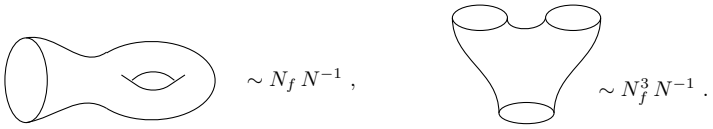

Figure 2.9: *The parameter N_f allows one to distinguish otherwise indistinguishable surfaces.*

Continuum limit and double scaling

In analogy to the bubble number we defined in (2.2.26) for cactus diagrams, we can define the 'vertex number' for the polygonisation of Σ_h as

$$\langle n_h\rangle = \partial_{\log\alpha}\log\mathcal{F}^{(h)}(\alpha) \ . \tag{2.3.77}$$

For instance, given (2.3.45) we can compute $\langle n_0\rangle$ near α_c to find $\langle n_0\rangle \sim (\alpha - \alpha_c)^{-1}$. More generally, granting (2.3.47), we find $\langle n_h\rangle \sim (\alpha-\alpha_c)^{-1}$ for all h. Consequently, as α approaches α_c the number of vertices diverges suggesting the possibility for a continuum limit of the discretised surfaces Σ_h.

There is another limit of interest we can consider, known as the *double scaling limit*. The limit consists of simultaneously taking N large as well as α to it's critical value α_c, while keeping a particular combination α and N fixed. Recall (2.3.47), namely that the non-analytic part of $\mathcal{F}^{(h)}(\alpha)$ near α_c scales as

$$\lim_{\alpha\to\alpha_c}\mathcal{F}^{(h)}_{\text{n.a.}}(\alpha) = f_h(\alpha-\alpha_c)^{5\chi_h/4} \ , \qquad h\in\mathbb{N} \ , \tag{2.3.78}$$

with f_h being some proportionality constant and $h=1$ is understood to be logarithmic. It follows that the large N expansion near $\alpha=\alpha_c$ is approximately

$$\mathcal{F}_N(\alpha) \approx N^2\mathcal{F}^{(0)}(\alpha_c) + \sum_{h=0}^{\infty} f_h\, e^{\chi_h\log N}(\alpha-\alpha_c)^{5\chi_h/4} \ . \tag{2.3.79}$$

The above expression suggests the introduction of a new parameter

$$\kappa^{-1} \equiv N(\alpha - \alpha_c)^{5/4} \ . \tag{2.3.80}$$

The double scaling limit takes $N \to \infty$ and $\alpha \to \alpha_c$ while keeping κ fixed. In this way, we see how the continuum limit and the large N limit work harmoniously in producing a new function of potential interest

$$\mathcal{F}(\kappa) \equiv \lim_{N\to\infty,\ \kappa \text{ fixed}} \Big(\mathcal{F}_N(\alpha) - N^2 \mathcal{F}^{(0)}(\alpha) \Big) = \sum_{h=0}^{\infty} f_h \, \kappa^{-\chi_h} \ . \tag{2.3.81}$$

In the next subsection, by introducing a new method for dealing with the matrix integrals, we will produce a non-linear differential equation whose solution encodes $\mathcal{F}(\kappa)$.

***

An interesting system which naturally exhibits a genus expansion is the perturbative expansion of worldsheet string theory. At this stage there is no immediate reason for the two systems to be related, but one may speculate so. We shall see in section 2.8 that such speculations are materialised in a concrete and elegant sense.

2.4 Large N integrals over a single matrix II

In this section we introduce a different technique to solve matrix integrals. This technique will allow us to calculate contributions of the matrix integral beyond the planar approximation [80].

2.4.1 Orthogonal polynomials

Two polynomials are said to be orthogonal with respect to a weight function $w(x)$ if they satisfy

$$\text{ortho}_a : \quad \int \mathrm{d}x \, w(x) \, p_n(x) p_m(x) = h_n \delta_{m,n} \tag{2.4.1}$$

for some h_n. A familiar example is given by the Hermite polynomials

$$H_n(x) = (-1)^n e^{x^2} \frac{\mathrm{d}^n}{\mathrm{d}x^n} e^{-x^2}, \ n = 1, 2, \ldots \tag{2.4.2}$$

which satisfy

$$\int_{\mathbb{R}} \mathrm{d}x \, e^{-x^2} \, H_n(x) H_m(x) = 2^n \sqrt{\pi} \, n! \, \delta_{mn} \ . \tag{2.4.3}$$

In addition to (6.0.28), orthogonal polynomials satisfy the *three-term recurrence relation*

$$\begin{aligned} \text{ortho}_b: \quad & x\,p_n(x) = A_n\,p_n(x) + S_n\,p_{n+1}(x) + R_n\,p_{n-1}(x) \qquad \text{for} \qquad n>0\ , \\ & x\,p_0(x) = A_0\,p_0(x) + S_0\,p_1(x)\ , \end{aligned} \tag{2.4.4}$$

where A_n, S_n, and R_n are some real constants. The Hermite polynomials (2.4.2) satisfy

$$x\,H_n = \frac{1}{2}\,H_{n+1} + n\,H_{n-1}\ , \tag{2.4.5}$$

and thus for $n \geq 0$ we have $A_n = 0$, $S_n = 1/2$, and $R_n = n$. Other examples of orthogonal polynomials include the Legendre polynomials, Laguerre polynomials, and Chebychev polynomials.

In what follows we will focus on monic polynomials

$$P_n(\lambda) \equiv \lambda^n + \sum_{j=0}^{n-1} a_j \lambda^j\ , \qquad n = 0, \ldots, N-1\ . \tag{2.4.6}$$

It is worth mentioning that when the measure in (6.0.28) is even under $\lambda \to -\lambda$, the monic polynomials $P_n(\lambda)$ transform as $P_n(-\lambda) = (-1)^n P_n(\lambda)$. This implies that only even powers of λ appear in $P_{2n}(\lambda)$ whereas only odd powers of λ appear in $P_{2n-1}(\lambda)$. Moreover, invariance under $\lambda \to -\lambda$ implies that the coefficient A_n in the three-term recurrence relation vanishes, while being monic implies $S_n = 1$.

Orthogonal polynomials for matrix integrals

We will now use the properties of monic orthogonal polynomials to solve matrix integrals. In order to do so, we observe that the Vandermonde matrix can be expressed in the following way

$$\mathbf{V}_N = \begin{pmatrix} P_0(\lambda_1) & P_1(\lambda_1) & \ldots & P_{N-1}(\lambda_1) \\ P_0(\lambda_2) & \ldots & \ldots & \ldots \\ \vdots & \ldots & \ldots & \ldots \\ P_0(\lambda_N) & P_1(\lambda_N) & \ldots & P_{N-1}(\lambda_N) \end{pmatrix}\ . \tag{2.4.7}$$

The above expression is related to (2.3.10) by a similarity transformation. The determinant $\Delta_N(\lambda)$ depends only on the leading degree of each polynomial. Using the Leibniz formula for determinants, we can recast $\Delta_N(\lambda)$ as

$$\Delta_N(\lambda) = \sum_{\sigma \in S_N} \text{sgn}(\sigma) \prod_{I=1}^{N} P_{\sigma(I)-1}(\lambda_I)\ . \tag{2.4.8}$$

Consequently, we can re-express the matrix integral (2.3.1) as

$$\operatorname{vol}\frac{U(1)^N\times S_N}{U(N)}\,\mathcal{M}_N=\sum_{\sigma,\tau\in S_N}\operatorname{sgn}(\sigma)\operatorname{sgn}(\tau)\prod_{I=1}^{N}\int_{\mathbb{R}}\mathrm{d}\mu(\lambda_I)P_{\sigma(I)-1}(\lambda_I)P_{\tau(I)-1}(\lambda_I)$$
$$=N!\prod_{I=0}^{N-1}h_I\ , \quad (2.4.9)$$

where for notational convenience we have defined $\mathrm{d}\mu(\lambda)\equiv\mathrm{d}\lambda\, e^{-NV(\lambda)}$. Using the three-term recurrence relation we can relate h_n to R_n in (6.0.29) and rewrite (2.4.9) entirely in terms of R_n, which are themselves determined by the weight function $w(\lambda)=e^{-NV(\lambda)}$. It will also prove convenient to express h_n in the following way

$$h_n=\int_{\mathbb{R}}\mathrm{d}\mu(\lambda)\lambda P_{n-1}(\lambda)P_n(\lambda)\ . \quad (2.4.10)$$

An additional relation that will be useful is

$$nh_n=\int_{\mathbb{R}}\mathrm{d}\mu(\lambda)P_n'(\lambda)\,\lambda P_n(\lambda)=NR_n\int_{\mathbb{R}}\mathrm{d}\mu(\lambda)V'(\lambda)P_n(\lambda)P_{n-1}(\lambda)\ . \quad (2.4.11)$$

For example, when combined with (2.4.10) the above relation informs us that for a Gaussian potential $V(\lambda)=\lambda^2/2$ we have $h_0=\sqrt{2\pi/N}$ and $R_n=n/N$. Hence the orthogonal polynomials are the Hermite polynomials for $V(\lambda)=\lambda^2/2$. From the above expressions, we can recursively calculate the sub-leading coefficients a_J in (6.0.30). Applying ortho_b to (2.4.10) leads to the recursion $h_n=R_n\,h_{n-1}$, which implies that (2.4.9) can be rewritten as

$$\mathcal{M}_N=\operatorname{vol}\frac{U(N)}{U(1)^N\times S_N}\times N!\,h_0^N R_1^{N-1}R_2^{N-2}\cdots R_{N-1}\ . \quad (2.4.12)$$

As a simple check of the above expression we note that for $\alpha=0$

$$\mathcal{M}_N=\operatorname{vol}\frac{U(N)}{U(1)^N\times S_N}\times N!\left(\frac{2\pi}{N}\right)^{N/2}\prod_{n=1}^{N-1}\left(\frac{n}{N}\right)^{N-n}=\left(\frac{2\pi}{N}\right)^{N^2/2}\ , \quad (2.4.13)$$

where we have used (2.3.33), $\operatorname{vol}S_N=N!$, and $\operatorname{vol}U(1)=2\pi$.

Finally, we obtain a relation between the quantities defined and $\mathcal{F}_N(\alpha)$:

$$\frac{1}{N^2}\mathcal{F}_N(\alpha)=-\frac{1}{N}\log\frac{h_0(\alpha)}{h_0(0)}-\frac{1}{N}\sum_{n=1}^{N-1}\left(1-\frac{n}{N}\right)\log\frac{R_n(\alpha)}{R_n(0)}\ . \quad (2.4.14)$$

The argument of h_n and R_n indicates their dependence on the coefficient α

parametrising a non-Gaussian piece of $V(\lambda)$. We now delve into a detailed example.

2.4.2 Non-planar contributions

We are now ready to see how the orthogonal polynomials can be used to go beyond the planar approximation of the large N expansion of $\mathcal{F}_N(\alpha)$. For concreteness we take $V_\alpha(\lambda) = \lambda^2/2 + \alpha\lambda^4$. From (2.4.11) we find

$$\frac{n}{N} = R_n(\alpha)\Big(1 + 4\alpha\left(R_{n+1}(\alpha) + R_n(\alpha) + R_{n-1}(\alpha)\right)\Big) \,, \tag{2.4.15}$$

where the term multiplying 4α follows from the quartic interaction term in the potential and the relation

$$\int_{\mathbb{R}} \mathrm{d}\mu(\lambda)\lambda^3 P_{n-1}(\lambda)P_n(\lambda) = \big(R_{n+1}(\alpha) + R_n(\alpha) + R_{n-1}(\alpha)\big)h_n(\alpha) \,, \tag{2.4.16}$$

which is obtained using the three-term-recurrence relation (6.0.29). In appendix 6 we provide a graphical procedure to obtain relations similar to (2.4.16) also for higher order potentials. We can use equation (6.0.32) to study the large N limit. Let us define the variables $\varepsilon \equiv 1/N$ and $x \equiv n\varepsilon$. In the large N limit, x is well approximated by a continuous parameter. In view of this, it is convenient to set $r(x,\alpha) \equiv R_n(\alpha)$. We note that $r(x,\alpha)$ is also a function of N, but we suppress this dependence for notational simplicity. We can rewrite (6.0.32) as

$$x = r(x,\alpha) + 4\alpha r(x,\alpha)\left[r(x+\varepsilon,\alpha) + r(x,\alpha) + r(x-\varepsilon,\alpha)\right] \,. \tag{2.4.17}$$

It follows from (6.0.33) that $r(x,\alpha)$ is symmetric under $\varepsilon \leftrightarrow -\varepsilon$ and we can expand it in even powers of ε

$$r(x,\alpha) = r_0(x,\alpha) + \varepsilon^2\, r_2(x,\alpha) + \varepsilon^4\, r_4(x,\alpha) + \cdots \,. \tag{2.4.18}$$

Collecting terms with equal powers of ε we obtain the expression:

$$r(x+\varepsilon,\alpha) + r(x-\varepsilon,\alpha) = 2\sum_{n=0}^{\infty}\varepsilon^{2n}\sum_{k+p=n}\frac{1}{(2p)!}\frac{\mathrm{d}^{2p}}{\mathrm{d}x^{2p}}\, r_{2k}(x,\alpha) \,. \tag{2.4.19}$$

Re-inserting this into (6.0.33) and comparing powers of ε we conclude

$$x\,\delta_{s,0} = r_{2s}(x,\alpha) + 4\alpha\sum_{m+n=s} r_{2m}(x,\alpha)\left[r_{2n}(x,\alpha) + 2\sum_{k+p=n}\frac{1}{(2p)!}\frac{\mathrm{d}^{2p}}{\mathrm{d}x^{2p}}\, r_{2k}(x,\alpha)\right] \,. \tag{2.4.20}$$

For the cases $s = 0$ and $s = 1$ we readily find

$$r_0(x,\alpha) = \frac{-1+\sqrt{1+48\alpha x}}{24\alpha} \qquad \text{and} \qquad r_2(x,\alpha) = \frac{96\alpha^2 r_0(x,\alpha)}{(1+48\alpha x)^2} \tag{2.4.21}$$

Our final ingredient will be the Euler-Maclaurin formula

$$\frac{1}{N}\sum_{n=1}^{N} f\left(\frac{n}{N}\right) = \int_0^1 \mathrm{d}x f(x) + \frac{1}{2N} f(x)\Big|_0^1 + \sum_{n=1}^{p-1} \frac{B_{2n}}{(2n)!}\frac{1}{N^{2n}} f(x)^{(2n-1)}\Big|_0^1 + \mathcal{R}_N \ . \tag{2.4.22}$$

In the above, $f(x)$ is a $2p$ times continuously differentiable function, $\mathcal{R}_N$ is a remainder term scaling as $\mathcal{O}(1/N^{2p+1})$, and the B_{2n} denote the Bernoulli numbers. Applying the Euler-Maclaurin formula to

$$f\left(x\right) = (1-x)\log\frac{r(x,\alpha)}{x} \ , \tag{2.4.23}$$

and expanding (6.0.31) in inverse powers of N, we find

$$\begin{aligned}\frac{1}{N^2}\mathcal{F}_N(\alpha) = &-\int_0^1 \mathrm{d}x(1-x)\log\frac{r(x,\alpha)}{x} - \frac{1}{N}\log\frac{h_0(\alpha)}{h_0(0)} + \frac{1}{2N}\lim_{x\to 0}\log\frac{r(x,\alpha)}{x} \\ &- \frac{1}{12N^2}\left((1-x)\log\frac{r(x,\alpha)}{x}\right)^{(1)}\Bigg|_0^1\end{aligned} \tag{2.4.24}$$

up to order $\mathcal{O}(1/N^4)$ corrections. To obtain $h_0(\alpha)$ we simply evaluate

$$h_0(\alpha) = \int_{\mathbb{R}} \mathrm{d}\mu(\lambda) = \frac{e^{\frac{N}{32\alpha}}}{2\sqrt{2}}\sqrt{\frac{1}{\alpha}}\,K_{\frac{1}{4}}\left(\frac{N}{32\alpha}\right) = \sqrt{\frac{2\pi}{N}}\left(1 - \frac{3}{N}\,\alpha + \frac{105}{2N^2}\,\alpha^2 + \ldots\right) \ , \tag{2.4.25}$$

where $K_n(x)$ is the modified Bessel function of the second kind. Expanding all three terms in (6.0.34) up to powers of order $\mathcal{O}(1/N^2)$ we find [80]

$$\begin{aligned}\frac{1}{N^2}\mathcal{F}_N(\alpha) = &-\int_0^1 \mathrm{d}x\,(1-x)\,\log\frac{r_0(x,\alpha)}{x} \\ &- \frac{1}{N^2}\left[\int_0^1 \mathrm{d}x\,(1-x)\,\frac{r_2(x,\alpha)}{r_0(x,\alpha)} + \frac{1}{12}\left[(1-x)\log\frac{r_0(x,\alpha)}{x}\right]^{(1)}\Bigg|_0^1 - 3\,\alpha\right] \ .\end{aligned} \tag{2.4.26}$$

Using (2.4.21) both integrals in (6.0.38) can be evaluated analytically. The expression obtained for $\mathcal{F}^{(0)}(\alpha)$ agrees with the re-summed expression in (2.3.45) and

near $\alpha_c = -1/48$ we recover

$$\lim_{\alpha\to\alpha_c} \partial_\alpha^{(3)} \mathcal{F}^{(0)}_{\text{n.a.}}(\alpha) \sim (\alpha - \alpha_c)^{-1/2} + \dots \ . \tag{2.4.27}$$

For $\mathcal{F}^{(1)}(\alpha)$ we obtain

$$\mathcal{F}^{(1)}(\alpha) = \frac{1}{24}\left(\log 4 + \log(1+48\alpha) - 2\log\left(1+\sqrt{1+48\alpha}\right)\right) \ . \tag{2.4.28}$$

Interestingly, in the case of $\mathcal{F}^{(1)}(\alpha)$, the non-analyticity near α_c comes in the form of a logarithm. Finally, a small α expansion leads to

$$\mathcal{F}^{(0)}(\alpha) = 2\alpha - 18\alpha^2 + 288\alpha^3 - 6048\alpha^4 + \frac{746496}{5}\alpha^5 - 4105728\alpha^6 + \mathcal{O}\left(\alpha^7\right) \ , \tag{2.4.29}$$

$$\mathcal{F}^{(1)}(\alpha) = \alpha - 30\alpha^2 + 1056\alpha^3 - 40176\alpha^4 + \frac{8004096}{5}\alpha^5 - 65774592\alpha^6 + \mathcal{O}\left(\alpha^7\right) \ . \tag{2.4.30}$$

In addition to $\mathcal{F}^{(0)}(\alpha)$ and $\mathcal{F}^{(1)}(\alpha)$, we present $\mathcal{F}^{(h)}(\alpha)$ for $h = 2$, 3, and 4 in appendix 6. Their non-analytic behaviour near α_c agrees with the general form (2.3.78).

2.4.3 Full genus expansion & non-perturbative effects

The orthogonal polynomial method allows us to systematically compute non-planar contributions. Near the critical coupling, however, one might expect that only a small piece of the detailed functions $\mathcal{F}^{(h)}(\alpha)$ should matter. To this end, let us revisit equation (6.0.33). Recall that ε is parameterically small at large N, admitting an expansion of the type (6.0.34). We also note from our expressions (2.4.21) and (6.0.1) that if we also take $\alpha \to \alpha_c$, expressions are dominated by the region near $x = 1$. To render the expressions finite near $x = 1$ we must keep $\kappa^{-1} = (\alpha - \alpha_c)^{5/4} N$ fixed as we take $N \to \infty$. This is the double scaling limit we encountered earlier. Thus, we are prompted to study the full equation (6.0.33) in the double scaling limit. If we take

$$x = 1 + (\alpha - \alpha_c) z \ , \quad r(x,\alpha) = r_0(1,\alpha_c) + (\alpha - \alpha_c)^{1/2} \delta r(z) \ , \quad \varepsilon = (\alpha - \alpha_c)^{5/4} \kappa \ , \tag{2.4.31}$$

we can readily show that in the limit $\alpha \to \alpha_c$, and recalling that $\alpha_c = -1/48$, equation (6.0.33) implies

$$\frac{1}{4}\delta r(z)^2 + \frac{\kappa^2}{6}\delta r''(z) + z = 0 \ . \tag{2.4.32}$$

Thus, at least in the double scaling limit, the full genus expansion (2.3.81) is reduced to solving the above Painlevé I equation [102–105]. This is a remarkable simplification of the original problem.

It is worth mentioning some features of the Painlevé I equation. For instance, the Painlevé I equation remains unchanged under the rescaling

$$z \to \lambda z \ , \qquad \delta r(z) \to \lambda^{1/2} \delta r(z) \ , \qquad \kappa \to \lambda^{5/4} \kappa \ . \tag{2.4.33}$$

Given the above scaling symmetry, it only makes sense to build perturbative expansions out of a scale invariant quantity such as $\kappa(-z)^{-5/4}$ rather than, say, small κ. The first few terms of this expansion are given by

$$\delta r_{\pm}(z) = (-z)^{1/2} \left(\pm 2 + \frac{1}{12} \frac{\kappa^2}{(-z)^{5/2}} \mp \frac{49}{576} \frac{\kappa^4}{(-z)^5} + \frac{1225}{3456} \frac{\kappa^6}{(-z)^{15/2}} + \sum_{n=4}^{\infty} a_n^{(\pm)} \frac{\kappa^{2n}}{(-z)^{5n/2}} \right) . \tag{2.4.34}$$

Expanding further, one observes that the coefficients of the negative branch $\delta r_-(z)$ are all positive while those of the positive branch $\delta r_+(z)$ alternate. To specify a solution of the Painlevé I equation, we must pick a set of initial conditions for $\delta r(z)$ and $\delta r'(z)$ at some value of z. Upon fixing half of the initial data, most choices for the remaining data lead to the oscillatory branch $\delta r_+(z)$ [108].

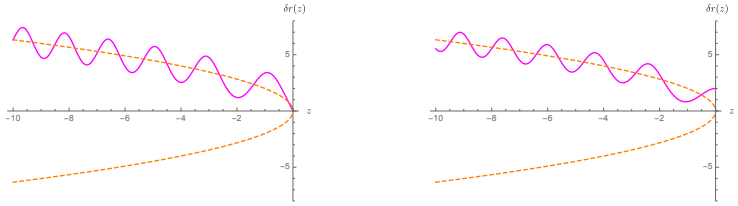

Figure 2.10: *Solutions of the Painlevé equation with $\kappa = 1$. We take the initial conditions $\{\delta r(0), \delta r'(0)\} = \{0, -5\}$ (left) and $\{\delta r(0), \delta r'(0)\} = \{2, 0\}$ (right). The orange dashed lines are $\pm 2\sqrt{-z}$.*

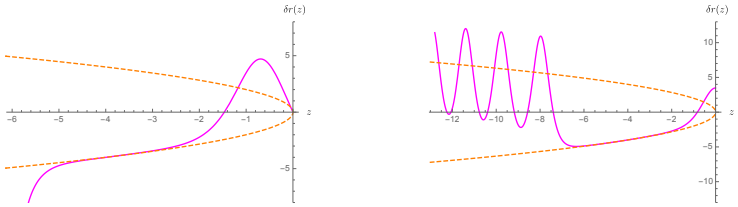

Figure 2.11: *Solutions of the Painlevé equation with $\kappa = 1$. We take the initial conditions $\{\delta r(0), \delta r'(0)\} = \{0, -9.44761388485\}$ (left) and $\{\delta r(0), \delta r'(0)\} = \{3.482113278, 0\}$ (right). The orange dashed lines are $\pm 2\sqrt{-z}$.*

Of the two branches (2.4.34), only the negative branch $\delta r_-(z)$ connects to the double scaling limit stemming from the matrix integral. From now on we focus on this branch. The coefficients for $\delta r_-(z)$ satisfy the recursion relation

$$a_{n+1} = \frac{25n^2-1}{24}\, a_n + \frac{1}{4}\sum_{m=1}^{n} a_m a_{n+1-m} \ , \qquad a_0 = -2 \ , \qquad n \geq 0 \ . \tag{2.4.35}$$

For large n the coefficients above grow as $\sim 5/(4\sqrt{6})\,\Gamma(2n-1/2)$ [100]. This implies that the branch reproducing the perturbative expansion (2.4.34) is not Borel summable [103]. In fact, there is a family of solutions to (2.4.32) containing non-perturbative terms [97, 100] of the type

$$\epsilon(z) = c\left(\frac{-z}{\kappa^{4/5}}\right)^{-1/8} \times e^{-\frac{4}{5\kappa}\sqrt{6}\,(-z)^{5/4}} \ . \tag{2.4.36}$$

This family admits the same perturbative expansion (2.4.34) at large $(-z)^{5/4}/\kappa$. The parameter c is an undetermined integration constant. The form (2.4.36) is obtained by considering a small deviation $\delta r(z) = \delta r_0(z) + \epsilon(z)$ and solving for $\epsilon(z)$ in a WKB approximation. To linear order in $\epsilon(z)$ we have

$$\frac{1}{4}\delta r_0(z)^2 + \frac{\kappa^2}{6}\delta r_0''(z) + z = 0 \ , \qquad \frac{\kappa^2}{6}\epsilon''(z) + \frac{1}{2}\delta r_0(z)\epsilon(z) = 0 \ . \tag{2.4.37}$$

For completeness, we mention that one can also construct a perturbative expansion for solutions near a double pole at $z = z_0$

$$\delta r(z) = -\frac{4}{(z-z_0)^2} + \frac{3z_0}{5}(z-z_0)^2 + (z-z_0)^3 + a_4(z-z_0)^4 - \frac{3z_0^2}{100}(z-z_0)^6 + \dots \ , \tag{2.4.38}$$

where we have set $\kappa = 1$. Both the location of the pole, z_0, as well as the value of a_4 are free parameters.

We now relate $\delta r_-(z)$ to the double scaling limit expression $\mathcal{F}(\kappa)$ introduced in (2.3.81). To do so, we note that in the double scaling limit, the expression (6.0.37) is dominated by

$$\mathcal{F}_N(\alpha) \approx -N^2 \int_0^1 \mathrm{d}x (1-x) \log\frac{r(x,\alpha)}{x} + \cdots \ . \tag{2.4.39}$$

Combining the above expression with (2.4.31) we obtain

$$\begin{aligned}\mathcal{F}(\kappa) &\equiv \lim_{\text{d.s.l.}} \left(\mathcal{F}_N(\alpha) - N^2\mathcal{F}^{(0)}(\alpha)\right) \\ &= \frac{12288\sqrt{3}}{5\kappa^2} + \frac{1}{2\kappa^2}\lim_{\varepsilon\to 0^+}\int_{-(\kappa/\varepsilon)^{4/5}}^{0} \mathrm{d}z z\left(\delta r_-(z) + 2(-z)^{1/2}\right) \ . \end{aligned} \tag{2.4.40}$$

It follows from (2.3.45) that $\mathcal{F}^{(0)}(\alpha_c) = (7/24 - \log 2/2)$. We now recall the perturbative expansion (2.4.34) which is reliable for $(\kappa/\varepsilon)^{4/5} \geq -z \gg \kappa^{4/5}$. Since the first term in the expansion (2.4.34) is κ independent and grows at large z it is convenient to subtract it from $\delta r_-(z)$, as we have done in (2.4.40). It is of interest to see how the perturbative expansion (2.4.34) is encoded in $\mathcal{F}(\kappa)$. We must recall that there is in fact no actual small κ expansion since the scaling symmetry (2.4.33) always allows us to rescale κ. Instead, it is convenient to consider a slightly generalised integral given by

$$\mathcal{F}(\kappa;\eta) \equiv \frac{1}{2\kappa^2}\lim_{\varepsilon\to 0^+}\int_{-(\kappa/\varepsilon)^{4/5}}^{-\eta} \mathrm{d}z\,(z+\eta)\left(\delta r_-(z) + 2(-z)^{1/2}\right) \ . \tag{2.4.41}$$

We have introduced a cutoff at some small value $-\eta \gtrsim \kappa^{4/5}$ to avoid entering a region where the perturbative expansion (2.4.34) is invalidated. We note that $\partial_\eta^2\mathcal{F}(\kappa;\eta) = -\left(\delta r_-(-\eta) + 2\eta^{1/2}\right)/2\kappa^2$. Evaluating $\mathcal{F}(\kappa;\eta)$ in a small $\kappa/\eta^{5/4}$ expansion we find

$$\mathcal{F}(\kappa;\eta) = \frac{1}{24}\left(\log\left(\eta\left(\frac{\varepsilon}{\kappa}\right)^{4/5}\right) + 1\right) - \frac{7\kappa^2}{1440\,\eta^{5/2}} - \frac{245\kappa^4}{41472\,\eta^5} + \dots \ . \tag{2.4.42}$$

We recognise the coefficient of the logarithm from our previous expression (2.4.28).

Double scaling limit for multicritical models

One can perform a similar analysis for the multicritical model introduced in (2.3.51). Using the methods discussed in appendix 6 it is straightforward to derive the equation

$$r_0(x,\boldsymbol{\alpha}) + 3\alpha_2 r_0(x,\boldsymbol{\alpha})^2 + 10\alpha_3 r_0(x,\boldsymbol{\alpha})^3 = x \ . \tag{2.4.43}$$

Crucially however, compared to the quartic matrix integral with a single coupling the double scaling limit for a multicritical matrix integral is far more ambiguous as there are multiple different ways to approach the multicritical point $(-1/9, 1/270)$. As explained more in chapter 3 and in the outlook of this thesis the m^{th} multicritical matrix integral has at least $(m-1)$ distinct ways to approach the multicritical

point. One particularly easy path is parametrised by the path in coupling space

$$\gamma(t) = \begin{pmatrix} -1/9t \\ 1/270t^2 \end{pmatrix} \ , \quad t \in [0,1] \ . \tag{2.4.44}$$

The equation governing $\delta r(z)$ in the double scaling limit reads

$$\delta r(z)^3 - \frac{1}{2}\delta r'(z)^2 - \delta r(z)\delta r''(z) + \frac{1}{10}\delta r^{(4)}(z) - z = 0 \ . \tag{2.4.45}$$

We can solve the above equation in a large z expansion

$$\delta r(z) = z^{1/3}\left(1 + \sum_{n=1}^{\infty} b_k z^{-7n/3}\right) \ , \tag{2.4.46}$$

with the first few terms given by

$$\begin{aligned}\delta r(z) = z^{1/3}\Big(1 - \frac{1}{18}z^{-7/3} - \frac{7}{108}z^{-14/3} - \frac{4199}{17496}z^{-21/3} - \frac{409297}{262440}z^{-28/3} \\ - \frac{101108329}{9447840}z^{-35/3} + \frac{25947984239}{191318760}z^{-42/3} + \dots\Big) \ .\end{aligned} \tag{2.4.47}$$

Expanding further the coefficients of the above expansion are found to be alternating. Contrary to the coefficients (2.4.35) of the Painlevé I equation, the coefficients (2.4.46) of the perturbative expansion of (2.4.45) are Borel summable [100]. Related to this, $\mathcal{M}_N$ (2.3.1) for the polynomial $V(M)$ (2.3.51) is well defined at finite N for all positive γ. Furthermore choosing a different path the coefficients of this expansion change.

It is also interesting to assess whether the above series can admit non-perturbative corrections. Expanding about the $\delta r(z)$ solution given by the large z expansion (2.4.47), we find that to linear order the small deviation $\epsilon(z)$ must satisfy

$$\frac{1}{10}\epsilon^{(4)}(z) - z^{1/3}\epsilon''(z) - \frac{1}{3}z^{-2/3}\epsilon'(z) + 3z^{2/3}\epsilon(z) = 0 \ . \tag{2.4.48}$$

Performing a WKB analysis we obtain $\epsilon(z) \approx c_\pm \, z^{-1/4} \, e^{-\frac{6}{7}\sqrt{5\pm i\sqrt{5}}\, z^{7/6}}$. It is interesting to note that the exponent is now complex. Interestingly, the polynomial governing the eigenvalues, $V(\lambda)$ given in (2.3.51), has no maxima. Rather it has critical points at the complex values $\lambda_\pm^2 = \frac{1}{4}(5 \pm i\sqrt{5})$.

2.4.4 Eigenvalues & instantons

As a final note, we discuss a connection between the non-perturbative corrections of the Painlevé I equation and the original matrix integral (2.3.1). To do so, we

consider configurations for which one (or multiple) of the eigenvalues is sitting outside of the densely filled eigenvalue distribution. Such a configuration will give a subdominant contribution to the matrix integral whose size we will now compute.

For simplicity, we focus on the case where a single eigenvalue $\lambda \equiv \lambda_N$ is separated from the remaining $N-1$ eigenvalues. The matrix integral $\mathcal{M}_N$ can be written in the following form

$$\text{vol}\,\frac{U(1)^N \times S_N}{U(N)}\mathcal{M}_N = \int_{\mathbb{R}} \mathrm{d}\lambda e^{-NV(\lambda)} \int_{\mathbb{R}^{N-1}} \prod_{I=1}^{N-1} \mathrm{d}\mu_I \Delta_{N-1}(\mu)^2\, e^{-N\sum_{I=1}^{N-1} V(\mu_I)} \times \prod_{I=1}^{N-1} (\lambda-\mu_I)^2 \ , \quad (2.4.49)$$

where the expectation value is defined in (2.3.53). We define the effective polynomial

$$V_{\text{eff}}(\lambda) \equiv V(\lambda) - \frac{1}{N}\left\langle \text{Tr}\log\left(\lambda\,\mathbb{I}_{N-1} - M_{N-1}\right)^2 \right\rangle \ , \quad (2.4.50)$$

which is the leading order correction of the polynomial $V(\lambda)$ in the large N limit. Explicitly, assuming that $\mathcal{M}_N$ admits a single cut eigenvalue density $\rho(\lambda)$ symmetric about the origin, we find

$$V_{\text{eff}}(\lambda) = V(\lambda) - \int_{-a}^{a} \mathrm{d}\mu\, \rho(\mu) \log(\lambda-\mu)^2 \ , \quad (2.4.51)$$

to leading order in the large N limit. It follows from (2.3.16) that within the range $\lambda \in (-a,a)$, $V_{\text{eff}}(\lambda)$ must be a constant V_0 given by

$$V_0 \equiv V(0) - \int_{-a}^{a} \mathrm{d}\mu\, \rho(\mu) \log \mu^2 \ . \quad (2.4.52)$$

The effective polynomial ceases to be constant for $\lambda^2 > a^2$. To leading order in the large N limit, the piece of the integral pertinent to the separated eigenvalue is given by

$$\mathcal{I}_N \equiv \int_{\mathbb{R}} \mathrm{d}\lambda\, e^{-NV_{\text{eff}}(\lambda)} = 2a\, e^{-NV_0}\left(1 + \frac{1}{2a}\int_{\lambda\notin[-a,a]} \mathrm{d}\lambda\, e^{-N(V_{\text{eff}}(\lambda)-V_0)}\right) . \quad (2.4.53)$$

The critical points of $V_{\text{eff}}(\lambda)$ for $\lambda^2 > a^2$ can be found by solving

$$V'_{\text{eff}}(\lambda) = \text{sign}\,\lambda\, \text{Re}\sqrt{V'(\lambda)^2 - 4\mathcal{P}(\lambda)} = 0 \ , \quad (2.4.54)$$

where $\mathcal{P}(\lambda)$ is defined in (2.3.61).

At large N we can apply the saddle point approximation to the integral in (2.4.53), which requires evaluating its exponent at its critical points. We are interested in contributions that stem from a single eigenvalue sitting at a critical point outside the interval containing the dense set of remaining $N-1$ eigenvalues. These contributions can lead to corrections which are exponentially suppressed in N. Consequently they do not contribute to the perturbative $1/N$ expansion – they are non-perturbative. In certain contexts, such suppressed configurations bear the name instantons.

Example. As a concrete example, we consider the quartic polynomial (2.3.35). Taking $\alpha \in (\alpha_c, 0)$, we find the following two maxima for the effective polynomial:

$$\lambda_\pm = \pm\sqrt{-\frac{1}{6\alpha} - \frac{\sqrt{1+48\alpha}}{12\alpha}} \ . \tag{2.4.55}$$

For $\lambda \in (-a_+, a_+)$, with a_+ given in (2.3.38) and the eigenvalue density in (2.3.39), we find

$$V_0 = -\frac{1}{48\alpha} + \frac{\sqrt{1+48\alpha} + 24\alpha\left(1 + \log 576 - 2\log\frac{\sqrt{1+48\alpha}-1}{\alpha}\right)}{48\alpha} \ . \tag{2.4.56}$$

Evaluating $V_{\text{eff}}(\lambda)$ at $\lambda = \lambda_\pm$ one finds

$$V_{\text{eff}}(\lambda_\pm) - V_0 = \sqrt{3}\frac{\sqrt{2+\sqrt{y}}}{(1-y)}\, y^{1/4} - 2\,\text{Re}\left(\text{arctanh}\frac{\sqrt{2+\sqrt{y}}}{\sqrt{3}y^{1/4}}\right) \ , \tag{2.4.57}$$

where we have defined $y \equiv 1 - \alpha/\alpha_c$. A small y expansion reveals

$$V_{\text{eff}}(\lambda_\pm) - V_0 = \frac{4}{5}\sqrt{6}\, y^{5/4} + \frac{2}{7}\sqrt{\frac{3}{2}}\, y^{7/4} + \dots \ . \tag{2.4.58}$$

Interestingly, in the double scaling limit, where N is taken to infinity while keeping $Ny^{5/4}$ fixed, the leading term in the above expansion gives a contribution to (2.4.53) that remains finite [100]. The correction is reminiscent of the non-perturbative correction (2.4.36) found in our discussion of the Painlevé I equation.

2.5 Large N integrals over two matrices

In this section we will generalize the one matrix integral (2.3.1) to an integral involving two $N \times N$ Hermitian matrices A and B

$$\mathcal{T}_N(c) = \int_{\mathbb{R}^{2N^2}} [\mathrm{d}A]\,[\mathrm{d}B]\, e^{-N\,\mathrm{Tr}\,(V(A)+V(B)-2\,c\,A\,B)} \,. \tag{2.5.1}$$

$V(A)$ and $V(B)$ are two polynomials and $c \in \mathbb{R}$. The measures $[\mathrm{d}A]$ and $[\mathrm{d}B]$ are as in (2.3.2). Part of the motivation for studying such models is that they will form an interesting bridge between the quantum mechanical models explored in later sections and the matrix integrals explored so far. We note that the integral is invariant under a single $U(N)$ transformation that rotates both A and B concurrently. Given that we have two matrices and only a single $U(N)$ symmetry, the eigenvalue decomposition is slightly more involved.

2.5.1 Eigenvalue decomposition

Following an approach inspired by that pursued in section 2.3, we parameterise A and B in terms of their eigenvalues

$$A = \mathcal{U}_A D_A \mathcal{U}_A^\dagger \,, \qquad D_A = \mathrm{diag}(a_1, \ldots, a_N) \,, \tag{2.5.2}$$

and similarly for B. Recalling the discussion in subsection 2.3.1, the matrices $\mathcal{U}_A$ and $\mathcal{U}_B$ are general elements of $U(N)/U(1)^N$. Integrating over the angular variables in (2.5.1) leads to

$$\mathcal{T}_N(c) = \mathrm{vol}\,\frac{U(N)}{U(1)^N \times S_N} \int_{\mathbb{R}^{2N}} \prod_{I=1}^{N} \mathrm{d}a_I\,\mathrm{d}b_I\,\Delta_N(a)^2\Delta_N(b)^2\, e^{-N\sum_{I=1}^{N}(V(a_I)+V(b_I))} I(a,b,c) \,, \tag{2.5.3}$$

where $I(a,b,c)$ is known as the Harish-Chandra-Itzykson-Zuber (HCIZ) integral

$$I(a,b,c) \equiv \frac{1}{\mathrm{vol}\,S_N} \int [\mathrm{d}\mathcal{L}]\, e^{2cN\,\mathrm{Tr}\,D_A\mathcal{U}D_B\mathcal{U}^\dagger} \,, \qquad \mathcal{U} \equiv \mathcal{U}_A^\dagger \mathcal{U}_B \,. \tag{2.5.4}$$

The integral $I(a,b,c)$ evaluates to [122]

$$I(a,b,c) = \mathrm{vol}\,\frac{U(N)}{U(1)^N \times S_N}\,\frac{G(N+1)}{(2cN)^{N(N-1)/2}}\,\frac{\det\left(e^{2cNa_Ib_J}\right)_{1\le I,J\le N}}{\Delta_N(a)\Delta_N(b)} \,, \tag{2.5.5}$$

where $G(N+1) = \prod_{K=1}^{N-1} K!$ denotes Barnes G-function. Finally, using the Leibniz formula for the determinant we obtain for a measure $\mathrm{d}\tilde{\mu}(a,b)$ completely anti-

symmetric under $a_I \leftrightarrow a_J$ and $b_I \leftrightarrow b_J$

$$\int \mathrm{d}\tilde{\mu}(a,b)\,\det\left(e^{2cNa_Ib_J}\right)_{1\le I,J\le N} = \mathrm{vol}\,S_N \int \mathrm{d}\tilde{\mu}(a,b)\,e^{2cN\sum_{I=1}^N a_Ib_I}\ . \tag{2.5.6}$$

We can thus write (2.5.3) as

$$\begin{aligned}&\mathcal{T}_N(c)\\ &= \left(\mathrm{vol}\,\frac{U(N)}{U(1)^N}\right)^2 \frac{G(N+1)}{\mathrm{vol}\,S_N}\int\prod_{I=1}^N \mathrm{d}a_I\mathrm{d}b_I\,\frac{\Delta_N(a)\Delta_N(b)}{(2cN)^{N(N-1)/2}}\,e^{-N\sum_I (V(a_I)+V(b_I)-2\,c\,a_Ib_I)}\ ,\end{aligned} \tag{2.5.7}$$

The above expression resembles the single matrix expression (2.3.12). However, it has some differences such as the Vandermonde determinant for each collection of eigenvalues appearing with a single power.

HCIZ integral for $N = 2$. As a simple example, we consider the case $N = 2$. We note that $[d\mathcal{L}]$ is the line element on the sphere

$$\mathrm{d}s^2 = \frac{1}{2}(\mathrm{d}\theta^2 + \sin\theta^2\mathrm{d}\phi^2)\ . \tag{2.5.8}$$

The HCIZ integral for $N = 2$ is thus equal to

$$\begin{aligned} I(a,b,c) &= \frac{1}{4}\int_0^{2\pi}\mathrm{d}\phi\int_0^{\pi}\mathrm{d}\theta\sin\theta\,e^{4c\left(\sin^2\frac{\theta}{2}(a_1b_1+a_2b_2)+\cos^2\frac{\theta}{2}(a_1b_2+a_2b_1)\right)}\\ &= \frac{\pi}{4c}\,\frac{1}{\Delta_2(a)\Delta_2(b)}\,\det\begin{pmatrix}e^{4c\,a_1b_1} & e^{4c\,a_1b_2}\\ e^{4c\,a_2b_1} & e^{4c\,a_2b_2}\end{pmatrix}\ ,\end{aligned} \tag{2.5.9}$$

confirming (2.5.5) for $N = 2$.

2.5.2 Orthogonal polynomials & the quartic polynomial

Having reached the expression (2.5.7), we can proceed to use the techniques developed in the previous to solve the integral at large N. One approach is to introduce an eigenvalue density for the a_I and b_I eigenvalues and study a generalisation of the loop equations introduced in section 2.3.4 for multi-matrix models [92, 93]. Here, we will consider the orthogonal polynomial approach. We take $V(a)$ and $V(b)$ to be the quartic polynomial previously considered in the single matrix case (2.3.35). Thus, we would like to solve

$$\mathcal{T}_N(\alpha,c) = \mathcal{C}_N\int_{\mathbb{R}^{2N}}\prod_{I=1}^N \mathrm{d}a_I\,\mathrm{d}b_I\,\Delta_N(a)\Delta_N(b)\,e^{-N\sum_{I=1}^N W(a_I,b_I)}\ , \tag{2.5.10}$$

with

$$W(a,b) = \frac{1}{2}(a^2+b^2) + \alpha(a^4+b^4) - 2c\,a\,b\ , \quad c^2 \in (0,1/4)\ . \tag{2.5.11}$$

We have absorbed the volume pre-factors into an N-dependent constant $\mathcal{C}_N$. It is worth reiterating that the Vandermonde for each set of eigenvalues only appears linearly in (2.5.10).

At this stage we introduce a set of monic polynomials $Q_n(x)$, with $x \in \mathbb{R}$, subject to the condition $Q_n(-x) = (-1)^n Q_n(x)$. A priori we should have introduced two different sets of monic polynomials for the eigenvalues of A and B respectively. However due to the symmetry of $W(a,b)$ under interchanging these eigenvalues we can choose the same set of monic polynomials. Orthogonality of the $Q_n(x)$ is expressed as

$$\int_{\mathbb{R}^2} \mathrm{d}\mu(a,b)\, Q_n(a) Q_m(b) = k_n(\alpha,c)\delta_{mn}\ , \qquad \mathrm{d}\mu(a,b) \equiv \mathrm{d}a\,\mathrm{d}b\, e^{-NW(a,b)}\ , \tag{2.5.12}$$

and the three-term recurrence relation is given by

$$x\, Q_n(x) = Q_{n+1}(x) + R_n\, Q_{n-1}(x) + S_n\, Q_{n-3}(x)\ . \tag{2.5.13}$$

Notice that for the two-matrix model we have to introduce an additional variable S_n. We can only choose a polynomial that has the same parity as $xQ_n(x)$ under $x \leftrightarrow -x$ since we have an even measure. Thus, we exclude $Q_n(x)$ and $Q_{n-2}(x)$. Following the same steps leading to (2.4.12) we rewrite (2.5.10) as

$$\mathcal{T}_N(\alpha,c) = \mathcal{C}_N N! \prod_{n=0}^{N-1} k_n(\alpha,c)\ . \tag{2.5.14}$$

Combining orthogonality and the three-term recurrence relation we obtain, using an integration by parts, three independent equations for the three unknowns k_n, R_n and S_n

$$\int_{\mathbb{R}^2} \mathrm{d}\mu(a,b)\, Q_{n-1}(a) Q_n(b) \partial_a W(a,b) = 0\ , \tag{2.5.15}$$

$$\int_{\mathbb{R}^2} \mathrm{d}\mu(a,b)\, Q_n(a) Q_{n-1}(b) \partial_a W(a,b) = \frac{n}{N} k_{n-1}(\alpha,c)\ , \tag{2.5.16}$$

$$\int_{\mathbb{R}^2} \mathrm{d}\mu(a,b)\, Q_{n-3}(a) Q_n(b) \partial_a W(a,b) = 0\ . \tag{2.5.17}$$

Solving the three integrals on the left hand side is straightforward. The only slightly more difficult one is the second integral where we have to apply the three-

term recurrence relation multiple times. It is now convenient to define $z_n(\alpha, c) \equiv 2\alpha k_n(\alpha, c)/(ck_{n-1}(\alpha, c))$ for $\alpha \neq 0$ and $z_n(0, c) \equiv 2k_n(0, c)/(ck_{n-1}(0, c))$ for $\alpha = 0$. For $\alpha \neq 0$, the above three equations then imply

$$z_n(\alpha, c) = 4\alpha\, R_n(\alpha, c)\left(1 + 4\alpha\Big(R_{n+1}(\alpha, c) + R_n(\alpha, c) + R_{n-1}(\alpha, c)\Big)\right)^{-1} , \tag{2.5.18}$$

$$\begin{aligned} z_n(\alpha, c) = {} & \frac{\alpha}{c^2}\, R_n(\alpha, c)\left(1 + 4\alpha\Big(R_{n+1}(\alpha, c) + R_n(\alpha, c) + R_{n-1}(\alpha, c)\Big)\right) \\ & + \frac{4\alpha^2}{c^2}\Big(S_{n+2}(\alpha, c) + S_{n+1}(\alpha, c) + S_n(\alpha, c)\Big) - \frac{\alpha}{c^2}\frac{n}{N} , \end{aligned} \tag{2.5.19}$$

and

$$z_n(\alpha, c) z_{n-1}(\alpha, c) z_{n-2}(\alpha, c) = \frac{4\alpha^2}{c^2} S_n(\alpha, c) . \tag{2.5.20}$$

For $\alpha = 0$ the three equations become

$$z_n(0, c) = 4R_n(0, c) , \quad c^2 z_n(0, c) = R_n(0, c) - \frac{n}{N} , \quad S_n(0, c) = 0 . \tag{2.5.21}$$

Upon introducing $\varepsilon = 1/N$ and $x = n\varepsilon$, at large N we can express $z_n(\alpha, c)$, $R_n(\alpha, c)$, and $S_n(\alpha, c)$ in terms of continuous functions

$$z_n(\alpha, c) \equiv z(x, \alpha, c), \qquad R_n(\alpha, c) \equiv r(x, \alpha, c), \qquad S_{n+1}(\alpha, c) \equiv s(x, \alpha, c) . \tag{2.5.22}$$

To leading order in a small ε-expansion the expressions (2.5.18), (2.5.19), and (2.5.20) are given by

$$z(x, \alpha, c) = 4\alpha\, r(x, \alpha, c)\,(1 + 12\alpha\, r(x, \alpha, c))^{-1} , \tag{2.5.23}$$

$$z(x, \alpha, c) = \frac{\alpha}{c^2}\, r(x, \alpha, c)\big(1 + 12\alpha\, r(x, \alpha, c)\big) + \frac{12\alpha^2}{c^2} s(x, \alpha, c) - \frac{\alpha x}{c^2} \tag{2.5.24}$$

$$z(x, \alpha, c)^3 = \frac{4\alpha^2}{c^2}\, s(x, \alpha, c) . \tag{2.5.25}$$

Eliminating $r(x, \alpha, c)$ and $s(x, \alpha, c)$ in the above equations we find the following expressions

$$\frac{\omega(z(x, \alpha, c))}{(1 - 3z(x, \alpha, c))^2} = 0 \qquad \text{and} \qquad z(x, 0, c) = \frac{4x}{(1 - 4c^2)} , \tag{2.5.26}$$

where we have defined

$$\omega(z) \equiv -108c^2 z^5 + 72c^2 z^4 + 24c^2 z^3 + 3(12\alpha x - 8c^2) z^2 - (24\alpha x - 4c^2 + 1) z + 4\alpha x . \tag{2.5.27}$$

We have thus boiled down the large N approximation of our problem to solving a quintic polynomial. Generally speaking, quintic polynomials do not admit simple solutions. Nevertheless, for certain special values of α and c the quintic of interest (2.5.27) admits simple solutions. These turn out to encode a certain critical behaviour in the planar approximation. For instance, when

$$\alpha_1 x = \frac{1}{9}\left(\sqrt{2c}+3c-2c^2\right)\ , \quad \alpha_2 x = -\frac{1}{9}\left(\sqrt{2c}-3c+2c^2\right)\ , \quad \alpha_3 x = -\frac{1}{48}\left(1-\frac{32c^2}{3}\right)\ ,$$
$$\alpha_4 x = \frac{1}{9}\left(\sqrt{-2c}-3c-2c^2\right)\ , \quad \alpha_5 x = -\frac{1}{9}\left(\sqrt{-2c}+3c+2c^2\right)\ . \tag{2.5.28}$$

the discriminant of the quintic (2.5.27) vanishes. Consequently, $\omega(z)$ shares a zero with its derivative $\omega'(z)$. For $\alpha_2 x$ and $\alpha_4 x$ the discriminant of $\omega'(z)$, which now is a polynomial in c, vanishes provided $c = \pm 1/8$. A quartic polynomial with a vanishing discriminant contains a multiple root, which for the specific case of $\omega'(z)$ lies at $z = -1/3$. It can be easily checked that (2.5.27) at $c = \pm 1/8$ and $\alpha x = -5/288$ can be written as

$$\omega(z) = -\frac{3}{16}\left(z+\frac{1}{3}\right)^3 (9z^2-15z+10)\ . \tag{2.5.29}$$

To identify the non-analytic structure of interest, it is enough to solve (2.5.26) with $c = \pm 1/8$, in a small $\delta = (\alpha x + 5/288)$ expansion about the $z = -1/3$ solution. To leading order we find

$$z(x,\alpha,\pm 1/8) = -\frac{1}{3}+\frac{1}{3}\sqrt[3]{\frac{5}{6}}\sqrt[3]{1+\frac{288}{5}\alpha x}+\dots\ . \tag{2.5.30}$$

The above expansion exhibits the leading non-analyticity we were after. Away from $c = \pm 1/8$ the quintic (2.5.27) has at most a second order zero leading to a different non-analytic structure more akin to that of the single matrix case.

Planar contribution. As for the study of single matrix integrals, we can apply the orthogonal polynomial technique to evaluate $\mathcal{G}_N(\alpha,c) \equiv -\log \mathcal{T}_N(\alpha,c)/\mathcal{T}_N(0,c)$ in a systematic large N expansion. Here $\mathcal{T}_N(\alpha,c)$ is obtained from (2.5.14) in the same way that (2.4.12) was obtained for the single matrix integral:

$$\mathcal{T}_N(\alpha,c) = \mathcal{C}_N N! \left(\frac{c}{2\alpha}\right)^{N(N-1)/2} k_0^N\, z_1^{N-1} z_2^{N-2}\cdots z_{N-1}\ . \tag{2.5.31}$$

Performing steps analogous to those leading to (6.0.31) and combining the resulting expression for $\mathcal{G}_N(\alpha,c)$ with the Euler-Maclaurin formula (6.0.35) results in the

expression

$$\frac{1}{N^2}\,\mathcal{G}_N(\alpha,c) = -\int_0^1 \mathrm{d}x\,(1-x)\log\frac{z(x,\alpha,c)}{z(x,0,c)} + \frac{1}{2}\log\alpha + \mathcal{O}\left(N^{-2}\right)\ . \tag{2.5.32}$$

Evaluating (2.5.32) for $c = \pm 1/8$ by using the expansion (2.5.30), we conclude that the non-analytic behaviour is given by

$$\lim_{\alpha\to\alpha_c}\partial_\alpha^{(3)}\mathcal{G}^{(0)}_{\text{n.a.}}(\alpha,\pm 1/8) \sim (\alpha-\alpha_c)^{-2/3}\ , \tag{2.5.33}$$

where we recall the critical value $\alpha_c = -5/288$.

Non-planar contributions. One can continue along these lines and calculate non-planar contributions. As for the single matrix case, one can argue that the non-analytic structure of the non-planar contributions takes the form

$$\lim_{\alpha\to\alpha_c}\mathcal{G}^{(h)}_{\text{n.a.}} = g_h\,(\alpha-\alpha_c)^{7\chi_h/6}\ , \qquad h\in\mathbb{N}\ , \tag{2.5.34}$$

where the $h = 1$ case is understood to be logarithmic. Near criticality, the essential difference [16, 56, 118] from the single matrix case (2.3.78) is that the critical exponent is now $7/6$ instead of $5/4$.

Double scaling limit. As for the single matrix mode, one can consider a double scaling limit in which the combination $\kappa^{-1} = N\,(\alpha-\alpha_c)^{7/6}$ is kept fixed as N tends to infinity. Though we do not provide the details, it is worth mentioning that the Painlevé I equation (2.4.32) uncovered in the double scaling limit of the single matrix model has an avatar for the two-matrix case under consideration. For the curious reader, we state that the analogous equation can be put in the following form [109, 110, 112]

$$\delta r(z)^3 - \delta r(z)\delta r''(z) - \frac{1}{2}\delta r'(z)^2 + \frac{2}{27}\,\delta r^{(4)}(z) - z = 0\ . \tag{2.5.35}$$

The assymptotic expansion is given by [100]

$$\delta r(z) = z^{1/3}\left(1+\sum_{n=1}^{\infty}a_k z^{-7n/3}\right)\ , \tag{2.5.36}$$

where the first few coefficients are given by

$$\delta r(z) = z^{1/3}\Big(1-\frac{1}{18}\,z^{-7/3} - \frac{1925}{26244}\,z^{-14/3} - \frac{509575}{1417176}\,z^{-21/3} - \frac{445712575}{114791256}\,z^{-28/3} + \dots\Big)\ . \tag{2.5.37}$$

As for the single-matrix case, the above expansion admits non-perturbative corrections of the type

$$\epsilon(z) = c_1\, z^{-1/4}\, e^{-\frac{18}{7} z^{7/6}} + c_2\, z^{-1/4}\, e^{-\frac{9\sqrt{2}}{7} z^{7/6}} \ . \tag{2.5.38}$$

We note that the integration constants can not be fixed by the WKB analysis. The appearance of multiple solutions has been discussed in [101].

2.5.3 A diagrammatic expansion: decorated Riemann surfaces

As a final note, we consider how the perturbative expansion in the 't Hooft limit is modified due to the appearance of a second matrix. Taking into account that the quadratic part of the exponent in the integral (2.5.1) contains a mixed term, we have the following set of propagators

$$\langle A_{IK} B_{JL} \rangle = \frac{2c}{N(1-4c^2)}\, \delta_{IL}\delta_{JK} \ , \quad \langle A_{IK} A_{JL} \rangle = \langle B_{IK} B_{JL} \rangle = \frac{1}{N(1-4c^2)}\, \delta_{IL}\delta_{JK} \ . \tag{2.5.39}$$

Thus, we have additional structure at each face indicating whether it has edges built from AA, BB or AB type propagators

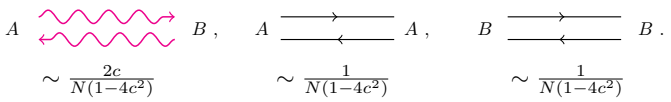

Figure 2.12: *Various propagators in the two-matrix model.*

We might envision a continuum limit in which the vertices densely fill the discretised Riemann surface. In such a situation, the additional structure at the vertices may be viewed as an additional field taking two values living on each vertex of the continuous surface. More generally, we could have added an additional coupling weighting the two quartic vertices differently. This would generalise (2.5.11) to

$$W(a,b) = \frac{1}{2}(a^2+b^2) + \alpha(g\, a^4 + g^{-1}\, b^4) - 2c\, a\, b \ , \tag{2.5.40}$$

where $g > 0$ parametrises the relative weight of the A and B vertices.

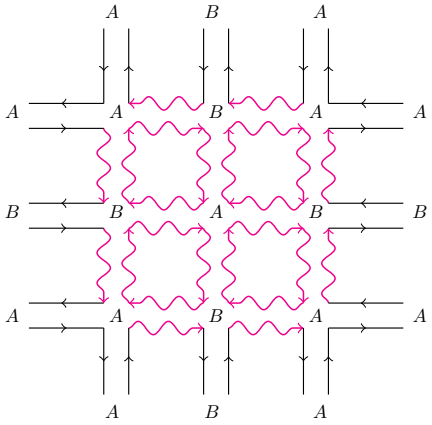

Figure 2.13: *Piece of a planar diagram in the two-matrix model.*

At this stage, we have no immediate reason to suspect that such a two-dimensional field theory is itself local. Nevertheless, and somewhat remarkably, we will discuss evidence for this in section 2.8 where we will also provide an interpretation for the three couplings in (2.5.40), namely α, c, and g.

***

Adding more matrices further decorates the Feynman diagrams. One might imagine a limit where we have an infinite chain of matrices such that they effectively carry a continuous label t. We will now consider precisely such a situation.

2.6 Quantum mechanical matrices

In the previous sections, we considered certain classes of integrals in the limit of a large number of variables. In this section we will consider the quantum mechanical generalisation of those integrals over a single matrix. The original $\mathbb{C}$-number elements of our $N \times N$ Hermitian matrices will be promoted to operators acting on a Hilbert space, and the matrix integral will be naturally replaced by a matrix path integral. Our most important goal in this section will be to characterise the ground state for such systems.

2.6.1 Action and Hamiltonian

We begin by introducing the following class of classical actions

$$S_N[M(t)] = N \,\mathrm{Tr} \int \mathrm{d}t \left(\frac{1}{2} \dot{M}(t)^2 - V(M(t)) \right) \,. \tag{2.6.1}$$

Here, $V(M(t))$ is a polynomial potential governing the $N \times N$ Hermitian matrix valued path $M(t)$, and the dot denotes a derivative with respect to time. We can view the above as a class of classical theories comprising N^2 degrees of freedom whose dynamical features are governed by the potential $V(M(t))$. Quantum mechanical transition amplitudes are given by the Feynman path integral

$$\mathcal{A}_N(M_f, M_i) = \int \mathcal{D}M(t)\, e^{\frac{i}{\hbar} S_N[M(t)]} \ , \tag{2.6.2}$$

with boundary conditions $M(t_i) = M_i$ and $M(t_f) = M_f$, and our measure is now given by

$$\mathcal{D}M(t) \equiv \prod_{t \in \mathbb{R}} [\mathrm{d}M(t)] \ . \tag{2.6.3}$$

The path integral (2.6.2) serves as the quantum mechanical generalisation of the matrix integrals previously explored.

As for the ordinary matrix integrals, we can exploit the global $U(N)$ symmetry of (2.6.1) by parametrising $M(t)$ as

$$M(t) \to \mathcal{U}(t)\, D_M(t)\, \mathcal{U}(t)^\dagger \ , \qquad D_M(t) = \mathrm{diag}(\lambda_1(t), \lambda_2(t), ..., \lambda_N(t)) \ . \tag{2.6.4}$$

Here, $\mathcal{U}(t)$ is a time dependent element of $U(N)/U(1)^N$, and the $\lambda_I(t)$ are the real valued time dependent eigenvalues of $M(t)$. Under (2.6.4) the kinetic term in the action (2.6.1) is expressed as

$$\mathrm{Tr}\, \dot{M}(t)^2 = \mathrm{Tr}\, \dot{D}_M(t)^2 + \mathrm{Tr}[D_M(t), \dot{\mathcal{U}}(t)\mathcal{U}(t)^\dagger]^2 \ . \tag{2.6.5}$$

We note that $\dot{\mathcal{U}}(t)\,\mathcal{U}(t)^\dagger$ is again a Hermitian matrix which can be expressed as

$$\dot{\mathcal{U}}(t)\,\mathcal{U}(t)^\dagger = \frac{i}{\sqrt{2}} \sum_{a=1}^{N(N-1)/2} \left(T_a^S\, \dot{\beta}_a(t) + T_a^A\, \dot{\gamma}_a(t) \right) \ , \tag{2.6.6}$$

where T_a^S and T_a^A are a basis of real symmetric, and pure imaginary antisymmetric $N \times N$ generators of $U(N)/U(1)^N$, with normalisation $\mathrm{Tr}\, T_a^\epsilon T_b^{\epsilon'} = \delta_{ab}\, \delta^{\epsilon\epsilon'}$ with $\epsilon, \epsilon' \in \{S, A\}$. Thus,

$$\mathrm{Tr}\, \dot{M}^2 = \mathrm{Tr}\, \dot{D}_M^2 + \frac{1}{2} \sum_{I<J} (\lambda_I - \lambda_J)^2 (\dot{\beta}_{IJ}^2 + \dot{\gamma}_{IJ}^2) \ , \tag{2.6.7}$$

where for notational convenience we suppressed the explicit time dependence, β_{IJ} are the matrix elements of $\sum_a T_a^S\, \dot{\beta}_a$ and analogously γ_{IJ} the matrix elements of $\sum_a T_a^A\, \dot{\gamma}_a$.

Turning to the Hamiltonian formalism, we calculate the canonical momenta for λ, β_{IJ} and γ_{IJ} respectively:

$$\pi_I = N\dot{\lambda}_I, \qquad \pi_{IJ} = \frac{N}{2}(\lambda_I - \lambda_J)^2\,\dot{\beta}_{IJ}\ , \qquad \tilde{\pi}_{IJ} = \frac{N}{2}\,(\lambda_I - \lambda_J)^2\,\dot{\gamma}_{IJ}\ . \quad (2.6.8)$$

From these, we can construct the classical Hamiltonian

$$H = \sum_{I=1}^{N}\left(\frac{1}{2N}\,\pi_I^2 + NV(\lambda_I)\right) + \frac{1}{N}\sum_{I<J}\frac{\pi_{IJ}^2 + \tilde{\pi}_{IJ}^2}{(\lambda_I - \lambda_J)^2}\ . \quad (2.6.9)$$

At the classical level, the lowest energy configuration lies at the minimum of $V(\lambda_I)$ with all classical momenta vanishing. As we shall soon see, the quantum mechanical ground state differs considerably from its classical counterpart.

2.6.2 Quantisation & free fermions

It is straightforward to promote (2.6.9) to a quantum Hamiltonian. Recall that in the eigenvalue basis (2.6.4), the N^2 degrees of freedom are living on a curved space. Moreover, this curved space is merely a coordinate transformation of the flat metric on $\mathbb{R}^{N^2}$. Consequently, the quantum kinetic term is nothing other than the Laplace-Beltrami differential operator associated to our curved space. The quantum version of the Hamiltonian in (2.6.9) is consequently given by

$$\hat{H} = \sum_{I=1}^{N}\left(-\frac{1}{2N}\frac{1}{\Delta_N(\lambda)}\frac{\partial^2}{\partial\lambda_I^2}\,\Delta_N(\lambda) + NV(\lambda_I)\right) + \frac{1}{N}\sum_{I<J}\frac{\hat{\pi}_{IJ}^2 + \hat{\tilde{\pi}}_{IJ}^2}{(\lambda_I - \lambda_J)^2}\ , \quad (2.6.10)$$

where we have explicitly written the eigenvalue dependence for the Laplacian, we are working in units for which $\hbar = 1$ and $\Delta_N(\lambda)$ is the determinant of the Vandermonde matrix introduced in (2.3.11). The angular part in (2.6.10) describes the motion on the compact coset space $U(N)/U(1)^N$.[2] Due to the compactness of the coset space, the eigenfunctions of H can be annihilated by $\hat{\pi}_{IJ}$ and $\hat{\tilde{\pi}}_{IJ}$ whilst retaining normalisability. Thus, it is natural to study wavefunctions $\Psi(\lambda_I)$ that are functions only of the eigenvalues, but not the coordinates on the compact coset space $U(N)/U(1)^N$. Acting on such wavefunctions, the Hamiltonian is reduced to

$$\hat{H} = \sum_{I=1}^{N}\left(-\frac{1}{2N}\frac{1}{\Delta_N(\lambda)}\frac{\partial^2}{\partial\lambda_I^2}\,\Delta_N(\lambda) + NV(\lambda_I)\right)\ . \quad (2.6.11)$$

[2]It is worth mentioning that for certain values of $\hat{\pi}_{IJ}$ and $\hat{\tilde{\pi}}_{IJ}$ the above Hamiltonian is of the form of a Calogero model [139, 140].

A subsequent redefinition of the wavefunctions

$$\Psi(\lambda_1, \ldots, \lambda_N) = \frac{\psi(\lambda_1, \ldots, \lambda_N)}{\Delta_N(\lambda)} \ , \tag{2.6.12}$$

leads to a Hamiltonian with standard kinetic term. Thus, we have reduced our eigenvalue problem to the following single particle problem

$$\left(-\frac{1}{2N} \frac{\partial^2}{\partial \lambda^2} + NV(\lambda) \right) \psi_{\varepsilon_n}(\lambda) = N\varepsilon_n \psi_{\varepsilon_n}(\lambda) \ , \qquad n = 1, 2, \ldots, N \ . \tag{2.6.13}$$

Recall that $\Delta_N(\lambda)$ is antisymmetric under exchange of any two eigenvalues λ_I. It then follows from (2.6.12) that a general state Ψ invariant under the permutation subgroup $S_N \subset U(N)$ enforces the rescaled wavefunction ψ to be an *anti-symmetric* function of the λ_I. In particular, the problem has been reduced to solving a system of N free particles subject to the Pauli exclusion principle [25]. It is already clear at this stage that the quantum mechanical state, particularly at large N, differs substantially from its classical counterpart. In other words, quantum effects play a dominant role in the description of the system.

The ground state of the matrix quantum mechanical systems is described by N free fermions, each governed by the potential $V(\lambda)$. The fermions fill up the first N energy levels, all the way up to the Fermi level $\varepsilon_F \equiv \varepsilon_N$. We will be interested in small energy excitations or ripples above the filled Fermi sea. Rather generally, in the large N limit, the low energy physics near a filled Fermi sea has a linear dispersion relation in two-dimensions [133].

2.6.3 Non-analyticity & the inverted harmonic oscillator

We now assume that the potential has a maximum at some value of λ. Recall that in our study of ordinary matrix integrals, we uncovered non-analytic behaviour for particular choices of the polynomial $V(\lambda)$. For instance, for $V_\alpha(\lambda) = \lambda^2/2 + \alpha\lambda^4$ we uncovered non-analytic behaviour for a negative value of $\alpha = \alpha_c < 0$. For negative values of α, $V_\alpha(\lambda)$ contains a maximum. Thus, in tuning the value of α beyond α_c, the confining effect of the quadratic term in the Lagrangian will no longer be strong enough to compete with the repulsion of eigenvalues from both the Vandermonde and the quartic contribution to $V_\alpha(\lambda)$. Recall further that for the matrix integrals the non-analyticities were important in obtaining a continuum limit with a divergent number of vertices in the discretised Riemann surface.

It is natural, then, to ask what kind of non-analyticities might we expect from the free fermions stemming from quantum mechanical matrices? As a simple test

observable, we can consider the Fermi energy for a potential given by

$$V(\lambda) = \frac{1}{2}\gamma^2\lambda^2 - \alpha\lambda^4 \ . \tag{2.6.14}$$

We have maxima at $\lambda_\pm = \pm\gamma\,(2\sqrt{\alpha})^{-1}$, such that $V(\lambda_\pm) = \gamma^4(16\alpha)^{-1}$. Given a fixed number, N, of fermions we can consider how the Fermi energy ε_F behaves as a function of the dimensionless parameter $\tilde{\alpha} \equiv \alpha\,\gamma^{-3}$. As we vary $\tilde{\alpha}$, the Fermi level will begin to approach the maximum of the potential. In the large N limit we can resort to a semi-classical approximation. This approximation can be cast in the form of a Bohr-Sommerfeld condition

$$\int_0^{\lambda_+} \mathrm{d}\lambda\sqrt{\varepsilon_F - V(\lambda)} = \frac{\pi}{2\sqrt{2}}\left(1 + \frac{1}{2N}\right) \ . \tag{2.6.15}$$

Examining the above integral reveals that upon tuning ε_F to the maximum value of the potential gives rise to non-analytic behaviour. This stems from the part of the integral near the maxima. The same non-analyticity is captured by the following, simpler, integral which we evaluate in a small $\delta\varepsilon_F$-expansion [124–127]:

$$\int_0^{\lambda_+} \mathrm{d}\lambda\sqrt{\delta\varepsilon_F - V''(\lambda_+)(\lambda-\lambda_+)^2/2} = -\frac{\delta\varepsilon_F}{4\gamma}\,\log\tilde{\alpha}\frac{\delta\varepsilon_F}{\gamma} + \text{analytic} \ . \tag{2.6.16}$$

We should view $-\delta\varepsilon_F$ as the difference between the Fermi level and the maximum value of the potential. So long as the Fermi level is close to the top of the potential the detailed features of the potential will not affect the preceding analysis.

For the sake of generality, it is perhaps worth pointing out that tuning the potential to have a non-quadratic maximum would affect the non-analytic behaviour. For instance

$$\int_0^{\lambda_+} \mathrm{d}\lambda\sqrt{\delta\varepsilon_F + (\lambda-\lambda_+)^m} = \sqrt{\delta\varepsilon_F}\,\lambda_+ \times {}_2F_1\left(-\frac{1}{2};\frac{1}{m};1+\frac{1}{m};-\frac{(-\lambda_+)^m}{\delta\varepsilon_F}\right) \ , \tag{2.6.17}$$

from which we extract a non-analytic behaviour of the type $\sim \delta\varepsilon_F^{1/2+1/m}$ for $m \neq 2$ [125, 127]. In what follows we focus on the $m = 2$ case.

2.6.4 A scattering problem

A final (albeit somewhat a posteriori) motivation for assuming a local maximum is that we will eventually compare calculations for the matrix quantum mechanical theory to a certain worldsheet string theory. The natural observable from the worldsheet perspective is an S-matrix. In the presence of a local maximum, the low energy excitations naturally encode an S-matrix. This is most evident, if we

consider the physics localised near the maximum, where the model reduces to N fermions in an inverse harmonic well. Let us introduce the following dimensionless quantities

$$x = 2^{3/4} N^{1/2} \, (\lambda - \lambda_+) \, \gamma^{1/2} \, , \qquad \nu = \frac{N}{2^{1/2}} \left(\frac{\varepsilon_F + \delta\varepsilon - V(\lambda_+)}{\gamma} \right) \, , \quad (2.6.18)$$

and consider excitations with energy near ε such that at large N we have $\delta\varepsilon/\varepsilon_F \ll 1$. The single particle Schrödinger equation (2.6.13) near the maximum of the potential now becomes

$$\left(-\partial_x^2 - \frac{x^2}{4} \right) \psi_{\nu,p} = \nu \, \psi_{\nu,p} \, . \quad (2.6.19)$$

Note further that the rescaling (2.6.18) involves N in such a way that the range of x and ν becomes effectively infinite as N tends to infinity. The parity index in $\psi_{\nu,p}$, $p \in \{\pm\}$, reflects the behaviour of the wavefunction under the discrete symmetry $x \to -x$, namely $\psi_{\nu,p}(-x) = p \, \psi_{\nu,p}(x)$.

When considering the scattering problem, we take the Fermi level ν_F of our new Schrödinger problem (2.6.19) to be negative, such that we can send in an incoming wave from negative x, let it bounce against the wall, and compute the reflected wavefunction. The Schrödinger equation (2.6.19) admits solutions whose explicit form is given by the parabolic cylinder functions $D_a(z)$. Explicitly,

$$\Psi_{\nu,\pm}(x) = e^{-i\pi(1/2 - i\nu)/4} \left(D_{i(\nu+i/2)} \left(e^{\frac{3\pi i}{4}} x \right) \pm D_{i(\nu+i/2)} \left(e^{-\frac{\pi i}{4}} x \right) \right) \, . \quad (2.6.20)$$

It will also prove convenient to express the above wavefunctions in a basis of incoming/outgoing waves near large and negative values of x. These can be expressed as follows

$$\psi_\nu^{(out)}(x) = \frac{1}{2} \left(\Psi_{\nu,+}(x) + \Psi_{\nu,-}(x) \right) \, , \qquad \psi_\nu^{(in)}(x) = \left(\psi_\nu^{(out)}(x) \right)^* \, . \quad (2.6.21)$$

The outgoing wavefunctions admit an asymptotic expansion of the following form

$$\lim_{x \to -\infty} \psi_\nu^{(out)}(x) = e^{ix^2/4} (-x)^{-1/2 + i\nu} + \dots \, . \quad (2.6.22)$$

Notice that in addition to the energy, ν parameterises the wavelength of the spatial oscillations. It is easiest to see this by considering a coordinate transformation to the spatial coordinate $x = -e^{-u}$. The Wronskian for the above wavefunctions is

given by

$$W(\nu) = \psi_\nu^{(out)}(x)\partial_x\psi_\nu^{(out)}(-x) - \psi_\nu^{(out)}(-x)\partial_x\psi_\nu^{(out)}(x) = i\frac{\sqrt{2\pi}}{\Gamma\left(1/2 - i\nu\right)}\, e^{-\pi\nu/2} \ . \tag{2.6.23}$$

As expected, $W(\nu)$ is independent of x. We can also express the parity eigenstates in terms of $\psi^{(out)}(x)$ as follows

$$\psi_{\nu,+}(x) \equiv \frac{1}{\sqrt{2}}\,\frac{\psi_\nu^{(out)}(x) + \psi_\nu^{(out)}(-x)}{W(\nu)} \ , \qquad \psi_{\nu,-}(x) \equiv \frac{1}{\sqrt{2}}\,\frac{\psi_\nu^{(out)}(x) - \psi_\nu^{(out)}(-x)}{W(\nu)^*} \ , \tag{2.6.24}$$

where we have rescaled (2.6.20) with respect to the Wronskian.

By virtue of the discrete symmetry $x \leftrightarrow -x$, $\psi_\nu^{(out)}(-x)$ and its complex conjugate also describe solutions to (2.6.19). These are waves that are purely incoming or outgoing on the other side of the potential barrier.

2.6.5 Releasing the particle number

So far we kept the particle number N fixed. It will be convenient to also allow the particle number to vary, thus constructing a second quantised picture of the quantum mechanical theory. To do so, we introduce lowering and raising operators, $\hat{a}_{\nu,p}$ and $\hat{a}^\dagger_{\nu,p}$ satisfying the standard anti-commutation relations

$$\{\hat{a}_{\nu,p}, \hat{a}_{\nu',p'}\} = 0 \ , \qquad \{\hat{a}_{\nu,p}, \hat{a}^\dagger_{\nu',p'}\} = 2\pi\,\delta_{\nu,\nu'}\delta_{p,p'} \ . \tag{2.6.25}$$

The ground state is filled until the Fermi level and we introduce the state $|\text{Fermi}\rangle$ corresponding to a filled Fermi sea by

$$\begin{aligned} \hat{a}_{\nu,p}\,|\text{Fermi}\rangle &= 0 \ , \qquad \nu > \nu_F \qquad \& \qquad p \in \{\pm\} \ , \\ \hat{a}^\dagger_{\nu,p}\,|\text{Fermi}\rangle &= 0 \ , \qquad \nu < \nu_F \qquad \& \qquad p \in \{\pm\} \ , \end{aligned} \tag{2.6.26}$$

where we recall that $\nu_F < 0$. The above Fermi sea is filled on both sides of the potential.[3] We can create multi-particle energy eigenstates on top of $|\text{Fermi}\rangle$ by acting with $\hat{a}^\dagger_{\nu,p}$ with $\nu > \nu_F$, and hole type excitations by acting with $\hat{a}_{\nu,p}$ with $\nu < \nu_F$.

We can thus introduce field operators for the creation and annihilation of wave-

[3] One can also consider filling one of the two sides, or perhaps filling the two sides with Fermi seas with different levels. The case where both sides are filled equally was considered in [134,135].

functions at x:

$$\hat{\Psi}_p(t,x) = \int_{\mathbb{R}} \frac{\mathrm{d}\nu}{2\pi}\, e^{-i\nu t}\, \hat{a}_{\nu,p}\, \psi^*_{\nu,p}(x) \ , \qquad \hat{\Psi}^\dagger_p(t,x) = \int_{\mathbb{R}} \frac{\mathrm{d}\nu}{2\pi}\, e^{i\nu t}\, \hat{a}^\dagger_{\nu,p}\, \psi_{\nu,p}(x) \ , \tag{2.6.27}$$

where the integration is over the continuous energy levels ν and $\psi^*_{\nu,p}(x)$ and $\psi_{\nu,p}(x)$ are the parity eigenstates introduced in (2.6.24). In the expression above $*$ denotes the complex conjugation of $\mathbb{C}$-numbers, while $\dagger$ denotes the complex conjugation of quantum operators. Given the above fermionic operators, we can define a number density operator

$$\hat{n}(t,x) = \hat{\Psi}^\dagger(t,x)\hat{\Psi}(t,x) \ . \tag{2.6.28}$$

In the above, we have defined $\hat{\Psi}(t,x) \equiv \hat{\Psi}_+(t,x) + \hat{\Psi}_-(t,x)$ and its conjugate, satisfying

$$\{\hat{\Psi}(t,x), \hat{\Psi}^\dagger(t,x')\} = 2\,\delta(x-x') \ . \tag{2.6.29}$$

The operator $\hat{\Psi}^\dagger(t,x)$ creates states that can be perceived as single particle states on top of the filled Fermi sea when viewed near the left boundary at large negative values of x.

Feynman propagator

Given a second quantised theory we can construct various propagators for the fermions. For instance, the Feynman propagator is given by

$$S_F(t,x;t',x') = -i\,\langle \text{Fermi}|\, T_F\, \hat{\Psi}(t,x)\hat{\Psi}^\dagger(t',x')|\text{Fermi}\rangle \ , \tag{2.6.30}$$

where T_F denotes Fermionic time-ordering. It satisfies

$$\left(-\partial_x^2 - \frac{x^2}{4} - i\partial_t\right) S_F(t,x;t',x') = \delta(t-t')\delta(x-x') \ . \tag{2.6.31}$$

More explicitly, we can express $S_F(t,x;t',x')$ as

$$\begin{aligned} i\,S_F(t,x;t',x') = \Theta(s) \int_{\nu_F}^{\infty} \frac{\mathrm{d}\nu}{2\pi}\, e^{-i\nu s}\, \psi^*_{\nu,p}(x)\psi_{\nu,p}(x') - \\ \Theta(-s) \int_{-\infty}^{\nu_F} \frac{\mathrm{d}\nu}{2\pi}\, e^{-i\nu s}\, \psi^*_{\nu,p}(x)\psi_{\nu,p}(x') \ , \end{aligned} \tag{2.6.32}$$

where we sum over the parity index, and for notational simplicity we have defined $s \equiv t-t'$. We can also write down the Fourier transform of the Fermion propagator with respect to s. For this we use the contour integral representation of the

Heaviside function

$$\Theta(s) = \lim_{\varepsilon\to 0^+} \int_{\mathbb{R}} \frac{\mathrm{d}\Omega}{2\pi i} \frac{e^{i\Omega s}}{\Omega - i\varepsilon} \ . \tag{2.6.33}$$

The Fourier transform then reads

$$\tilde{S}_F(x,x';\omega) = -\lim_{\varepsilon\to 0^+} \int_{\mathbb{R}} \frac{\mathrm{d}\nu}{2\pi} \psi^*_{\nu,p}(x)\psi_{\nu,p}(x') \left(\frac{\Theta(\nu-\nu_F)}{\nu-\omega-i\varepsilon} + \frac{\Theta(\nu_F-\nu)}{\nu-\omega+i\varepsilon} \right) , \tag{2.6.34}$$

and we use the following conventions for the Fourier transform:

$$f(t) = \int_{\mathbb{R}} \frac{\mathrm{d}\omega}{2\pi} e^{-i\omega t} \tilde{f}(\omega) \qquad \& \qquad \tilde{f}(\omega) = \int_{\mathbb{R}} \mathrm{d}t\, e^{+i\omega t} f(t) \ . \tag{2.6.35}$$

Complex conjugation at the level of the Fourier transform mirrors itself in $x \leftrightarrow x'$ and a particle hole exchange. Finally, we note that for large negative values of x and x' the parity states behave as

$$\begin{aligned} &\lim_{x,x'\to-\infty} \left(\psi^*_{+,\nu}(x)\psi_{+,\nu}(x') + \psi^*_{-,\nu}(x)\psi_{-,\nu}(x')\right) = \\ &\quad \frac{1}{\sqrt{xx'}} \left(e^{-i(x^2-x'^2)/4 - i\nu\log x/x'} + R^*_\nu\, e^{-i(x^2+x'^2)/4 - i\nu\log xx'} \right) + \text{h.c.} \ , \end{aligned} \tag{2.6.36}$$

where we defined

$$R_\nu \equiv -i\, \frac{\Gamma(1/2 - i\nu)}{\sqrt{2\pi}}\, e^{-\pi\nu/2} \ . \tag{2.6.37}$$

We will provide a physical interpretation of the definition of R_ν in the next section. For large negative values of x and x', with $x > x'$, we then find the asymptotic form for (2.6.36):

$$\begin{aligned} \tilde{S}_F(x,x';\omega) \approx &-\frac{i}{\sqrt{xx'}} \left(e^{i(x^2-x'^2)/4 + i\omega\log x/x'} + R_\omega\, e^{i(x^2+x'^2)/4 + i\omega\log xx'} \right) \Theta(\omega-\nu_F) \\ &+ \frac{i}{\sqrt{xx'}} \left(e^{-i(x^2-x'^2)/4 - i\omega\log x/x'} + R^*_\omega\, e^{-i(x^2+x'^2)/4 - i\omega\log xx'} \right) \Theta(\nu_F-\omega) \, . \end{aligned} \tag{2.6.38}$$

For $x' > x$, both large and negative we find

$$\begin{aligned} \tilde{S}_F(x,x';\omega) \approx &-\frac{i}{\sqrt{xx'}} \left(e^{-i(x^2-x'^2)/4 - i\omega\log x/x'} + R_\omega\, e^{i(x^2+x'^2)/4 + i\omega\log xx'} \right) \Theta(\omega-\nu_F) \\ &+ \frac{i}{\sqrt{xx'}} \left(e^{i(x^2-x'^2)/4 + i\omega\log x/x'} + R^*_\omega\, e^{-i(x^2+x'^2)/4 - i\omega\log xx'} \right) \Theta(\nu_F-\omega) \ . \end{aligned} \tag{2.6.39}$$

We will now put all these expressions to good use, as they have provided us the basic building blocks to construct an S-matrix for our quantum mechanical matrices.

2.7 Scattering from quantum mechanical matrices

As briefly mentioned in the previous section, one can setup an S-matrix problem for the fermions propagating near the filled Fermi sea. These excitations reflect off the region near the maximum of the potential. In this section, we provide some details for the scattering amplitude introduced in [31, 32] of the number density operator $\hat{n}(t, x)$ defined in (2.6.28). These are simple observables in our theory.

2.7.1 Reflection coefficient & Green's function

Recall the Hamiltonian (2.6.19) we obtained at the end of the previous section

$$\hat{H} = -\partial_x^2 - \frac{x^2}{4} \ . \tag{2.7.1}$$

A natural object to consider is given by the reflection coefficient, R_ν, of a wave of frequency ν coming in from the asymptotic region at large and negative values of x and reflecting back, as depicted in figure 2.14.

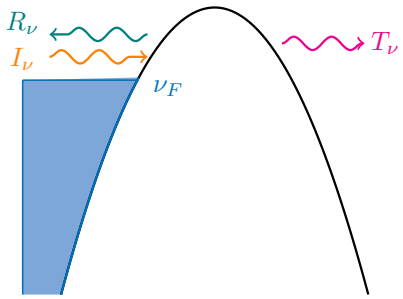

Figure 2.14: *We consider an incoming wave from negative infinity (orange), part of which is reflected (teal), and part of which is transmitted (magenta) from the inverted harmonic oscillator potential. The ground state configuration fills the Fermi sea up to ν_F.*

As our boundary condition we impose that the incoming flux from large positive values of x vanishes. In this regard, it is convenient to note that $\psi_\nu^{(out)}(-x)$ is a

wave that is purely outgoing for large positive values of x. Expanding for large negative values of x we find a superposition of an incoming and reflected wave

$$\frac{\psi_\nu^{(out)}(-x)}{W(\nu)} \approx \frac{e^{-ix^2/4-i\nu\log(-x)}}{\sqrt{-x}} - i\,\frac{\Gamma(1/2-i\nu)}{\sqrt{-2\pi x}}e^{-\pi\nu/2}e^{ix^2/4+i\nu\log(-x)} + \dots \ , \tag{2.7.2}$$

where we have normalised the wavefunction such that the incoming (first) part has unit coefficient. To obtain the reflection and transmission coefficient we calculate the probability current

$$\mathcal{J}(t,x) = -i\left(\psi^*\partial_x\psi - \psi\partial_x\psi^*\right) \ , \qquad \partial_t\rho + \partial_x\mathcal{J} = 0 \ . \tag{2.7.3}$$

From the probability current one can readily obtain the reflection and transmission coefficients

$$|R_\nu|^2 = \frac{|\mathcal{J}_{ref|}}{|\mathcal{J}_{in}|} = \frac{1}{1+e^{2\pi\nu}} \ , \quad |T_\nu|^2 = \frac{|\mathcal{J}_{trans}|}{|\mathcal{J}_{in}|} = \frac{1}{1+e^{-2\pi\nu}} = 1-|R_\nu|^2 \ , \tag{2.7.4}$$

where we obtain $\mathcal{J}_{in}$ from (2.7.3) by using the purely incoming part of (2.7.2) and similarly the purely reflected and transmitted wave for $\mathcal{J}_{ref}$ and $\mathcal{J}_{trans}$ respectively. For negative values of ν, which is the situation we are most interested in, the transmission coefficient is exponentially suppressed. In fact, the expression (2.7.2) encodes more information. For instance, it encodes the reflection coefficient

$$R_\nu = -i\,\frac{\Gamma(1/2-i\nu)}{\sqrt{2\pi}}\,e^{-\pi\nu/2} \ , \tag{2.7.5}$$

which can be viewed as an S-matrix element for the scattering of a single wave against the potential barrier. Perturbative unitarity of the S-matrix is given by the fact that R_ν is a pure phase up to $e^{-\pi\nu/2}$ corrections. Using the Gamma function identity

$$|\Gamma(1/2-i\nu)|^2 = \frac{\pi}{\cosh(\pi\nu)} \ , \tag{2.7.6}$$

the absolute value of (2.7.5) reduces to (2.7.4).

The Green's function is given by evaluating the matrix elements of the resolvent

$$G(x,x';z) = \langle x'|\left(\hat{H}-z\right)^{-1}|x\rangle \ , \qquad \left(G(x,x';z)\right)^* = G(x',x;z^*) \ , \tag{2.7.7}$$

where z takes values across the whole complex plane, modulo the spectrum of $\hat{H}$.

The Green's function satisfies the equation

$$\left(-\partial_x^2 - \frac{x^2}{4} - z\right) G(x,x';z) = \delta(x-x') \ . \tag{2.7.8}$$

It is often convenient to express $G(x,x';z)$ in terms of eigenfunctions of $\hat{H}$ with complex eigenvalue z. Concretely,

$$G(x,x';z) = \frac{1}{W(z)} \left(\psi_z^R(x)\psi_z^L(x')\Theta(x'-x) + \psi_z^R(x')\psi_z^L(x)\Theta(x-x')\right) \ , \tag{2.7.9}$$

where $\psi_z^L(x)$ decays at $x=-\infty$, and $\psi_z^R(x)$ decays at $x=\infty$, and $W(z)$ is the Wronskian (2.6.23). As an example, when z takes values in the upper half of the complex plane we can express $\psi_z^{L,R}(x)$ as

$$\psi_z^L(x) = \psi_z^{(out)}(x) \ , \qquad \psi_z^R(x) = \psi_z^{(out)}(-x) \ . \tag{2.7.10}$$

For large negative and large positive values of x these wave functions scale as

$$\lim_{x\to-\infty} \psi_z^L(x) = \frac{1}{\sqrt{-x}}\, e^{ix^2/4 + iz\log(-x)} \qquad \text{and} \qquad \lim_{x\to\infty} \psi_z^R(x) = \frac{1}{\sqrt{x}}\, e^{ix^2/4+iz\log x} \ . \tag{2.7.11}$$

Using the expressions for the wavefunctions in (2.7.2), we can obtain an asymptotic expansion of $G(x,x';z)$ for large and negative values of x and x'. For z in the upper half plane we obtain

$$\begin{aligned} G(x,x';z) \approx & -\frac{i}{\sqrt{xx'}} \left(e^{-i(x^2-x'^2)/4 - iz\log x/x'} + R_z\, e^{i(x^2+x'^2)/4 + iz\log xx'}\right)\Theta(x'-x) \\ & -\frac{i}{\sqrt{xx'}} \left(e^{i(x^2-x'^2)/4 + iz\log x/x'} + R_z\, e^{i(x^2+x'^2)/4 + iz\log xx'}\right)\Theta(x-x') \ . \end{aligned} \tag{2.7.12}$$

A similar expression can be derived for z in the lower half plane. The reflection coefficient R_ν given in (2.7.5) and the above Green's function are the basic building blocks for the scattering problem of interest – namely, the scattering of the probability density $\rho(t,x) = \psi^*(t,x)\psi(t,x)$ about the filled Fermi sea. We note that $\rho(t,x)$ is a quantum mechanical analogue of the eigenvalue density $\rho(\lambda)$ introduced in (2.3.15).

As a final remark, before embarking on the calculation of various scattering processes we would like to relate the Green's function introduced in (2.7.9) to the Feynman propagator (2.6.32) discussed in the previous section. These obey the same equation. Comparing the first line in (2.6.38) with the lower line of the

Green's function in (2.7.12), we note that the two expressions take the same form. The difference lies in the Heaviside function appearing in $\tilde{S}_F(x, x'; \omega)$. This is a simple manifestation of the fact that $G(x, x'; z)$ stems from a first quantised setup, whereas $\tilde{S}_F(x, x'; \omega)$ stems from a 'second quantised' picture allowing for particle creation and annihilation.

2.7.2 Multi-particle scattering

To ensure a large range of admissible scattering frequencies we take $\nu_F^2 \gg 1$. This condition will also ensure that the transmitted wave is exponentially suppressed, such that we can aptly refer to scattering processes leaking across the barrier as non-perturbative phenomena. The physical problem we are after consists of sending in an incoming density wave $\rho_\omega(x)$ at some incoming frequency ω near the spatial boundary at large and negative values of x, and measuring the scattered wave at some outgoing frequency ω', again at large negative values of x. Since we are scattering a composite object, the elements of our perturbative S-matrix will be given by certain convolutions of the reflection coefficients R_ν. In what follows, we will often express results in terms of the spatial coordinate

$$u = -\log(-x) \ , \qquad x < 0 \ . \tag{2.7.13}$$

Notice that for large negative values of x, u is also large and negative and u increases monotonically with x.

To compute scattering processes for multiple incoming and outgoing waves[4] it is convenient to resort to the multi-particle picture described in section 2.6.5. We begin by considering the n-point function

$$\mathcal{Q}\left(\{t_k, x_k\}\right) = \langle \text{Fermi} | T_B \prod_{k=1}^{n} \hat{n}(t_k, x_k) | \text{Fermi} \rangle \ , \tag{2.7.14}$$

where now T_B indicates bosonic time ordering and we defined $\hat{n}(t_k, x_k)$ in (2.6.28). Given that our theory is non-interacting, we can calculate $\mathcal{Q}$ via multiple Wick contractions using (2.6.32). We note that the above correlation function is invariant under $(t_i, x_i) \leftrightarrow (t_j, x_j)$.

General approach. Before delving into concrete examples, it is worth explaining the general strategy. Starting with the quantum correlation function (2.7.14) we perform all possible Wick contractions. Keeping the fully connected part we

[4]The S-matrix in a two-dimensional world is a rather subtle object due to the absence of an infinitely large celestial sphere at null infinity. This implies we cannot have parametrically separated asymptotic states. Instead, in two-dimensions the celestial sphere collapses to a celestial point.

obtain

$$\mathcal{Q}_c\left(\{t_k, x_k\}\right) = -\frac{i^n}{n} \sum_{\sigma \in \text{Perm}(n)} \prod_{k=1}^{n} S_F(t_{\sigma_k}, x_{\sigma_k}; t_{\sigma_{k+1}}, x_{\sigma_{k+1}}) \ , \tag{2.7.15}$$

where $\text{Perm}(n)$ denotes the set of order $n!$ permuting the elements in $\{1, 2, \ldots, n\}$. We also compute indices modulo n (e.g. $\sigma_{n+1} \equiv \sigma_1$ and so on). The subscript c is a reminder that we are considering the fully connected part. Notice that (2.7.15) is invariant under $(t_i, x_i) \leftrightarrow (t_j, x_j)$. Going to Fourier space the above leads to an expression manifestly invariant under $(\omega_i, x_i) \leftrightarrow (\omega_j, x_j)$. From this expression we extract the fully connected part $\tilde{\mathcal{Q}}_c(\{\omega_i, x_i\})$ and obtain the one-to-n scattering amplitude $S(\omega_1, \ldots, \omega_{n-1}|\omega_n)$ defined as the part of the correlation function taking the form

$$\delta\left(\omega_1 + \cdots + \omega_n\right) \exp\left(i\omega_n u_n - i\sum_{k=1}^{n-1} \omega_k u_k\right) \ S(\omega_1, \ldots, \omega_{n-1}|\omega_n) \ . \tag{2.7.16}$$

Outgoing frequencies ω_k are positive for $k = 1, \ldots, n-1$ and as a result, the frequency of the incoming wave ω_n must be negative. Since the original correlation function (2.7.14) is invariant under $(t_i, x_i) \leftrightarrow (t_j, x_j)$ we impose a specific ordering of the spatial coordinates, namely $x_1 > x_2 > \ldots > x_n$, to avoid overcounting. For $m > 1$ we can similarly define the m-to-n amplitude. We now proceed to study some concrete examples.

One-to-one scattering. As a warm up exercise, we compute the one-to-one scattering problem in the second quantised picture. We wish to calculate the Fourier transform of the connected part of

$$\mathcal{Q}\left(\{t_i, x_i\}\right) = \langle \text{Fermi}|\, T_B\, \hat{n}(t_1, x_1)\, \hat{n}(t_2, x_2)|\text{Fermi}\rangle \ , \tag{2.7.17}$$

where now T_B corresponds to bosonic time ordering. Keeping track of the various Wick contractions and using the Fermion propagator (2.6.32), we find

$$\mathcal{Q}_c(t_1, x_1; t_2, x_2) = \frac{1}{2} \sum_{\sigma \in \text{Perm}(2)} \prod_{k=1}^{2} S_F(t_{\sigma_k}, x_{\sigma_k}; t_{\sigma_{k+1}}, x_{\sigma_{k+1}}) \ . \tag{2.7.18}$$

In appendix 6 we provide some steps leading to (2.7.18). Going to Fourier space we obtain

$$\tilde{\mathcal{Q}}_c(\omega_1, x_1; \omega_2, x_2) = \int_{\mathbb{R}^2} \mathrm{d}t_1 \mathrm{d}t_2 \, e^{+i\omega_1 t_1 + i\omega_2 t_2} \, \mathcal{Q}_c(t_1, x_1; t_2, x_2) \ . \tag{2.7.19}$$

Performing the integrals over t_1 and t_2, we are led to the following expression

$$\tilde{\mathcal{Q}}_c(\omega_1, x_1; \omega_2, x_2) = \frac{2\pi}{2}\delta(\omega_1+\omega_2)\times \int_{\mathbb{R}} \frac{\mathrm{d}\upsilon}{2\pi}\left(\tilde{S}_F(x_1,x_2;\upsilon+\omega_1)\tilde{S}_F(x_2,x_1;\upsilon) + \tilde{S}_F(x_2,x_1;\upsilon+\omega_2)\tilde{S}_F(x_1,x_2;\upsilon)\right) . \tag{2.7.20}$$

We can expand the above expression at large and negative values of x_1 and x_2. There are various pieces in this regime. Of these, we would like to keep those terms corresponding to particles that have been scattered by the barrier, and moreover do not exhibit large oscillations of the type $\sim e^{\pm ix^2/4}$. Expressing the result in terms of the spatial coordinate $u = -\log(-x)$ we find

$$\tilde{\mathcal{Q}}_c(\omega_1, u_1; \omega_2, u_2) = 2\pi\delta(\omega_1+\omega_2)\left(\omega_2\,\frac{e^{i\omega_1 u_1 - i\omega_2 u_2}}{2\pi} + \frac{e^{-i\omega_1 u_1 + i\omega_2 u_2}}{2\pi}\,S(\omega_1|\omega_2)\right) . \tag{2.7.21}$$

and $S(\omega_1|\omega_2)$ is defined as

$$S(\omega_1|\omega_2) \equiv e^{-i\omega_2\log(-\nu_F)}\int_0^{\omega_1}\mathrm{d}\upsilon\, R^*_{\nu_F-\upsilon}R_{\nu_F-\upsilon-\omega_2} . \tag{2.7.22}$$

The phase $e^{-i\omega_2\log(-\nu_F)}$ subtracts the phase appearing in the perturbative expansion of the reflection coefficient (6.0.13). (One can also remove this phase by a redefinition of the u-coordinate.) Notice that the frequency of R_ν is always above the Fermi level since it corresponds to particle scattering, whereas the frequency of R^*_ν is always below the Fermi level since it corresponds to the scattering of a hole. Performing a large ν_F expansion, we obtain

$$S(\omega_1|\omega_2) = \omega_1 + \frac{1}{24\nu_F^2}\left(i\omega_1^2 - \omega_1^4(\omega_1-2i)\right) + \mathcal{O}\left(\nu_F^{-4}\right) . \tag{2.7.23}$$

It is worth noting that the leading piece of $S(\omega_1|\omega_2)$, including the energy conserving delta-function, is the one-to-one scattering amplitude we would have obtained for a theory of massless fields in two-spacetime dimensions in a theory subject to Poincaré invariance. The terms subleading in $1/\nu_F$ are corrections which indicate any such Poincaré invariance is ultimately broken. We will comment on this from the perspective of a continuum description in the next section. Finally dimensional analysis may raise concerns about the above expression. We must remember, however, that in going to the Hamiltonian (2.7.1) we have set several dimensionful parameters to unity. Upon restoring them, we can also restore our faith in dimensional analysis.

One-to-two scattering. We now move on to the case of one-to-two scattering. This scattering amplitude encodes the type of interactions present in the theory. The correlation function of interest is

$$\mathcal{Q}\left(\{t_i, x_i\}\right) = \langle \text{Fermi}|\, T_B\, \hat{n}(t_1, x_1)\hat{n}(t_2, x_2)\hat{n}(t_3, x_3)|\text{Fermi}\rangle \ , \tag{2.7.24}$$

The resulting expression for the connected part reads

$$\mathcal{Q}_c\left(\{t_i, x_i\}\right) = \frac{i}{3} \sum_{\sigma \in \text{Perm}(3)} \prod_{k=1}^{3} S_F(t_{\sigma_k}, x_{\sigma_k}; t_{\sigma_{k+1}}, x_{\sigma_{k+1}}) \ . \tag{2.7.25}$$

Fourier transforming with respect to the time coordinates, we obtain

$$\tilde{\mathcal{Q}}_c(\omega_1, x_1; \omega_2, x_2; \omega_3, x_3) = \int_{\mathbb{R}^3} \mathrm{d}t_1 \mathrm{d}t_2 \mathrm{d}t_3\, e^{i\omega_1 t_1 + i\omega_2 t_2 + i\omega_3 t_3}\, \mathcal{Q}_c(t_1, x_1; t_2, x_2; t_3, x_3) \ . \tag{2.7.26}$$

Due to time-translation invariance, we obtain an overall delta function imposing the conservation of energy. Combining (2.7.16) with (2.7.26) we obtain

$$S(\omega_1, \omega_2|\, \omega_3) \equiv e^{-i\omega_3 \log(-\nu_F)} \left[\int_0^{\omega_1} \mathrm{d}\upsilon\, R^*_{\nu_F - \upsilon} R_{\nu_F - \upsilon - \omega_3} - \int_{\omega_2}^{\omega_1 + \omega_2} \mathrm{d}\upsilon\, R^*_{\nu_F - \upsilon} R_{\nu_F - \upsilon - \omega_3} \right] . \tag{2.7.27}$$

We can express the above expression in a large ν_F expansion using (6.0.13)

$$\begin{aligned} S(\omega_1, \omega_2|\, \omega_3) = \frac{i}{\nu_F}\, \omega_1\omega_2\omega_3 - \frac{i}{24\nu_F^3} \omega_1\omega_2\omega_3\, (\omega_3 + i)\, (\omega_3 + 2i) \\ \times \left(\omega_1\, (\omega_1 - i) + \omega_2\, (\omega_2 - i) + 1\right) + \mathcal{O}\left(\nu_F^{-5}\right) \ . \end{aligned} \tag{2.7.28}$$

Note that the alternating signs arise from the alternating signs in (2.6.38) and we take the frequencies of the scattered waves $\omega_1, \omega_2 > 0$.

One-to-three scattering. In direct analogy to the one-to-one and one-to-two case, we can work out the one-to-three scattering amplitude. After obtaining the possible Wick contractions of

$$\mathcal{Q}\left(\{t_k, x_k\}\right) = \langle \text{Fermi}|\, T_B\, \hat{n}(t_1, x_1)\hat{n}(t_2, x_2)\hat{n}(t_3, x_3)\hat{n}(t_4, x_4)|\text{Fermi}\rangle \ , \tag{2.7.29}$$

we can express the connected piece as

$$\mathcal{Q}_c\left(\{t_k, x_k\}\right) = -\frac{1}{4}\sum_{\sigma\in\text{Perm}(4)}\prod_{k=1}^{4} S_F(t_{\sigma_k}, x_{\sigma_k}; t_{\sigma_{k+1}}, x_{\sigma_{k+1}}) \ . \tag{2.7.30}$$

Fourier transforming, extracting the term without the $e^{\pm ix^2/4}$ oscillations, and using (2.7.16) we end up with

$$\begin{aligned} S(\omega_1,\omega_2,\omega_3\,|\,\omega_4) \equiv e^{-i\omega_4\log(-\nu_F)}\Bigg[&\int_{\omega_2+\omega_3}^{\omega_1+\omega_2+\omega_3} \mathrm{d}\upsilon\, R^*_{\nu_F-\upsilon}R_{\nu_F-\upsilon-\omega_4} \\ &- \int_{\omega_2}^{\omega_1+\omega_2} \mathrm{d}\upsilon\, R^*_{\nu_F-\upsilon}R_{\nu_F-\upsilon-\omega_4} - \int_{\omega_3}^{\omega_1+\omega_3} \mathrm{d}\upsilon\, R^*_{\nu_F-\upsilon}R_{\nu_F-\upsilon-\omega_4} \\ &+ \int_{0}^{\omega_1} \mathrm{d}\upsilon\, R^*_{\nu_F-\upsilon}R_{\nu_F-\upsilon-\omega_4}\Bigg] \ . \end{aligned} \tag{2.7.31}$$

Note that there is an overall minus sign arising from our original definition of the scattering amplitude (2.7.16) and (2.7.30). Expanding the above expression at large ν_F by making use of (6.0.13) we find

$$\begin{aligned} S(\omega_1,\omega_2,\omega_3\,|\,\omega_4) = &-\frac{1}{\nu_F^2}\,\omega_1\omega_2\omega_3\omega_4(\omega_4+i)+\frac{1}{24\nu_F^4}\,\omega_1\omega_2\omega_3\omega_4\,(\omega_4+i)\,(\omega_4+2i)\,(\omega_4+3i) \\ &\times\left(\omega_1\,(\omega_1-i)+\omega_2\,(\omega_2-i)+\omega_3\,(\omega_3-i)+1\right)+\mathcal{O}\left(\nu_F^{-6}\right) \ . \end{aligned} \tag{2.7.32}$$

One-to-$(n-1)$ scattering. From the above scattering amplitudes we observe

$$S(\omega_1,\ldots,\omega_{n-1}|\,\omega_n) = \sum_{L=0}^{\infty}\nu_F^{n-1+2L}S^{(L)}(\omega_1,\ldots,\omega_{n-1}|\,\omega_n) \ , \tag{2.7.33}$$

where for the case of one-to-(n-1) scattering the left hand side is given by [32]

$$S(\omega_1,\ldots,\omega_{n-1}|\,\omega_n) \equiv e^{-i\omega_n\log(-\nu_F)}\sum_{\Omega\subseteq\{\omega_1,..,\omega_{n-1}\}}(-1)^{|\Omega|+1}\int_0^{\omega(\Omega)}\mathrm{d}\upsilon\, R^*_{\nu_F-\upsilon}R_{\nu_F-\upsilon-\omega_n} \ . \tag{2.7.34}$$

where $\omega(\Omega)$ is the sum of all elements in Ω. Furthermore, for the leading term in a large ν_F expansion of the one-to-$(n-1)$ scattering amplitude, we observe

$$S^{(0)}(\omega_1,\ldots,\omega_{n-1}|\,\omega_n) = -i^n\,\omega_1\cdots\omega_{n-1}\prod_{k=0}^{n-3}(\omega_n+ik) \ , \qquad n\geq 3 \ . \tag{2.7.35}$$

For the the first sub-leading term and $n \geq 3$ we find

$$S^{(1)}(\omega_1, \ldots, \omega_{n-1} | \, \omega_n) = (i)^n \, \frac{1}{24} \, \omega_1 \cdots \omega_{n-1} \prod_{k=0}^{n-1} (\omega_n + ki) \left(\sum_{\ell=1}^{n-1} \omega_\ell (\omega_\ell - i) + 1 \right) \, , \tag{2.7.36}$$

where $\omega_n = -\sum_{k=1}^{n-1} \omega_k$. For both expressions we made use of the large ν_F expansion (6.0.13). In appendix 6 we obtain some higher-point scattering amplitudes that confirm the above expressions, at least for low enough particle number.

Two-to-two scattering. To obtain the two-to-two amplitude, instead of looking for terms of the form (2.7.16) we must extract the term proportional to

$$e^{-i\omega_1 u_1 - i\omega_2 u_2 + i\omega_3 u_3 + i\omega_4 u_4} \, \delta(\omega_1 + \omega_2 + \omega_3 + \omega_4) \, S(\omega_1, \omega_2 \, | \, \omega_3, \omega_4) \tag{2.7.37}$$

from the connected part of the four point correlation function (2.7.30). This defines for us the two-to-two amplitude $S(\omega_1, \omega_2 \, | \, \omega_3, \omega_4)$. In the above expression we assume that ω_1 and ω_2 are the positive frequencies of the outgoing waves, while ω_3 and ω_4 are the negative frequencies of the two incoming waves. Additionally we have to order the frequencies. We choose

$$\omega_2 > \omega_1 \, , \quad \omega_4 > \omega_3 \, , \quad \omega_2 > -\omega_3 \, , \quad \omega_2 > -\omega_4 \, , \tag{2.7.38}$$

such that $\omega_2 = \max\{\omega_1, \omega_2, |\omega_3|, |\omega_4|\}$. Combining with (2.7.37) and (2.7.30) we obtain [32, 141, 142]

$$\begin{aligned} S(\omega_1, \omega_2 | \omega_3, \omega_4) \equiv e^{-i(\omega_3+\omega_4)\log(-\nu_F)} \Bigg[& \int_{\omega_3}^{\omega_1+\omega_3} \mathrm{d}\upsilon R^*_{\nu_F - \upsilon + \omega_3} R_{\nu_F - \upsilon - \omega_4} \\ + \int_{\omega_2}^{\omega_1+\omega_2} \mathrm{d}\upsilon R^*_{\nu_F - \upsilon} R_{\nu_F - \upsilon + \omega_1 + \omega_2} & - \int_{\omega_3}^{\omega_1+\omega_3} \mathrm{d}\upsilon R_{\nu_F - \upsilon} R^*_{\nu_F - \upsilon + \omega_3} R_{\nu_F - \upsilon + \omega_1 + \omega_3} R^*_{\nu_F - \upsilon - \omega_2} \\ - \int_{\omega_4}^{\omega_1+\omega_4} \mathrm{d}\upsilon R_{\nu_F - \upsilon} R^*_{\nu_F - \upsilon + \omega_4} R_{\nu_F - \upsilon + \omega_1 + \omega_4} R^*_{\nu_F - \upsilon - \omega_2} & \Bigg] \\ = -\frac{1}{\nu_F^2} \omega_1 \omega_2 \omega_3 \omega_4 (\omega_2 - i) + \mathcal{O}(\nu_F^{-4}) \, , & \end{aligned} \tag{2.7.39}$$

as the two-to-two scattering amplitude.

Two-to-three scattering. To obtain the two-to-three amplitude we consider the connected correlation function (6.0.17). We are then looking for terms in

proportional to

$$e^{-i\omega_1 u_1 - i\omega_2 u_2 - i\omega_3 u_3 + i\omega_4 u_4 + i\omega_5 u_5}\,\delta(\omega_1+\omega_2+\omega_3+\omega_4+\omega_5)\,S(\omega_1,\omega_2,\omega_3\,|\,\omega_4,\omega_5) \tag{2.7.40}$$

with $\omega_1,\omega_2,\omega_3$ outgoing and positive and ω_4,ω_5 incoming negative. The above expression defines for us the scattering amplitude for two-to-three scattering. Additionally we assume

$$\omega_3 > \omega_2 > \omega_1\ , \quad \omega_5 > \omega_4\ , \quad \omega_3 > -\omega_4\ , \quad \omega_2 < -\omega_5\ , \quad \omega_1 < -\omega_5\ , \tag{2.7.41}$$

and $x_1 > x_2 > x_3 > x_4 > x_5$. In particular (2.7.41) implies that $\omega_3 = \max\{\omega_1,\omega_2,\omega_3,|\omega_4|,|\omega_5|\}$. We then find :

$$\begin{aligned}
&S(\omega_1,\omega_2,\omega_3\,|\,\omega_4,\omega_5)\\
&\equiv e^{-i(\omega_4+\omega_5)\log(-\nu_F)}\Bigg[\int_0^{\omega_1}\mathrm{d}\upsilon\, R_{\nu_F-\upsilon-\omega_2-\omega_4}R^*_{\nu_F-\upsilon+\omega_1+\omega_5}R_{\nu_F-\upsilon+\omega_1}R^*_{\nu_F-\upsilon-\omega_2}\\
&-\int_{\omega_4}^{\omega_1+\omega_4}\mathrm{d}\upsilon\, R_{\nu_F-\upsilon-\omega_3-\omega_5}R^*_{\nu_F-\upsilon+\omega_4}R_{\nu_F-\upsilon}R^*_{\nu_F-\upsilon-\omega_3}-\int_{\omega_2+\omega_3}^{\omega_1+\omega_2+\omega_3}\mathrm{d}\upsilon\, R_{\nu_F-\upsilon-\omega_4-\omega_5}R^*_{\nu_F-\upsilon}\\
&-\int_{\omega_5}^{\omega_1+\omega_5}\mathrm{d}\upsilon\, R_{\nu_F-\upsilon-\omega_3-\omega_4}R^*_{\nu_F-\upsilon+\omega_5}R_{\nu_F-\upsilon}R^*_{\nu_F-\upsilon-\omega_3}+\int_{\omega_3}^{\omega_1+\omega_3}\mathrm{d}\upsilon\, R_{\nu_F-\upsilon-\omega_4-\omega_5}R^*_{\nu_F-\upsilon}\\
&+\int_0^{\omega_1}\mathrm{d}\upsilon\, R_{\nu_F-\upsilon-\omega_2-\omega_5}R^*_{\nu_F-\upsilon+\omega_1+\omega_4}R_{\nu_F-\upsilon+\omega_1}R^*_{\nu_F-\upsilon-\omega_2}+\int_0^{\omega_1}\mathrm{d}\upsilon\, R_{\nu_F-\upsilon-\omega_4-\omega_5}R^*_{\nu_F-\upsilon}\\
&-\int_{\omega_2}^{\omega_1+\omega_2}\mathrm{d}\upsilon\, R_{\nu_F-\upsilon-\omega_4-\omega_5}R^*_{\nu_F-\upsilon}\Bigg]=\frac{i}{\nu_F^3}\omega_1\omega_2\omega_3\omega_4\omega_5(\omega_3-i)(\omega_1+\omega_2+\omega_3-2i)+\mathcal{O}\left(\nu_F^{-5}\right)\ .
\end{aligned} \tag{2.7.42}$$

We note that any two-to-n amplitude contains factors of either two or four reflection coefficients.

In such a way we can continue to compute higher amplitudes from our basic building blocks. We thus observe the emergence of a perturbative S-matrix admitting a small $1/\nu_F$ expansion. So far, we obtained the S-matrix directly from the large N quantum mechanical matrix model. It is natural to ask whether the same S-matrix can be obtained directly from some weakly coupled system. Before turning to this we summarise the results of the $(n-m)$-to-m scattering amplitudes $S(\omega_1,\ldots,\omega_m\,|\,\omega_{m+1},\ldots,\omega_n)$ calculated in this section and appendix 6.

$*$	$S(\omega_1 \,\vert\, \omega_2)$	$S(\omega_1, \omega_2 \,\vert\, \omega_3)$	$S(\omega_1, \omega_2, \omega_3 \,\vert\, \omega_4)$
ν_F^0	ω_1	0	0
ν_F^{-1}	0	$i\omega_1\omega_2\omega_3$	0
ν_F^{-2}	$\frac{1}{24}\left(i\omega_1^2 - \omega_1^4(\omega_1 - 2i)\right)$	0	$-\omega_1\omega_2\omega_3\omega_4(\omega_4 + i)$
ν_F^{-3}	0	$-\frac{i}{24}\,\omega_1\omega_2 \prod_{k=0}^{2}(\omega_3 + ki)$ $\times\left(\sum_{\ell=1}^{2}\omega_\ell(\omega_\ell - i) + 1\right)$	0
ν_F^{-4}	x	0	$\frac{1}{24}\,\omega_1\omega_2\omega_3 \prod_{k=0}^{3}(\omega_4 + ki)$ $\times\left(\sum_{\ell=1}^{3}\omega_\ell(\omega_\ell - i) + 1\right)$
	0	x	0
	x	0	x

Table 2.1: *Each box contains the contribution to the scattering amplitude at the inverse power of ν_F in the leftmost box. An x indicates a nonzero result easily obtained by expanding the reflection coefficients to higher order in $1/\nu_F$. Within $S(\omega_1, \ldots, \omega_{n-1} \,\vert\, \omega_n)$, ω_n denotes the incoming (negative) frequency, whereas $\{\omega_1, \ldots, \omega_{n-1}\}$ denote the $n-1$ outgoing (positive) frequencies.*

$*$	$S(\omega_1,\omega_2\,\vert\,\omega_3,\omega_4)$	$S(\omega_1,\omega_2\,\vert\,\omega_3,\omega_4,\omega_5)$	$S(\omega_1,\omega_2,\omega_3\,\vert\,\omega_4,\omega_5)$
	0	0	0
ν_F^{-2}	$-\omega_1\omega_2\omega_3\omega_4(\omega_2-i)$	0	0
ν_F^{-3}	0	$-i\omega_1\omega_2\omega_3\omega_4\omega_5$ $\times(\omega_2-i)(\omega_2-2i)$	$i\omega_1\omega_2\omega_3\omega_4\omega_5$ $\times(\omega_3-i)(\omega_1+\omega_2+\omega_3-2i)$
ν_F^{-4}	x	0	0
ν_F^{-5}	0	x	x
	x	0	0
	0	x	x

Table 2.2: *Summary of the scattering amplitudes calculated in this section and appendix 6. Each box contains the contribution to the scattering amplitude at the inverse power of ν_F in the leftmost box. An x indicates a nonzero result easily obtained by expanding the reflection coefficients to higher order in $1/\nu_F$. Within $S(\omega_1,\ldots,\omega_m\,\vert\,\omega_{m+1},\ldots,\omega_n)$, $\{\omega_{m+1},\ldots,\omega_n\}$ denote the $n-m$ incoming (negative) frequencies and $\{\omega_1,\ldots,\omega_m\}$ the m outgoing (positive) frequencies. Note in particular that we choose an ordering of the frequencies which implies that ω_2 is the maximum for the two-to-two and three-to-two amplitude, whereas ω_3 is the maximum for the two-to-three amplitude.*

2.8 A glimpse into the continuum

Up until this point, we have focused on the large N limit of a variety of systems. We have mentioned on several instances that upon taking the large N limit, and further tuning certain coefficients, the systems often exhibit certain critical behaviour. In the case of large N matrices, one might then imagine the emergence of a continuous theory residing on a genus h Riemann surface Σ_h. The goal of this section is to briefly elaborate on these two-dimensional continuum theories.

2.8.1 Random pure geometry in two-dimensions

We begin our discussion by considering a theory of pure geometry in two-dimensions. The question of interest is as follows. Let us endow a compact genus h Riemann surface, Σ_h, with a metric g_{ij}. The most general local, diffeomorphism invariant,

two-derivative action is given by

$$S_{\text{grav}}[g_{ij};\Sigma_h] = -\frac{\vartheta}{4\pi}\int_{\Sigma_h} \mathrm{d}^2x\sqrt{g}\,R + \Lambda\int_{\Sigma_h}\mathrm{d}^2x\sqrt{g}\ , \tag{2.8.1}$$

where ϑ and Λ are real parameters and R is the Ricci scalar. By the Gauss-Bonnet theorem, the first term is a topological invariant proportional to the Euler characteristic χ_h. The second term, which is the cosmological constant term, computes the area of the surface. Motivated by the continuum limit of the discrete picture discussed in section 2.3 and the resulting expression (2.3.79), we are prompted to study the path integral

$$\mathcal{Z}_{\Sigma_h}[\vartheta;\Lambda] = e^{\vartheta\,\chi_h}\int\frac{\mathcal{D}g_{ij}}{\text{vol diff}}\,\exp\left(-\Lambda\int_{\Sigma_h}\mathrm{d}^2x\sqrt{g}\right)\ . \tag{2.8.2}$$

At this stage, it is useful to recall that a two-dimensional metric is diffeomorphic, at least locally, to the following

$$g_{ij}(x) = e^{\varphi(x)}\tilde{g}_{ij}(x)\ , \tag{2.8.3}$$

where $\tilde{g}_{ij}$ is a fixed reference metric, often referred to as the fiducial metric, and $\varphi(x)$ is a local Weyl factor that remains unfixed. The parameterization (2.8.3) leaves a particular subgroup of diffeomorphisms unfixed. Indeed, if we consider the set of coordinate transformations that map $\tilde{g}_{ij}$ to itself times a local Weyl factor $e^{\sigma(x)}$, we can return to the original expression by shifting $\varphi(x)\to\varphi(x)-\sigma(x)$. That the group of residual diffeomorphisms in the gauge (2.8.3) is the two-dimensional conformal group will play an important role in what comes. In fact, the transformation

$$\tilde{g}_{ij}(x)\to e^{\tilde{\sigma}(x)}\tilde{g}_{ij}(x)\ ,\qquad \varphi(x)\to\varphi(x)-\tilde{\sigma}(x) \tag{2.8.4}$$

for general $\tilde{\sigma}(x)$ is a redundancy of the parameterization (2.8.3). As such, the resulting theory governing $\varphi(x)$ and the accompanying Fadeev-Popov ghost fields should be invariant under the more general Weyl transformations (2.8.4). In the gauge (2.8.3), the ghost theory is described by a conformal field theory of bc-ghosts in a fixed background $\tilde{g}_{ij}$ whose central charge is $c_g=-26$. The resulting theory consisting of the $\mathfrak{bc}$-ghosts and the φ-field should be invariant under the redundancy (2.8.4). Thus, the theory governing the Weyl mode $\varphi(x)$ must be a two-dimensional conformal field theory with central charge $c_L=26$ such that the net conformal anomaly vanishes. If we further assume the φ-sector admits a local

description, one can postulate an action of the following type [29, 30]

$$S_L[\varphi, \tilde{g}_{ij}] = \frac{1}{4\pi} \int_{\Sigma_h} \mathrm{d}^2x \sqrt{\tilde{g}} \left(\tilde{g}^{ij} \partial_i \varphi \partial_j \varphi + Q \tilde{R} \varphi + 4\pi \Lambda \, e^{2b\varphi} \right) \ . \tag{2.8.5}$$

The above action is known as the Liouville action and has been studied extensively [33, 35, 73]. In order for the kinetic term to have a standard normalisation, we have allowed for a constant rescaling of φ by $2b$, such that the resulting theory should be invariant under the following redundancy

$$\tilde{g}_{ij}(x) \to e^{\tilde{\sigma}(x)} \tilde{g}_{ij}(x) \ , \qquad \varphi(x) \to \varphi(x) - \tilde{\sigma}(x)/2b \ . \tag{2.8.6}$$

When $Q = b + 1/b$, the Liouville action describes a two-dimensional conformal field theory. It has some unusual features such as a continuous spectrum and the absence of a normalisable vacuum state. Nevertheless, it admits a consistent quantisation and many of its properties are known explicitly. For instance, its central charge is given by $c_L = 1 + 6Q^2$, and the theory contains spinless primary operators $\mathcal{O}^{(\alpha)} = e^{2\alpha\varphi}$ whose conformal dimensions are

$$\Delta_\alpha = \alpha \left(Q - \alpha \right) \ , \qquad \bar{\Delta}_\alpha = \alpha \left(Q - \alpha \right) \ . \tag{2.8.7}$$

These conformal dimensions can be used to fix b in (2.8.5), since conformal invariance requires $\mathcal{O}^{(b)} = e^{2b\varphi}$ to have conformal dimensions $(\Delta_b, \bar{\Delta}_b) = (1, 1)$. One thus finds

$$b = \frac{Q}{2} \pm \sqrt{\frac{Q^2}{4} - 1} \ . \tag{2.8.8}$$

Requiring $c_L + c_g = 0$ fixes $Q = \pm 5/\sqrt{6}$. Given the discrete symmetry $Q \to -Q$, $b \to -b$, and $\varphi \to -\varphi$, we can pick $Q > 0$ without loss of generality. One then finds the two solutions $b = b_\pm$ with $b_+ = \sqrt{3/2}$ and $b_- = \sqrt{2/3}$. If one further requires the existence of a semi-classical limit, i.e. a limit where $Q \to \infty$ gives rise to a sensible saddle-point approximation, one is forced to pick the negative root in (2.8.8). We will consider the negative root in what follows even in the absence of a semiclassical limit.

In this way we obtain a description of the path integral for a theory of pure two-dimensional geometry in terms of Liouville theory. A natural collection of observables is given by the set of diffeomorphism invariant functionals of g_{ij}. In the Weyl gauge, this is given by the set of conformal primaries built from φ with conformal dimensions $\left(\Delta, \bar{\Delta}\right) = (1, 1)$. A particularly important one is the area operator

$$\mathcal{A}_h = \int_{\Sigma_h} \mathrm{d}^2x \sqrt{g} = \int_{\Sigma_h} \mathrm{d}^2x \sqrt{\tilde{g}} \, e^{2b\varphi} \ , \tag{2.8.9}$$

where b is given by (2.8.8). Expectation values of $\mathcal{A}_h$ are calculated by taking derivatives of $-\log \mathcal{Z}_{\Sigma_h}[\vartheta;\Lambda]$ with respect of Λ.

2.8.2 Sprinkling matter

Generally speaking a local quantum field theory can be placed on an arbitrary curved background. If the theory has no diffeomorphism anomaly, we can further gauge the diffeomorphism group. Thus, it would seem we can couple arbitrary matter content to two-dimensional gravity. Following this reasoning, and going to the Weyl gauge (2.8.3), a consistent theory of matter coupled to two-dimensional gravity is described by the following action

$$S_{\text{eff}} = S_L[\varphi, \tilde{g}_{ij}] + S_{\text{ghost}}[\mathfrak{b}, \mathfrak{c}, \tilde{g}_{ij}] + S_{\text{matter}}[X, \varphi, \tilde{g}_{ij}] \ . \tag{2.8.10}$$

Invariance under the redundancy (2.8.4) and the residual diffeomorphisms implies that the above theory must be a two-dimensional conformal field theory with vanishing central charge. This statement must be true, curious as it may sound, even for a massive matter theory. Somehow, the Liouville mode must 'dress' the matter theory in such a way as to make the resulting system conformal. Of course, given that the original matter theory is not conformal, the resulting conformal theory obtained upon coupling to the Liouville mode must be strongly interacting even if the original matter theory is not [147].

In what follows we will consider the simpler situation, namely, a matter theory which is itself a two-dimensional conformal field theory with central charge c_m. In this case, the matter action S_{matter} becomes solely a function of the matter fields and $\tilde{g}_{ij}$. However, the path integration measures for the matter and ghost fields produce the Liouville action in the Weyl gauge [8].[5] Thus, one can postulate that (2.8.5) continues to govern the φ sector, except now we must fix the parameters Q and b such that $c_L + c_m - 26 = 0$. Proceeding along similar lines to the previous sub-section, we end up with the expressions

$$Q = \sqrt{\frac{25 - c_m}{6}} \ , \qquad b = \frac{\sqrt{25 - c_m} \pm \sqrt{1 - c_m}}{2\sqrt{6}} \ . \tag{2.8.11}$$

For $c_m = 0$, we recover (2.8.8).

The expressions (2.8.11) demonstrate an important point. The resulting theory is highly sensitive to c_m. For $c_m \leq 1$, we have that b is real and positive. For $c_m \in (1, 25)$ the parameter b becomes complex with non-vanishing real and imaginary

[5] More generally, there is no reason to insist on the existence of a matter action. The relevant point is that the conformal anomaly of a two-dimensional conformal field theory on the background (2.8.3) is governed by the Liouville theory.

parts, while Q remains real. Finally, for $c_m \geq 25$, we have that b and Q become pure imaginary. If we take $c_m = 25$ and tune $\Lambda = 0$, we observe that (2.8.5) reduces to the action of a free scalar, such that our resulting theory is nothing more than the critical bosonic string. All other cases describe non-critical string theories.

In the presence of matter, we can extend the space of admissible observables. For instance, a spinless weight (Δ, Δ) conformal primary $\mathcal{O}_\Delta$ of the matter theory can be combined with the Liouville exponential operator to produce a 'dressed' operator $\tilde{\mathcal{O}}_\Delta = e^{2\sigma\varphi}\mathcal{O}_\Delta$ with

$$\sigma = \frac{\sqrt{25 - c_m} \pm \sqrt{24\Delta + 1 - c_m}}{2\sqrt{6}} \ . \tag{2.8.12}$$

In this way, we can obtain a significant collection of observables. It is worth noticing that for certain values of c_m and Δ, σ may become complex. For such situations, $\mathcal{O}^{(\sigma)} = e^{2\sigma\varphi}$ becomes a complex (rather than Hermitian) operator. To render it Hermitian we can consider linear combinations of $\mathcal{O}^{(\sigma)}$ with its complex conjugate.

Small and/or negative central charge. The most understood situation occurs when $c_m < 1$. For example, we could take the matter conformal field theory to be one of the minimal models [27, 28] with central charge

$$c_m^{(p,q)} = 1 - \frac{6(p-q)^2}{pq} \ , \qquad (p,q) \ \text{coprime} \ , \tag{2.8.13}$$

and operators of conformal dimension

$$\Delta_{r,s} = \frac{(rq - sp)^2 - (p-q)^2}{4pq} \ , \quad r = 1, \ldots, p-1 \ , \quad s = 1, \ldots, q-1 \ . \tag{2.8.14}$$

The limit $c_m \to -\infty$ leads to a parameterically large Q and, for the negative branch, a parametrically small b. In this limit, the system is driven to a semi-classical regime where saddle point techniques may be employed. Though there are several known minimal models with large and negative c_m, they are all non-unitary.[6]

Large central charge. For $c_m > 25$, we could imagine a contour rotation $\varphi \to i\varphi$ that yields the action (2.8.5) real. This comes at the price (or perhaps reward) of changing the sign of the kinetic term of φ. In critical string theory, we would

[6] Nevertheless, upon coupling to gravity many of the states in the original matter theory are removed from the resulting Hilbert space possibly rendering the non-unitarity less severe.

interpret a wrong sign scalar as a time-like direction in the target space. Perhaps the same is true for $c_m > 25$, in which case non-critical string theory might provide an interesting window into time-dependent backgrounds in string theory. In such circumstances caution must be exercised, as many of the techniques we understand require rotating time-like target space coordinates back to their spacelike values, which for $c_m > 25$ would take us back to a complex action.

Intermediate central charge. For $c_m \in (1, 25)$ the situation is far less understood. In this case, the action is intrinsically complex, and new methods are required to deal with it. Curiously, and perhaps interestingly, this case includes a matter conformal field theory with $c_m = 3$ and $c_m = 4$.

Matter matters

The regime $c_m \in (1, 25)$ teaches us an important lesson. The ability to couple a particular matter theory to gravity at the classical level does not guarantee that the combined system makes sense at the quantum level. Even if sense can be made of the path integral for a matter theory with $c_m \in (1, 25)$, it seems the resulting theory will not resemble an ordinary theory of two-dimensional geometry. The difficulties surrounding the $c_m > 1$ regime have been dubbed the $c_m > 1$ *barrier* in the literature.

In the next section we will discuss several contexts in which this barrier has been surpassed. As a general rule, addressing which matter theories can indeed be consistently coupled to gravity at the quantum level, particularly in higher-dimensions, seems to require a more complete understanding of the theory in the deep ultraviolet.

2.8.3 Critical exponents & the area operator

At this stage we have equipped ourselves with the necessary tools to compute the following quantity

$$\tilde{\mathcal{Z}}_{\Sigma_h}[\upsilon;\Lambda] = \int \frac{\mathcal{D}g_{ij}}{\text{vol diff}} \mathcal{D}_{g_{ij}} X \, e^{-S_{\text{grav}}[g_{ij}]-S_{\text{matter}}[X,g_{ij}]} \, \delta\left(\int_{\Sigma_h} \mathrm{d}^2x\sqrt{g} - \upsilon\right) . \tag{2.8.15}$$

The δ-function in the above expression fixes the area to the particular value υ. By fixing the area operator (2.8.9) to take a fixed value, the fixed area partition function (2.8.15) tames any potential divergences in the original path integral which can subsequently be analysed in a clearer fashion.

Once again, resorting to the Weyl gauge (2.8.3) and keeping in mind the rescaling of φ, we can make progress in evaluating (2.8.15). We obtain the path integral

expression

$$\tilde{\mathcal{Z}}_{\Sigma_h}[\upsilon;\Lambda] = e^{\vartheta\,\chi_h}\int\frac{\mathcal{D}\varphi}{\mathrm{vol}\,\mathcal{G}}\,e^{-S_L[\varphi,\tilde{g}_{ij}]}\,\delta\left(\int_{\Sigma_h}\mathrm{d}^2x\sqrt{\tilde{g}}\,e^{2b\varphi}-\upsilon\right)\,. \tag{2.8.16}$$

Any local ultraviolet divergences arising upon integrating out the matter and ghost fields are absorbed in the bare couplings of the gravitational theory. The group $\mathcal{G}$ is the residual gauge group upon fixing the Weyl gauge. For instance, when $h=0$ we could fix $\tilde{g}_{ij}$ to be the round metric on the two-sphere in which case $\mathcal{G}=PSL(2,\mathbb{C})$. In contrast to the critical string, dividing by the potentially divergent volume of $\mathcal{G}$ does not mean that the partition function vanishes. This is due to the fact that φ transforms non-trivially under the residual gauge transformations.

Given (2.8.16), the approach is to consider a constant shift $\varphi\to\varphi+\log\upsilon^{1/2b}$ that allows us to remove υ from the δ-function while only affecting the remaining Liouville theory in a simple way [29, 30]. Using $\delta(\zeta x)=\delta(x)/|\zeta|$ and (2.8.5) it is readily found that

$$\tilde{\mathcal{Z}}_{\Sigma_h}[\upsilon;\Lambda] = \mathcal{N}_h\,e^{\vartheta\chi_h}\,e^{-\Lambda\upsilon}\,\upsilon^{-Q\chi_h/2b-1}\,, \tag{2.8.17}$$

where $\mathcal{N}_h$ is a normalisation constant that may depend on the genus h but is independent of υ, ϑ, and Λ. We recall that b is given by (2.8.11). The continuum partition function can be recovered by integrating over υ as follows

$$\mathcal{Z}_{\Sigma_h}[\vartheta;\Lambda] = e^{\vartheta\chi_h}\int_0^\infty\mathrm{d}\upsilon\,\tilde{\mathcal{Z}}_{\Sigma_h}[\upsilon;\Lambda] = \mathcal{N}_h\,e^{\vartheta\chi_h}\,\Lambda^{\frac{Q\chi_h}{2b}}\,\Gamma\left(-Q\chi_h/2b\right)\,,\qquad h\neq 1\,, \tag{2.8.18}$$

where we have regularised the integral near $\upsilon=0$ by analytic continuation. When $h=1$ the resulting expression is logarithmic in Λ, regardless of the value of $Q/2b$.

It is tempting to view (2.8.18) from the perspective of critical systems near a phase transition, with Λ being a tuneable parameter driving the system towards criticality. To this end, it is customary in the literature to define a critical exponent $\Gamma_{\mathrm{str}}\equiv 2-Q/b$, often referred to as the string susceptibility. Combining Q and b in (2.8.11) and choosing the negative branch for b, we obtain the KPZ relation [143]

$$\Gamma_{\mathrm{str}} = \frac{1}{12}\left(c_m-1-\sqrt{(c_m-1)(c_m-25)}\right)\,. \tag{2.8.19}$$

Some examples are given by [54–56, 118, 119, 123]

$$\left(\Gamma_{\mathrm{str}},Q/2b\right) = \begin{cases}(-1/2,5/4) & \text{for} \quad c_m=0\,,\\ (-1/3,7/6) & \text{for} \quad c_m=1/2\,,\\ (0,1) & \text{for} \quad c_m=1\,.\end{cases} \tag{2.8.20}$$

At large negative c_m we have

$$\mathcal{Z}_{\Sigma_h}[\vartheta;\Lambda] = \tilde{\mathcal{N}}_h\, e^{\vartheta\chi_h}\left(\frac{1}{\sqrt{\Lambda}}\right)^{\frac{c_m\chi_h}{6}} , \tag{2.8.21}$$

where $\tilde{\mathcal{N}}_h$ is again independent of Λ. For genus zero (2.8.21) is reminiscent of the partition function of a CFT of central charge c_m on a round two-sphere with Ricci scalar $\tilde{R} = 2\Lambda$ [146], and consequently an entanglement entropy [157–159]. For a genus h Riemann surface (2.8.21) is reminiscent of the partition function obtained from Euclidean $\mathrm{AdS}_3/\mathrm{CFT}_2$ considerations at large positive central charge (see for instance [145]).

A gravitational conformal weight

When coupling a conformal field theory to gravity, one is naturally led to the question of what replaces the conformal weights of a spinless conformal primary $\mathcal{O}_\Delta$. One way to quantify this is by computing the following quantity

$$\begin{aligned}\langle\mathcal{O}_\Delta\rangle_\upsilon = \frac{1}{\tilde{\mathcal{Z}}_{\Sigma_h}[\upsilon;\Lambda]} \times e^{\vartheta\,\chi_h}\int\frac{\mathcal{D}\varphi}{\mathrm{vol}\,\mathcal{G}}\mathcal{D}X\, e^{-S_L[\varphi,\tilde{g}_{ij}]-S_{\mathrm{matter}}[X,\tilde{g}_{ij}]} \\ \delta\left(\int_{\Sigma_h}\mathrm{d}^2x\sqrt{\tilde{g}}\,e^{2b\varphi}-\upsilon\right)\int_{\Sigma_h}\mathrm{d}^2x\sqrt{\tilde{g}}\,e^{2\sigma\varphi}\mathcal{O}_\Delta\ ,\end{aligned} \tag{2.8.22}$$

where σ was given in (2.8.12) and b in (2.8.11). Once again, using the technique of [29, 30], we can shift $\varphi \to \varphi + \log\upsilon^{1/(2b)}$ to conclude

$$\langle\mathcal{O}_\Delta\rangle_\upsilon = \mathcal{N}_h\,\upsilon^{\sigma/b} , \tag{2.8.23}$$

with a υ-independent normalisation constant $\mathcal{N}_h$. Rescaling the area parameter $\upsilon \to k^2\upsilon$ we find $\langle\mathcal{O}_\Delta\rangle_\upsilon \to k^{2\sigma/b}\langle\mathcal{O}_\Delta\rangle_\upsilon$. In an ordinary two-dimensional conformal field theory, an integrated spinless conformal operator with weights $(\tilde{\Delta},\tilde{\Delta})$ would scale as $k^{2(1-\tilde{\Delta})}$. We are thus prompted to define the quantity $\Delta_{\mathrm{grav}} \equiv 1-\sigma/b$ as the gravitational analogue of the conformal weight. Explicitly

$$\Delta_{\mathrm{grav}} = \frac{\sqrt{24\Delta+1-c_m}-\sqrt{1-c_m}}{\sqrt{25-c_m}-\sqrt{1-c_m}} , \tag{2.8.24}$$

which is our second KPZ relation. For the identity operator both $\Delta = 0$ and $\Delta_{\mathrm{grav}} = 0$. We also have that $\Delta_{\mathrm{grav}} = 1$ when $\Delta = 1$. For large and negative c_m we have $\Delta_{\mathrm{grav}} = \Delta + \mathcal{O}(1/c_m)$. More generally, the two differ.

2.8.4 Large N matrices & the continuum

We are now in a position to connect the continuum description developed in this section to the matrix models we examined throughout the previous ones.

Single matrix integrals. Let us consider first the integrals over single matrices considered in section 2.3. There, we argued for the existence of a continuum limit in which the expectation number $\langle n_h \rangle$ defined in (2.3.77) diverges as we approach a critical coupling. We presented evidence that near criticality and at large N

$$\mathcal{F}_N(\alpha) \approx \sum_{h=0}^{\infty} f_h \, e^{\chi_h \log N} \, (\alpha - \alpha_c)^{5\chi_h/4} \ . \tag{2.8.25}$$

How should we compare the above to our continuum expressions? We might expect that the sum (2.3.70) should be viewed as the discrete version of the pure geometry path integral (2.8.2), with $\vartheta = \log N$. In such a case, we should compare the critical limit (2.3.78) to (2.8.18). Using the $c_m = 0$ result for $Q/2b$, and recalling (2.3.78), we conclude that the cosmological constant of the continuum theory Λ is propotional to the deviation from criticality, i.e. $\Lambda \propto (\alpha - \alpha_c)$. Notice that we recover the logarithmic behaviour in (2.4.28) for $h = 1$.

That the continuum cosmological constant is defined as a deviation from the critical coupling α_c is part of a recurring theme. It is the same theme that led us to consider physics just above the filled Fermi sea.

Multicritical matrix model. It has been argued [16, 103, 110] that multicritical matrix models correspond to two-dimensional gravity coupled to a non-unitary minimal CFT (2.8.13) with $(p, q) = (2, 2m - 1)$ and string susceptibility $\Gamma_{\rm str} = -1/m$. For instance, the multicritical model discussed in (2.3.51) corresponds to $m = 3$: i.e. two-dimensional gravity coupled to the Lee-Yang minimal model with $c_m = -22/5$. For these models, one has to use a slightly modified version [110] of the KPZ relation due to the presence of negative weight operators in the spectrum of the matter CFT. It is remarkable that tuning the parameters of $V(M)$ for a *single* matrix leads to a continuum description of gravity coupled to conformal field theories with varying central charges.

Double matrix integrals. Given (2.5.34) and using $\Lambda \propto (\alpha - \alpha_c)$ one is led to a theory with $Q/(2b) = 7/6$. Looking at (2.8.20) we see that this occurs for $c_m = 1/2$. It is natural to propose [118] that the two matrix model corresponds to $c_m = 1/2$ matter, and in particular two-dimensional gravity coupled to a free massless fermion. The free massless fermion in two dimensions is a minimal model which has three spinless conformal primaries, namely the identify operator with

$\Delta_0 = 0$, the σ-operator with $\Delta_\sigma = 1/16$, and the energy operator with $\Delta_\epsilon = 1/2$. These operators are sourced by the cosmological constant Λ, the magnetic field H and the temperature β. These sources make their appearance in the matrix model as simple functions of the couplings α, g, and c of the potential (2.5.40). Using (2.8.24) we infer the gravitational conformal weight of these primaries to be $\Delta_{\text{grav},0} = 0$, $\Delta_{\text{grav},\sigma} = 1/6$, and $\Delta_{\text{grav},\epsilon} = 2/3$. These were obtained from considerations of the generalised two-matrix model (2.5.40) in [110] where it was found that there are certain non-analyticities of the large N two-matrix integral with potential (2.5.40) upon tuning α, c, and g. The critical coefficients stemming from these non-analyticities are expressed in terms of the gravitational conformal weights $\Delta_{\text{grav},0}$, $\Delta_{\text{grav},\epsilon}$, and $\Delta_{\text{grav},\sigma}$ via the scaling relations of the two-dimensional Ising model. Concretely, the critical exponents associated to c and g, which we denote by $\boldsymbol{\alpha}$ and $\boldsymbol{\beta}$ respectively, are related to the gravitational conformal weights as

$$\boldsymbol{\alpha} = \frac{1 - 2\Delta_{\text{grav},\epsilon}}{1 - \Delta_{\text{grav},\epsilon}} = -1 \ , \qquad \boldsymbol{\beta} = \frac{\Delta_{\text{grav},\sigma}}{1 - \Delta_{\text{grav},\epsilon}} = \frac{1}{2} \ . \tag{2.8.26}$$

It might be worth recalling that a free massless fermion describes the critical behaviour of the two-dimensional Ising model. The Ising model has two states at every point on the lattice. This may remind us, somewhat, of the decorated Feynman diagrams discussed in section 2.5.3. This bears some truth, but caution should be exercised before decorating the Feynman diagrams too elaborately. For instance, the continuum limit of mulitcritical single matrix models corresponds to non-unitary minimal models with $c_m < 0$ coupled to gravity. It has been further argued [120, 121] that the whole remaining family of minimal models can be obtained from particularly selected two-matrix models.

Upon coupling a minimal model to two-dimensional quantum gravity one obtains a new set of dressed and integrated operators generalising to the area operator in (2.8.22). In addition to their gravitional conformal weights (2.8.24), one can also study the correlation functions of these operators and compare them to quantities obtained from matrix integral calculations. Work in this direction includes [161, 162, 166–168].

Non-perturbative features from the continuum. In our discussion of large N matrices we touched upon the possibility of non-perturbative corrections to the planar expansion. In the double scaling limit, these manifest themselves in terms of small WKB type corrections of the series expansion solutions to the various non-linear differential equations, such as the Painlevé I equation. We are naturally led to the question of whether such non-perturbative terms can be recovered in the continuum picture.

In [188] it was shown that Liouville theory can be studied on the disk topology, which is a manifold with a boundary. In this case, the Liouville field diverges near the boundary of the disk. Taking the metric $\tilde{g}_{ij}$ on the disk to be $\mathrm{d}s^2 = \mathrm{d}\rho^2 + \rho^2 \mathrm{d}\theta^2$ with $\rho \in (0,1)$, in the semiclassical $b \to 0$ limit the solution of φ is given by

$$e^{2b\varphi_{cl}} = \frac{1}{\pi b^2 \Lambda} \frac{1}{(1-\rho^2)^2} \,, \tag{2.8.27}$$

such that the physical metric $g_{ij} = e^{2b\varphi}\tilde{g}_{ij}$ is the Poincaré disk. The authors of [188] showed the existence of a family of boundary states labelled by two integers (m,n). These configurations are known as ZZ-branes or instantons. Processes involving Liouville theory on the disk have been argued [137,190,191] to be related to non-perturbative features in the matrix models. For instance, [189] recovered the exponent (2.4.36) and (2.5.38) of the non-perturbative corrections in the double scaling limit by calculating the Liouville disk partition function. In [160], the ZZ-instantons were interpreted as single eigenvalues sitting on critical points of the potential away from the dense eigenvalue distribution.

There is another type of boundary condition that arises in the study of Liouville theory on a disk topology. Here, one adds a boundary interaction [186,187]

$$S_{\mathrm{bdy}} = \int_{S^1} \mathrm{d}u \sqrt{h} \left(\frac{Q}{2\pi} K\varphi + \Lambda_B e^{b\varphi} \right) \tag{2.8.28}$$

to the Liouville action (2.8.5). The boundary cosmological constant Λ_B is a new continuous parameter labelling the states in this theory. The induced metric at the S^1 boundary of the disk is h and K is the extrinsic curvature at the boundary. Λ_B can be viewed as a chemical potential for the size of the boundary of the physical metric on a disk topology. For $\Lambda_B > 0$, the boundary action S_{bdy} suppresses configurations at large values of φ. These configurations are known as FZZT branes and can be viewed as extended across the weakly coupled region $\varphi \lesssim -(\log \Lambda_B)/b$. From the matrix model perspective, an interpretation of the FZZT brane should be an object that is parameterised by a continuous variable. Once again, one may ask whether FZZT branes are related to non-perturbative features of the matrix integral. In [160], the FZZT branes were argued to be described by the single trace $\mathrm{Tr}\log(\Lambda_B - M)$. Indeed, the relation of $\mathrm{Tr}\log(\Lambda_B - M)$ to triangulated Riemann surfaces with a boundary was explored in section 2.3.5.

Quantum mechanical matrices. In the case of quantum mechanical matrices, we uncovered a rich structure in the form of a two-dimensional S-matrix. We now turn to its realisation in the continuum picture.

2.8.5 Scattering from the continuum

We now discuss how to recover the scattering discussed in the previous section from the continuum theory, in particular the one-to-one and one-to-two amplitudes. In order to do so, we must first understand what is being scattered in the continuum picture. For instance the two-dimensional theory (2.8.10) lives on a Euclidean compact surface Σ_h which has no asymptotic regions to scatter to and from. If, on the other hand, we view the two-dimensional theory as the worldsheet theory of a string propagating some target space, there may be room for a scattering amplitude in the assymptotia of the target space. To this end we take the $c_m = 1$ theory to be a free scalar field denoted by X^0. In particular for $c_m = 1$ we conclude using (2.8.11) that $b = 1$ and $Q = 2$. Our worldsheet theory is then given by

$$S_{\text{w.s.}} = -\frac{1}{4\pi}\int_{\Sigma_h} \mathrm{d}^2x\sqrt{\tilde{g}}\,\tilde{g}^{ij}\,\partial_i X^0\partial_j X^0 + \frac{1}{4\pi}\int_{\Sigma_h}\mathrm{d}^2x\sqrt{\tilde{g}}\left(\tilde{g}^{ij}\partial_i\varphi\partial_j\varphi + 2\tilde{R}\,\varphi + 4\pi\Lambda\, e^{2\varphi}\right) . \tag{2.8.29}$$

The free scalar X^0 encodes the time coordinate of the target space, and as such comes with a kinetic term with the wrong sign. The Liouville mode φ is then associated to the spatial coordinate of the target space, such that the target space is two-dimensional. Taking the contribution of the ghost conformal field theory into account, the net theory has vanishing central charge.[7] A string propagating in two-dimensions has no transverse excitations. Consequently, its spectrum is given by a single scalar field encoding the target space centre of mass position of the string. The natural asymptotic region in the target space is given by the region $\varphi \to -\infty$, where the Liouville interaction is switched off.

We can now compute the S-matrix elements as is done for more familiar worldsheet theories. We calculate the expectation value of several vertex operator insertions. For a free scalar we can construct conformal operators by exponentiating X^0. It follows from our discussion in section 2.8.2, that we can construct the dressed integrated vertex operator

$$\mathcal{V}^{\pm}_{\omega} = g_s\int_{\Sigma_h}\mathrm{d}^2x\sqrt{\tilde{g}}\;:e^{\pm i\omega X^0}:\mathcal{O}(\omega)\;, \qquad \omega \geq 0\;. \tag{2.8.30}$$

In the above, $\mathcal{O}(\omega)$ is taken to be a Hermitian Liouville operator of the form

$$\mathcal{O}(\omega) \equiv S(\omega)e^{(2+i\omega)\varphi} + S(\omega)^* e^{(2-i\omega)\varphi}\;, \qquad \omega \geq 0\;. \tag{2.8.31}$$

The phase factors have been chosen such that the two-point function of the Liou-

[7] Said otherwise, given that the central charge of a worldsheet matter theory consisting of a free scalar and the Liouville conformal field theory can be tuned to equal 26, we can regard the system as a bosonic critical string.

ville operator $\mathcal{O}(\omega; z, \bar{z})$ has standard δ-function normalisation

$$\langle \mathcal{O}(\omega_1; z_2, \bar{z}_2)\mathcal{O}(\omega_2; z_2, \bar{z}_2)\rangle = 2\pi\delta(\omega_1 - \omega_2) \times \frac{1}{|z_1 - z_2|^{4+\omega_1^2}} \ , \tag{2.8.32}$$

where z and $\bar{z}$ label points on $\mathbb{C}$, and we adhere to the conventions of [69] with $\alpha' = 1$. The phase factor is given by [33]

$$S(\omega) = \sqrt{\frac{\Gamma(i\omega)}{\Gamma(1-i\omega)}\frac{\Gamma(1+i\omega)}{\Gamma(-i\omega)}} \ . \tag{2.8.33}$$

To compute target space S-matrix elements we must calculate expectation values for the above vertex operators. The parameter ω corresponds to the energy of the asymptotic state, and the sign determines whether it is incoming (negative) or outgoing (positive).[8]

One-to-one from the continuum. We begin by considering the one-to-one amplitude in the continuum picture. For this, we require the expectation value for two vertex operator insertions on the two-sphere. Given the two-point function (2.8.32), and following the discussion in [182], one finds

$$A_{S^2}(\omega_1|\omega_2) = 2\pi\omega_1\delta(\omega_1 - \omega_2) \times \left(\frac{g_s^2 c_{S^2}}{4\pi}\right) \ , \tag{2.8.34}$$

where c_{S^2} is a coefficient which we will soon relate to the one-to-two amplitude. Comparing to (2.7.23) we fix $c_{S^2} = 4\pi/g_s^2$.

One-to-two from the continuum. Next we consider three insertions on a genus zero surface

$$A_{S^2}(\omega_1, \omega_2 \,|\, \omega_3) \equiv \langle \mathfrak{c}\tilde{\mathfrak{c}}\mathcal{V}^+_{\omega_1} \, \mathfrak{c}\tilde{\mathfrak{c}}\mathcal{V}^+_{\omega_2} \, \mathfrak{c}\tilde{\mathfrak{c}}\mathcal{V}^-_{\omega_3}\rangle_{S^2} \ . \tag{2.8.35}$$

We follow the presentation in [38]. To evaluate the above expression requires knowledge of the three-point function for the Liouville operator $\mathcal{O}(\omega; z, \bar{z})$

$$\begin{aligned}&\langle \mathcal{O}(\omega_1; z_1, \bar{z}_1)\, \mathcal{O}(\omega_2; z_2, \bar{z}_2)\, \mathcal{O}(\omega_3; z_3, \bar{z}_3)\rangle \\ &\qquad = \frac{\mathcal{C}(\omega_1, \omega_2, \omega_3)}{|z_{12}|^{2+(\omega_1^2+\omega_2^2-\omega_3^2)/2}|z_{23}|^{2+(\omega_2^2+\omega_3^2-\omega_1^2)/2}|z_{31}|^{2+(\omega_3^2+\omega_1^2-\omega_2^2)/2}} \ .\end{aligned} \tag{2.8.36}$$

This quantity was studied by Dorn-Otto [34] and Zamolodchikov-Zamolodchikov

[8] This is a different convention from our previous section where ω could take either sign. We choose it to comply with recent literature on Liouville theory.

[36] which gives it the name DOZZ formula. The structure constant $\mathcal{C}(\omega_1,\omega_2,\omega_3)$ is given by

$$\mathcal{C}(\omega_1,\omega_2,\omega_3) \equiv \left(S(\omega_1)S(\omega_2)S(\omega_3)\right)^{-1} C(\omega_1,\omega_2,\omega_3) \ , \tag{2.8.37}$$

with the DOZZ coefficient

$$\begin{aligned} C(\omega_1,\omega_2,\omega_3) = & \frac{\Upsilon_1'(0)}{\Upsilon_1(1+i(\omega_3+\omega_2+\omega_1)/2)} \frac{\Upsilon_1(2+i\omega_1)}{\Upsilon_1(1+i(\omega_1+\omega_2-\omega_3)/2)} \\ & \times \frac{\Upsilon_1(2+i\omega_2)}{\Upsilon_1(1+i(\omega_2+\omega_3-\omega_1)/2)} \frac{\Upsilon_1(2+i\omega_3)}{\Upsilon_1(1+i(\omega_3+\omega_1-\omega_2)/2)} \ . \end{aligned} \tag{2.8.38}$$

In the literature the three-point function contains an additional phase has been absorbed in a shift of the Liouville field. The function $\Upsilon_b(z)$ is a holomorphic function that admits an integral expression as

$$\log \Upsilon_b(z) = \int_0^\infty \frac{\mathrm{d}t}{t} \left[\left(\frac{Q}{2}-z\right)^2 e^{-t} - \frac{\sinh^2\left[\left(\frac{Q}{2}-z\right)\frac{t}{2}\right]}{\sinh\frac{tb}{2}\sinh\frac{t}{2b}} \right] \ , \tag{2.8.39}$$

where the real part of z is restricted to the interval $z \in (0,Q)$ and $b+b^{-1}=Q$. To evaluate $\Upsilon_b(z)$ at complex values of z we must analytically continue the above expression. It is useful to note that we can express $\Upsilon_b(z)$ in terms of the Barnes double Gamma-function $\Gamma_2(z\,|\,b_1,b_2)$:

$$\Upsilon_b(z) = \frac{1}{\Gamma_b(z)\Gamma_b(Q-z)} \ , \qquad \Gamma_b(z) \equiv \frac{\Gamma_2(z\,|\,b,b^{-1})}{\Gamma_2(Q/2\,|\,b,b^{-1})} \ . \tag{2.8.40}$$

In particular we have $\Gamma_2(z\,|\,1,1) = (2\pi)^{z/2}/G(z)$ with $G(z)$ being the Barnes G-function. $\Upsilon_b(z)$ also satisfies

$$\Upsilon_b(z+b) = \gamma(bz)\, b^{1-2bz}\, \Upsilon_b(z) \ , \quad \Upsilon_b(z) = \Upsilon_{b^{-1}}(z) \ , \quad \Upsilon_b(Q-z) = \Upsilon_b(z) \ , \tag{2.8.41}$$

with $\gamma(z) \equiv \Gamma(z)/\Gamma(1-z)$. The phase $S(\omega)$ in (2.8.33) can be expressed as $S(\omega) = \gamma(i\omega)^{1/2}\gamma(1+i\omega)^{1/2}$.

Additionally (2.8.30) contains a piece stemming from the operator $e^{\pm i\omega X^0}$. The structure constants for this piece (as may be familiar from the critical string) will not produce non-trivial functions of the ω_i. Nevertheless, due to the symmetry $X^0 \to X^0 + a$, it yields a delta-function imposing the conservation of target space energy.

At this point we have asembled the tools required to evaluate (2.8.35). Using the

relations (2.8.41) for $(Q,b)=(2,1)$ we can rewrite $\Upsilon_1(2+i\omega_k)$ as

$$\Upsilon_1(2+i\omega_k)=\Upsilon_1(2+i\omega_k)^{1/2}\Upsilon_1(2+i\omega_k)^{1/2}=\Upsilon_1(-i\omega_k)^{1/2}\Upsilon_1(i\omega_k)^{1/2}\gamma(i\omega_k)^{1/2}\gamma(-i\omega_k)^{-1/2}\,, \tag{2.8.42}$$

with $\gamma(x)$ defined below (2.8.41) satisfying in particular $\gamma(1+i\omega_k)=\gamma(-i\omega_k)^{-1}$. This way we obtain for (2.8.37)

$$\begin{aligned}\mathcal{C}(\omega_1,\omega_2,\omega_3)&=\frac{1}{\Upsilon_1(1+i(\omega_1+\omega_2+\omega_3)/2)}\left(\frac{\Upsilon_1(i\omega_1)^{1/2}\Upsilon_1(-i\omega_1)^{1/2}}{\Upsilon_1(1+i(\omega_1+\omega_2-\omega_3)/2)}\times 2\text{ perm.}\right)\\&=\frac{1}{\Upsilon_1(1+i(\omega_1+\omega_2+\omega_3)/2)}\left(\frac{\omega_1\Upsilon_1(1+i\omega_1)}{\Upsilon_1(1+i(\omega_1+\omega_2-\omega_3)/2)}\times 2\text{ perm.}\right)\,,\end{aligned} \tag{2.8.43}$$

where we made use of (2.8.40) to evaluate $\Upsilon_1'(0)=1$ and in going to the second line we used

$$\Upsilon_1(-i\omega_k)=\Upsilon_1(2+i\omega_k)=\gamma(1+i\omega_k)\Upsilon_1(1+i\omega_k)\,. \tag{2.8.44}$$

Putting everything together, and in particular applying the energy conservation obtained from the delta function as well as $\Upsilon_1(1)=1$, we have that

$$A_{S^2}(\omega_1,\omega_2\,|\,\omega_3)=i\,c_{S^2}\,g_s^3\,\delta(\omega_1+\omega_2-\omega_3)\mathcal{C}(\omega_1,\omega_2,\omega_3)=i\,c_{S^2}\,g_s^3\,\delta(\omega_1+\omega_2-\omega_3)\,\omega_1\omega_2\omega_3\,, \tag{2.8.45}$$

where c_{S^2} is a non-vanishing constant. Comparing to (2.7.28), we see that the amplitude matches the leading term in the large ν_F expansion [65–67], so long as we identify $1/|\nu_F|=c_{S^2}g_s^3=4\pi g_s$.

The terms (2.7.28) which are subleading in $1/\nu_F$ are predictions about higher genus contributions to the one-to-two scattering process in the continuum picture. We note that this identification is consistent with the powers of ν_F appearing in the various scattering amplitudes computed in section 2.7.2. A scattering amplitude on a Riemann surface of genus h and n vertex operator insertions scales as g_s^{2h-2+n}. A similar picture holds for other perturbative scattering amplitudes.

Further remarkable comparisons between the quantum mechanical matrix model S-matrix and Liouville theory have been obtained more recently in [38]. It is interesting to note that the whole structure of the perturbative string amplitudes is encoded in the reflection coefficient (2.7.5). Though manifest from the quantum mechanical matrix model, the explicit form of R_ν is far from obvious from the Liouville perspective.

Two-dimensional target space picture

To end the section, we would like to make some remarks about the target space picture of the non-critical string theory (2.8.29). For $\varphi \to -\infty$ the exponential interaction of the Liouville mode is switched off, and the theory is approximated by the combination of a free scalar and a linear dilaton CFT. From this perspective, at least in the limit of large and negative φ, we have a two-dimensional target space with a running dilaton Φ. The free scalar encodes the time direction of the target space, whereas φ encodes the spatial direction. The target space metric and dilaton field are given by

$$\frac{\mathrm{d}s^2}{\alpha'} = -(\mathrm{d}X^0)^2 + \mathrm{d}\varphi^2 \ , \qquad \Phi(X^0, \varphi) = 2\varphi \ , \tag{2.8.46}$$

such that the space-dependent string coupling $g_s = e^{\Phi}$ becomes parameterically weak as $\varphi \to -\infty$ and increasingly strong in the positive φ region. We also have reinstated the string tension α'.

Due to the space-dependence, the vacuum is not Poincaré invariant. As φ increases, so does the string coupling, and we moreover enter a regime where the Liouville interaction becomes significant. This regime is often referred to as the *Liouville wall* in the literature. As was mentioned, the spectrum of a string embedded in a two-dimensional target space consists of a single propagating degree of freedom, which is the 'tachyon field' τ. It is the target space field corresponding to the vertex operator (2.8.30). In two-dimensions, τ is in fact a massless field, so tachyon is somewhat of a misnomer. From the target space perspective, the S-matrix is given by sending an incoming tachyon wave from $\varphi \to -\infty$, which reflects off the Liouville wall, finally heading back to $\varphi \to -\infty$. Finally, we note that the background (2.8.46) is intrinsically stringy since the slope of Φ is the string length.

2.9 Outlook and speculative remarks

We would like to end our discussion with a brief outlook, some questions, and speculative remarks.

AdS/CFT & criticality. Over the last two-decades there has been tremendous progress in the development of the AdS/CFT correspondence. This has led to wonderful insights into the nature of quantum gravity and black holes. At the same time, it is important to keep in mind how the various large N models leading to gravity and string theories differ in their detailed form. For instance, many of the large N models considered throughout this work lead to a continuum picture only upon tuning the parameters to certain critical values. At the critical point

the Feynman diagrams in the 't Hooft expansion become densely filled Riemann surfaces. This type of criticality seems to be of a different nature than the underlying mechanism in the known examples of AdS/CFT. For instance in $\mathcal{N} = 4$ SYM theory at large N we have a continuum worldsheet picture for all values of the 't Hooft coupling λ. In this picture, different values of λ correspond to different values of the AdS length in string units. It remains possible that upon extending λ to the complex plane, one may encounter critical behaviour akin to that exhibited by the matrix models we have studied. Interestingly, complex values of λ would correspond to complex values of the IIB string coupling.

In the D0-brane picture the string coupling is space dependent and in some region becomes strongly coupled. This is reminiscent of the running dilaton in the two-dimensional target space picture of the non-critical string. From the D0-brane quantum mechanics perspective, this is understood from the fact that the 't Hooft coupling is dimensionful and thus flows. As such it cannot be tuned to some critical value. It seems less clear for the case of the D0-brane quantum mechanics theory that there is an analogue for tuning the level of the Fermi sea we saw for the quantum mechanical matrix model.

$\mathcal{Q}$: Does such critical behaviour of the microscopic model at large N and the emergence of a continuum picture play a role for more general considerations of the emergence of spacetime or is it an artefact of the lower dimensional models?

Wigner's black holes. In the introduction we mentioned Wigner's hypothesis that complex systems can be treated in statistical fashion. Though heavy nuclei were Wigner's main concern, from the perspective of gravity a natural candidate seems to be a black hole. Indeed, recent ideas motivated by the chaotic nature of the SYK system and its randomised couplings, as well as other considerations [149, 150] might provide novel avenues to explore the idea of a Wignerian black hole.

Another place where matrix integrals have recently played an important role in the context of black hole physics comes from applying ideas of supersymmetric localisation towards calculations of supersymmetric black hole partition functions [151, 152]. This context (at least naively [153]) is conceptually different from the Wignerian case described above. Nevertheless, it is interesting to note yet again the appearance of random matrices.

$\mathcal{Q}$: Is there a role for Wigner's hypothesis, namely that complex systems are well approximated by averaging ensembles of theories, in the theory of black holes?

Non-perturbative phenomena: Matrix integrals. The matrix models discussed throughout exhibit interesting non-perturbative features. For instance, the perturbative expansion of solutions to the non-linear differential equations discussed in section 2.4 and 2.5 may contain exponentially suppressed terms capturing non-perturbative behaviour. In [101] an equation determining the coefficients in the non-perturbative exponent for general multicritical matrix models has been presented. This equation implies, in particular, Borel summablility for some of the perturbative expansions.

$\mathcal{Q}$: The relation between non-perturbative effects of matrix models and the corresponding Liouville theory coupled to unitary minimal models has been explored in [189]. Can the non-perturbative effects observed for multicritical matrix models be related to the corresponding Liouville theory coupled to a non-unitary minimal model, particularly in the limit of large and negative central charge?

Non-perturbative phenomena & the non-singlet sector: MQM. The quantum mechanical matrix model discussed in sections 2.6 and 2.7 also exhibits interesting non-perturbative features. For instance, depending on how we fill the Fermi sea on the other side of the barrier, the perturbative S-matrix may admit different non-perturbative completions. At a more practical level, it is interesting to explore non-perturbative corrections to the perturbative S-matrix from the continuum string perspective. Although these corrections may disrupt the unitarity of the perturbative S-matrix, they may do so in a calculable form. For instance, as recently explored in [200–202], ZZ-instantons may capture certain non-perturbative contributions. Moreover, when the eigenvalue potential is not infinitely deep, the half-filled Fermi sea will be metastable. Any precise microscopic description of a 'metastable string vacuum' might be viewed as encouraging given that many vacua of interest in more realistic string theories may well be metastable [209, 211] (see also [197]).

Finally, in 2.6 and 2.7 we have only focused on the singlet sector of the quantum mechanical matrix model. Much less is known about the non-singlet sector, although it has been argued [138] and recently re-examined [181] that the adjoint sector in the matrix quantum mechanics is dual to a long string with specific boundary conditions corresponding to FZZT branes. More generally, one could study the implications of releasing other non-singlet sectors, particularly with regard to the problem of black holes [183, 184, 192].

$\mathcal{Q}$: Can the metastability of the quantum mechanical matrix model and the instantons mediating it sharpen our holographic understanding of the decay of D-branes [193] and more realistic metastable string vacua? Is there a target picture

of the general non-singlet sector?

Quantum mechanics & **worldline holography.** Throughout our discussion we focused on large N matrix integrals and quantum mechanical matrix models rather than large N quantum field theories. There are several differences between quantum mechanical and quantum field theoretic models. For instance, a quantum mechanical model has a finite number of (non-locally) interacting degrees of freedom, and potentially even a finite dimensional Hilbert space. Aside from topological field theories, continuum quantum field theory has an infinite dimensional Hilbert space and number of degrees of freedom. In quantum mechanics, gauging a symmetry is nothing more than imposing a constraint on the space of states, whereas in quantum field theory one generally introduces additional degrees of freedom. As has been recently emphasised [221–224], quantum mechanical models can be coupled to a worldine gravity and the quantisation of the resulting 'gravitational' theory remains straightforward. This might still be so in two-dimensional quantum field theory, but becomes increasingly complicated in higher dimensions. Finally, quantum mechanical theories are distinguished from quantum field theories in the sense that the degrees of freedom are not required to interact in a local/nearest neighbor type way. From a Wilsonian perspective, in the absence of locality we are confronted with the challenge of which degrees of freedom to integrate out in large N quantum mechanical models to capture the low energy effective theory.

$\mathcal{Q}$: Are there important differences from the perspective of the emergent worldsheet theory/ holographic dual when the microscopic theory is quantum mechanical rather than quantum field theoretic?

Finiteness & **cosmology?** One of our motivations for considering these topics is related to cosmological spacetimes, and in particular ones with positive cosmological constant [214]. In cosmology one often considers spacetimes with compact Cauchy surfaces, and consequently no asymptotic spatial boundary. From this perspective, the two-dimensional models of gravity coupled to minimal models seem to have the desired property of being more 'finite' examples of quantum gravity, albeit in a two-dimensional world. They can be quantised on a compact Cauchy surface and the constraints of gravity impose severe restrictions on the allowed space of states, rendering it essentially finite.

Moreover, the two-dimensional quantum gravity path integrals discussed in 2.8 make sense for positive (rather than negative) cosmological constant. From the large N matrix model perspective, this manifests itself in the appearance of branch cut ambiguities as we cross from $\alpha > \alpha_c$ to $\alpha < \alpha_c$. It is interesting to note

that from the perspective of the matrix model at fixed N, tuning $\Lambda \propto (\alpha - \alpha_c)$ corresponds to tuning the number of vertices of the triangulated Riemann surface. As Λ increases, the number goes down. This bears some resemblance to the de Sitter horizon entropy [5] being inversely related to the cosmological constant. Interestingly, the Euclidean continuation of a two-dimensional de Sitter universe continues to the Euclidean two-sphere. (It has been suggested that any microscopic description of de Sitter will involve a finite number of degrees of freedom or, more extremely, even a finite dimensional Hilbert space [212].) Perhaps, then, the quantum gravity path integrals studied in section 2.8 on an S^2 topology are of some relevance [191, 213, 215–217]. We saw that the S^2 path integral of gravity coupled to conformal matter with $c_m < 1$ is dual to a large N matrix integral.[9] It would be interesting to understand the Lorentzian interpretation (if any) of the matrix integral in terms of a Hilbert space and a collection of operators directly from the matrix picture. One possible avenue may be to consider inserting a macroscopic loop operator W_ℓ introduced in section 2.3.4. In the continuum limit, this creates a hole in the Riemann surface leading to a picture similar to that of Hartle and Hawking's wavefunction [205].[10] A cosmological time emerging from an underlying statistical/Euclidean model remains an elusive but fascinating idea [210].

As a final remark, connecting to the beginning of our discussion, we return to Wigner. There seems to be a certain degree of complexity in constructing de Sitter vacua in string theory. Perhaps this should be taken as a starting point, in the spirit of Wigner, and we could attempt to build a framework for de Sitter based on an ensemble of theories [218, 219].

[9] Matrix integrals have also appeared in other considerations of quantum de Sitter. For instance, it was shown in [220] that a matrix integral captures gauge invariant correlation functions in a four-dimensional de Sitter theory with an infinite tower of interacting massless higher spin fields. In [225–227] matrix integrals were discussed in relation to a two-dimensional de Sitter solution of Jackiw-Teitelboim gravity.

[10] One might even imagine inserting multiple W_ℓ's creating multiple boundaries whose interpretation [206, 207] seems less clear.

3 Matrix integrals & finite holography

3.1 Introduction

Being $0+0$ systems, matrix integrals are of a more finite nature than large N quantum field theories traditionally explored in holography. In this work we explore in detail a particular class of matrix integrals, known as multicritical matrix integrals (MMI) [15,16]. These are matrix integrals built out of a single Hermitian $N \times N$ matrix organised in an even polynomial of order $2m$ with $(m-1)$ free parameters (couplings). Despite being constructed from a single matrix, MMI admit $(m-1)$ distinct critical exponents in the leading order planar expansion, which are encoded in the non-analytic behaviour of the matrix integral as a function of its couplings. In the large N limit and upon tuning the couplings to a set of special values, MMI are conjectured to be dual to the series $(2m-1,2)$ of minimal models [27, 28] — which we denote by $\mathcal{M}_{2m-1,2}$ — on a fluctuating background. This can be described by coupling $\mathcal{M}_{2m-1,2}$ to two-dimensional quantum gravity, where the theory of quantum gravity at hand upon fixing the Weyl gauge is given by Liouville theory [8].

For $m \geq 2$, $\mathcal{M}_{2m-1,2}$ is a non-unitary two-dimensional CFT consisting of $(m-1)$ distinct Virasoro primaries, each accompanied with an infinite tower of Virasoro descendants. The conformal dimensions of the Virasoro primaries are increasingly negative, with the highest being the vanishing conformal dimension of the identity operator. While the norm of the Virasoro primaries of $\mathcal{M}_{2m-1,2}$ is positive, the norm of the Virasoro descendants is negative, leading to the non-unitarity of the models. We note that the non-unitary minimal models $\mathcal{M}_{2m-1,2}$ are related to integrable lattice models. The Lee-Yang singularity [175] characterising the zeroes of the partition function of the Ising model in an imaginary magnetic field in the thermodynamic limit has been identified with $\mathcal{M}_{5,2}$ [171]. On the other side $\mathcal{M}_{7,2}$ has been conjectured [176] to correspond to the tricritical phase (the crossing point of the three lowest energy levels) of a generalisation of the Ising model with three state classical variables, known as the Blume-Capel model [177].

As explored extensively throughout this work, an important piece of evidence in establishing the conjectured duality between MMI and Liouville theory coupled to $\mathcal{M}_{2m-1,2}$ is the matching of critical exponents between MMI and the continuum theory. We uncover the relation between the continuum theory on an S^2 topology and the explicit form of the MMI through its (finite) coupling dependence in the leading order planar expansion, as well as its perturbative multi-vertex expansion. This approach is orthogonal and complementary to the approach in [163–166] where the authors compare correlation functions of integrated operators (correlation numbers) to analogous quantities in the matrix integral. In our analysis of the partition function of the continuum theory we are turning on a single operator at finite coupling of the minimal model, the calculation of correlation numbers involves turning on multiple operators with an infinitesimal coupling. MMI have also made an appearance, initiated by [149], in the context of JT gravity [241]. In that context the continuum theory is studied on manifolds with boundary as compared to our analysis on S^2 and more generally on compact Riemann surfaces.

One of the key motivations of our work is the existence of a semiclassical limit exhibited by Liouville theory coupled to $\mathcal{M}_{2m-1,2}$. This is the large m limit, and was first observed in [20]. Specifically, upon fixing the area of the physical metric, restricting to an S^2 topology, and turning on only the identity operator of $\mathcal{M}_{2m-1,2}$ one finds a round two-sphere geometry as the saddle point solution. This is the geometry of Euclidean two-dimensional de Sitter space. Two-dimensional de Sitter space supports finiteness [17–19], and its conjectured entropy is finite [5].

Outline

In section 3.3 and 3.4 we study the diagrammatic expansion of MMI, providing new combinatorial expressions for Feynman diagrams whose vertices emanate an arbitrary even number of edges. As an example there are 243180821057048715513033825248570669471308484796973569520429442294243 321168794098389867298816000000000000000000 diagrams consisting of fifteen distinct vertices emanating an even number between four and thirty-two edges. We provide a concrete framework identifying each of the $(m-1)$ distinct planar critical exponents of the MMI in section 3.5. Geometrically these critical exponents are living on distinct fine-tuned "hypersurfaces" in coupling space. We match the critical exponents of the MMI to those of the continuum theory of Liouville theory coupled to $\mathcal{M}_{2m-1,2}$ in section 3.6. This matching comes with an important subtlety. Whereas for unitary minimal models the identification of critical exponents in the matrix integral with critical exponents of the emergent large N continuum theory uses the KPZ relation [29, 30, 143], the minimal models at hand are non-unitary and require a generalisation of the KPZ formula [16, 110]. In section 3.7 we consider the operator content of $\mathcal{M}_{2m-1,2}$ on a fluctuating background. On a fluctuating background the number of operators of the $\mathcal{M}_{2m-1,2}$ is subject to the Virasoro constraints.

Gauge fixing to the Weyl gauge further introduces the $\mathfrak{bc}$-ghost system. Initiated by work of Lian-Zuckerman (LZ) [230] and subsequent work [231–233] it was observed that the resulting BRST cohomology admits an infinite number of operators with non-vanishing ghost number and matter and Liouville descendants. The infinite set of LZ operators is still much smaller than the infinite tower of Virasoro descendants arising for each primary operator of $\mathcal{M}_{2m-1,2}$ on a fixed sphere. As a consequence of the Riemann-Roch theorem we do however infer that LZ operators do not lead to additional critical exponents on an S^2 topology. This may render the non-unitarity of $\mathcal{M}_{2m-1,2}$ on S^2 less severe. On the other hand the LZ operators contribute to the torus partition function [228, 229], which we match to the leading non-planar result of the MMI. We observe that the partition function on S^2 dominates (in absolute value) over the partition function on T^2 only for a sufficiently large cosmological constant Λ, whereas for small $\Lambda > 0$, the partition function on T^2 dominates. We do not yet have a clear understanding of this phenomenon but it would be interesting to explore its consequences for the Hartle-Hawking picture [205]. Some more open questions we present in section 3.8.

3.2 Multicritical matrix integrals

In [16, 103, 110] it has been conjectured that a certain class of matrix integrals — known as multicritical matrix integrals [15] — in the large N limit and upon tuning certain couplings are dual to two-dimensional quantum gravity coupled to $\mathcal{M}_{2m-1,2}$. We explore this conjecture by drawing explicit connections between the $(m-1)$ primaries of $\mathcal{M}_{2m-1,2}$ and properties of the multicritical matrix integral.

We consider the matrix integral

$$\mathcal{M}_N^{(m)}(\boldsymbol{\alpha}) = \int_{\mathbb{R}^{N^2}} [\mathrm{d}M]\, e^{-N\mathrm{Tr}V_m(M,\boldsymbol{\alpha})} \ , \quad m \geq 2 \ , \tag{3.2.1}$$

known as the m^{th} multicritical matrix integral, in the planar large N limit. M is a Hermitian $N \times N$ matrix and the measure factor is given by

$$[\mathrm{d}M] \equiv \prod_J \mathrm{d}M_{JJ} \prod_{I<J} \mathrm{dRe}M_{IJ} \prod_{I<J} \mathrm{dIm}M_{IJ} \ . \tag{3.2.2}$$

For $V_m(M, \boldsymbol{\alpha})$ we choose the even, order $2m$ polynomial

$$V_m(M, \boldsymbol{\alpha}) = \sum_{n=1}^{m} \frac{1}{2n} \alpha_n M^{2n} \ , \quad \alpha_1 \equiv 1 \ , \tag{3.2.3}$$

with $\boldsymbol{\alpha} \equiv (\alpha_2, \ldots, \alpha_m) \in \mathbb{R}^{m-1}$. We will denote the set of numbers $\boldsymbol{\alpha}$ as the couplings of the polynomial (3.2.3). We highlight that the number of free parameters $\boldsymbol{\alpha}$ is equal to the number of primaries of $\mathcal{M}_{2m-1,2}$.

Upon diagonalisation of M, we can analyse the planar contribution of (3.2.1) in the large N limit using a saddle point approximation. This reduces the exponent of (3.2.1) to

$$S[\rho^{(m)}_{\text{ext}}(\lambda, \boldsymbol{\alpha})] = \frac{1}{2}\int_{-a}^{a} \mathrm{d}\lambda \rho^{(m)}_{\text{ext}}(\lambda, \boldsymbol{\alpha}) V_m(\lambda, \boldsymbol{\alpha}) - 2\int_0^a \mathrm{d}\lambda \rho^{(m)}_{\text{ext}}(\lambda, \boldsymbol{\alpha}) \log(\lambda) \ , \quad (3.2.4)$$

where we assumed that the eigenvalues $\lambda \in \text{spec}(M)$ are distributed in the interval $[-a, a]$ and $\rho^{(m)}_{\text{ext}}(\lambda, \boldsymbol{\alpha})$ is the eigenvalue density obtained as the solution of

$$V_m'(\lambda, \boldsymbol{\alpha}) = 2\int_{-a}^{a} \mathrm{d}\mu \frac{\rho^{(m)}(\mu, \boldsymbol{\alpha})}{\lambda - \mu} \ . \quad (3.2.5)$$

The prime indicates a derivative with respect to λ. For more details we refer to [63, 68]. Another important quantity is the resolvent [25]

$$\mathrm{R}_N(z) \equiv \frac{1}{N}\mathrm{Tr}\,(z\,\mathbb{I}_N - M)^{-1} = \frac{1}{N}\sum_{I=1}^{N} \frac{1}{z - \lambda_I} \ , \qquad z \in \mathbb{C}/\{\lambda_I\} \ . \quad (3.2.6)$$

Sending $N \to \infty$ the sum can be replaced by an integral, where each eigenvalue is weighted by its average density

$$\lim_{N\to\infty} \mathrm{R}_N(z) \equiv \mathrm{R}(z) = \int_{-a}^{a} \mathrm{d}\mu \, \frac{\rho(\mu)}{z - \mu} \ . \quad (3.2.7)$$

For a higher order even polynomial it is convenient to express the resolvent as [83]

$$\mathrm{R}(z) = \int_0^a \frac{\mathrm{d}x}{\pi} \frac{xV'(x)}{z^2 - x^2} \frac{\sqrt{z^2 - a^2}}{\sqrt{a^2 - x^2}} \ . \quad (3.2.8)$$

From the definition of the resolvent (3.2.7) one obtains its large z scaling $\mathrm{R}(z) \sim 1/z$ reducing (3.2.8) to the condition[1]

$$1 = \int_0^a \frac{\mathrm{d}x}{\pi} \frac{xV'(x)}{\sqrt{a^2 - x^2}} \ . \quad (3.2.10)$$

[1] To evaluate (3.2.10) the following integral identity is useful:

$$\int_0^y \frac{\mathrm{d}x}{\pi} \frac{x^{2n}}{z^2 - x^2} \frac{\sqrt{z^2 - y^2}}{\sqrt{y^2 - x^2}} = \frac{1}{2B(n, 1/2)} \int_0^{y^2} \mathrm{d}A \frac{A^{n-1}}{\sqrt{z^2 - A}} \ . \quad (3.2.9)$$

For the polynomial $V_m(M, \boldsymbol{\alpha})$ (3.2.3), (3.2.10) implies

$$0 = \mathcal{N}_m(\boldsymbol{\alpha}) \equiv 1 - \sum_{n=1}^{m} \frac{\alpha_n u^n}{2nB(n,1/2)} , \qquad u \equiv a^2 . \tag{3.2.11}$$

$B(n, 1/2)$ denotes the beta function. We will call the condition $\mathcal{N}_m(\boldsymbol{\alpha}) = 0$ the normalisation condition for our matrix integral. For a particular choice of $\boldsymbol{\alpha}$ we can turn the normalisation condition into

$$(u - 4m)^m = 0 , \tag{3.2.12}$$

in other words $u = 4m$ is an m^{th} order zero. The values of $\boldsymbol{\alpha}$ leading to this behaviour can be easily obtained by recursively solving the discriminant of $\mathcal{N}_m(\boldsymbol{\alpha}) = 0$ [15, 82]:

$$\alpha_{n,c}^{(m)} \equiv (-1)^{n+1} \binom{m}{n} \frac{2n}{(4m)^n} B(n,1/2) , \quad 2 \leq n \leq m . \tag{3.2.13}$$

Finally we define the expectation value of the loop operator W_ℓ [83], which is related to the resolvent (3.2.7) through a Laplace transform

$$\langle W_\ell \rangle \equiv \int_{-a}^{a} \mathrm{d}\lambda \rho_{\text{ext}}(\lambda)\, e^{\lambda \ell} , \quad \mathrm{R}(z) = \int_0^\infty \mathrm{d}\ell\, \langle W_\ell \rangle\, e^{-\ell z} . \tag{3.2.14}$$

We use (3.2.9) to obtain the large z expansion of the resolvent for the multicritical matrix integrals (3.2.3):

$$\mathrm{R}_m(z, \boldsymbol{\alpha}) = \sum_{k \geq 0} \frac{1}{4^k} \binom{2k}{k} z^{-2k-1} \sum_{n=1}^{m} \frac{\alpha_n u^{n+k}}{2(n+k)B(n,1/2)} . \tag{3.2.15}$$

Using (3.2.14), we relate the large z expansion of the latter to the small ℓ expansion of the loop operator. For small ℓ we find

$$\langle W_\ell^{(m)}(\boldsymbol{\alpha}) \rangle = \sum_{n \geq 0} \frac{\ell^{2n}}{(2n)! 4^n} \binom{2n}{n} \sum_{k=1}^{m} \frac{\alpha_k u^{n+k}}{2(n+k)B(k,1/2)} = \sum_{n \geq 0} \omega_n^{(m)}(\boldsymbol{\alpha}) \ell^{2n} , \tag{3.2.16}$$

where we defined

$$\omega_n^{(m)}(\boldsymbol{\alpha}) \equiv \frac{1}{(n!)^2 4^n} \sum_{k=1}^{m} \frac{\alpha_k u^{n+k}}{2(n+k)B(k,1/2)} . \tag{3.2.17}$$

As a final remark we note that evaluating (3.2.7) close to the real axis $z = x \pm i\epsilon$

we obtain the important relations

$$\text{res}_a: \quad \rho(x) = \frac{1}{2\pi i}\left(\mathrm{R}(x-i\epsilon) - \mathrm{R}(x+i\epsilon)\right) , \quad \text{res}_b: \quad V'(x) = \mathrm{R}(x-i\epsilon)+\mathrm{R}(x+i\epsilon) . \tag{3.2.18}$$

Combining res_a with the definition of the resolvent (3.2.7) and the integral identity (3.2.9) we obtain the extremal eigenvalue density for $V_m(\lambda, \boldsymbol{\alpha})$

$$\begin{aligned}\rho^{(m)}_{\text{ext}}(z,\boldsymbol{\alpha}) &= \frac{1}{\pi}\sum_{n=1}^{m}\frac{\alpha_n}{B(n,1/2)} z^{2n-2}\, {}_2F_1\left(\frac{1}{2}, 1-n; \frac{3}{2}; 1-\frac{u}{z^2}\right)\sqrt{u-z^2} \\ &= \frac{1}{\pi}\sum_{n=1}^{m}\frac{\alpha_n}{B(n,1/2)} z^{2n-2}\sum_{k=0}^{\infty}\frac{(-1)^k}{2k+1}\binom{n-1}{k}\left(1-\frac{u}{z^2}\right)^k\sqrt{u-z^2}\end{aligned} \tag{3.2.19}$$

where we used that the hypergeometric ${}_2F_1(a,b;c;z)$ can be written as a polynomial as soon as either a or b become non-positive integers. At the multicritical point $\boldsymbol{\alpha}_c \equiv (\alpha^{(m)}_{2,c}, \ldots, \alpha^{(m)}_{m,c})$ (3.2.13) and close to the boundary of the eigenvalue interval where $u = 4m$ (3.2.12) the density scales as $\rho^{(m)}_{\text{ext}}(z,\boldsymbol{\alpha}_c) \propto (4m-z^2)^{(2m-1)/2}$ generalising the well-known exponent $3/2$ [25] in the quartic $m = 2$ model.

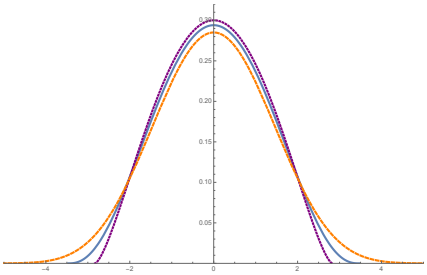

Figure 3.1: *Extremal eigenvalue density for $\boldsymbol{\alpha} = \boldsymbol{\alpha}_c$ and $m = 2, 3$ and $m = 12$ (purple dotted, teal, orange dashed). At the edges the eigenvalue distribution scales as $3/2, 5/2$ and $23/2$ respectively.*

Using (3.2.16) we obtain the planar on-shell action (3.2.4) for arbitrary m:

$$S[\rho^{(m)}_{\text{ext}}(\lambda,\boldsymbol{\alpha})] = \sum_{n=1}^{m}\frac{(2n)!}{4n}\,\alpha_n\,\omega^{(m)}_n + \sum_{n=1}^{m}\frac{\alpha_n u^n}{4n^2 B(n,1/2)} - \frac{1}{2}\log u + \log 2 , \tag{3.2.20}$$

At the critical point we find

$$S_c[\rho^{(m)}_{\text{ext}}(\lambda,\boldsymbol{\alpha}_c)] = \frac{1}{2}H_{2m} - \frac{1}{2}\log 4m + \log 2 , \tag{3.2.21}$$

where H_n denotes the n^{th} harmonic number. The subscript c indicates that we

zoom into criticality (3.2.13). At large m (3.2.21) scales as

$$\lim_{m\to\infty} S_c[\rho_{\text{ext}}^{(m)}(\lambda, \boldsymbol{\alpha}_c)] = \frac{1}{2}(\gamma + \log 2) + \frac{1}{8m} - \sum_{k=1}^{\infty} \frac{B_{2k}}{4k(2m)^{2k}} \ , \tag{3.2.22}$$

where γ denotes the Euler-Mascheroni constant and B_k the k^{th} Bernoulli number.

3.3 Planar diagrams with a single vertex

In this section we discuss the diagrammatic expansion of the matrix integral (3.2.1). We expand the normalisation condition (3.2.11) and the planar on-shell action (3.2.20) for small couplings $\boldsymbol{\alpha}$. For the $m = 2$ model with a single coupling this was first explored by [25]. To account for the two indices of the matrix M one uses the 't Hooft double line notation [78]. We will denote the resulting diagrams as ribbon diagrams. Whereas for the $m = 2$ model one only encounters ribbon diagrams whose vertices emanate four edges, for the multicritical matrix integrals (3.2.3) we have to deal with vertices emanating an arbitrary even number of edges.

3.3.1 An $m = 2$ refresher

Before delving into the multi-coupling perturbation theory we quickly review the $m = 2$ case. For more details we refer to [63]. For $m = 2$ we have the polynomial (3.2.3)

$$V_2(M, \alpha_2) = \frac{1}{2}M^2 + \frac{1}{4}\alpha_2 M^4 \ . \tag{3.3.1}$$

Normalisation of the eigenvalue density implies the vanishing of $\mathcal{N}_2(\alpha_2)$ in (3.2.11) with solutions $u_{\pm}^{(2)}$ given by

$$u_{\pm}^{(2)} = -\frac{2}{3\alpha_2} \pm \frac{2}{3\alpha_2}\sqrt{1 + 12\alpha_2} \ . \tag{3.3.2}$$

Of the two solutions, only $u_{+}^{(2)}$ is well-behaved near $\alpha_2 = 0$. The other solution $u_{-}^{(2)}$ exhibits a pole at $\alpha_2 = 0$, and is ordinarily discarded. Nonetheless, it is worth noting that knowledge of the residue of the pole at α_2 is sufficient to reconstruct $u_{+}^{(2)}$ from $u_{-}^{(2)}$. We also note that (3.3.2) exhibits a non-analytic behaviour close to $\alpha_2 = -1/12$ which we recognise as the $m = 2$ multicritical point (3.2.13). For $\alpha_2 < \alpha_{2,c}^{(2)}$ the normalisation condition has no real solution.

We now discuss the $m = 2$ model from a perturbative perspective in small α_2. For

$\alpha_2 > \alpha_{2,c}^{(2)}$ we obtain the small α_2 expansion of $u_+^{(2)}$

$$u_+^{(2)} = 4\sum_{k=0}^{\infty}(-1)^k \frac{(3\alpha_2)^k}{k+1}\binom{2k}{k} = 4\,{}_2F_1\left(\frac{1}{2}, 1; 2;\ \frac{\alpha_2}{\alpha_{2,c}^{(2)}}\right) . \tag{3.3.3}$$

Inspecting the above expression, one recognises the Catalan numbers

$$\mathcal{C}_k^{(2)} \equiv \frac{1}{k+1}\binom{2k}{k} . \tag{3.3.4}$$

Further to this, we see that the critical value $\alpha_{2,c}^{(2)} = -1/12$ controls the radius of convergence of the power series. At large k, the summand in (3.3.3) goes as $\sim k^{-\mathbf{3/2}}(\alpha_2/\alpha_{2,c}^{(2)})^k$. This behaviour encodes the fact that there is a **square root** non-analyticity in the solution $u_+^{(2)}$ and as we shall soon see, it is intimately related to the growth of planar diagrams.

Defining $\mathcal{F}_2^{(0)}(\alpha_2) \equiv -\log \mathcal{M}_N^{(2)}(\alpha_2)/\mathcal{M}_N^{(2)}(0)$ we obtain for small α_2 [25]

$$\mathcal{F}_2^{(0)}(\alpha_2) = -\sum_{k=1}^{\infty}(-1)^k(3\alpha_2)^k \frac{(2k-1)!}{k!(k+2)!} = \frac{1}{2}\alpha_2\,{}_3F_2\left(1, 1, \frac{3}{2}; 2, 4;\ \frac{\alpha_2}{\alpha_{2,c}^{(2)}}\right) . \tag{3.3.5}$$

$\mathcal{F}_2^{(0)}(\alpha_2)$ is the generating function of the connected planar bubble diagrams generated by the matrix integral with a quartic interaction. From a small α_2 expansion of

$$\mathcal{M}_N^{(2)}(\alpha_2) = \int_{\mathbb{R}^{N^2}} [\mathrm{d}M]\, e^{-\frac{N}{2}\mathrm{Tr}M^2} \sum_{k=0}^{\infty} \frac{(-1)^k}{k!}\left(\frac{\alpha_2 N}{4}\right)^k \left(\mathrm{Tr}M^4\right)^k , \tag{3.3.6}$$

we can read off the propagator and quartic vertex (fig. 3.2)

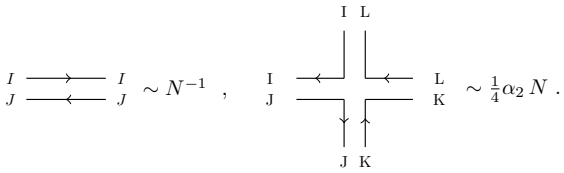

Figure 3.2: *Propagator and quartic vertex.*

Explicitly the propagator is given by

$$\langle M_{IK} M_{JL}\rangle = \mathcal{M}_N^{-1}(0) \int_{\mathbb{R}^{N^2}} [\mathrm{d}M]\, e^{-\frac{N}{2}\mathrm{Tr}\,M^2} M_{IJ} M_{KL} = \frac{1}{N}\delta_{IL}\delta_{KJ} . \tag{3.3.7}$$

$\mathcal{F}_2^{(0)}(4\alpha_2)$ counts planar diagrams with four edges emanating from each vertex, with the shift $\alpha_2 \to 4\alpha_2$ accounting for the $1/4$ weighting each vertex. We have

$$\mathcal{F}_2^{(0)}(4\alpha_2) = 2\alpha_2 - 18\alpha_2^2 + 288\alpha_2^3 + \dots \ . \tag{3.3.8}$$

The summand in (3.3.5) scales as $\sim k^{-\mathbf{7/2}}(\alpha_2/\alpha_{2,c}^{(2)})^k$ at large k. This behaviour encodes the growth of discrete Riemann surfaces with a fixed number of vertices k [234].

3.3.2 Binomial matrix integrals

We discuss the polynomials

$$\tilde{V}_n(M, \alpha_n) \equiv \frac{1}{2}M^2 + \frac{1}{2n}\alpha_n M^{2n} \ . \tag{3.3.9}$$

For $n = 2$ the above polynomial is equal to the $m = 2$ multicritical polynomial (3.3.1) discussed in the last section. By setting all of the couplings but α_n to zero in (3.2.19) we obtain the normalisation condition

$$0 = \tilde{\mathcal{N}}_n(\alpha_n) \equiv 1 - \frac{1}{4}u - \frac{\alpha_n}{2nB(n, 1/2)}u^n \ . \tag{3.3.10}$$

For $\alpha_n = \tilde{\alpha}_{n,c}$, where

$$\tilde{\alpha}_{n,c} \equiv -\frac{2n}{(4n)^n}(n-1)^{n-1}B(n, 1/2) \ , \quad 2 \leq n \leq m \ , \tag{3.3.11}$$

(3.3.10) has a second order zero at $u = 4n/(n-1)$, whereas for any other non-vanishing value of the coupling $\tilde{\alpha}_n$, (3.3.10) has n distinct solutions. We further note that

$$|\tilde{\alpha}_{2,c}| < |\alpha_{2,c}^{(m)}| \ , \quad |\tilde{\alpha}_{n,c}| > |\alpha_{n,c}^{(m)}| \ , \quad m \geq 3 \ . \tag{3.3.12}$$

For small α_n only one of the solutions of (3.3.10) can be uniformly approximated by a perturbative expansion which is a power series in the coupling α_n.

To obtain the leading expression in the perturbative expansion (3.3.10) we set $\alpha_n = 0$, however this prevents us from obtaining the other $n-1$ solutions. Solutions which cannot be obtained in a perturbative expansion when setting the perturbation parameter to zero are discussed within the field of singular perturbation theory.

Singular perturbation theory. To recover the perturbative expansion of the $n-1$ solutions of (3.3.10) singular for $\alpha_n \to 0$ we start by rescaling $u \to \alpha_n^{-\nu}u$,

$\nu \in \mathbb{R}_+$. For the case at hand (3.3.10) we obtain the rescaled equation

$$0 = \alpha_n^\nu - \frac{1}{4}u - \frac{1}{2nB(n,1/2)}\alpha_n^{1-\nu(n-1)}u^n \ . \tag{3.3.13}$$

For small α_n and $0 < \nu < 1/(n-1)$ or $\nu > 1/(n-1)$ (3.3.13) we only obtain the trivial solution $u = 0$. We are left with two special points $\nu \in \{0, 1/(1-n)\}$, where we find a non-trivial solution for u. The perturbative solution for $\nu = 0$ is the regular solution $u_\star^{(n)}$.[2] A superscript indicates that u solves (3.3.10). For $\nu = 1/(1-n)$ we obtain

$$0 = -\frac{1}{4}u - \frac{1}{2nB(n,1/2)}u^n \ , \tag{3.3.14}$$

solved by the $n-1$ roots of unity

$$u^{(n)}_{1,\dots,n-1} = e^{i\frac{\pi(2\ell+1)}{n-1}}\left(\frac{nB(n,1/2)}{2\alpha_n}\right)^{\frac{1}{n-1}} \ , \qquad \ell \in \{0,\dots,n-2\} \ . \tag{3.3.15}$$

We then obtain the n distinct perturbative expressions

$$\begin{aligned} u_\star^{(n)} &= 4 - 4\binom{2n-1}{n-1}\alpha_n + \mathcal{O}(\alpha_n^2) \ , \\ u^{(n)}_{1,\dots,n-1} &= e^{i\frac{\pi(2\ell+1)}{n-1}}\left(\frac{nB(n,1/2)}{2\alpha_n}\right)^{\frac{1}{n-1}} - \frac{4}{n-1} + \mathcal{O}\left(\alpha_n^{1/(n-1)}\right) \ , \end{aligned} \tag{3.3.16}$$

where $\ell \in \{0,\dots,n-2\}$, approximating all n solutions of (3.3.10).

To discuss the perturbative analysis of (3.3.10) we take the regular solution $u_\star^{(n)}$. For $n \geq 3$ Its small α_n expansion reads

$$u_\star^{(n)} = 4\sum_{k=0}^{\infty}(-1)^k\mathcal{C}_k^{(n)}\binom{2n-1}{n-1}^k\alpha_n^k = 4\,{}_{n-1}F_{n-2}\left[\begin{matrix}\frac{1}{n} & \frac{2}{n} & \cdots & \cdots & \frac{n-1}{n} \\ & \frac{2}{n-1} & \cdots & \frac{n-2}{n-1} & \frac{n}{n-1}\end{matrix}; \frac{\alpha_n}{\tilde{\alpha}_{n,c}}\right] . \tag{3.3.17}$$

where we defined $\tilde{\alpha}_{n,c}$ in (3.3.11) and

$$\mathcal{C}_k^{(n)} \equiv \frac{1}{(n-1)k+1}\binom{nk}{k} \ , \tag{3.3.18}$$

are known as Pfaff-Fuss-Catalan numbers generalising the Catalan numbers (3.3.4)

[2] Here and hereafter we introduce the subscript $\star$ to indicate the solution regular at the origin in coupling space.

for $n = 2$. For large k the summand in (3.3.17) scales as

$$\sim k^{-\mathbf{3/2}} e^{-k(n-1)\log(n-1)} \tilde{\alpha}_{n,c}^{-k} \ . \tag{3.3.19}$$

Note that the exponent $\mathbf{3/2}$ is universal for all binomial matrix integrals. Introducing $\tilde{\mathcal{F}}_n^{(0)}(\alpha_n)$ analogously to $\mathcal{F}_2^{(0)}(\alpha_2)$ and using (3.3.17) we obtain the perturbative α_n expansion

$$\begin{aligned}\tilde{\mathcal{F}}_n^{(0)}(\alpha_n) &= -\sum_{k=1}^{\infty}(-1)^k \frac{\left(\binom{2n-1}{n-1}\alpha_n\right)^k}{k!}\frac{(nk-1)!}{((n-1)k+2)!} \\ &= \frac{1}{2n}\,\mathcal{C}_n^{(2)}\,\alpha_n\,{}_{n+1}F_n\left[\begin{matrix}1 & 1 & \frac{n+1}{n} & \dots & \dots & \frac{2n-2}{n} & \frac{2n-1}{n} \\ & 2 & \frac{n+2}{n-1} & \dots & \dots & \frac{2n-1}{n-1} & \frac{2n}{n-1}\end{matrix}\,;\,\frac{\alpha_n}{\tilde{\alpha}_{n,c}}\right] \ . \end{aligned} \tag{3.3.20}$$

Since $\tilde{\alpha}_{2,c} = \alpha_{2,c}^{(2)}$ and using $\mathcal{C}_2^{(2)} = 2$, (3.3.20) reduces to (3.3.5) for $n = 2$. For large k the summand of this expression scales universally as

$$\sim k^{-\mathbf{7/2}} e^{-k(n-1)\log(n-1)} \tilde{\alpha}_{n,c}^{-k} \ . \tag{3.3.21}$$

3.4 Planar diagrams with multiple vertices

In this section we consider the diagrammatic multi-vertex expansion of the multicritical matrix integrals (3.2.3). We discuss the $m = 3$ and $m = 4$ (3.2.3) cases in some detail since the normalisation condition (3.2.11) for these matrix integrals is a cubic and a quartic polynomial whose roots admit explicit expressions. For $m \geq 5$ the normalisation condition is a quintic or higher polynomial, and in general not solvable by radicals.

3.4.1 $m = 3$ analysis

The normalisation condition $\mathcal{N}_3(\alpha_2, \alpha_3) = 0$ is the cubic equation (3.2.11)

$$1 - \frac{1}{4}u - \frac{3}{16}\alpha_2 u^2 - \frac{5}{32}\alpha_3 u^3 = 0 \ , \tag{3.4.1}$$

whose general solutions can be expressed as

$$u_\ell^{(3)} = \frac{32}{15\alpha_3}\left(-\frac{3}{16}\alpha_2 + \Delta_0\,\zeta_\ell^{-1}\,\Gamma^{-1/3} + \zeta_\ell\,\Gamma^{1/3}\right) \ , \qquad \ell = 1,2,3 \ . \tag{3.4.2}$$

Here, $\zeta_\ell = e^{2\pi i(\ell-1)/3}$ is a third root of unity and we have defined

$$\Delta_0 \equiv \frac{3}{256}\left(3\alpha_2^2 - 10\alpha_3\right) , \tag{3.4.3}$$

$$\Delta_1 \equiv -\frac{27}{2048}\left(\alpha_2^3 - 5\alpha_2\alpha_3 - 50\alpha_3^2\right) , \tag{3.4.4}$$

$$\Gamma \equiv \frac{1}{2}\left(\Delta_1 + \sqrt{\Delta_1^2 - 4\Delta_0^3}\right) . \tag{3.4.5}$$

We further define

$$D_3 \equiv \Delta_1^2 - 4\Delta_0^3 = \frac{675}{4194304}\alpha_3^2\left(-9(12\alpha_2+1)\alpha_2^2 + 20(27\alpha_2+2)\alpha_3 + 2700\alpha_3^2\right) . \tag{3.4.6}$$

Expanding D_3 at small α_3, we identify $\alpha_2 = -1/12$ as a special value, corresponding to $\alpha_{2,c}^{(2)}$. Expanding D_3 at small α_2 reveals $\alpha_3 = -2/135$ as a special value, corresponding to $\tilde{\alpha}_{3,c}$ (3.3.11). Near both $(\alpha_2, \alpha_3) = (-1/12, 0)$ and $(\alpha_2, \alpha_3) = (0, -2/135)$, where $D_3 = 0$, Δ_1 remains non-vanishing such that the non-analytic behaviour of the solutions $u_\ell^{(3)}$ near these points is that of a **square root**. On the other hand, expanding D_3 near $\alpha_2 = -1/9$ reveals $\alpha_3 = 1/270$ as a special value, the multicritical point (3.2.13). At $\alpha_2 = -1/9$ we have that $\Delta_1 = (135\alpha_3 - 1)(270\alpha_3 - 1)/55296$, which vanishes for $\alpha_{3,c}^{(3)}$. This implies that the non-analytic behaviour of $u_\ell^{(3)}$ near the multicritical point is that of a **cubic root**.

Single-variable perturbation theory. We start by discussing the normalisation condition (3.4.1) along the path $\gamma_\star^{(3)}$ in coupling space [82]

$$\gamma_\star^{(3)} : \ [0,1] \to \mathbb{R}^2 , \qquad t \mapsto \begin{pmatrix} \alpha_{2,c}^{(3)} t \\ \alpha_{3,c}^{(3)} t^2 \end{pmatrix} , \tag{3.4.7}$$

leading to the rescaled normalisation condition

$$0 = 1 - \frac{1}{4}u - \frac{3}{16}\alpha_{2,c}^{(3)} t u^2 - \frac{5}{32}\alpha_{3,c}^{(3)} t^2 u^3 . \tag{3.4.8}$$

Of all paths, the path $\gamma_\star^{(3)}$ is special in that upon rescaling $u \to u/t$, t^{-1} takes the role of an overall pre-factor for $V_3(M, \boldsymbol{\alpha})$ (3.2.3). The solution of (3.4.8) regular for $t \in [0,1]$ reads

$$u_\star^{(3)} = \frac{12}{t}\left(1 - (1-t)^{1/3}\right) = 12\sum_{k=0}^{\infty}(-1)^k \binom{1/3}{k+1} t^k . \tag{3.4.9}$$

At large k the summand scales as $\sim k^{-\mathbf{4/3}}$, different from the $\sim k^{-\mathbf{3/2}}$ for $m = 2$ (3.3.3). Note that (3.4.9) converges for $|t| \leq 1$.

Two-variable perturbation theory. The solution of $\mathcal{N}_3(\alpha_2, \alpha_3) = 0$ regular near the origin in coupling space is

$$u_\star^{(3)} = 4 \sum_{k_1,k_2=0}^{\infty} \frac{(-1)^{k_1+k_2}}{(1+k_1+2k_2)} \frac{\prod_{s=1}^{k_2}(k_1+s)}{k_2!} \binom{3k_2+2k_1}{2k_2+k_1} (10\alpha_3)^{k_2} (3\alpha_2)^{k_1} \ . \tag{3.4.10}$$

Performing the substitution $k = k_1 + 2k_2$, $n = k_1 + k_2$ we find the single sum expression

$$u_\star^{(3)} = 4\sqrt{\pi} \sum_{k=0}^{\infty} \left(\frac{20\alpha_3}{3\alpha_2}\right)^k \frac{1}{\Gamma(2+k)} \, {}_3\tilde{F}_2\left(1, -k, 1+k; \frac{1}{2} - \frac{k}{2}, 1 - \frac{k}{2}; \frac{9\alpha_2^2}{40\alpha_3}\right) \ . \tag{3.4.11}$$

Along the path $\gamma_\star^{(3)}$ we recover (3.4.9), as shown in appendix 6. Equation (3.4.11) provides a perturbative expansion regular for small couplings α_2 and α_3. Depending on the range of the couplings (3.4.11) arises from a different solution (3.4.2) of the normalisation condition $\mathcal{N}_3(\alpha_2, \alpha_3) = 0$. Switching for simplicity to polar coordinates $(\alpha_2, \alpha_3) = (r\cos\phi, r\sin\phi)$, we observe that the function

$$B_3(r, \phi) = u_1(r, \phi)\Theta(\pi - \phi) + u_3(r, \phi)\Theta(\phi - \pi) \ , \tag{3.4.12}$$

is well behaved and real near the origin.

On-shell action for $m = 3$. We define

$$\mathcal{F}_3^{(0)}(\alpha_2, \alpha_3) \equiv -\log \frac{\mathcal{M}_N^{(3)}(\alpha_2, \alpha_3)}{\mathcal{M}_N^{(3)}(0, 0)} \ . \tag{3.4.13}$$

Using (3.2.20) for $m = 3$ and the regular solution (3.4.10) we obtain the small α_2, α_3 expansion

$$\begin{aligned} \mathcal{F}_3^{(0)}(\alpha_2, \alpha_3) = &- \sum_{k_2=1}^{\infty} (-1)^{k_2} \frac{(10\alpha_3)^{k_2}}{k_2!} \frac{(3k_2-1)!}{(2k_2+2)!} \\ &- \sum_{k_2=0}^{\infty} \sum_{k_1=1}^{\infty} (-1)^{k_1+k_2} \frac{(10\alpha_3)^{k_2}}{k_2!} \frac{(3\alpha_2)^{k_1}}{k_1!} \frac{(3k_2+2k_1-1)!}{(2k_2+k_1+2)!} \ . \end{aligned} \tag{3.4.14}$$

It is convenient to perform again the substitution $k = k_1 + 2k_2$, $n = k_1 + k_2$ leading to

$$\mathcal{F}_3^{(0)}(\alpha_2, \alpha_3) = -\sqrt{\pi} \sum_{k=1}^{\infty} \left(\frac{20\alpha_3}{3\alpha_2} \right)^k \frac{1}{k\Gamma(3+k)} \, {}_3\tilde{F}_2 \left(1, -k, k; \frac{1}{2} - \frac{k}{2}, 1 - \frac{k}{2}; \frac{9\alpha_2^2}{40\alpha_3} \right) . \tag{3.4.15}$$

Evaluating (3.4.15) at the multicritical point $\alpha_{2,c}^{(3)} = -1/9$, $\alpha_{3,c}^{(3)} = 1/270$ (3.2.13) we recover the value of the on-shell action at criticality (3.2.21). Note that in the definition of $\mathcal{F}_3^{(0)}(\alpha_2, \alpha_3)$ in (3.4.13) we subtract the Gaussian term which evaluates to 3/4. In appendix 6 we show that the summand scales as $\sim k^{-\mathbf{10/3}}$, which differs from the $\sim k^{-\mathbf{7/2}}$ encountered in (3.3.5). $\mathcal{F}_3^{(0)}(4\alpha_2, 6\alpha_3)$ counts planar diagrams with four or six edges emanating from each vertex

$$\mathcal{F}_3^{(0)}(4\alpha_2, 6\alpha_3) = 2\alpha_2 + 5\alpha_3 - 18\alpha_2^2 - 300\alpha_3^2 - 144\alpha_2\alpha_3 + \dots . \tag{3.4.16}$$

To see some of these coefficients explicitly we expand the exponential in (3.2.1)

$$\begin{aligned} &\mathcal{M}_N^{(3)}(\alpha_2, \alpha_3) \\ &= \int_{\mathbb{R}^{N^2}} [\mathrm{d}M] \, e^{-\frac{N}{2}\mathrm{Tr}M^2} \sum_{k_1,k_2=0}^{\infty} \frac{(-1)^{k_1+k_2}}{k_1!k_2!} \left(\frac{\alpha_2 N}{4} \right)^{k_1} \left(\frac{\alpha_3 N}{6} \right)^{k_2} \left(\mathrm{Tr}M^4 \right)^{k_1} \left(\mathrm{Tr}M^6 \right)^{k_2} , \end{aligned} \tag{3.4.17}$$

leading to the graphical representation of the propagator, the quartic and the sextic vertex

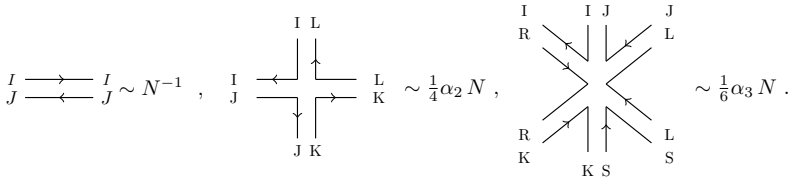

Figure 3.3: *Propagator, quartic and sextic vertex.*

In fig. 3.4 we show the diagrams contributing to $\mathcal{O}(\alpha_2\alpha_3)$ in (3.4.16)

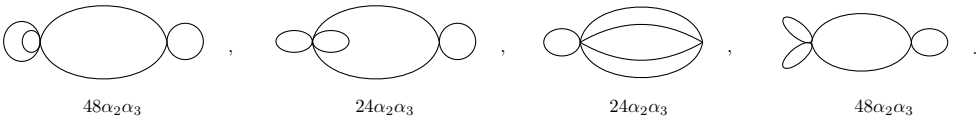

Figure 3.4: *Diagrams combining vertices with four and six edges emanating. Each line represents a thick double line. The number below each diagrams counts the number of diagrams including the symmetry factor.*

3.4.2 $m = 4$ analysis

The normalisation condition $\mathcal{N}_4(\boldsymbol{\alpha}) = 0$ is the quartic equation (3.2.11)

$$0 = 1 - \frac{1}{4}u - \frac{3}{16}\alpha_2 u^2 - \frac{5}{32}\alpha_3 u^3 - \frac{35}{256}\alpha_4 u^4 \ , \tag{3.4.18}$$

admitting four solutions $u^{(4)}_{\ell,\pm}$, $\ell = 1, 2$ whose properties we discuss in appendix 6.

Single-variable perturbation theory. Along the path $\gamma^{(4)}_\star$

$$\gamma^{(4)}_\star : \ [0,1] \to \mathbb{R}^3 \ , \qquad t \mapsto \begin{pmatrix} \alpha^{(4)}_{2,c}\, t \\ \alpha^{(4)}_{3,c}\, t^2 \\ \alpha^{(4)}_{4,c} t^3 \end{pmatrix} \ , \tag{3.4.19}$$

the regular solution of (3.4.18) reads

$$u^{(4)}_\star = \frac{16}{t}\left(1 - (1-t)^{1/4}\right) = 16 \sum_{k=0}^{\infty} (-1)^k \binom{1/4}{k+1} t^k \ , \tag{3.4.20}$$

converging for $|t| \leq 1$. At large k the summand scales as $\sim k^{-\mathbf{5/4}}$ as compared to $\sim k^{-\mathbf{4/3}}$ for $m = 3$ (3.4.9) and $\sim k^{-\mathbf{3/2}}$ for $m = 2$ (3.3.3) and the binomial matrix integrals (3.3.19).

Three-variable perturbation theory. Solving (3.4.18) and expanding the regular solution for α_2, α_3 and α_4 close to zero we obtain

$$u^{(4)}_\star = 4 \sum_{k_1,k_2,k_3=0}^{\infty} \frac{(-1)^{k_1+k_2+k_3}}{(1+k_1+2k_2+3k_3)} (35\alpha_4)^{k_3} (10\alpha_3)^{k_2} (3\alpha_2)^{k_1} \\ \times \frac{\prod_{s=1}^{k_2+k_3}(k_1+s)}{(k_2+k_3)!} \frac{\prod_{s=1}^{k_3}(k_2+s)}{k_3!} \binom{4k_3+3k_2+2k_1}{3k_3+2k_2+k_1} \ . \tag{3.4.21}$$

Performing the substitution $k = k_1 + 2k_2 + 3k_3$, $n = k_1 + k_2 + k_3$, $l = k_2 + k_3$

$$u_\star^{(4)} = 4\sqrt{\pi}\sum_{k=0}^{\infty}\sum_{n=0}^{k}(-1)^n\left(\frac{7\alpha_4}{\alpha_3}\right)^k\left(\frac{3\alpha_2\alpha_3}{7\alpha_4}\right)^n\frac{\Gamma(1+k+n)}{\Gamma(2+k)\Gamma(1+n)\Gamma(1+k-n)}$$
$$\times\ {}_3\tilde{F}_2\left(1,-n,-k+n;\frac{1}{2}+\frac{1}{2}(-k+n),1+\frac{1}{2}(-k+n);\frac{5\alpha_3^2}{21\alpha_2\alpha_4}\right)\ . \tag{3.4.22}$$

We conjecture

$$\sum_{n=0}^{k}\frac{(-3)^n}{8^k}\frac{\Gamma(1+k+n)}{\Gamma(2+k)\Gamma(1+n)\Gamma(1+k-n)}$$
$$\times\ {}_3\tilde{F}_2\left(1,-n,-k+n;\frac{1}{2}+\frac{1}{2}(-k+n),1+\frac{1}{2}(-k+n);\frac{4}{6}\right) = \frac{4}{\sqrt{\pi}}\binom{1/4}{k+1} \tag{3.4.23}$$

According to this conjecture (3.4.22) reduces to (3.4.20) along $\gamma_\star^{(4)}$. Equation (3.4.22) provides a perturbative expansion regular for small couplings $\boldsymbol{\alpha}$. Depending on the range of the couplings it arises from a different solution (6.0.43) of the normalisation condition $\mathcal{N}_4(\boldsymbol{\alpha}) = 0$, as we elucidate further in appendix 6.

On-shell action for $m = 4$. We define

$$\mathcal{F}_4^{(0)}(\alpha_2,\alpha_3,\alpha_4) \equiv -\log\frac{\mathcal{M}_N^{(4)}(\alpha_2,\alpha_3,\alpha_4)}{\mathcal{M}_N^{(4)}(0,0,0)}\ . \tag{3.4.24}$$

Using (3.2.20) for $m = 4$ and (3.4.22) we obtain the small $\alpha_2, \alpha_3, \alpha_4$ expansion

$$\mathcal{F}_4^{(0)}(\alpha_2,\alpha_3,\alpha_4) = -\sum_{k_3=1}^{\infty}(-1)^{k_3}\frac{(35\alpha_4)^{k_3}}{k_3!}\frac{(4k_3-1)!}{(3k_3+2)!}$$
$$-\sum_{k_3=0}^{\infty}\sum_{k_2=1}^{\infty}(-1)^{k_2+k_3}\frac{(35\alpha_4)^{k_3}}{k_3!}\frac{(10\alpha_3)^{k_2}}{k_2!}\frac{(4k_3+3k_2-1)!}{(3k_3+2k_2+2)!}$$
$$-\sum_{k_3,k_2=0}^{\infty}\sum_{k_1=1}^{\infty}(-1)^{k_1+k_2+k_3}\frac{(35\alpha_4)^{k_3}}{k_3!}\frac{(10\alpha_3)^{k_2}}{k_2!}\frac{(3\alpha_2)^{k_1}}{k_1!}\frac{(4k_3+3k_2+2k_1-1)!}{(3k_3+2k_2+k_1+2)!}\ . \tag{3.4.25}$$

Along $\gamma_\star^{(4)}$ and using (3.4.20) we obtain

$$\lim_{t\to 1-\epsilon}\mathcal{F}_{4,\text{n.a.}}^{(0)}(\boldsymbol{\alpha})|_{\gamma_\star^{(4)}} \sim \epsilon^{\mathbf{9/4}}\ . \tag{3.4.26}$$

$\mathcal{F}_4^{(0)}(4\alpha_2, 6\alpha_3, 8\alpha_4)$ counts planar diagrams with four, six or eight edges emanating from each vertex

$$\begin{aligned}\mathcal{F}_4^{(0)}(4\alpha_2, 6\alpha_3, 8\alpha_4) = {} & 2\alpha_2 + 5\alpha_3 + 14\alpha_4 - 18\alpha_2^2 - 300\alpha_3^2 - 4900\alpha_4^2 \\ & - 144\alpha_2\alpha_3 - 560\alpha_2\alpha_4 - 2400\alpha_3\alpha_4 + 201600\alpha_2\alpha_3\alpha_4 + \dots \ . \end{aligned} \tag{3.4.27}$$

We obtain a graphical representation of the eight-order vertex (fig.3.5) following the steps in (3.4.17).

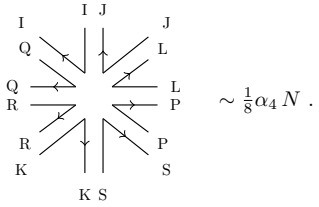

$\sim \frac{1}{8}\alpha_4 N$.

Figure 3.5: *Eight-order vertex.*

3.4.3 $m \geq 5$ analysis

For general $m \geq 5$ we cannot solve the normalisation condition (3.2.11) by radicals. Instead we conjecture generalisations of (3.4.10) and (3.4.21) for the normalisation condition and the expressions (3.4.14) and (3.4.25) for the on-shell action relying on numerical results.

Single-variable perturbation theory. We start by parametrising a path connecting the origin in coupling space to the multicritical point

$$\gamma_\star^{(m)} : \ [0,1] \to \mathbb{R}^{m-1} \ , \quad t \mapsto \begin{pmatrix} \alpha_{2,c}^{(m)}\, t \\ \vdots \\ \alpha_{m,c}^{(m)}\, t^{m-1} \end{pmatrix} \ . \tag{3.4.28}$$

This leads to the regular solution of $\mathcal{N}_m(\boldsymbol{\alpha}) = 0$

$$u_\star^{(m)} = \frac{4m}{t}\left(1 - (1-t)^{1/m}\right) = 4m \sum_{k=0}^{\infty} (-1)^k \binom{1/m}{k+1} t^k \ , \tag{3.4.29}$$

convergent for $|t| \leq 1$. For large k the summand scales as $\sim \Gamma(1+1/m) k^{-\mathbf{1}-\frac{\mathbf{1}}{\boldsymbol{m}}}$.

Multi-variable perturbation theory. For general small couplings $\boldsymbol{\alpha}$ the per-

turbative expansion of the regular solution reads

$$u_\star^{(m)} = 4 \sum_{k_1,\ldots,k_{m-1}=0}^{\infty} \frac{(-1)^{k_1+\ldots+k_{m-1}}}{(1+k_1+\ldots+(m-1)k_{m-1})} \prod_{\ell=2}^{m} \left[\binom{2\ell-1}{\ell-1} \alpha_\ell \right]^{k_{\ell-1}} \times \binom{2k_1+\ldots+mk_{m-1}}{k_1+\ldots+(m-1)k_{m-1}} \times \frac{\prod_{s=1}^{k_2+\ldots+k_{m-1}}(k_1+s)}{(k_2+\ldots+k_{m-1})!} \frac{\prod_{s=1}^{k_3+\ldots+k_{m-1}}(k_2+s)}{(k_3+\ldots+k_{m-1})!} \cdots \frac{\prod_{s=1}^{k_{m-1}}(k_{m-2}+s)}{(k_{m-1})!} \,. \quad (3.4.30)$$

The above expression accounts for mixing of the couplings. Note that if we set all but one of the couplings (e.g. α_ℓ) to zero (3.4.30) reduces to (3.3.17). We conjecture that this reduces to (3.4.29) along the path $\gamma_\star^{(m)}$. Similarly to the case $m = 3$ and $m = 4$ we believe that also for $m \geq 5$ there exists a smooth function which leads to (3.4.30) when approached from different directions in coupling space.

We note that we can also express (3.4.30) in terms of incomplete exponential Bell polynomials. Using the Lagrange inversion theorem to solve the normalisation condition perturbatively (3.2.11) we have

$$u_\star^{(m)} = \sum_{k=1}^{\infty} \frac{4^k}{k!} \sum_{\ell=0}^{k-1} (-1)^\ell k^{(\ell)} \mathcal{Y}_{k-1,\ell}\left(\hat{f}_1, \ldots, \hat{f}_{k-\ell}\right) \,, \quad \hat{f}_k \equiv 4k! \frac{\alpha_{k+1}}{2(k+1)B(k+1,1/2)} \,, \quad (3.4.31)$$

where $\mathcal{Y}_{k,\ell}(x_1,\ldots,x_n)$ denote the incomplete exponential Bell-polynomials, defined recursively through

$$\mathcal{Y}_{k,\ell}(x_1,\ldots,x_n) \equiv \sum \frac{n!}{j_1!j_2!\ldots j_{n-k+1}!} \left(\frac{x_1}{1!}\right)^{j_1} \left(\frac{x_2}{2!}\right)^{j_2} \cdots \left(\frac{x_{n-k+1}}{(n-k+1)!}\right)^{j_{n-k+1}} \,, \quad (3.4.32)$$

where the summation is subject to the additional constraints

$$j_1 + j_2 + \ldots + j_{n-k+1} = k \,, \quad j_1 + 2j_2 + 3j_3 + \ldots + (n-k+1)j_{n-k+1} = n \,. \quad (3.4.33)$$

The Bell polynomial encodes information on the partitions of a set. $\mathcal{Y}_{k,\ell}(x_1,\ldots,x_n)$ tells us how many partitions with block size between 1 and $(n-k+1)$ a set with n elements can have when divided into k blocks. As an example

$$\mathcal{Y}_{4,2}(x_1,x_2,x_3) = 3x_2^2 + 4x_1x_3 \,, \quad (3.4.34)$$

reflects that the set $\boldsymbol{y} \equiv \{y_1,y_2,y_3,y_4\}$ can be divided into blocks of size 2 in two different ways. We can have 3 mutually, non-overlapping subsets, each consisting of a block of size two. Additionally we have 4 different ways to break $\boldsymbol{y}$ into a

1-block and a 3-block.

On-shell action for general m. We define

$$\mathcal{F}_m^{(0)}(\boldsymbol{\alpha}) \equiv -\log \frac{\mathcal{M}_N^{(m)}(\boldsymbol{\alpha})}{\mathcal{M}_N^{(m)}(\mathbf{0})} \ . \tag{3.4.35}$$

Using (3.2.20) and (3.4.30) we obtain the perturbative expansion

$$\begin{aligned}\mathcal{F}_m^{(0)}(\boldsymbol{\alpha}) = &-\sum_{k_{m-1}=1}^{\infty}(-1)^{k_{m-1}}\frac{\left(\binom{2m-1}{m-1}\alpha_m\right)^{k_{m-1}}}{k_{m-1}!}\frac{(mk_{m-1}-1)!}{((m-1)k_{m-1}+2)!}+\\ &-\sum_{k_{m-1}=0}^{\infty}\sum_{k_{m-2}=1}^{\infty}(-1)^{k_{m-1}+k_{m-2}}\prod_{j=m-1}^{m}\frac{\left(\binom{2j-1}{j-1}\alpha_j\right)^{k_{j-1}}}{k_{j-1}!}\frac{(\sum_{j=m-2}^{m-1}(j+1)k_j-1)!}{(\sum_{j=m-2}^{m-1}jk_j+2)!}+\dots\\ &-\sum_{k_2,\dots,k_{m-1}=0}^{\infty}\sum_{k_1=1}^{\infty}(-1)^{\sum_{j=1}^{m-1}k_j}\prod_{j=2}^{m}\frac{\left(\binom{2j-1}{j-1}\alpha_j\right)^{k_{j-1}}}{k_{j-1}!}\frac{(\sum_{j=1}^{m-1}(j+1)k_j-1)!}{(\sum_{j=1}^{m-1}jk_j+2)!}\ .\end{aligned} \tag{3.4.36}$$

Assuming that all but one of the couplings is very small the above reduces to (3.3.20). Along $\gamma_\star^{(m)}$ (3.4.28) and using (3.4.29) we obtain

$$\lim_{t\to 1-\epsilon}\mathcal{F}_{m,\text{n.a.}}^{(0)}(\boldsymbol{\alpha})|_{\gamma_\star^{(m)}} \sim \epsilon^{\mathbf{2}+\frac{\mathbf{1}}{\mathbf{m}}} \ . \tag{3.4.37}$$

Upon shifting $\alpha_\ell \to 2\ell\alpha_\ell$, $\ell = 2,\dots,m$, $\mathcal{F}_m^{(0)}(\boldsymbol{\alpha})$ (3.4.35) counts planar diagrams with vertices emanating $4,\dots,2m$ edges. As an example we infer that $\mathcal{F}_{10}^{(0)}(\boldsymbol{\alpha})$ contains the term

$$4654905553625015743787991537108910080000000\alpha_2\alpha_3\alpha_4\alpha_5\alpha_6\alpha_7\alpha_8\alpha_9\alpha_{10} \ , \tag{3.4.38}$$

which counts diagrams with nine distinct vertices emanating an even number between four and twenty edges. After this shift the terms linear in the couplings have coefficients given by the Catalan numbers $\mathcal{C}_k^{(2)}$ with $k = 2,\dots,m$. In fig. 3.6 we illustrate diagrams with a single vertex emanating four to twelve edges.

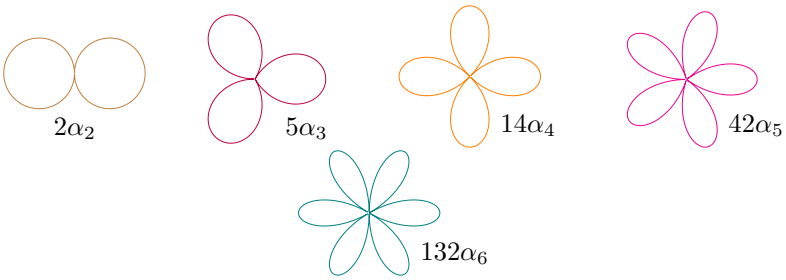

Figure 3.6: *Vertices with four to twelve edges emanating. Each line represents a thick line. The number below each diagram enumerates the number of such diagrams as counted by* $\mathcal{F}_m^{(0)}(4\alpha_2, \ldots, 2m\alpha_m)$ *for* $m \geq 6$.

3.5 Non-analytic behaviour of multicritical matrix integrals

In this section, we uncover the non-analytic behaviour of the planar on-shell action (3.2.20) as a function of its couplings near the multicritical point (3.2.13).

An $m = 2$ refresher. For $m = 2$ the polynomial (3.2.3) reduces to the quartic polynomial

$$V_2(M, \alpha_2) = \frac{1}{2}M^2 + \frac{1}{4}\alpha_2 M^4 \ . \tag{3.5.1}$$

From (3.2.8) it is straightforward to obtain the resolvent and using res_a (3.2.18) we find the eigenvalue distribution (3.2.5):

$$\begin{aligned} \mathrm{R}_2(z, \alpha_2) &= \frac{1}{2}V_2'(z, \alpha_2) - \frac{1}{4}(2 + \alpha_2 u + 2\alpha_2 z^2)\sqrt{z^2 - u} \ , \\ \rho_{\mathrm{ext}}^{(2)}(z, \alpha_2) &= \frac{1}{4\pi}(2 + \alpha_2 u + 2\alpha_2 z^2)\sqrt{u - z^2} \ , \quad u = a^2 \ . \end{aligned} \tag{3.5.2}$$

Combining the above leads to the planar on-shell action (3.2.20)

$$S[\rho_{\mathrm{ext}}^{(2)}(\lambda, \alpha_2)] = \sum_{n=1}^{2} \frac{(2n)!}{4n}\, \alpha_n\, \omega_n^{(2)} + \sum_{n=1}^{2} \frac{\alpha_n u^n}{4n^2 B(n, 1/2)} - \frac{1}{2}\log u + \log 2 \ , \tag{3.5.3}$$

with $\omega_n^{(2)}$ defined in (3.2.17). Using $u_+^{(2)}$ (3.3.2) this implies

$$\mathcal{F}_{2,\mathrm{n.a.}}^{(0)}(\alpha_2^\epsilon) = \frac{7}{24} - \frac{1}{2}\log 2 + \epsilon - 18\epsilon^2 + \frac{384}{5}\sqrt{3}\,\epsilon^{\mathbf{5/2}} + \mathcal{O}(\epsilon^3) \ , \tag{3.5.4}$$

where the subscript n.a. indicates the leading non-analyticity. The leading non-analytic behaviour, encoded in the critical exponent **5/2**, characterises the particular universality class associated to the $m = 2$ (3.5.1) and binomial matrix integrals (3.3.9) and is intimately related to the exponent **7/2** we observed in (3.3.5) at large k.

3.5.1 Critical exponents for $m = 3$

For $m = 3$ we have

$$V_3(M, \alpha_2, \alpha_3) = \frac{1}{2}M^2 + \frac{1}{4}\alpha_2 M^4 + \frac{1}{6}\alpha_3 M^6 \ . \tag{3.5.5}$$

The resolvent and the eigenvalue density are given by

$$\begin{aligned} &\mathrm{R}_3(z, \alpha_2, \alpha_3) \\ &= \frac{1}{2}V_3'(z, \alpha_2, \alpha_3) - \frac{1}{16}\left(8 + 4u\alpha_2 + 3u^2\alpha_3 + z^2(8\alpha_2 + 4u\alpha_3) + 8\alpha_3 z^4\right)\sqrt{z^2 - u} \ , \\ &\rho^{(3)}_{\text{ext}}(z, \alpha_2, \alpha_3) = \frac{1}{16\pi}\left(8 + 4u\alpha_2 + 3u^2\alpha_3 + z^2(8\alpha_2 + 4u\alpha_3) + 8\alpha_3 z^4\right)\sqrt{u - z^2} \ . \end{aligned} \tag{3.5.6}$$

For the $m = 3$ multicritical matrix integral, in contradistinction to the $m = 2$ model (3.5.1), we obtain two different non-analyticities – one along a fine-tuned path, another one along a generic path in coupling space.

Fine-tuned path. Normalising the above eigenvalue density we obtain the normalisation condition $\mathcal{N}_3(\alpha_2, \alpha_3) = 0$ (3.4.1) whose solutions we discussed in (3.4.2). Recall that the discriminant (3.4.6)

$$D_3 = \frac{675}{4194304}\alpha_3^2\left(-9(12\alpha_2 + 1)\alpha_2^2 + 20(27\alpha_2 + 2)\alpha_3 + 2700\alpha_3^2\right) \ , \tag{3.5.7}$$

vanishes at the multicritical point. More generally D_3 vanishes for

$$\alpha_{3,\pm} = \alpha^{(3)}_{3,c} - \frac{1}{10}\epsilon \pm \frac{1}{5}\epsilon^{3/2} \ , \quad \alpha_2^\epsilon \equiv \alpha^{(2)}_{2,c} + \epsilon \ . \tag{3.5.8}$$

and we restrict $\epsilon > 0$. Solving $\mathcal{N}_3(\alpha^{(3)}_{2,c}, \alpha_{3,\pm}) = 0$ we find $u = 12 + \tilde{x}\,\epsilon^{1/2} + \mathcal{O}(\epsilon^2)$, with the three solutions $\tilde{x}_{1,2} = \pm 36$ and $\tilde{x}_3 = 72$. WLOG we focus on $\tilde{x} = \pm 36$. Expanding the on-shell action leads to a leading non-analyticity of the form

$$\mathcal{F}^{(0)}_{3,\text{n.a.}}(\alpha_2^\epsilon, \alpha_{3,\pm}) = \frac{19}{40} - \frac{1}{2}\log 3 + \frac{9}{10}\epsilon \pm \frac{9}{10}\epsilon^{\mathbf{3/2}} - \frac{243}{40}\epsilon^2 + \mathcal{O}(\epsilon^{5/2}) \ . \tag{3.5.9}$$

The constant term is the action at criticality (3.2.21) for $m = 3$ with the Gaussian piece, which is equal to 3/4, subtracted. The critical exponent is given by **3/2**, which differs from the **5/2** critical exponent of the $m = 2$ model (3.5.4). Note that had we not kept the solution $\alpha_{3,\pm}$ to order $\mathcal{O}(\epsilon^{3/2})$ we would have not obtained the correct leading non-analytic behaviour in (3.5.9).

Generic path. Further to this, one can uncover another critical exponent by zooming into criticality while adding a linear deformation to one of the couplings. This leads to the ansatz

$$(\alpha_2, \alpha_3) = (\alpha_{2,c}^{(3)}, \alpha_3^{\epsilon}) \ , \quad u = 12 - 36 \cdot 10^{1/3}\epsilon^{1/3} + 108 \cdot 10^{2/3}\epsilon^{2/3} - 3240\epsilon + \mathcal{O}(\epsilon^2) \ . \tag{3.5.10}$$

The solution u is expanded up to order $\mathcal{O}(\epsilon)$ to avoid the appearance of spurious non-analyticities. Expanding the action around (3.5.10) we find

$$\mathcal{F}_{3,\text{n.a.}}^{(0)}(\alpha_{2,c}^{(3)}, \alpha_3^{\epsilon}) = \frac{19}{40} - \frac{1}{2}\log 3 + \frac{9}{2}\epsilon - 206550\epsilon^2 + \frac{11208375}{7}10^{1/3}\epsilon^{\mathbf{7/3}} + \mathcal{O}(\epsilon^2) \ . \tag{3.5.11}$$

The critical exponent is given by **7/3**, which again differs from the **5/2** critical exponent of the $m = 2$ model.

We believe that there are no other critical exponents near the multicritical point for $m = 3$ in the leading order planar expansion.

3.5.2 Critical exponents for general m

Since for $m \geq 4$ the normalisation condition is a higher order polynomial, we now outline a perturbative approach for the fine-tuned path.

Fine-tuned path. We would like to deform the couplings near the multicritical point $\boldsymbol{\alpha}_c$ (3.2.13) in the following manner

$$\boldsymbol{\alpha}^{\epsilon} = \boldsymbol{\alpha}_c + \boldsymbol{s}\,\epsilon \ , \quad u = 4m + x \ , \tag{3.5.12}$$

where x and ϵ are small parameters, and $\boldsymbol{s} \equiv (s_2, \ldots, s_m) \in \mathbb{R}^{m-1}$. Expanding the normalisation condition (3.2.11) we find

$$\mathcal{N}_m(\boldsymbol{\alpha}) = \left(-\frac{x}{4m}\right)^m - \epsilon \sum_{n=2}^{m} \frac{(4m)^n s_n}{2nB(n, 1/2)} \sum_{\ell=0}^{n} \binom{n}{\ell} \left(\frac{x}{4m}\right)^{\ell} + \mathcal{O}(\epsilon^2) \ . \tag{3.5.13}$$

For those $\boldsymbol{s}$ satisfying

$$\bigcup_{j=1}^{r'} \mathcal{H}_m^{(j)} = 0 \ , \quad r' = 1, \dots, m-2 \ , \tag{3.5.14}$$

where $\mathcal{H}_m^{(j)}$ (hypersurfaces) are defined as

$$\mathcal{H}_m^{(j)} \equiv m^{-j-1} \sum_{n=j+1}^{m} \frac{(4m)^n}{2nB(n,1/2)} \binom{n-2}{j-1} s_n = 0 \ , \tag{3.5.15}$$

the coefficients of x^ℓ in (3.5.13) with $0 \leq \ell \leq r'-1$ vanish. The proof of this can be found in appendix 6. Consequently on (3.5.14), the solutions of $\mathcal{N}_m(\boldsymbol{\alpha}) = 0$ in x will scale as $\epsilon^{1/(m-r')}$. To indicate that the deformations $\boldsymbol{s}$ are living on (3.5.14) we introduce an additionial superscript to the normalisation condition $\mathcal{N}_m^{(r')}(\boldsymbol{\alpha})$ and $\mathcal{F}_{m,\text{n.a.}}^{(r')}(\boldsymbol{\alpha})$, where $r' \in \{1, \dots, m-2\}$. We are thus led to the following ansatz

$$\boldsymbol{\alpha}^\epsilon \equiv \boldsymbol{\alpha}_c + \boldsymbol{s}\,\epsilon \ , \quad u = 4m + \tilde{x}\,\epsilon^{\frac{1}{m-r'}} \ , \quad \tilde{x} \in \mathbb{R} \ , \tag{3.5.16}$$

giving rise to the normalisation condition

$$\mathcal{N}_m^{(r')}(\boldsymbol{\alpha}^\epsilon) = \left[(-1)^m \frac{\tilde{x}^m}{(4m)^m} - \frac{\tilde{x}^{r'}}{4^{r'}} m^2\, \mathcal{H}_m^{(r'+1)} \right] \epsilon^{\frac{m}{m-r'}} + \mathcal{O}\left(\epsilon^{\frac{m+1}{m-r'}}\right) \ . \tag{3.5.17}$$

We refer to appendix 6 for a proof of (3.5.17). Recalling the discussion near (3.5.9) for $m = 3$, to ensure that we obtain the correct non-analytic behaviour for $\mathcal{F}_{m,\text{n.a.}}^{(0)}(\boldsymbol{\alpha})$, we must expand one of the couplings to subleading order. For $p \in \{2, \dots, m\}$ arbitrary we take

$$\alpha_{n\neq p}^\epsilon = \alpha_{c,n\neq p}^{(m)} + s_{n\neq p}\,\epsilon \ , \quad \alpha_p^\beta = \alpha_{c,p}^{(m)} + s_p\,\epsilon + \tilde{s}\,\epsilon^\beta \ , \quad u = 4m + \tilde{x}\,\epsilon^{\frac{1}{m-r'}} \ . \tag{3.5.18}$$

For $\beta < m/(m-r')$ the last term gives additional contributions spoiling the $\epsilon^{m/(m-r')}$ non-analyticity. For $\beta > m/(m-r')$ the leading non-analyticity is unaffected. For $\beta = m/(m-r')$ we are led to

$$\mathcal{N}_m^{(r')}(\alpha_{n\neq p}^\epsilon, \alpha_p^\beta) = \left[(-1)^m \frac{\tilde{x}^m}{(4m)^m} - \frac{\tilde{x}^{r'}}{4^{r'}} m^2\, \mathcal{H}_m^{(r'+1)} - \frac{(4m)^p}{2pB(p,1/2)} \tilde{s} \right] \epsilon^{\frac{m}{m-r'}} + \mathcal{O}\left(\epsilon^{\frac{m+1}{m-r'}}\right) \ . \tag{3.5.19}$$

It can be checked that adding subleading corrections to more than one of the α_n does not lead to additional non-analyticities.

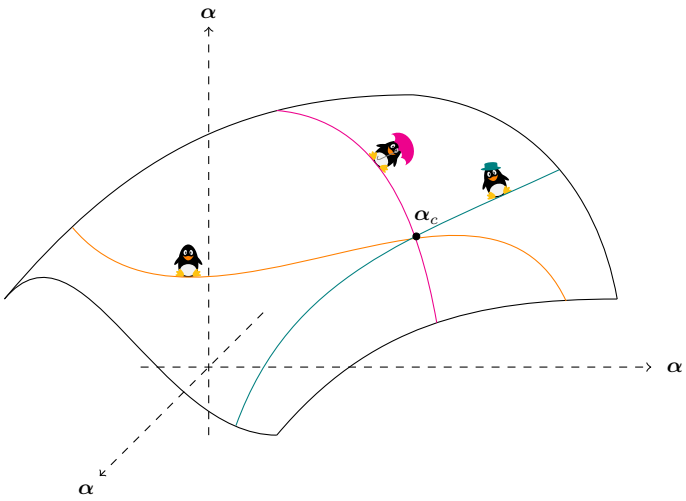

Figure 3.7: *We zoom into the critical point $\boldsymbol{\alpha}_c$ and then start moving into special directions to recover the different non-analyticities.*

We now determine the non-analytic behaviour of $\mathcal{F}^{(0)}_{m,\text{n.a.}}(\boldsymbol{\alpha})$ once we move away from the critical point (3.5.16). Using $\beta = m/(m-r')$ in (3.5.18) we are led to

$$S^{(r')}_m[\rho^{(m)}_{\text{ext}}(\lambda,\boldsymbol{\alpha}^\epsilon)] = \mathcal{S}^{(r')}_m[\boldsymbol{s},\epsilon,\epsilon^2] - \frac{1}{2}H_m\left[(-1)^m\frac{\tilde{x}^m}{(4m)^m} - \frac{\tilde{x}^{r'}}{4^{r'}}m^2\,\mathcal{H}^{(r'+1)}_m - \frac{(4m)^p}{2pB(p,1/2)}\tilde{s}\right]\epsilon^{\frac{m}{m-r'}} + \frac{(4m)^p}{2p^2B(p,1/2)}\frac{m!p!}{(m+p)!}\,\tilde{s}\,\epsilon^{\frac{m}{m-r'}} + \mathcal{O}\left(\epsilon^{\frac{m+1}{m-r'}}\right)\,, \quad (3.5.20)$$

where $\mathcal{S}^{(r')}_m[\boldsymbol{s},\epsilon,\epsilon^2]$ is an $\tilde{x}$-independent expression whose explicit form we present in appendix 6. Taking $\tilde{x} = \tilde{x}_*$ to be a solution of the normalisation condition $\mathcal{N}^{(r')}_m(\alpha^\epsilon_{n\neq p},\alpha^\beta_p) = 0$ at order $\epsilon^{m/(m-r')}$ we finally obtain for $r' = 1,2,\ldots,m-2$

$$\mathcal{F}^{(0)}_{m,\text{n.a.}}(\alpha^\epsilon_{n\neq p},\alpha^\beta_p) - \mathcal{S}^{(r')}_m[\boldsymbol{s},\epsilon,\epsilon^2] + \frac{3}{4} = \frac{(4m)^2}{2p^2B(p,1/2)}\frac{m!p!}{(m+p)!}\,\tilde{s}\,\epsilon^{\frac{m}{m-r'}} + \mathcal{O}\left(\epsilon^{\frac{m+1}{m-r'}}\right)\,, \quad (3.5.21)$$

where $2 \leq p \leq m$. In summary for the m^{th} multicritical matrix integral (3.2.3) we have so far obtained $(m-2)$ distinct critical exponents given by $\boldsymbol{m/(m-r')}$, $r' = 1,2,\ldots,m-2$.

Example $m = 3$**.** Let us take

$$(\alpha_2, \alpha_3) = (\alpha_2^\epsilon, \alpha_3^\epsilon) \ , \quad u = 12 + x \ , \qquad 0 < \epsilon \ll 1 \ . \tag{3.5.22}$$

The parameter x is itself small and fixed in terms of s_2, s_3, and ϵ through $\mathcal{N}_3(\boldsymbol{\alpha}) = 0$. For generic values of s_2 and s_3, expanding the normalisation condition $\mathcal{N}_3(\boldsymbol{\alpha}) = 0$ for small ϵ leads to the following three solutions

$$x = 36\, z\, \epsilon^{1/3} (s_2 + 10 s_3)^{1/3} \ , \qquad z^3 = -1 \ . \tag{3.5.23}$$

We thus recover the non-analytic behaviour observed in (3.5.10).

For the finely tuned combination $\mathcal{H}_3^{(1)} = s_2 + 10 s_3 = 0$ (3.5.15), we find the leading order behaviour

$$x = \pm 36 \sqrt{3 s_2 \epsilon} \ , \tag{3.5.24}$$

recovering the non-analytic behaviour observed in (3.5.19). To obtain the subleading $\epsilon^{3/2}$ dependence in (3.5.22), we must add a subleading piece $\tilde{s}\epsilon^\beta$, $\beta > 1$ to one of the couplings. WLOG we take α_3. Expanding the normalisation condition we infer that only $\beta = 3/2$ is consistent with the perturbative expansion. Our ansatz becomes (3.5.18)

$$\alpha_2^\epsilon = \alpha_{2,c}^{(3)} + s_2 \epsilon \ , \quad \alpha_3^\beta = \alpha_{3,c}^{(3)} - \frac{1}{10} s_2 \epsilon + \tilde{s} \epsilon^{3/2} \ , \quad u = 12 + \tilde{x}\, \epsilon^{1/2} \ . \tag{3.5.25}$$

Adding further subleading terms will not change the leading non-analytic behaviour. Setting $s_2 = 1$ and $\tilde{s} = \pm 1/5$ we recover (3.5.8). Expanding $\mathcal{N}_3^{(1)}(\alpha_2^\epsilon, \alpha_3^\beta)$ for small ϵ, we find (3.5.19)

$$\mathcal{N}_3^{(1)}(\alpha_2^\epsilon, \alpha_3^\beta) = \left(-\frac{1}{1728} \tilde{x}^3 + \frac{9}{4} s_2 \tilde{x} - 270 \tilde{s} \right) \epsilon^{3/2} + \mathcal{O}(\epsilon^2) \ . \tag{3.5.26}$$

Evaluating the action in a perturbative expansion along (3.5.25), we obtain (3.5.21)

$$\begin{aligned} &\mathcal{F}_{3,\text{n.a.}}^{(0)}(\alpha_2^\epsilon, \alpha_3^\beta) \\ &= \frac{19}{40} - \frac{1}{2} \log 3 + \frac{9}{10} s_2 \epsilon - \frac{1}{2} H_3 \left(-\frac{1}{1728} \tilde{x}^3 + \frac{9}{4} s_2 \tilde{x} - 270 \tilde{s} \right) \epsilon^{\mathbf{3/2}} + \frac{9}{2} \tilde{s}\, \epsilon^{\mathbf{3/2}} + \mathcal{O}(\epsilon^2) \ , \end{aligned} \tag{3.5.27}$$

recovering (3.5.9) for $s_2 = 1$ and $\tilde{s} = \pm 1/5$. From the above expression we infer that for vanishing $\tilde{s}$ the coefficient multiplying the leading non-analyticity vanishes, since its solution in $\tilde{x} = \tilde{x}_\star$ agrees with the solution of the leading order term in (3.5.26). The non-analytic behaviour in (3.5.27) is robust against other deformations of the ansatz (3.5.25).

Generic path for general m. In addition to the $(m-2)$ critical exponents in (3.5.21) the matrix integrals (3.2.1) exhibit one more multicritical exponent.

To obtain (3.5.4) for $m=2$ we observed the reaction of the action when allowing α_2 to slightly deviate from its critical value $\alpha_{2,c}^{(2)}$ (3.2.13). We can generalise this for the polynomials $V_m(M,\boldsymbol{\alpha})$ for $m\geq 3$. Here we observe the reaction of the action when allowing one arbitrary coupling to deviate away from the multicritical point. In other words we consider

$$\alpha_2=\alpha_{2,c}^{(m)},\ \ldots,\ \alpha_{m-1}=\alpha_{m-1,c}^{(m)}\ ,\ \alpha_m=\alpha_{m,c}^{(m)}+\epsilon\ ,\quad 0<\epsilon\ll 1\ , \tag{3.5.28}$$

where WLOG α_m deviates away from its critical value $\alpha_{m,c}^{(m)}$. The leading reaction of the normalisation condition away from its critical value $4m$ is of the form $\epsilon^{1/m}$ easily extracted from (3.5.13).[3] To avoid spurious critical exponents in $\mathcal{F}^{(0)}_{m,\text{n.a.}}(\boldsymbol{\alpha})$, we need to expand the solution to the normalisation condition to order $\mathcal{O}(\epsilon)$. In addition to (3.5.28) we take the following ansatz[4] for u

$$u=4m+\tilde{A}\epsilon^{1/m}+\sum_{\ell=2}^{2m}\tilde{C}_\ell\,\epsilon^{\ell/m}+\mathcal{O}\left(\epsilon^{(2m+1)/m}\right)\ . \tag{3.5.29}$$

The coefficients $\{\tilde{A},\tilde{C}_\ell\}\in\mathbb{C}$ we obtain by comparing coefficients of equal powers of ϵ in the normalisation condition. The coefficients $\tilde{A}$ are given by

$$\tilde{A}^{(n)}=e^{i\pi n/m}\left(\frac{(4m)^{2m}}{2mB(m,1/2)}\right)^{1/m}\ ,\quad n=1,\ldots,m\ . \tag{3.5.30}$$

Upon choosing one $\tilde{A}^{(n)}$ the $\tilde{C}_\ell$ for $2\leq\ell\leq 2m-1$ are fixed uniquely. WLOG we choose $\tilde{A}^{(m)}$ and find

$$u=4m\sum_{\ell=0}^{2m}(-1)^\ell m^\ell\binom{2m-1}{m-1}^{\ell/m}\epsilon^{\ell/m}+\mathcal{O}\left(\epsilon^{(2m+1)/m}\right)\ . \tag{3.5.31}$$

The leading non-analyticity is thus given by

$$\mathcal{F}^{(0)}_{m,\text{n.a.}}(\alpha_{2,c}^{(m)},\ldots,\alpha_{m-1,c}^{(m)},\alpha_m^\epsilon)=S_c[\rho^{(m)}_{\text{ext}}(\lambda,\boldsymbol{\alpha}_c)]-\frac{3}{4}+\beta_1\,\epsilon+\beta_2\,\epsilon^2+\beta_3\,\epsilon^{\mathbf{2}+\frac{\mathbf{1}}{\mathbf{m}}}+\mathcal{O}\left(\epsilon^{2+\frac{2}{m}}\right)\ , \tag{3.5.32}$$

[3] Comparing (3.5.12) to our ansatz (3.5.28) we set $s_n=0$, $n\leq m-1$ and $s_m=1$.

[4] We would obtain the right critical exponent already if we stopped at linear order in ϵ. However the coefficient is affected by terms up to order $\mathcal{O}(\epsilon^2)$

with β_3 given by

$$\beta_3 = \frac{m^{2m+3}}{2(2m+1)} \binom{2m-1}{m-1}^{1+1/m} \mathcal{C}_m^{(2)} \ . \tag{3.5.33}$$

$\mathcal{C}_m^{(2)}$ are the Catalan numbers (3.3.4). On the other side β_1 and β_2 are ϵ-independent expressions in m. From (3.5.32) we infer the leading non-analyticity $\mathbf{2+1/m}$ which is intimately related to the critical exponent (3.4.29) observed for large k in the perturbative expansion.

Example $m = 3$**.** For the multicritical matrix integral with $m = 3$ we make the ansatz

$$\alpha_2 = \alpha_{2,c}^{(3)} \ , \quad \alpha_3 = \alpha_{3,c}^{(3)} + \epsilon \ , \quad u = 12 + \tilde{A}\epsilon^{1/3} + \sum_{\ell=2}^{6} \tilde{C}_\ell \, \epsilon^{\ell/3} + \mathcal{O}\left(\epsilon^{7/3}\right) \ . \tag{3.5.34}$$

Expanding the normalisation condition $\mathcal{N}_3(\alpha_{2,c}, \alpha_3^\epsilon) = 0$ (3.2.11) we obtain to leading order

$$\tilde{A}^{(n)} = 36\, e^{i\pi n/3} \times 10^{1/3} \ , \quad n = 1, 2, 3 \ . \tag{3.5.35}$$

Choosing $\tilde{A}^{(3)}$ and repeating (3.5.34) after including subleading corrections in the normalisation condition we obtain the ansatz

$$u = 12 \sum_{\ell=0}^{6} (-1)^\ell 3^\ell (10)^{\ell/m} \epsilon^{\ell/3} + \mathcal{O}\left(\epsilon^{7/3}\right) \ . \tag{3.5.36}$$

Expanding the action around (3.5.36) we obtain

$$\mathcal{F}_{3,\text{n.a.}}^{(0)}(\alpha_{2,c}^{(3)}, \alpha_3^\epsilon) = \frac{19}{40} - \frac{1}{2}\log 3 + \frac{9}{2}\epsilon - 6075\epsilon^2 + \frac{492075}{7} \times (10)^{1/3} \epsilon^{\mathbf{7/3}} + \mathcal{O}\left(\epsilon^{8/3}\right) \ . \tag{3.5.37}$$

We observe the leading critical exponent $\mathbf{7/3}$.

General remarks. It is worth noting that only ϵ and ϵ^2 appear at orders lower than the leading non-analytic behaviour of $S_m^{(r)}[\rho_{\text{ext}}^{(m)}(\lambda, \boldsymbol{\alpha}^\epsilon)]$ (3.5.20). This is a consequence of our particular choice of deformation (3.5.15). For m prime the full set of critical exponents are elements of $\mathbb{Q}^+/\mathbb{Z}$. For non-prime m some of the critical exponents are integers. Whether or not we should refer to these integers as critical exponents is a subtle matter.[5] A point of concern for integer critical

[5] It can often happen that when a critical exponent is naïvely integer valued there is in fact a logarithmic dependence on the coupling. Logarithmic behaviour is also present for the critical exponent of a two-matrix model [119] whose continuum description has been argued to be the free fermion coupled to two-dimensional gravity. It is relatively straightforward to prove that

exponents is that they may be sensitive to analytic redefinitions of the couplings. For $m = 4$, $k = 2$ and WLOG taking $p = 2$ we have

$$u = 16+\tilde{x}\epsilon^{1/2}\,, \quad \alpha_2 = -\frac{1}{8}+\frac{560}{3}s_4\epsilon+\delta\epsilon^2\,, \quad \alpha_3 = \frac{1}{160}-28s_4\epsilon\,, \quad \alpha_4 = -\frac{1}{8960}+s_4\epsilon \tag{3.5.38}$$

and (3.5.21) reduces to

$$S_4^{(2)}[\rho_{\rm ext}^{(4)}(\lambda,\boldsymbol{\alpha}^\epsilon)] - \mathcal{S}_4^{(2)}[\boldsymbol{s},\epsilon,\epsilon^2] = \frac{8}{5}\,\delta\,\epsilon^{\mathbf{2}} + \mathcal{O}\left(\epsilon^{5/2}\right)\,, \tag{3.5.39}$$

where

$$\mathcal{S}_4^{(2)}[\boldsymbol{s},\epsilon,\epsilon^2] = S_c[\rho_{\rm ext}^{(4)}(\lambda,\boldsymbol{\alpha}_c)] + 160s_4\epsilon - 143360s_4^2\epsilon^2\,. \tag{3.5.40}$$

If s_4 and δ obey

$$\frac{8}{5}\delta - 143360s_4^2 = 0\,, \tag{3.5.41}$$

we can cancel the integer critical exponent **2**.

Furthermore we note that the matrix integral (3.2.3) admits $(m-1)$ distinct critical exponents only upon considering deformations away from the multicritical point. The only other critical exponent is that of a **square root** non-analyticity in the normalisation condition leading to $\mathcal{F}^{(0)}_{m,\rm n.a.}(\boldsymbol{\alpha}) \sim \epsilon^{\mathbf{5/2}}$ which occurs on surfaces connecting the $m^{\rm th}$ polynomial $V_m(M,\boldsymbol{\alpha})$ to a binomial matrix integral $\tilde{V}_n(M,\alpha)$, $n \leq m$ (3.3.9).

⋆ ⋆ ⋆

Summary. In summary, the set of $(m-1)$ critical exponents for the $m^{\rm th}$ multicritical matrix integral (3.2.3) are given by $\boldsymbol{m/(m-r')}$, $r' = 1,\ldots,m-2$ (3.5.21) and $\boldsymbol{2+1/m}$ (3.5.32).

3.6 Critical exponents in the continuum picture

In section 3.5 we uncovered a set of non-analyticities arising from the deformation of multicritical matrix integrals (3.2.3) slightly away from the multicritical point (3.2.13). We showed that the $m^{\rm th}$ multicritical matrix integral has $(m-1)$ distinct non-analyticities (3.5.21) and (3.5.32). In this section we will uncover the same non-analyticities within the continuum picture of $\mathcal{M}_{2m-1,2}$ coupled to two-dimensional quantum gravity.

our integer valued critical exponents are indeed integers exhibiting no logarithmic dependence on the coupling.

3.6.1 A minimal model refresher

Minimal models are two-dimensional CFTs characterised by two coprime integers (p, p') with $p, p' \geq 2$ and WLOG we assume $p > p'$.[6] We will denote the (p, p') minimal model by $\mathcal{M}_{p,p'}$. The central charge of $\mathcal{M}_{p,p'}$ is given by

$$c^{(p,p')} \equiv 1 - \frac{6(p-p')^2}{pp'} \ . \tag{3.6.1}$$

Each $\mathcal{M}_{p,p'}$ has a finite number of conformal primaries $\mathcal{O}_{r,s}$ whose (holomorphic) conformal dimension is given by

$$\Delta_{r,s} = \frac{(rp'-sp)^2-(p-p')^2}{4pp'} \ , \quad r = 1, \ldots, p-1 \ , \quad s = 1, \ldots, p'-1 \ . \tag{3.6.2}$$

These obey

$$\Delta_{r,s} = \Delta_{p-r,p'-s} = \Delta_{r+p,s+p'} \ , \tag{3.6.3}$$

such that the number of distinct conformal primaries is given by $n_{p,p'} \equiv (p-1)(p'-1)/2$. The identity operator $\mathbb{I}$ of vanishing conformal dimension is always present and given by $\mathcal{O}_{1,1} = \mathcal{O}_{p-1,p'-1}$. The anti-holomorphic conformal dimensions are denoted by $\bar{\Delta}_{r,s}$ and take the same values as (3.6.2).

The simplest minimal model is $\mathcal{M}_{3,2}$, which is a two-dimensional CFT with central charge $c^{(3,2)} = 0$ and the unique operator $\mathbb{I}$, of vanishing conformal dimension.

(Non)-unitary minimal models. It will prove useful to distinguish between unitary and non-unitary minimal models. In addition to a positive definite inner product, unitary minimal models have positive central charge and non-negative conformal dimensions. As shown in [28], the unitary models are given by the series $\mathcal{M}_{m+1,m}$ with $m > 2$. Unitary minimal models have $n_{m+1,m} = m(m-1)/2$ primaries.

Non-unitary minimal models have negative central charge. Although the highest weight states have positive norm, their Virasoro descendants have negative norm. The simplest example of a non-unitary minimal model is $\mathcal{M}_{5,2}$, the Yang-Lee model with $c^{(5,2)} = -22/5$. $\mathcal{M}_{5,2}$ has two conformal primaries of holomorphic conformal dimension $\Delta_{1,1} = 0$ and $\Delta_{2,1} = -1/5$.

In what follows we will focus on $\mathcal{M}_{2m-1,2}$ with $m \geq 2$. The general expression for

[6] In addition to the original work [27], an excellent resource discussing their detailed properties is given by [172, 173].

their central charge is

$$c^{(2m-1,2)} = 1 - \frac{3(3-2m)^2}{2m-1} \ . \tag{3.6.4}$$

The number of conformal primaries is $n_{2m-1,2} = (m-1)$, and their holomorphic dimensions are given by

$$\Delta_{r,1} = \frac{(2m-1-2r)^2 - (2m-3)^2}{8(2m-1)} \ , \quad r = 1, \dots, m-1 \ . \tag{3.6.5}$$

The conformal dimensions are increasingly negative for increasing r, and the lowest weight primary $\mathcal{O}_{\rm min} \equiv \mathcal{O}_{m-1,1}$ has holomorphic conformal dimension

$$\Delta_{\rm min} = \frac{(m-1)(m-2)}{2(1-2m)} \ . \tag{3.6.6}$$

From (3.6.4) and (3.6.6) we infer the large m expansions

$$c^{(2m-1,2)} = -6m + 16 + \dots \ , \quad \Delta_{\rm min} = -\frac{m}{4} + \frac{5}{8} + \dots \ . \tag{3.6.7}$$

Although $c^{(2m-1,2)}$ grows at large m, it has been argued [178, 235] that a better measure of the number of degrees of freedom is captured by

$$c_{\rm eff}^{(2m-1,2)} \equiv c^{(2m-1,2)} - 24\Delta_{\rm min} = 1 + \frac{3}{1-2m} \ . \tag{3.6.8}$$

We note that $c_{\rm eff}^{(2m-1,2)} < 1$ goes to one in the large m limit.

3.6.2 Critical exponents

To compute critical exponents associated to a given conformal field theory, we consider the partition function of the theory deformed by a small amount of a particular conformal primary $\mathcal{O}_\Delta$. We first discuss critical exponents for CFTs on a fixed background, and then proceed to a fluctuating background.

2d CFT on a fixed flat background. From the perspective of a path-integral, we would like to compute

$$Z[\lambda_\Delta, \ell] = \int [\mathcal{D}\Phi] e^{-S_{\rm CFT}[\Phi] - \lambda_\Delta \int {\rm d}^2x \, \mathcal{O}_\Delta} \ , \quad \lambda_\Delta \in \mathbb{R} \ , \tag{3.6.9}$$

where ℓ denotes the size of the flat square on which the CFT resides. The conformal primary $\mathcal{O}_\Delta$ has dimension $(\Delta, \bar{\Delta})$ and for simplicity we take $\Delta = \bar{\Delta}$.

The dimensionful scales of the problem are the volume of space ℓ^2, the ultraviolet length scale $\ell_{\rm uv} \ll \ell$, and the coupling λ_Δ whose holomorphic scaling dimension is $\Delta_\lambda = \Delta - 1$. Following the line of argumentation from the scaling hypothesis $Z[\lambda_\Delta, \ell] = Z[q^{-\Delta_\lambda}\lambda_\Delta, q\ell]$, $q \in \mathbb{R}^+$ [174] we would like the UV independent part of $\log Z[\lambda_\Delta, \ell]$ to be extensive in the volume. Given that $Z[\lambda_\Delta, \ell]$ is dimensionless, we must have

$$\log Z[\lambda_\Delta, \ell] = \mathcal{N}\ell^2(\lambda_\Delta)^{\boldsymbol{\nu}_\Delta} \ , \quad \boldsymbol{\nu}_\Delta \equiv 1/(1-\Delta) \ . \tag{3.6.10}$$

$\mathcal{N}$ is a normalisation constant independent of λ_Δ. Notice that the critical exponent associated to the identity operator is simply $\boldsymbol{\nu}_0 = 1$. Furthermore, for $\Delta > 1$, corresponding to an irrelevant $\mathcal{O}_\Delta$, the critical exponent would be negative.

2d CFT on a fluctuating background. We now consider a two-dimensional CFT with central charge $c_{\rm m} < 1$ coupled to two-dimensional gravity. Integrating over all metrics renders the extensivity condition of the scaling hypothesis somewhat subtle. In the Weyl gauge the two-dimensional metric is chosen to be $g_{ij} = e^{2b\varphi}\tilde{g}_{ij}$. The problem then maps to studying the matter CFT with central charge $c_{\rm m}$, trivially coupled to a Liouville CFT with central charge $c_L = 26 - c_{\rm m}$, and the $\mathfrak{bc}$-ghost system with central charge $c_g = -26$ [8]. The Liouville action is given by [8]

$$S_L[\varphi, \Lambda] = \frac{1}{4\pi}\int \mathrm{d}^2x\sqrt{\tilde{g}}\left(\tilde{g}^{ij}\partial_i\varphi\partial_j\varphi + QR[\tilde{g}_{ij}]\varphi + 4\pi\Lambda\, e^{2b\varphi}\right) \ , \tag{3.6.11}$$

where $\tilde{g}_{ij}$ is taken to be the round metric on S^2 such that $R[\tilde{g}_{ij}] = 2$ and $\Lambda \geq 0$ is the cosmological constant. Moreover, $Q = b + 1/b$ with [33, 63, 66, 68]

$$b = \frac{\sqrt{25 - c_{\rm m}} - \sqrt{1 - c_{\rm m}}}{2\sqrt{6}} \ , \quad Q = \sqrt{\frac{25 - c_{\rm m}}{6}} \ . \tag{3.6.12}$$

The residual gauge invariance in the Weyl gauge enforces that all operators of the combined theory are spinless primaries with conformal dimension $\Delta = 1$. In the trivial ghost sector this is achieved by dressing the matter primaries of weight $\Delta_{\rm m}$ by a Liouville operator of weight $\Delta_L = 1 - \Delta_{\rm m}$.

Unitary 2d CFT on a fluctuating background. We now specify to a unitary two-dimensional CFT with $c_{\rm m} \in (0, 1)$. The simplest critical exponent corresponds to the matter identity whose coupling is Λ. The partition function of interest is

$$\mathcal{Z}[\Lambda] = \int [\mathcal{D}\varphi] e^{-S_L[\varphi,\Lambda]} = \Lambda^{\boldsymbol{Q/b}} \ . \tag{3.6.13}$$

We indicate the partition function on a fluctuating background by $\mathcal{Z}$. A simple derivation of the above follows from performing a shift in φ [29,30]. Due to the Liouville dressing, the critical exponent of the identity is no longer simply given by $\boldsymbol{\nu}_0 = 1$ (3.6.10), but rather [143]

$$\boldsymbol{\nu}_{\text{grav}} \equiv Q/b = \frac{1}{12}\sqrt{(1-c_{\text{m}})\,(25-c_{\text{m}})} + \frac{25-c_{\text{m}}}{12} \ . \tag{3.6.14}$$

The critical exponent for $\boldsymbol{\nu}_{\text{grav}}$ informs us how to modify the scaling behaviour of length upon coupling to gravity. On a fixed background the total scaling dimension of a length scale is minus one, whereas now we must take it to be $\boldsymbol{\nu}_{\text{grav}}/2$. $\boldsymbol{\nu}_{\text{grav}}$ is also known as the string scusceptibility.

Now, rather than the identity we consider turning on a matter conformal primary $\mathcal{O}_\Delta$. The partition function of interest, in the Weyl gauge, becomes

$$\mathcal{Z}[\lambda_\Delta] = \int [\mathcal{D}\varphi][\mathcal{D}\Phi] e^{-S_L[\varphi,\Lambda=0]-S_{\text{CFT}}[\Phi]-\lambda_\Delta \int \mathrm{d}^2x\sqrt{\hat{g}}\, e^{2\sigma_\Delta\varphi}\mathcal{O}_\Delta} \ , \tag{3.6.15}$$

where we set $\Lambda = 0$ since we are interested in turning on $\mathcal{O}_\Delta$ alone. We further have

$$\sigma_\Delta \equiv \frac{\sqrt{25-c_{\text{m}}} - \sqrt{24\Delta+1-c_{\text{m}}}}{2\sqrt{6}} \ , \tag{3.6.16}$$

which ensures that the matter operator is dressed appropriately. We note that $b = \sigma_{\Delta=0}$. Upon shifting $\varphi \to \varphi - (\log\lambda_\Delta)/2\sigma_\Delta$, [29,30] and noting that the path-integration measure over φ is invariant under such shifts, it is straightforward to deduce

$$\mathcal{Z}[\lambda_\Delta] = \mathcal{N}\,(\lambda_\Delta)^{\boldsymbol{Q/\sigma_\Delta}} \ , \tag{3.6.17}$$

where $\mathcal{N}$ is a λ_Δ independent normalisation. For more details we refer to [63].

$\mathcal{M}_{2m-1,2}$ on a fluctuating background. For non-unitary models with $c_{\text{m}} \leq 0$, further care must be taken due to the presence of operators with negative conformal dimension. Our main interest is in $\mathcal{M}_{2m-1,2}$, whose most relevant operator $\mathcal{O}_{\text{min}}$ has negative conformal dimension Δ_{min} (3.6.6). The lowest weight operator replaces the identity in that all other operators are 'irrelevant' with respect to $\mathcal{O}_{\text{min}}$. Thus, in the non-unitary case we might be inclined [16,110] to replace (3.6.13) with

$$\mathcal{Z}[\Lambda_{\text{min}}] = \int [\mathcal{D}\varphi][\mathcal{D}\Phi] e^{-S_L[\varphi,\Lambda=0]-S_{\text{CFT}}[\Phi]-\Lambda_{\text{min}} \int \mathrm{d}^2x\sqrt{\hat{g}}\, e^{2\sigma_{\text{min}}\varphi}\mathcal{O}_{\text{min}}} \ , \tag{3.6.18}$$

where $\sigma_{\text{min}} \equiv \sigma_{\Delta_{\text{min}}}$ (3.6.16). Using similar techniques to those discussed previ-

ously one finds

$$\mathcal{Z}[\Lambda_{\min}] = (\Lambda_{\min})^{\boldsymbol{Q/\sigma_{\min}}} \ . \tag{3.6.19}$$

In effect, one is replacing $\sigma_{\Delta=0}$ with $\sigma_{\Delta_{\min}}$ (3.6.13). Note that

$$Q/\sigma_{\min} = \mathbf{2 + 1/}\boldsymbol{m} \ . \tag{3.6.20}$$

Turning on other operators $\mathcal{O}_{r,1}$ while setting $\Lambda_{\min} = 0$ leads to

$$\mathcal{Z}[\lambda_{\Delta_{r,1}}] = \mathcal{N}\left(\lambda_{\Delta_{r,1}}\right)^{\boldsymbol{Q/\sigma_{\Delta_{r,1}}}} \quad , \quad Q/\sigma_{\Delta_{r,1}} = (\mathbf{1} + \mathbf{2m})/(\mathbf{r} + \mathbf{1}) \ , \tag{3.6.21}$$

where $r = 1, 2, \ldots, m-2$. Finally we note the useful relation

$$\sigma_{\min}/\sigma_{\Delta_{r,1}} = \mathbf{m}/(\mathbf{1} + \mathbf{r}) \ , \qquad r = 1, \ldots, m-2 \ . \tag{3.6.22}$$

Summary. In summary, we obtain $(m-1)$ critical exponents: Turning on the operator of lowest conformal dimension we obtain **2+1/m** (3.6.20). Turning on any of the other $(m-2)$ operators we obtain the critical exponents **m/(1+r)**, $r = 1, \ldots, m-2$ (3.6.22).

A fixed "area" perspective. In order to compare to the perturbative discussion of section 3.4 it proves instructive to consider the gravitational path integrals with a constraint fixing the total area of space to a fixed value υ. This can be achieved by inserting a δ-function inside of the gravitational path-integral (3.6.9). For two-dimensional conformal field theories with $c_{\rm m} < 1$, we have

$$\mathcal{Z}_{\rm area}[\upsilon] = \mathcal{N}\,\upsilon^{\boldsymbol{-1-Q/b}} \times e^{-\upsilon\Lambda} \ , \qquad \int \mathrm{d}^2x\sqrt{\tilde{g}}\, e^{2b\varphi} = \upsilon \ . \tag{3.6.23}$$

where $\mathcal{N}$ is independent of υ and Λ. Integrating $\mathcal{Z}_{\rm area}[\upsilon]$ against υ, we recover $\mathcal{Z}[\Lambda]$ (3.6.13). For $c_{\rm m} = 0$, we note that $1 + Q/b = \mathbf{7/2}$, the value observed in (3.3.5). For $c_{\rm m} = c^{(2m-1,2)}$ in (3.6.4), we find instead $1 + Q/b = \mathbf{3/2+m}$. Let us now consider those non-unitary minimal models whose lowest weight operator $\mathcal{O}_{\min}$ is different from the identity. We can also consider fixing

$$\int \mathrm{d}^2x\sqrt{\tilde{g}}\, \mathcal{O}_{\min}\, e^{2\sigma_{\min}\varphi} = \upsilon \ . \tag{3.6.24}$$

This leads to the following partition function

$$\mathcal{Z}_{\min}[\upsilon] = \mathcal{N}\,\upsilon^{\boldsymbol{-1-Q/\sigma_{\min}}} e^{-\upsilon\Lambda_{\min}} \ . \tag{3.6.25}$$

For the Lee-Yang model $\mathcal{M}_{5,2}$ with $c^{(5,2)} = -22/5$, we have $1 + Q/\sigma_{\min} = \mathbf{10/3}$.

For general $\mathcal{M}_{2m-1,2}$ we have $1 + Q/\sigma_{\min} = (\mathbf{3} + \mathbf{1/m})$.

3.6.3 Comparison to matrix integrals

At this stage it behooves us to compare our results to those of the multicritical matrix integrals. We take inspiration from 't Hooft's diagrammatic picture [78], whereby the perturbative diagrams of the matrix integrals correspond to discretised Riemann surfaces. Care must be taken in identifying the appropriate quantities between the matrix integrals and the continuum picture.

$\mathcal{M}_{3,2}$ on a fluctuating background. Let us begin by discussing the simplest case, namely $m = 2$. In this case the matrix diagrammatics (3.3.5) indicates that the dependence on the number of vertices k goes as $\sim k^{-\mathbf{7/2}}(\alpha_2/\alpha_{2,c}^{(2)})^{-k}$ at large k. One is motivated to identify the number of vertices, k, with the area of the surface in the continuum picture. Both are extensive quantities sensitive to the total number of points on the surface. In doing so, one finds a match between the behaviour of the fixed area partition function (3.6.23) and the matrix diagrammatics. This suggests that the identification of k in the matrix diagrammatics and v in the continuum is indeed sensible.[7] Going from the diagrammatics to the critical exponent is simply a matter of integrating (summing) over v (k), and identifying $\Lambda \propto (\alpha_2 - \alpha_{2,c}^{(2)})$.

$\mathcal{M}_{2m-1,2}$ on a fluctuating background. We would like to compare the asymptotics at large vertex number from the multicritical matrix diagrammatics to the continuum picture. Part of the issue is that there are multiple couplings, and consequently multiple paths in coupling space to reach the multicritical point. Along the path (3.4.28) which simultaneously tunes several couplings, the growth of vertices goes as $\sim k^{-(\mathbf{3}+\mathbf{1/m})}t^k$ (3.4.37). Recalling (3.6.25) and noting that for general m, $1 + Q/\sigma_{\min} = (\mathbf{3} + \mathbf{1/m})$, we find evidence that such a tuning corresponds to fixing the extensive quantity (3.6.24), rather than the area (3.6.23). The remaining task is to identify $\Lambda_{\min}$, and the additional $(m-2)$ couplings $\lambda_{\Delta_{r,1}}$ from the perspective of the multicritical matrix integral. This is precisely the problem of non-analyticities solved in section 3.5. The non-analyticities found in the m^{th} multicritical matrix integral correspond to the values $Q/\sigma_{\min}$ (3.6.20) and $\sigma_{\min}/\sigma_{\Delta_{r,1}}$, $r = 1, \ldots, m-2$ (3.6.22) arising from $\mathcal{M}_{2m-1,2}$ on a fluctuating background. We thus identify $\Lambda_{\min} = \epsilon$ in (3.5.32), $\lambda_{\Delta_{r,1}} = \epsilon^{\sigma_{\min}/Q}$ and $r' = m - r - 1$ in (3.5.21). We observe that $\sigma_{\min}/Q$ is independent of r. Further to this, our hypersurface

[7] Although we do not discuss it here, this identification continues to be sensible for those matrix integrals argued to describe the unitary minimal models coupled to gravity. As an explicit example, the $\mathcal{M}_{4,3}$ model on a fluctuating background was studied in [119], leading to the fixed area behaviour $\sim v^{-\mathbf{10/3}}$ which agrees with the prediction from the corresponding two-matrix model.

equation (3.5.15) provides the detailed relation between the matrix deformation and the corresponding matter primary.

3.7 Remarks on a Hilbert space

In this section we remark on the Hilbert space of $\mathcal{M}_{2m-1,2}$ coupled to two-dimensional gravity, and its manifestation from the matrix integral perspective.

3.7.1 S^2 considerations

On a fixed background, $\mathcal{M}_{2m-1,2}$ has a finite number of primaries equal to $n_{2m-1,2} = (m-1)$, each accompanied by an infinite tower of descendants. On a fluctuating background these operators must satisfy constraints arising from the diffeomorphism invariance. Additionally we need to consider the contribution from the Liouville and $\mathfrak{bc}$-ghost sector.

Concretely we must identify the set of BRST invariant operators. This was examined in early work of Lian-Zuckerman (LZ) [230] and subsequent work [231–233]. Under the assumption that the Liouville sector can be treated as a linear dilaton theory, it was noted that the BRST cohomology comprises of an *infinite* collection of operators. In particular LZ operators have a non-trivial ghost number and generally contain matter and Liouville descendants. Though also infinite, this infinity is far smaller than the infinite operator content of the matter theory on a fixed background arising from the Virasoro descendants. The origin of these operators is intimately connected to the presence of null operators in the Liouville sector [236][8] and the matter sector. In conformal gauge $\mathrm{d}s^2 = e^{2b\varphi(z,\bar{z})}\mathrm{d}z\mathrm{d}\bar{z}$ the LZ operators are given by

$$\mathcal{R}^{\mathrm{LZ}}_{r,\pm}(t) \equiv \mathcal{O}^{\mathrm{LZ}}_{r,\pm}(\mathfrak{b},\mathfrak{c},\varphi,\Phi;t)\otimes\bar{\mathcal{O}}^{\mathrm{LZ}}_{r,\pm}(\tilde{\mathfrak{b}},\tilde{\mathfrak{c}},\varphi,\Phi;t)\otimes\mathcal{O}_{r,1}\otimes e^{2\sigma_{\mathrm{LZ}}\varphi}\ , \tag{3.7.1}$$

where $t\in\mathbb{Z}$ and $\pm$ denote the particular LZ operator. The holomorphic conformal dimensions of these operators are given by

$$\Delta^{\mathrm{LZ}}_{r,\pm}(t) + \Delta_{r,1} + \sigma_{\mathrm{LZ}}(Q-\sigma_{\mathrm{LZ}}) = 0\ , \tag{3.7.2}$$

where $Q = b + b^{-1}$ and LZ operators are graded by the ghost number. The LZ weights for $\mathcal{M}_{2m-1,2}$ are given by

$$\Delta^{\mathrm{LZ}}_{r,\pm}(t) = A_{r,\pm}(t) - \Delta_{r,1} - 1\ , \tag{3.7.3}$$

[8] Indeed, one can always find primary operators in Liouville theory with central charge $c_L = 26 - c^{(2m-1,2)}$ whose conformal dimension lies on one of the values in the Kac table, and hence admit null states in their Verma module. The null operators are themselves primary.

where $A_{r,\pm}(t)$ are given by [170]

$$A_{r,\pm}(t) \equiv \frac{(4(2m-1)t + 2r \pm (2m-1))^2 - (2m-3)^2}{8(2m-1)} \ . \tag{3.7.4}$$

The anti-holomorphic conformal dimension has to be equal to the holomorphic conformal dimension. The argument t is related to the ghost number, whereas the subscript $\pm$ indicates whether the ghost number is even $(+)$ or odd $(-)$.

Example $\mathcal{M}_{3,2}$. For $\mathcal{M}_{3,2}$ the LZ operators with ghost number $(\mathfrak{n}_b, \mathfrak{n}_c) = (0,0)$ and $(\mathfrak{n}_b, \mathfrak{n}_c) = (0,2)$ respecetively associated to the matter primary $\mathcal{O}_{1,1}$ are [231, 233]

$$\mathcal{R}^{\rm LZ}_{1,+}(0) = \mathbb{I} \ , \qquad \mathcal{R}^{\rm LZ}_{1,+}(0) = \mathfrak{c}(z)\partial^2\mathfrak{c}(z)\tilde{\mathfrak{c}}(\bar{z})\partial^2\tilde{\mathfrak{c}}(\bar{z}) \otimes e^{2Q\varphi} \ , \tag{3.7.5}$$

with $\sigma_{\rm LZ} = 0$ and $\sigma_{\rm LZ} = Q$ respectively. The operators (3.7.5) have non-trivial ghost number as compared to the vertex-operators considered in section 3.6 whose BRST invariant form takes $\mathcal{O}^{\rm LZ}_{1,-}(\mathfrak{b}, \mathfrak{c}, \varphi, \Phi; 0) = \mathfrak{c}$ and $\bar{\mathcal{O}}^{\rm LZ}_{1,-}(\tilde{\mathfrak{b}}, \tilde{\mathfrak{c}}, \varphi, \Phi; 0) = \tilde{\mathfrak{c}}$ and $\sigma_{\rm LZ} = b$. On the other side the LZ operators with lowest ghost number $(\mathfrak{n}_b, \mathfrak{n}_c) = (1,1)$ associated to the matter primary $\mathcal{O}_{1,1}$ for $\mathcal{M}_{3,2}$ is

$$\mathcal{R}^{\rm LZ}_{1,+}(-1) = \Big(\mathfrak{b}(z)\mathfrak{c}(z) - b^{-1}\partial\varphi(z,\bar{z})\Big)\Big(\tilde{\mathfrak{b}}(\bar{z})\tilde{\mathfrak{c}}(\bar{z}) - b^{-1}\bar{\partial}\varphi(z,\bar{z})\Big) \otimes e^{-b\varphi(z,\bar{z})} \ , \tag{3.7.6}$$

where combining (3.6.12) with $c^{(3,2)}$ (3.6.7) we have $b = \sqrt{2/3}$. Besides the operator (3.7.6) there exists another operator $\mathcal{R}^{\rm LZ}_{1,+}(-1)$ with $\sigma_{LZ} = 2/b$. To show the BRST invariance of these operators, it is useful to recall the (holomorphic) BRST current [69]

$$J_{\rm BRST} = \mathfrak{c}\, T^{\varphi} + \frac{1}{2} : \mathfrak{c}\, T^{g} : + \frac{3}{2}\,\partial^2\,\mathfrak{c} \ , \tag{3.7.7}$$

where T^{φ} and T^{g} are the Liouville and ghost stress tensor respectively

$$T^{\varphi} = -(\partial\varphi)^2 + Q\partial^2\varphi \ , \quad T^{g} =: (\partial\mathfrak{b})\mathfrak{c} : -2\partial\,(:\mathfrak{b}\mathfrak{c}:) \ . \tag{3.7.8}$$

In particular we find [231]

$$\delta\mathcal{R}^{\rm LZ}_{1,+}(-1) = \mathfrak{c}(0)\tilde{\mathfrak{c}}(0) \otimes \left(\frac{3}{2}\,L_{-1}^2 + L_{-2}\right)\left(\frac{3}{2}\,\tilde{L}_{-1}^2 + \tilde{L}_{-2}\right) e^{-b\varphi(0,0)} \ , \tag{3.7.9}$$

where $L_n, \tilde{L}_n$ are the Virasoro generators, satisfying

$$L_n \equiv \oint_{\mathcal{C}} \frac{\mathrm{d}z}{2\pi i z}\, z^{n+2} T^{\varphi}(z) \ , \quad \tilde{L}_n \equiv \oint_{\mathcal{C}} \frac{\mathrm{d}\bar{z}}{2\pi i \bar{z}}\, \bar{z}^{n+2} \tilde{T}^{\varphi}(\bar{z}) \ . \tag{3.7.10}$$

In other words the BRST variation leads to a null operator.

We note that we consider the stress tensor of the Liouville action arising when assuming it is a linear dilaton theory. This is justified when calculating the critical exponents (3.6.18) for which we set the cosmological constant to zero. The BRST transformation of a LZ operator can produce null operators in the matter or Liouville sector [231], which must subsequently be set to zero.

One may ask whether the LZ operators contribute additional critical exponents for the theory on S^2. By the Riemann-Roch theorem, non-vanishing $\mathfrak{bc}$-correlation functions on a compact Riemann surface with Euler characteristic χ require [69]

$$n_{\mathfrak{c}} - n_{\mathfrak{b}} = \frac{3}{2}\chi \ . \tag{3.7.11}$$

For S^2 we have $\chi = 2$. Given that LZ operators have a non-trivial ghost number, generically different from $n_{\mathfrak{c}} - n_{\mathfrak{b}} = 3$, we expect no new critical exponents from the LZ operators on an S^2 topology.

Assuming that some form of the operator-state correspondence holds for S^2 we are thus led to conclude that the associated Hilbert space is finite-dimensional. This might be related to observations on de Sitter space [17, 18].

Contrarily to S^2 the torus T^2 has Euler characteristic $\chi = 2$. As a consequence of the Riemann-Roch theorem (3.7.11) we thus infer that the LZ operators contribute to the torus partition function.

3.7.2 T^2 considerations

On the cylinder, the Hilbert space $\mathcal{H}_{T^2}$ lives on spatial S^1 constant time slices. States $|\Psi\rangle \in \mathcal{H}_{T^2}$ in the trivial ghost sector living on these spatial slices are subject to the Virasoro constraints

$$\left(L_0^{\text{tot}} + \tilde{L}_0^{\text{tot}} - 2\right)|\Psi\rangle = 0 \ , \qquad \left(L_0^{\text{tot}} - \tilde{L}_0^{\text{tot}}\right)|\Psi\rangle = 0 \ , \tag{3.7.12}$$

where L_n^{tot} and $\tilde{L}_n^{\text{tot}}$ are the Virasoro generators for the matter and Liouville sector. The first equation in (3.7.12) is what replaces the Hamiltonian constraint in canonical quantum gravity [237], while the second replaces the spatial diffeomorphism constraint. The above equations are the state analog of the constraint that vertex operators with trivial ghost contribution must have $\Delta \equiv \Delta_L + \Delta_{r,1} = 1$ and $\Delta = \bar{\Delta}$. Other states in $\mathcal{H}_{T^2}$, as first pointed out by Lian-Zuckerman [230], may also include non-trivial ghost excitations.

One way to characterise $\mathcal{H}_{T^2}$ is through the torus partition function [228, 229].

For fixed modular parameter $\tau = \tau_1 + i\tau_2$ the states in the BRST cohomology contribute

$$Z_{\text{fixed}}[\tau_2] = (q\bar{q})^{\frac{1}{24}\left(26-1-c^{(2m-1,2)}\right)} \sum_{r=1}^{m-1} \sum_{t\in\mathbb{Z}} \left((q\bar{q})^{\Delta^{\text{LZ}}_{r,+}(t)+\Delta_{r,1}} + (q\bar{q})^{\Delta^{\text{LZ}}_{r,-}(t)+\Delta_{r,1}} \right) , \tag{3.7.13}$$

where $q = e^{2\pi i\tau_2}$ and we used (3.7.4). The overall shift encodes the Casimir energy from the ghost, Liouville and matter sector. The τ_1-independence of $Z_{\text{fixed}}(\tau_2)$ is due to the diffeomorphism constraint (3.7.12).

What remains to be done is integrate over the modular parameter τ_2 and the zero modes of the Liouville sector

$$\mathcal{T}[\Lambda] = \log\Lambda \int_{\mathcal{F}} \frac{\mathrm{d}^2\tau}{\tau_2^{3/2}} Z_{\text{fixed}}(\tau_2) \ . \tag{3.7.14}$$

$\mathcal{F}$ is the fundamental domain of the modular group. The power of τ_2 is fixed by modular invariance and stems from the various zero modes in the $\mathfrak{bc}$-ghost and Liouville sector. The logarithm in Λ stems from the volume of the Liouville zero mode, and essentially encodes the fact that the Liouville interaction imposes a cutoff in the Liouville field space. Evaluating $\mathcal{T}[\Lambda]$ leads to [228]

$$\mathcal{T}[\Lambda] = \frac{2m-2}{24(2m-1)} \log\Lambda \ . \tag{3.7.15}$$

Comparing to the first non-planar contribution of the matrix integral as presented in appendix 6 we see that under the identification $\Lambda = \epsilon$ the results agree (6.0.39). In this way the LZ states appear in the leading non-planar contribution of the m^{th} multicritical matrix integral.

3.8 Discussion and open questions

We summarise some open questions and speculative remarks.

The large m limit. In [20] it has been observed that upon coupline $\mathcal{M}_{2m-1,2}$ to gravity whilst fixing the area υ and turning on only the identity operator of $\mathcal{M}_{2m-1,2}$ exhibits a saddle point solution in the large m limit. This saddle point solution is the round metric on S^2, which is Euclidean dS_2. Motivated by this, this work provides the basis to understand this observation from the matrix integral point of view. Recalling (3.5.21) for $r' = m-2$ we recover Zamolodchikov's continuum critical exponent from a matrix integral perspective. In the large m limit and upon tuning the couplings to the multicritical point (3.2.13) the polynomial

$V_m(\lambda, \boldsymbol{\alpha})$ (3.2.3) reduces to[9] [82]

$$\lim_{m\to\infty} V_m(\lambda, \boldsymbol{\alpha}_c) = \frac{1}{2}\lambda^2\, {}_2F_2\left(1,1;\frac{3}{2},2;-\frac{\lambda^2}{4}\right) . \tag{3.8.1}$$

Moreover the width of the eigenvalue distribution (3.2.19) scales with m and so becomes unbounded in the large m limit. We further remark that the most fine-tuned path where we switch on all the hypersurfaces and $\boldsymbol{s} \in \mathcal{H}_m^{(1)} \cup \ldots \cup \mathcal{H}_m^{(m-2)}$ (3.5.15) corresponds to the identity operator in the continuum theory.

Non-unitarity & torus Hilbert space. As a consequence of the Riemann-Roch theorem (3.7.11) the LZ operators contribute on T^2. In particular this implies that we have to deal with descendants of the Virasoro primaries of $\mathcal{M}_{2m-1,2}$. These are negative norm operators. The consequences of the non-unitarity from both the point of view of the MMI and the point of view of the continuum theory remain to be explored.

Diagrammatics & critical exponents. To evaluate the double sum (3.4.15), capturing the diagrammatic expansion of the $m = 3$ model, we introduced the path $\gamma_\star^{(3)}$ (3.4.7) in coupling space. This allowed us to explicitly determine the radius of convergence and for $m \geq 3$ using $\gamma_\star^{(m)}$ (3.4.28) we observed the critical exponent $\mathcal{F}^{(0)}_{m,\text{n.a.}}(\boldsymbol{\alpha})\big|_{\gamma_\star^{(m)}} \sim \epsilon^{\mathbf{2+1/m}}$ (3.4.37). However introducing the single parameter $t \in [0,1]$ connecting the origin in coupling space to the multicritical point prevents from observing the other $(m-2)$ critical exponents $\boldsymbol{m/(m-r')}$, $r' = 1, \ldots, m-2$, from a diagrammatic perspective. It would be interesting to uncover these.

Hartle-Hawking & topology. As a final remark, it is interesting to note that the partition function $\mathcal{Z}[\Lambda]$ on S^2 only dominates (in absolute value) over the partition function $\mathcal{T}[\Lambda]$ on T^2 for sufficiently large Λ, while for small enough $\Lambda > 0$, the T^2 partition function dominates. It would be interesting to understand if this has any consequences for the Hartle-Hawking picture [204, 205]. Further to this, being matrix integrals rather than matrix path integrals there is no a priori indication for the existence of Hilbert space from the matrix integral perspective. It would be interesting to uncover a Lorentzian picture directly from the matrix integral [203].

[9] We would like to acknowledge Jorge Russo for useful discussions.

4 Gravitational anomalies in $\mathrm{nAdS}_2/\mathrm{nCFT}_1$

4.1 Introduction

AdS_2 quantum gravity plays an important role in our understanding of black holes. A prominent example is the construction of the quantum entropy function via $\mathrm{AdS}_2/\mathrm{CFT}_1$ [11, 12], which encodes classical and quantum properties of extremal black holes in agreement with our microscopic understanding in string theory [238–240]. Unfortunately, relative to higher dimensional instances of AdS/CFT, we face some serious obstructions in building a holographic description of AdS_2. One crucial obstacle is that its symmetry prevents finite energy excitations, so capturing non-trivial dynamics requires a deformation that destroys the AdS_2 background [13, 14].

A proposal addressing this obstacle is known as the $\mathrm{nAdS}_2/\mathrm{nCFT}_1$ correspondence [9, 10]. The first insights relied on studies of 2D models of gravity coupled to a scalar field (i.e., a dilaton), which are colloquially referred to as JT gravity [241, 242]. Some generalisations are those in [243]. In these models the non-trivial profile of the dilaton breaks explicitly the conformal symmetry of AdS_2, while being at the same time tied to the large diffeomorphisms at the boundary of AdS_2. Moreover, these diffeomorphisms induce an anomaly via a Schwarzian derivative. This symmetry breaking pattern is important: It governs the gravitational backreaction, such as the thermodynamic response and the quantum chaos characterising black holes. And so the persistent trend in nAdS_2 holography, coined with a 'n' since we are 'near' to our original configuration, is that the deviations away from extremality are controlled by this pattern. For a review see [245].

The application of this new framework to black hole physics has shown that, while JT models capture common features [40, 248–250], the additional parameters for more general black holes display interactions that are not present in JT gravity [251–256]. This makes clear that there is new phenomena to be explored, that

simpler models do not take into account.

Our interest therefore is to further explore the properties of $\text{nAdS}_2/\text{nCFT}_1$ with the goal of building a more refined understanding of the dynamics near the horizon of (near-)extremal black holes. We will revisit the renown BTZ black hole in AdS_3 gravity [39, 257] using the framework of nAdS_2 holography. We will treat the angular direction in BTZ as a compact direction along which we will dimensionally reduce to two dimensions. The resulting 2D theory of gravity contains, in addition to the metric, a gauge field and a dilaton as expected in Kaluza-Klein theory. Our work builds upon the developments in [40, 258], where the 2D holographic dictionary was studied by dimensionally reducing the 3D Einstein-Hilbert action with a negative cosmological constant. Other relevant work includes [259], which focuses on the effects of $U(1)$ Chern-Simons fields in 2D; see also [260–262].

One question we investigate is the relation between the nCFT_1, that describes the near horizon physics of near-extremal BTZ, to the parent CFT_2, that is dual to AdS_3. This relation is subtle: The conformal (Weyl) anomaly in $\text{AdS}_3/\text{CFT}_2$ can easily be confused with the anomaly appearing in $\text{nAdS}_2/\text{nCFT}_1$. Both are controlled by a Schwarzian derivative after all.[1] In the present paper we explore this relation by adding to the Einstein-Hilbert action a gravitational Chern-Simons term: The resulting theory is topologically massive gravity (TMG). In the context of $\text{AdS}_3/\text{CFT}_2$, it is known that this theory contains both a conformal and gravitational anomaly, reflected in the boundary theory as a violation of parity that induces $c_L \neq c_R$ [266]. Here $c_{L/R}$ are the left/right central charges in the CFT_2.

Considering the gravitational Chern-Simons term adds a layer of complexity which, despite making some derivations more cumbersome, has several advantages. First, having a distinction between left and right movers will be particularly important when considering the thermodynamic responses in the nCFT_1, and its comparison to thermal properties of the CFT_2. Second, one of our main results is that the anomaly of $\text{nAdS}_2/\text{nCFT}_1$ is due to one chiral sector of the CFT_2, and hence it seems misleading to only discuss it as a Weyl anomaly. The dilaton and gauge field will play a crucial role in this interpretation: Different choices of boundary conditions will impact the holographic interpretation we aim to build. Our strategy therefore will be to divide the analysis of holographic properties into two:

UV perspective: This portion focuses on backgrounds in 2D that naturally uplift to asymptotically AdS_3 spacetimes. These are the running dilaton backgrounds in [258]. Our emphasis here is to keep track in the dimensionally reduced theory of the conformal and gravitational anomaly present in

[1] Related work that ties the Schwarzian derivative in the nCFT_1 to a Virasoro symmetry in a CFT_2 includes [263–265].

AdS_3/CFT_2. In this setup the reduced gravitational Chern-Simon term is somewhat dull: It modifies the conserved charges, but disappears from the Ward identities in the lower dimensional theory.

IR perspective: Here the starting point are solutions with a constant dilaton, leading to locally AdS_2 spacetimes. We coin these background IR, since they uplift to the near horizon physics of nearly extremal black holes. We will then turn on a deformation for the dilaton that ignites the key features of $nAdS_2$ holography. The asymptotic behaviour of the fields in this situation is different relative to the UV, and therefore changes various observables. In particular, the gravitational Chern-Simons term influences the anomalies appearing in $nAdS_2/nCFT_1$.

Finally, the 2D theory we will consider contains higher derivative interactions, and hence encapsulates a rich space of solutions. Some related work that studies certain classes of solutions includes [267–269]. Here we will exclusively focus on solutions of the 2D theory, that upon an uplift, can be interpreted as locally AdS_3 spacetimes; these are the solutions described in [258]. This subsector is a consistent truncation of the theory, and it will suffice to explore dynamics related to the BTZ black hole. There are of course plenty of other interesting configurations, in particular warped AdS_3 black holes [270–272], which would be interesting to study in future work using the tools of $nAdS_2$ holography.

The paper is organised as follows: In Sec. 4.2 we will introduce the 3D parent theory, i.e. TMG, alongside with a review of the holographic properties, and summarise the thermodynamic effects of the gravitational Chern Simons term on the BTZ black hole. In Sec. 4.3 we perform the dimensional reduction of TMG, and present its equations of motion in full generality. Sec. 4.4 focuses on holographic renormalisation of the 2D theory with our UV perspective: After setting the appropriate boundary conditions in 2D, we evaluate the one-point functions and derive the renormalised action. In Sec. 4.4.3 we compare the 3D results in Sec. 4.2.1 to our derivations in Sec. 4.4.2. This comparison illustrates that the 2D theory washes away some aspects of the gravitational anomaly, which we discuss. The results relevant to the near horizon physics of the BTZ are in Sec. 4.5. This is our IR setup, where the starting point are AdS_2 backgrounds with a constant dilaton. We perform holographic renormalisation in $nAdS_2$, and already at early stages of the computations the differences with the UV become manifest, as we advertised above. Finally, in Sec. 4.6 we make the symmetry breaking mechanism and anomalies in the 2D theory manifest. For this we derive the Schwarzian action for both the UV and IR perspective. We discuss the interpolation between the UV and IR, and the role these anomalies have in the entropy of 2D black holes. App. 6 contains useful relations that cast the BTZ black hole as a 2D solution.

4.2 Topologically massive gravity

The addition of a gravitational Chern-Simons term to the Einstein-Hilbert action in three dimensions defines topologically massive gravity [44–46]. The action is given by

$$\begin{aligned} I_{\rm 3D} &= I_{\rm EH} + I_{\rm CS} \ , \\ I_{\rm EH} &= \frac{1}{16\pi G_3}\int {\rm d}x^3\sqrt{-g}\,(R-2\Lambda) \ , \\ I_{\rm CS} &= \frac{1}{32\pi G_3\mu}\int {\rm d}x^3\sqrt{-g}\varepsilon^{MNL}\left(\Gamma^P_{MS}\partial_N\Gamma^S_{LP}+\frac{2}{3}\Gamma^P_{MS}\Gamma^S_{NQ}\Gamma^Q_{LP}\right) \ , \end{aligned} \tag{4.2.1}$$

where we have included a cosmological constant Λ, μ is a real coupling with dimensions of mass and we are using convention where $\sqrt{-g}\,\varepsilon^{012}=-1$. There is also a gauge theory formulation of this theory, which uses a Chern-Simons description of 3D gravity plus a constraint [46, 273, 274].

The equations of motion of TMG read

$$R_{MN}-\frac{1}{2}g_{MN}R-\frac{1}{\ell^2}g_{MN}=-\frac{1}{\mu}C_{MN} \ , \tag{4.2.2}$$

where C_{MN} is the Cotton tensor,

$$C_{MN}=\epsilon_M{}^{QP}\nabla_Q\left(R_{PN}-\frac{1}{4}g_{PN}R\right) \ . \tag{4.2.3}$$

Note that the equations of motion are covariant, even though the action has explicit dependence on Christoffel symbols. It is also important to highlight that *all* locally AdS_3 spacetimes have vanishing Cotton tensor, $C_{MN}=0$, which makes them automatically a solution to (4.2.2).

The novel solutions of TMG are those with $C_{MN}\neq 0$. An interesting subset of such solutions, denoted "warped AdS_3," were constructed in [270–272] along with warped black hole counterparts; see also [275–278]. Viewed holographically, the main feature of asymptotically warped AdS_3 geometries is that they do not obey Brown-Henneaux boundary conditions [41]. Indeed, the nature and symmetries of their holographic descriptions is more intricate than those in AdS_3 [279–283]. Our focus here will be on locally AdS_3 configurations; we will postpone the study of warped AdS_3 spacetimes for future work.

4.2.1 Holographic renormalisation

Some of the distinctive properties of the gravitational anomaly in TMG are very manifest in AdS_3/CFT_2 [266, 284–288]. In this section we will provide a quick summary of the resulting boundary stress tensor for TMG, which is mainly based on [266, 288]. We will focus only on locally AdS_3 solutions.[2]

The application of Brown-Henneaux boundary conditions for TMG shows that the classical phase space of asymptotically AdS_3 ($AAdS_3$) backgrounds is organised in two copies of the Virasoro algebra with central charges

$$c_R = \frac{3\ell}{2G_3}\left(1 - \frac{1}{\mu\ell}\right) , \quad c_L = \frac{3\ell}{2G_3}\left(1 + \frac{1}{\mu\ell}\right) . \tag{4.2.4}$$

This result uses the Fefferman-Graham expansion of the 3D metric, which is given by

$$\begin{aligned} ds_3^2 &= \mathrm{d}\eta^2 + g_{ij}(\eta, x)\mathrm{d}x^i\mathrm{d}x^j, \quad i,j \in \{0,1\} , \\ g_{ij}(\eta, x) &= g_{ij}^{(0)}(x)\, e^{2\eta/\ell} + g_{ij}^{(2)}(x) + O(e^{-2\eta/\ell}) , \end{aligned} \tag{4.2.5}$$

where as usual x^i denotes the boundary coordinates. In this context, the boundary stress tensor for the 3D theory is defined as the on-shell variation of the renormalised action with respect to the boundary metric

$$\delta I_{\mathrm{3D}}^{\mathrm{ren}} = \frac{1}{2}\int \mathrm{d}x^2 \sqrt{g^{(0)}}\, T^{ij}\, \delta g_{ij}^{(0)} . \tag{4.2.6}$$

Here $I_{\mathrm{3D}}^{\mathrm{ren}}$ contains, in addition to (4.2.1), the Gibbons-Hawking-York term, and a boundary cosmological constant, i.e. the standard counterterms in the holographic renormalisation of the 3D Einstein-Hilbert action with $AAdS_3$ boundary conditions [292–294]. One very interesting aspect of TMG is that the gravitational Chern-Simons term does not lead to new divergences: the variation with respect to $g_{ij}^{(0)}$ of I_{CS} is finite as $\eta \to \infty$. There are however some ambiguities in the variation of I_{CS}, due to the choice of renormalisation scheme in theories with a gravitational anomaly; we will review those choices in the following.

[2] At $\mu = 1$, i.e. chiral gravity, there are some additional subtleties due to an additional logarithmic branch in the classical phase space. This introduces solutions that are not locally AdS, while still being asymptotical AdS for appropriate boundary conditions. We will not dwell with this special point, and instead refer the reader to [289–291], and references within, for holographic properties of chiral gravity.

Consistent stress tensor [288]. The stress tensor that arises from a well defined variational principle is given by

$$T_{ij} = \frac{1}{8\pi G_3 \ell}\left(g^{(2)}_{ij} - g^{(0)}_{ij} g^{(2)}_{kl} g^{kl}_{(0)}\right) - \frac{1}{16\pi G_3 \mu \ell^2}\left(g^{(2)}_{ik}\varepsilon_{lj} g^{kl}_{(0)} + g^{(2)}_{jk}\varepsilon_{li} g^{kl}_{(0)}\right) - \frac{1}{16\pi G_3 \mu} A_{ij}\,, \tag{4.2.7}$$

where the additional term

$$A_{ij} = \frac{1}{4}\varepsilon^{kl} D_k \partial_l g^{(0)}_{ij} - \frac{1}{8}\varepsilon_i{}^k \varepsilon_j{}^l \varepsilon^{mn} D_l \partial_m g^{(0)}_{nk} - \frac{1}{8}\varepsilon_j{}^k \varepsilon_i{}^l \varepsilon^{mn} D_l \partial_m g^{(0)}_{nk}\,, \tag{4.2.8}$$

solely depends on the boundary metric $g^{(0)}_{ij}$. Here ε_{ij} is the epsilon tensor for the boundary metric, and we set $\sqrt{-g^{(0)}}\varepsilon^{01} = -1$; D_i is the covariant derivative with respect to $g^{(0)}_{ij}$.

The trace anomaly and Ward identity for this form of the stress tensor read

$$\begin{aligned} T^i{}_i &= \frac{c}{24\pi} R^{(0)} + \frac{\bar{c}}{12\pi} A^i{}_i\,, \\ D_i T^{ij} &= -\frac{\bar{c}}{24\pi} g^{ij}_{(0)} \varepsilon^{kl} \partial_m \partial_k \Gamma^m_{il}\,, \end{aligned} \tag{4.2.9}$$

where $R^{(0)}$ denotes the Ricci scalar for $g^{(0)}_{ij}$ and we also used (4.2.4) and introduced $c = (c_L + c_R)/2$ and $\bar{c} = (c_L - c_R)/2$. Casting the diffeomorphism anomaly as in (4.2.9) is in accordance with the Wess-Zumino consistency conditions, albeit the expressions are not covariant. The lack of covariance is reflected on the failure of A_{ij} to be a tensor.

Covariant stress tensor [266, 295]. The term A_{ij} in the stress tensor (4.2.7) does not carry information that depends on the "state", i.e. it does not depend on $g^{(2)}_{ij}$. If one removes A_{ij}, the resulting holographic stress tensor reads

$$t_{ij} = \frac{1}{8\pi G_3 \ell}\left(g^{(2)}_{ij} - g^{(0)}_{ij} g^{(2)}_{kl} g^{kl}_{(0)}\right) - \frac{1}{16\pi G_3 \mu \ell^2}\left(g^{(2)}_{ik}\varepsilon_{lj} g^{kl}_{(0)} + g^{(2)}_{jk}\varepsilon_{li} g^{kl}_{(0)}\right)\,. \tag{4.2.10}$$

The trace anomaly and Ward identity now are

$$t^i{}_i = \frac{c}{24\pi} R^{(0)}\,, \qquad D_j t^{ij} = \frac{\bar{c}}{24\pi}\varepsilon^{ij}\partial_j R^{(0)}\,. \tag{4.2.11}$$

In contrast to (4.2.9), these expressions are covariant with respect to the boundary metric, which makes this stress tensor receive the name 'covariant'. The sacrifice here is that it does not satisfies the Wess-Zumino conditions.

Conserved and Lorentz violating stress tensor [295]. Finally, one can also insist that the stress tensor is conserved. From (4.2.11) we see that this is easily achieved by defining

$$\hat{t}_{ij} = t_{ij} + \frac{\ell}{16\pi G_3 \mu}\varepsilon_{ij}R^{(0)} \ . \tag{4.2.12}$$

However, now we have an object that is not symmetric, which is a significant sacrifice in this definition. From here it is natural to cast $\hat{t}^{\hat{a}}{}_i = e_j{}^{\hat{a}}t^j{}_i$, where $\hat{t}^{\hat{a}}{}_i$ is the response of the action to variations of the vielbeins $e_i{}^{\hat{a}}$. Note that $\hat{t}^{\hat{a}}{}_i$ is also not invariant under local Lorentz transformations. At the price of loosing Lorentz invariance, the relevant identities for (4.2.12) are

$$\varepsilon_{\hat{a}}{}^i\,\hat{t}^{\hat{a}}{}_i = \frac{c}{12\pi}R^{(0)} \ , \qquad D^j\hat{t}^{\hat{a}}{}_j = 0 \ . \tag{4.2.13}$$

4.2.2 BTZ black hole

In this section we introduce the BTZ black hole in TMG and review some of its thermodynamic properties. The metric of the rotating BTZ solution is [257]

$$ds_3^2 = -\frac{(\rho^2-\rho_+^2)(\rho^2-\rho_-^2)}{\ell^2\rho^2}\mathrm{d}t^2 + \frac{\ell^2\rho^2}{(\rho^2-\rho_+^2)(\rho^2-\rho_-^2)}\mathrm{d}\rho^2 + \rho^2\left(\mathrm{d}\varphi - \frac{\rho_+\rho_-}{\ell\rho^2}\mathrm{d}t\right)^2 \ , \tag{4.2.14}$$

where $\rho_\pm$ are the position of the outer/inner horizon; without loss of generality, we will pick $\rho_+ > \rho_- > 0$. In the absence of the gravitational Chern-Simons term, mass and angular momentum are given by

$$m = \frac{\rho_+^2+\rho_-^2}{8G_3\ell^2} \ , \qquad j = \frac{\rho_+\rho_-}{4G_3\ell} \ . \tag{4.2.15}$$

The additional Chern Simons term contributes to the conserved charges in TMG. In particular the gravitational mass and angular momentum read

$$\begin{aligned} M &= \frac{1}{24\ell^3}\left(c_R\,(\rho_+ + \rho_-)^2 + c_L\,(\rho_+ - \rho_-)^2\right) \ , \\ J &= \frac{1}{24\ell^2}\left(c_R\,(\rho_+ + \rho_-)^2 - c_L\,(\rho_+ - \rho_-)^2\right) \ . \end{aligned} \tag{4.2.16}$$

It is worth noting that all variants of the boundary stress tensor presented above –i.e. (4.2.7), (4.2.10) and (4.2.12)– report the same answer for M and J. It is also

instructive to relate the charges in TMG to those in (4.2.15)

$$M\ell - J = \left(1 + \frac{1}{\mu\ell}\right)(m\ell - j) \ ,$$
$$M\ell + J = \left(1 - \frac{1}{\mu\ell}\right)(m\ell + j) \ . \tag{4.2.17}$$

Thermodynamics near Extremality

An important component of our holographic analysis of nAdS$_2$ encompasses the thermodynamic response in the presence of an irrelevant deformation. In the context of the 3D BTZ black hole this would correspond to the entropy near-extremality, which we review here. More details on this limit are presented in App. 6.

The Wald entropy of the BTZ black hole in TMG receives a non-trivial contribution which has been well documented and studied in [42, 285, 296–299]. The resulting expression is

$$S = \frac{\pi}{6\ell}\left(c_L\left(\rho_+ - \rho_-\right) + c_R\left(\rho_+ + \rho_-\right)\right) \ . \tag{4.2.18}$$

Using the expression for mass and angular momentum in (4.2.16), it is straight forward to verify the first law

$$dM = TdS - \Omega\, dJ \ , \tag{4.2.19}$$

where the temperature and angular velocity are

$$T = \frac{\rho_+^2 - \rho_-^2}{2\pi\ell^2\rho_+} \ , \qquad \Omega = -\frac{\rho_-}{\ell\rho_+} \ . \tag{4.2.20}$$

Note that these potentials are independent of the gravitational couplings, G_3 and μ, as expected since they are completely determined by the Euclidean regularity of the line element (4.2.14).

At extremality we have $\rho_+ = \rho_- \equiv \rho_0$. In this limit it follows from (4.2.20) that the temperature is zero, while the mass and entropy are

$$M_{\text{ext}} = \frac{c_R}{6\ell^3}\,\rho_0^2 \ , \qquad S_{\text{ext}} = 2\pi\sqrt{\frac{c_R}{6}M_{\text{ext}}\ell} \ . \tag{4.2.21}$$

Near extremality is a small deviation of ρ_+ away from its extremal value ρ_0, i.e. $\rho_+ = \rho_0 + \delta$ with δ a small parameter. In particular, we will deviate from extremality such that we increase the temperature T slightly away from zero, which

increases the mass M of the black hole while keeping the angular momentum J fixed. The implementation of this limit gives a mass increase by

$$\Delta E = M - M_{\text{ext}} = \frac{1}{M_{\text{gap}}} T^2 + \dots \ , \tag{4.2.22}$$

where the dots indicate that this is an expansion around small values of T. The response of the mass in this limit is quadratic with T as expected [40], where the coefficient that relates them is the mass gap

$$M_{\text{gap}} = \frac{8G_3}{\pi^2 \ell^2} \frac{1}{\left(1 + \frac{1}{\mu \ell}\right)} = \frac{12}{\pi^2 \ell c_L} \ . \tag{4.2.23}$$

It follows that the response of the entropy (4.2.18) near extremality is linear in the temperature

$$S = S_{\text{ext}} + \frac{2}{M_{\text{gap}}} T + \dots \ . \tag{4.2.24}$$

It is useful to cast these expressions in the language of the dual CFT_2. In this context the entropy (4.2.18) can be identified with the density of states distinctive of the Cardy regime,

$$S = S_L + S_R \ , \tag{4.2.25}$$

where the contribution to the entropy splits into a left and right moving part given by

$$S_{L/R} = 2\pi \sqrt{\frac{c_{L/R}}{6} h_{L/R}} \ , \qquad h_{L/R} = \frac{1}{2}(M\ell \mp J) \ . \tag{4.2.26}$$

At extremality, we have $S_L = 0$ and $S_R = S_{\text{ext}}$. The first deviation away from extremality in (4.2.24) is due to the response of S_L, while S_R remains dormant. The addition of the gravitational Chern-Simons term gives a way to disentangle the role of right versus left degrees of freedom in the CFT_2. And the interpretation is rather clear: The right movers control the ground state degeneracy at zero temperature, while the excitations near extremality are governed by the left moving excitations.

4.3 2D Theory

In this section we describe the 2D theory obtained via a dimensional reduction of (4.2.1). The ansatz for the 3D metric is

$$ds_3^2 = g_{MN} \mathrm{d}x^M \mathrm{d}x^N = g_{\mu\nu} \mathrm{d}x^\mu \mathrm{d}x^\nu + e^{-2\phi} \left(\mathrm{d}z + A_\mu \mathrm{d}x^\mu\right)^2 \ . \tag{4.3.1}$$

Here z is a compact direction with period $2\pi L$; the Greek indices run along the two dimensional directions, $\mu, \nu = 0, 1$. From the two dimensional perspective, $g_{\mu\nu}$ is the metric, A_μ is a gauge field and ϕ will be interpreted as the dilaton field.

The Kaluza-Klein reduction of I_{3D}, while tedious, is straight forward. The resulting action is [42, 43]

$$I_{2D} = I_{EMD} + I_{rCS} \ , \tag{4.3.2}$$

where the first term, coming from the Einstein-Hilbert piece in (4.2.1), reads

$$I_{EMD} = \frac{L}{8G_3} \int \mathrm{d}^2x \, \sqrt{-g} \, e^{-\phi} \left(R + \frac{2}{\ell^2} - \frac{1}{4} e^{-2\phi} \, F_{\mu\nu} F^{\mu\nu} \right) \ , \tag{4.3.3}$$

and the piece related to the gravitational Chern-Simons theory is

$$I_{rCS} = \frac{L}{32 G_3 \mu} \int \mathrm{d}^2x \, e^{-2\phi} \epsilon^{\mu\nu} \left(F_{\mu\nu} R + F_{\mu\rho} F^{\rho\sigma} F_{\sigma\nu} \, e^{-2\phi} - 2 F_{\mu\nu} D^2 \phi \right) \ . \tag{4.3.4}$$

Here $\epsilon^{\mu\nu}$ is the epsilon symbol, where $\epsilon^{01} = 1$, and D_μ is the covariant derivative with respect to the two dimensional metric $g_{\mu\nu}$.

In the following, we will refer to (4.3.3) as the Einstein-Maxwell-Dilation theory (EMD), which captures the two derivative dynamics of the dimensional reduction. The action (4.3.4) will be denoted as a reduced-Chern-Simons term (rCS), which contains the dynamics due to the 3D gravitational anomaly. As observed in [42], it is interesting to note that (4.3.4) is gauge and diffeomorphism invariant; this is related to the fact that the 3D equations of motion (4.2.2) are diffeomorphism invariant.

The equations of motion are

$$\begin{aligned} &\epsilon^{\alpha\beta} \partial_\beta \left(e^{-3\phi} f + \frac{1}{2\mu} \, e^{-2\phi} \left(R + 3 \, e^{-2\phi} f^2 - 2 D^2 \phi \right) \right) = 0 \ , \\ &e^{-\phi} \left(R + \frac{2}{\ell^2} + \frac{3}{2} \, e^{-2\phi} f^2 \right) + \frac{1}{\mu} \, e^{-2\phi} f \left(R + 2 \, e^{-2\phi} f^2 - 2 D^2 \phi \right) + \frac{1}{\mu} D^2 \left(e^{-2\phi} f \right) = 0 \ , \end{aligned} \tag{4.3.5}$$

which are the Maxwell and dilaton equations respectively. The variation with respect to the metric gives

$$g_{\alpha\beta} \left(D^2 e^{-\phi} - \frac{1}{\ell^2} \, e^{-\phi} + \frac{1}{4} \, e^{-3\phi} f^2 \right) - D_\alpha D_\beta e^{-\phi}$$

$$+\frac{1}{2\mu}\Big((D_\alpha e^{-2\phi}f)D_\beta\phi+(D_\beta e^{-2\phi}f)\mathrm{D}_\alpha\phi-D_\alpha D_\beta(e^{-2\phi}f)\Big)$$
$$+\frac{1}{2\mu}g_{\alpha\beta}\Big(\frac{1}{2}\,e^{-2\phi}fR-e^{-2\phi}fD^2\phi-D_\mu(e^{-2\phi}f)D^\mu\phi+D^2(e^{-2\phi}f)+e^{-4\phi}f^3\Big)=0\ . \tag{4.3.6}$$

It is also useful to record the trace of Einstein's equation, which reads

$$D^2e^{-\phi}-\frac{2}{\ell^2}\,e^{-\phi}+\frac{1}{2}\,e^{-3\phi}f^2+\frac{1}{2\mu}\,e^{-2\phi}f\left(R+2\,e^{-2\phi}f^2-2D^2\phi\right)+\frac{1}{2\mu}D^2\left(e^{-2\phi}f\right)=0\ . \tag{4.3.7}$$

In the above equations we introduced[3]

$$f\equiv\frac{1}{2\sqrt{-g}}\,\epsilon^{\alpha\beta}F_{\alpha\beta}\ , \tag{4.3.8}$$

which transforms as a scalar under diffeomorphisms. It is important to emphasise that (4.3.2) is a consistent truncation of TMG: All solutions to the equations of motion (4.3.5)-(4.3.6), when uplifted via (4.3.1), are solutions to (4.2.2).

4.4 Holographic renormalisation: UV perspective

One of our goals is to capture holographic properties of the 2D theory (4.3.2). We will start by considering backgrounds that have a running dilaton profile. In particular we will impose boundary conditions on the 2D fields that, upon an uplift to 3D, are interpreted as asymptotically AdS_3 backgrounds. For this reason, we coin this section a UV perspective to holographic renormalisation.

4.4.1 Background solution

To characterise the space of solutions, we will use throughout the gauge

$$ds^2=\mathrm{d}r^2+\gamma_{tt}\,\mathrm{d}t^2\ ,\qquad A_r=0\ . \tag{4.4.1}$$

Our interest here will be restricted to a very specific class of solutions: backgrounds that solve the equations of motion of $I_{\rm EMD}$. As in the three dimensional parent

[3] In terms of the epsilon tensor, $\varepsilon_{\alpha\beta}=\sqrt{-g}\,\epsilon_{\alpha\beta}$, we have

$$f=-\frac{1}{2}\varepsilon^{\alpha\beta}F_{\alpha\beta}\ ,\qquad F_{\alpha\beta}=\varepsilon_{\alpha\beta}f\ ,$$

where $\varepsilon^{\alpha\beta}\varepsilon_{\alpha\beta}=-2$.

theory, any solution to $I_{\rm EMD}$ will be a solution to $I_{\rm rCS}$. The most general solutions to EMD where constructed in [258], which we briefly summarise here. In EMD the gauge field is fixed to

$$F_{rt} = -2Q\, e^{3\phi}\sqrt{-\gamma}\ . \tag{4.4.2}$$

Solutions with a non-constant dilaton profile satisfy

$$\sqrt{-\gamma} = \frac{\alpha(t)}{\lambda'(t)}\,\partial_t e^{-\phi}\ , \tag{4.4.3}$$

where the dilaton is

$$e^{-2\phi} = \lambda(t)^2\, e^{2r/\ell}\left(1 + \frac{\ell^2}{2\lambda(t)^2}\,\mathfrak{m}(t)\, e^{-2r/\ell} + \frac{\ell^2}{16\lambda(t)^4}\left(\ell^2\,\mathfrak{m}(t)^2 - 4Q^2\right) e^{-4r/\ell}\right)\ , \tag{4.4.4}$$

and we introduced

$$\mathfrak{m}(t) \equiv m_0 - \left(\frac{\lambda'(t)}{\alpha(t)}\right)^2\ . \tag{4.4.5}$$

Here $\alpha(t)$ and $\lambda(t)$ are arbitrary functions of time that will be identified with the sources for the metric and dilaton, respectively; m_0 and Q are constants. For the subsequent analysis it will be useful to record the asymptotic behaviour of the solutions, which reads

$$\begin{aligned} e^{-2\phi} &= \lambda^2 e^{2r/\ell} + \frac{\ell^2}{2}\mathfrak{m} + O(e^{-2r/\ell})\ , \\ \gamma_{tt} &= -\alpha^2 e^{2r/\ell} + \frac{\ell^2\alpha^2}{2\lambda}\left(\frac{\mathfrak{m}}{\lambda} - \frac{\mathfrak{m}'}{\lambda'}\right) + O(e^{-2r/\ell})\ , \\ A_t &= \nu + \frac{\ell\alpha}{\lambda^3}\,Q\, e^{-2r/\ell} + O(e^{-4r/\ell})\ . \end{aligned} \tag{4.4.6}$$

The radial dependence of the gauge field A_t is fixed by (4.4.2); its source is $\nu(t)$, which is locally pure gauge. To be concise we have omitted the explicit time dependence of $\alpha(t)$, $\lambda(t)$, $\mathfrak{m}(t)$ and $\nu(t)$, and denoted time derivatives with a prime. The important feature here, to be contrasted with the asymptotic behaviour in Sec. 4.5, is that the gauge field has a sub-leading behaviour relative to the dilaton and 2D metric.

4.4.2 Renormalised observables

An important portion of performing holographic renormalisation is to obtain finite variations of the action provided a set of boundary conditions.[4] In this section we

[4] We are presenting here a very concise view on holographic renormalisation. For a current overview of the subject we refer to [300, 301].

will impose boundary conditions compatible with the leading behaviour in (4.4.6), and require that the renormalised on-shell variation of the action

$$\delta I_{\rm 2D}^{\rm UV} = \int {\rm d}t \left(\Pi^{tt}\, \delta\gamma_{tt} + \Pi_\phi\, \delta\phi + \Pi^t\, \delta A_t \right) \ , \tag{4.4.7}$$

remains finite and integrable. More explicitly, starting from the bulk action (4.3.2), we will add boundary terms leading to a functional $I_{\rm 2D}^{\rm UV}$ whose variations are finite when

$$\delta\gamma_{tt} = -2\,\alpha\, e^{2r/\ell}\, \delta\alpha \ , \quad \delta e^{-\phi} = e^{r/\ell}\delta\lambda \ , \quad \delta A_t = \delta\nu \ , \tag{4.4.8}$$

as we take $r \to \infty$. These are our UV boundary conditions. In terms of these sources, we have

$$\delta I_{\rm 2D}^{\rm UV} = \int {\rm d}t \left(\mathcal{T}_{\rm UV}\, \delta\alpha + \frac{\alpha}{\lambda}\, \mathcal{O}_{\rm UV}\, \delta\lambda - \alpha \mathcal{J}^t_{\rm UV}\, \delta\nu \right) \ , \tag{4.4.9}$$

where we have introduced the one-point functions conjugate to each source. The relation to the momenta variables in (4.4.7) is given by

$$\mathcal{T}_{\rm UV} \equiv \frac{2}{\alpha} \lim_{r\to\infty} \Pi_t{}^t \ , \quad \mathcal{O}_{\rm UV} \equiv -\frac{1}{\alpha} \lim_{r\to\infty} \Pi_\phi \ , \quad \mathcal{J}^t_{\rm UV} \equiv -\frac{1}{\alpha} \lim_{r\to\infty} \Pi^t \ . \tag{4.4.10}$$

Recall that our action has a contribution from the EMD action (4.3.3) and the rCS action in (4.3.4). Holographic renormalisation for EMD, with the boundary conditions (4.4.8), was done in detail in [258], and we will just highlight the main results. Varying the action (4.3.3) by itself leads to well known pathologies. These are cured by addition of the Gibbons-Hawking term

$$I_{\rm GH} = \frac{L}{4G_3} \int {\rm d}t\, \sqrt{-\gamma}\, e^{-\phi} K \ , \tag{4.4.11}$$

which leads to Dirichlet boundary conditions on the metric, and the counterterm[5]

$$I_{\rm c1} = -\frac{L}{4G_3\ell} \int {\rm d}t\, \sqrt{-\gamma}\, e^{-\phi} \ , \tag{4.4.12}$$

that renders the variation of the action finite for (4.4.8). In (4.4.11) K is the trace of the extrinsic curvature, which for our choice of gauge in (4.4.1) reads $K = \partial_r \log\sqrt{-\gamma}$. The renormalised action is then

$$I_{\rm EMD}^{\rm ren} = I_{\rm EMD} + I_{\rm GH} + I_{\rm c1} \ . \tag{4.4.13}$$

[5] As observed in [258], in (4.4.12) there is an additional term due to the conformal anomaly. It is a total derivative so it won't contribute to (4.4.10) and it will be ignored in the following.

The variation of $I^{\rm ren}_{\rm EMD}$ results in the renormalised canonical momenta

$$\begin{aligned}\delta I^{\rm ren}_{\rm EMD} =& \frac{L}{8G_3}\int {\rm d}t\sqrt{-\gamma}\left(\partial_r e^{-\phi}-\frac{1}{\ell}e^{-\phi}\right)\gamma^{tt}\delta\gamma_{tt}\\ &+\frac{L}{4G_3}\int {\rm d}t\sqrt{-\gamma}\left(K-\frac{1}{\ell}\right)e^{-\phi}\delta\phi-\frac{L}{4G_3}\int {\rm d}t\, Q\,\delta A_t\ . \end{aligned} \tag{4.4.14}$$

The contribution of the rCS action to (4.4.7) is rather interesting. The on- shell variation of $I_{\rm rCS}$ leads to

$$\begin{aligned}\delta I_{\rm rCS} =& -\frac{L}{16G_3\mu}\int {\rm d}t\, e^{-2\phi}\left(R+12Q^2\,e^{4\phi}-2D^2\phi\right)\delta A_t\\ &-\frac{L}{4G_3\mu}\int {\rm d}t\, Q\, e^{\phi}\delta\left(\sqrt{-\gamma}K\right)+\frac{L}{4G_3\mu}\int {\rm d}t\sqrt{-\gamma}\, Q\left((\partial_r e^{\phi})\delta\phi-e^{\phi}\,\delta\left(\partial_r\phi\right)\right)\ , \end{aligned} \tag{4.4.15}$$

where we used (4.4.2) to simplify this expression. This variation does not lead to divergences for (4.4.8) and falls off in (4.4.6), in accordance with the variation of the graviational Chern-Simons term in AAdS$_3$ spacetimes. Also, not surprisingly, we find variations of derivatives of the metric and dilaton. In order to restore Dirichlet boundary conditions for these fields, we add two extrinsic boundary terms:

$$I_{\rm c2}=\frac{L}{4G_3\mu}\int {\rm d}t\sqrt{-\gamma}\, Q\, e^{\phi}\, K+\frac{L}{4G_3\mu}\int {\rm d}t\sqrt{-\gamma}\, Q\,\partial_r e^{\phi}\ . \tag{4.4.16}$$

With this we obtain

$$\begin{aligned}\delta\left(I_{\rm rCS}+I_{\rm c2}\right) =& -\frac{L}{16G_3\mu}\int {\rm d}t\ e^{-2\phi}\left(R+12Q^2e^{4\phi}-2D^2\phi\right)\delta A_t\\ &+\frac{L}{8G_3\mu}\int {\rm d}t\sqrt{-\gamma}\, Q\left(\partial_r e^{\phi}\right)\gamma^{tt}\delta\gamma_{tt}\\ &+\frac{L}{4G_3\mu}\int {\rm d}t\sqrt{-\gamma}\, Q\ \left(2\,\partial_r e^{\phi}+Ke^{\phi}\right)\delta\phi\,. \end{aligned} \tag{4.4.17}$$

Gathering our contributions from (4.4.14) and (4.4.17) and using (4.4.6) the renormalised one-point functions are

$$\begin{aligned}\mathcal{T}_{\rm UV} &= -\frac{L\ell}{8G_3}\frac{\mathfrak{m}}{\lambda}-\frac{L}{4G_3\mu\ell}\frac{Q}{\lambda}\ ,\\ \mathcal{O}_{\rm UV} &= \frac{L\ell}{8G_3}\left(\frac{\mathfrak{m}}{\lambda}-\frac{\mathfrak{m}'}{\lambda'}\right)+\frac{L}{4G_3\mu\ell}\frac{Q}{\lambda}\ ,\\ \mathcal{J}^t_{\rm UV} &= \frac{L}{4G_3}\frac{Q}{\alpha}+\frac{L}{8G_3\mu}\frac{m_0}{\alpha} \end{aligned} \tag{4.4.18}$$

and the renormalised on-shell boundary action is

$$\begin{aligned} I_{\rm 2D}^{\rm UV} &= I_{\rm EMD}^{\rm ren} + I_{\rm rCS} + I_{\rm c2} \\ &= -\frac{L}{8G_3}\ell \int {\rm d}t \, \left(\frac{\alpha}{\lambda}\left[m_0 + 2\frac{Q}{\mu\ell^2}\right] + \frac{\lambda'^2}{\alpha\lambda} + \frac{2\nu}{\ell}\left[Q + \frac{m_0}{2\mu}\right]\right) \ . \end{aligned} \tag{4.4.19}$$

The above boundary action clearly satisfies

$$\mathcal{T}_{\rm UV} = \frac{\delta I_{\rm 2D}}{\delta\alpha} \ , \quad \mathcal{O}_{\rm UV} = \frac{\lambda}{\alpha}\frac{\delta I_{\rm 2D}}{\delta\lambda} \ , \quad \mathcal{J}^t_{\rm UV} = -\frac{1}{\alpha}\frac{\delta I_{\rm 2D}}{\delta\nu} \ . \tag{4.4.20}$$

At this stage, the effect of adding rCS to EMD is to shift $m_0 \to m_0 + 2\frac{Q}{\mu\ell^2}$ and $Q \to Q + \frac{m_0}{2\mu}$. Additionally we observe that (4.4.18) obeys

$$\mathcal{T}_{\rm UV} + \mathcal{O}_{\rm UV} = \frac{L\ell}{4G_3}\frac{1}{\alpha}\partial_t\left(\frac{\lambda'}{\alpha}\right) \ , \tag{4.4.21}$$

and

$$\partial_t \mathcal{J}^t_{\rm UV} + \mathcal{J}^t_{\rm UV}\,\partial_t \log\alpha = 0 \ , \quad \partial_t \mathcal{T}_{\rm UV} - \mathcal{O}_{\rm UV}\,\partial_t\log\lambda = 0 \ . \tag{4.4.22}$$

4.4.3 KK reduction of AdS_3/CFT_2

In this last portion we will dimensionally reduce the different boundary stress tensors in 3D of Sec. 4.2.1, and contrast them against the 2D quantitites in Sec. 4.4.2. To do so, we will first relate the 3D quantities to our 2D variables. From (4.3.1) we have

$$g_{tt} = \gamma_{tt} + e^{-2\phi}A_t^2 \ , \quad g_{tz} = e^{-2\phi}A_t \ , \quad g_{zz} = e^{-2\phi} \ , \tag{4.4.23}$$

which in turn implies that the boundary metric of the Fefferman-Graham expansion in (4.2.5) reads

$$g^{(0)}_{ij} = \begin{pmatrix} \lambda^2\nu^2 - \alpha^2 & \lambda^2\nu \\ \lambda^2\nu & \lambda^2 \end{pmatrix} \ , \tag{4.4.24}$$

where we used (4.4.6). In a similar fashion we can read off $g^{(2)}_{ij}$:

$$\begin{aligned} g^{(2)}_{tt} &= \frac{\ell^2}{2}\,\mathfrak{m}\left(\nu^2 + \frac{\alpha^2}{\lambda^2}\right) + 2\,\ell\,Q\,\frac{\alpha\,\nu}{\lambda} - \frac{\ell^2}{2}\,\frac{\alpha^2}{\lambda\,\lambda'}\,\mathfrak{m}' \ , \\ g^{(2)}_{zz} &= \frac{\ell^2}{2}\,\mathfrak{m} \ , \quad g^{(2)}_{tz} = \ell\,Q\,\frac{\alpha}{\lambda} + \frac{\ell^2}{2}\,\nu\,\mathfrak{m} \ . \end{aligned} \tag{4.4.25}$$

With these we will relate variations of the action with respect to $g^{(0)}_{ij}$ to variations with respect to α, λ and ν. This leads to

$$\frac{1}{2}\int \mathrm{d}x^2\sqrt{g^{(0)}}\,T^{ij}\,\delta g^{(0)}_{ij} = \pi L\int \mathrm{d}t\,\alpha\left(\frac{1}{\alpha}\mathcal{T}_{3\mathrm{D}}\,\delta\alpha + \frac{1}{\lambda}\mathcal{O}_{3\mathrm{D}}\,\delta\lambda - \mathcal{J}^t_{3\mathrm{D}}\,\delta\nu\right)\,, \quad (4.4.26)$$

where the relations among each side of this equation are

$$\begin{aligned}\mathcal{T}_{3\mathrm{D}} &= -2\pi L\,\frac{\lambda}{\alpha^2}\left(T_{tt}+\nu^2 T_{zz}-2\nu T_{tz}\right)\,,\\ \mathcal{O}_{3\mathrm{D}} &= \frac{2\pi L}{\lambda}\,T_{zz}\,,\\ \mathcal{J}^t_{3\mathrm{D}} &= 2\pi L\,\frac{\lambda}{\alpha^2}\left(T_{tz}-\nu T_{zz}\right)\,.\end{aligned} \quad (4.4.27)$$

In the 3D theory, the consistent stress tensor (4.2.7) arises from a well defined variational principle, for which it is meaningful to apply (4.4.27). Using (4.4.23) and (4.4.6) we obtain

$$\begin{aligned}\mathcal{T}_{3\mathrm{D}} &= -\frac{L\ell}{8G_3}\frac{\mathfrak{m}}{\lambda} - \frac{L}{4G_3\mu\ell}\left(\frac{Q}{\lambda}+\ell\,\frac{\lambda\lambda'\nu'}{2\alpha^3}\right)\,,\\ \mathcal{O}_{3\mathrm{D}} &= \frac{L\ell}{8G_3}\left(\frac{\mathfrak{m}}{\lambda}-\frac{\mathfrak{m}'}{\lambda'}\right) + \frac{L}{4G_3\mu\ell}\left(\frac{Q}{\lambda}+\frac{\ell}{2}\left(\frac{\alpha'\lambda^2\nu'}{\alpha^4}-\frac{\lambda^2\nu''}{2\alpha^3}\right)\right)\,,\\ \mathcal{J}^t_{3\mathrm{D}} &= \frac{L}{4G_3}\frac{Q}{\alpha} + \frac{L}{8G_3\mu}\left(\frac{m_0}{\alpha}-\frac{\alpha'\lambda\lambda'}{\alpha^4}+\frac{\lambda'^2}{2\alpha^3}+\frac{\lambda\lambda''}{2\alpha^3}\right)\,.\end{aligned} \quad (4.4.28)$$

In terms of these variables, the trace anomaly and Ward identity (4.2.9) take the form[6]

$$\mathcal{T}_{3\mathrm{D}}+\mathcal{O}_{3\mathrm{D}} = \frac{L\ell}{4G_3}\frac{1}{\alpha}\left(\partial_t\left(\frac{\lambda'}{\alpha}\right)-\frac{1}{4\mu\ell}\partial_t\left(\frac{\lambda^2\nu'}{\alpha^2}\right)\right)\,, \quad (4.4.29)$$

and

$$\begin{aligned}\partial_t\mathcal{J}^t_{3\mathrm{D}}+\mathcal{J}^t_{3\mathrm{D}}\,\partial_t\log\alpha &= \frac{L}{16G_3\mu\alpha}\,\partial_t^2\left(\frac{\lambda\lambda'}{\alpha^2}\right)\,,\\ \partial_t\mathcal{T}_{3\mathrm{D}}-\mathcal{O}_{3\mathrm{D}}\,\partial_t\log\lambda &= -\frac{L}{16G_3\mu}\left[\frac{\alpha}{\lambda\lambda'}\partial_t\left(\nu'\left(\frac{\lambda\lambda'}{\alpha^2}\right)^2\right)\right]\,.\end{aligned} \quad (4.4.30)$$

The renormalised boundary action $\tilde{I}_{\mathrm{ren}}$, which can be inferred by integrating

[6] Using (4.4.24) and (4.4.27), the divergence appearing in (4.2.9) translates to

$$D_iT^{it} = -\frac{1}{\alpha^2\lambda}\left(\partial_t\mathcal{T}-\mathcal{O}\,\partial_t\log\lambda\right)\,,\quad \mathrm{D}_iT^{iz} = \frac{\nu}{\alpha^2\lambda}\left(\partial_t\mathcal{T}-\mathcal{O}\,\partial_t\log\lambda\right)-\frac{1}{\lambda^3}\left(\partial_t\mathcal{J}^t+\mathcal{J}^t\partial_t\log\alpha\right)\,,$$

and the trace is $T^i_i = \frac{1}{\lambda}\left(\mathcal{T}+\mathcal{O}\right)$.

(4.4.26), reads

$$\tilde{I}_{\rm ren} = -\frac{L\ell}{8G_3}\int \mathrm{d}t\ \left(\frac{\alpha}{\lambda}\left[m_0 + 2\frac{Q}{\mu\ell^2}\right] + \frac{\lambda'^2}{\alpha\lambda} + \frac{2\nu}{\ell}\left[Q + \frac{m_0}{2\mu}\right]\right) + \frac{L}{16G_3\mu}\int \mathrm{d}t\ \frac{\lambda\lambda'\nu'}{\alpha^2}\ . \tag{4.4.31}$$

Clearly the covariant stress tensor, dimensionally reduced to 2D, does not coincide with the one-point functions in (4.4.18). Albeit the EMD contributions are in perfect agreement, as reported in [258], and the Q dependent pieces also agree, there is an additional term coming from the gravitational Chern-Simons term. The reason of this mismatch is not surprising: The last term in $\tilde{I}_{\rm ren}$ can be rewritten as

$$\frac{L}{16G_3\mu}\int \mathrm{d}t\ \frac{\lambda\lambda'\nu'}{\alpha^2} = -\frac{L}{32G_3\mu}\int \mathrm{d}t\ \gamma^{tt}\partial_t(e^{-2\phi})\,\partial_t A_t\ , \tag{4.4.32}$$

which is clearly not gauge invariant. It is as well finite, and methods for holographic renormalisation are not capable to fix finite counterterms unless another principle (or symmetry) is advocated for. From the 2D point of view, $I_{\rm rCS}$ is a gauge invariant action which makes the introduction of (4.4.32) somewhat awkward. The only meaningful observation we can make at this stage is that (4.4.32) can be achieved by integrating by parts either the first or second term in (4.3.4) and arranging time derivatives appropriately. This all illustrates that important parts of the anomalies are lost in the 2D theory (4.3.2), in particular if we don't make reference to the parent theory. Notably our one-point functions (4.4.18) lead to conserved currents (4.4.22), while in (4.4.30) we still encounter the effects of the gravitational anomaly.

It is instructive to compare our results with the dimensional reduction of the covariant stress tensor (4.2.10). Even though this choice of stress tensor does not comply with a variational principle, we simply inquire what the map (4.4.23) predicts in 2D. The result is

$$\begin{aligned} \sqcup_{\rm 3D} &= -\frac{L\ell}{8G_3}\frac{\mathfrak{m}}{\lambda} - \frac{L}{4G_3\mu\ell}\frac{Q}{\lambda}\ , \qquad \wr_{\rm 3D} = \frac{L\ell}{8G_3}\left(\frac{\mathfrak{m}}{\lambda} - \frac{\mathfrak{m}'}{\lambda'}\right) + \frac{L}{4G_3\mu\ell}\frac{Q}{\lambda}\ , \\ |^t_{\rm 3D} &= \frac{L}{4G_3}\frac{Q}{\alpha} + \frac{L}{8G_3\mu}\left(\frac{\mathfrak{m}}{\alpha} - \frac{\lambda}{2\lambda'\alpha}\,\mathfrak{m}'\right)\ . \end{aligned} \tag{4.4.33}$$

The trace anomaly and Ward identity (4.2.11) in this case reduce to

$$\sqcup_{\rm 3D} + \wr_{\rm 3D} = \frac{L\ell}{4G_3}\frac{1}{\alpha}\,\partial_t\left(\frac{\lambda'}{\alpha}\right)\ , \tag{4.4.34}$$

and

$$\partial_t |^t_{\rm 3D} + |^t_{\rm 3D}\, \partial_t \log\alpha = \frac{\lambda^2}{2\alpha}\,\partial_t\left(\frac{2}{\alpha\lambda}\partial_t\left(\frac{\lambda'}{\alpha}\right)\right)\ , \quad \partial_t \sqcup_{\rm 3D} - \wr_{\rm 3D}\,\partial_t \log\lambda = 0\ . \tag{4.4.35}$$

It is curious to report that in this case $\sqcup_{\rm 3D} = \mathcal{T}_{\rm UV}$ and $\wr_{\rm 3D} = \mathcal{O}_{\rm UV}$, while the currents $|^t_{\rm 3D}$ and $\mathcal{J}^t_{\rm UV}$ do not agree. Recall that the covariant stress tensor does not conform with the Wess-Zumino consistency conditions, so it is not surprising to find a disagreement between (4.4.18) and (4.4.33).

Finally, we have the 3D conserved stress tensor in (4.2.12). Because this object is not Lorentz invariant it is not clear how to treat it in the dimensionally reduced theory. One obstruction is that we cannot use the map (4.4.27): It assumes the 3D tensor is symmetric, and therefore contradicts the relations in (4.2.13).

4.5 Holographic renormalisation: IR perspective

In addition to the backgrounds considered in Sec. 4.4.1, the equations of motion (4.3.5)-(4.3.7) also admit a branch of solutions specified by a constant value of the dilaton. We will denote this branch IR fixed points, due to their role in describing the AdS$_2$ geometry of near extremal black holes.

In this section we will start with a derivation of the IR fixed point solutions, and then turn on an irrelevant deformation for the dilaton. This deformation drives also the metric away from its locally AdS$_2$ form attained at the fixed point. On this deformed background we will evaluate the appropriate one-point functions using holographic renormalisation.

4.5.1 Background solution

To construct the IR fixed point solution, we start by setting

$$e^{2\phi} = e^{2\phi_0}\ , \tag{4.5.1}$$

with ϕ_0 a constant. We will use the subscript '0' to refer to the values of the fields at the IR fixed point. Subtracting two times (4.3.7) from (4.3.5) we infer

$$R = -\frac{6}{\ell^2} - \frac{1}{2}\,e^{-2\phi_0} f^2\ , \tag{4.5.2}$$

which after plugging it back into the gauge field equation of motion (4.3.5) implies that the field strength f is constant as well. The values of f and R are then

determined by

$$R_0 + \frac{6}{\ell^2} + \frac{1}{2}\, e^{-2\phi_0} f_0^2 = 0 \ , \\ \left(-\frac{4}{\ell^2} + e^{-2\phi_0} f_0^2\right)\left(1 + \frac{3}{2\mu}\, e^{-\phi_0} f_0\right) = 0 \ . \tag{4.5.3}$$

There are two classes of solutions to (4.5.3). The first is

$$R_0 = -\frac{8}{\ell^2} \ , \qquad e^{-2\phi_0} f_0^2 = \frac{4}{\ell^2} \ , \tag{4.5.4}$$

which is the constant dilaton solution to EMD. The second branch is

$$R_0 = -\frac{6}{\ell^2} - \frac{2\mu^2}{9} \ , \qquad e^{-\phi_0} f_0 = -\frac{2\mu}{3} \ . \tag{4.5.5}$$

This configuration would uplift to warped AdS_3 solutions in TMG, such as those in [272, 275, 302]. Since the Ricci scalar is negative for real values of the variables, all fixed point solutions are locally AdS_2.

The focus for the reminder of this section will be on (4.5.4). Working in the same gauge as in (4.4.1), the background AdS_2 metric and gauge field are given by

$$\sqrt{-\gamma_0} = \alpha_{\rm ir}(t)\, e^{2r/\ell} + \beta_{\rm ir}(t)\, e^{-2r/\ell}, \\ A_t = \nu_{\rm ir}(t) - \ell\, Q\, e^{3\phi_0}\left(\alpha_{\rm ir}(t)\, e^{2r/\ell} - \beta_{\rm ir}(t)\, e^{-2r/\ell}\right) \ . \tag{4.5.6}$$

The subscript "ir" here is to distinguish the functions appearing in our IR analysis to those in (4.4.6) which are relevant for the UV. Here Q is defined as in (4.4.2) and from (4.5.4) we have

$$Q^2 = \frac{1}{\ell^2} e^{-4\phi_0} \ . \tag{4.5.7}$$

The functions $\alpha_{\rm ir}$, and $\nu_{\rm ir}$ act as sources for the AdS_2 metric and gauge field, respectively. $\beta_{\rm ir}$ parametrizes nearly-AdS_2 spacetimes: It is induced by large diffeomorphisms that preserve the boundary metric, as we shall see in Sec. 4.6.1.

Small perturbations around the IR background, will be ignited by a deviation of the dilaton away from its constant value:[7]

$$e^{-2\phi} = e^{-2\phi_0} + \mathcal{Y} \ , \tag{4.5.8}$$

with $\mathcal{Y}$ small. As the equations of motion will demand, this perturbation will

[7] We are adapting the same notation as in [254], and our subsequent derivations follow closely to those there. This is expected since 2D theories of gravity coupled to a dilaton follow universal trends that are present here too [9, 40, 244].

generate a backreaction of the metric which we parametrise as

$$\sqrt{-\gamma} = \sqrt{-\gamma_0} + \sqrt{-\gamma_1} \ . \tag{4.5.9}$$

The response of the gauge field follows automatically from (4.4.2). Here all fields depend explicitly on time and the radial coordinate, but we suppress it for notational convenience. We will determine the expressions of the perturbations $\sqrt{-\gamma_1}$ and $\mathcal{Y}$ by solving the perturbed EMD equations of motion, which we know leads to a solution of the full 2D theory (4.3.2). These linearised equations around the IR fixed point are

$$\left(\partial_r^2 - \frac{4}{\ell^2}\right) \mathcal{Y} = 0 \ , \tag{4.5.10}$$

$$\left(K_0\, \partial_r + D_{t,0}^2 - \frac{4}{\ell^2}\right) \mathcal{Y} = 0 \ , \tag{4.5.11}$$

$$\partial_r \left(\frac{\partial_t \mathcal{Y}}{\sqrt{-\gamma_0}}\right) = 0 \ , \tag{4.5.12}$$

$$\left(\partial_r^2 - \frac{4}{\ell^2}\right) \sqrt{-\gamma_1} + \frac{6}{\ell^2}\, e^{2\phi_0}\, \sqrt{-\gamma_0}\mathcal{Y} = 0 \ . \tag{4.5.13}$$

The subscript '0' for the trace of the extrinsic curvature K_0 and the Laplace Beltrami operator $D_{t,0}^2$ indicate again that they are evaluated in the IR geometry with metric γ_0

$$K_0 \equiv \partial_r \log \sqrt{-\gamma_0} \ , \qquad D_{t,0}^2 \equiv \frac{1}{\sqrt{-\gamma_0}} \partial_t \left(\sqrt{-\gamma_0}\, \gamma_0^{tt}\, \partial_t\right) \ . \tag{4.5.14}$$

Equation (4.5.10) implies

$$\mathcal{Y} = \lambda_{\rm ir}(t)\, e^{2r/\ell} + \sigma_{\rm ir}(t)\, e^{-2r/\ell} \ , \tag{4.5.15}$$

with $\lambda_{\rm ir}(t)$ the source for our deformation, and $\sigma_{\rm ir}(t)$ its vev. Also we can infer from this equation that $\mathcal{Y}$ has conformal dimension $\Delta = 2$ and is, as already anticipated, an irrelevant deformation moving us slightly away from the IR fixed point. The constraint in (4.5.12) relates $\mathcal{Y}$ to γ_0 by imposing

$$\beta_{\rm ir}(t) = \alpha_{\rm ir}(t)\, \frac{\sigma'_{\rm ir}(t)}{\lambda'_{\rm ir}(t)} \ . \tag{4.5.16}$$

This relation is a universal feature of nAdS$_2$ holography: It implies that the perturbation moving us away from the IR fixed point is related to the large diffeo-

morphisms in AdS_2. Finally combining (4.5.16) with (4.5.11) we obtain

$$\begin{aligned}\beta_{\rm ir}(t) &= -\frac{\ell^2}{16\lambda'_{\rm ir}(t)}\,\alpha_{\rm ir}(t)\,\partial_t\left(\frac{\mathfrak{q}(t)}{\lambda_{\rm ir}(t)}\right)\ ,\\ \sigma_{\rm ir}(t) &= -\frac{\ell^2}{16\lambda_{\rm ir}(t)}\,\mathfrak{q}(t)\ ,\end{aligned} \tag{4.5.17}$$

where we defined

$$\mathfrak{q}(t) \equiv c_0 + \left(\frac{\lambda'_{\rm ir}(t)}{\alpha_{\rm ir}(t)}\right)^2\ , \tag{4.5.18}$$

and c_0 is an integration constant, independent of the spacetime coordinates.

Now we examine the dilaton equation of motion (4.5.13). Its solution determines the form of the metric perturbation. The homogeneous solution is a locally AdS_2 metric, equal to the background solution $\sqrt{-\gamma_0}$. The inhomogeneous equation on the other side is solved by

$$\left(\sqrt{-\gamma_1}\right)_{\rm inh} = -\frac{e^{2\phi_0}}{2}\left(\mathcal{Y}\sqrt{-\gamma_0} + \frac{\ell^2}{2}\,\partial_t\left(\frac{\lambda'_{\rm ir}(t)}{\alpha_{\rm ir}(t)}\right)\right)\ . \tag{4.5.19}$$

4.5.2 Renormalised observables

We will now perform holographic renormalisation around the perturbed IR background. Our starting point is familiar: As in Sec. 4.4.2 we will build a 2D action, such that for the deformed IR background, the variation

$$\delta I^{\rm IR}_{\rm 2D} = \int {\rm d}t\left(\pi^{tt}\,\delta\gamma_{tt} + \pi_\phi\,\delta\phi + \pi^t\,\delta A_t\right)\ , \tag{4.5.20}$$

leads to a well defined variational principle. Here the lower case, relative to the upper case in (4.4.9), is to emphasis that the values of the canonical momenta will depend on our boundary conditions, and this affects the renormalisation of the action.

The boundary conditions on the metric and dilaton follow from (4.5.6) and (4.5.15),

$$\delta\gamma_{tt} = -2\alpha_{\rm ir}\,e^{4r/\ell}\delta\alpha_{\rm ir}\ ,\quad \delta e^{-2\phi} = e^{2r/\ell}\delta\lambda_{\rm ir}\ , \tag{4.5.21}$$

that is, their leading divergences are interpreted as sources, and as $r\to\infty$ we seek for finite responses under those variations. The deviations of $e^{-2\phi}$ away from its constant value are large in r, still we want to treat them as small perturbation around the IR fixed point. As we study the response of the action we will therefore

take

$$e^{2\phi_0}\,|\lambda_{\rm ir}|\,e^{2r/\ell} \;\ll\; 1\ , \tag{4.5.22}$$

which implies that we will keep only the first order effect of the deformation.

We have not mentioned the boundary conditions of the gauge field in (4.5.21) because the gauge field exhibits a crucial difference in the IR compared to the UV. This requires a separate discussion on how to treat its boundary conditions. The issue arises because in the AdS$_2$ region A_t is no longer dominated by the source $\nu_{\rm ir}$, but by the volume of AdS$_2$. From (4.5.6) we have

$$A_t = -\ell\, Q\, e^{3\phi_0}\alpha_{\rm ir}\, e^{2r/\ell} + \nu_{\rm ir} + O(e^{-2r/\ell})\ , \tag{4.5.23}$$

and for the canonical momenta on the AdS$_2$ background[8]

$$\pi^t = \frac{\delta I_{\rm 2D}}{\delta(\partial_r A_t)} = -\frac{L}{4G_3}\left(1 \mp \frac{1}{\mu\ell}\right) Q\ , \tag{4.5.24}$$

which reflects that $A_t \sim \sqrt{-\gamma_0}\,\pi^t$ as $r\to\infty$, and the source is being washed away. The problem therefore is the following: We have a space of asymptotic solutions characterised by a charge Q and source $\nu_{\rm ir}$, which we want to relate to the space of fields; and it is clear that the asymptotic behaviour of A_t and π^t does not capture this information. The solution to the dilemma is explained in [12, 254, 258]. Here we will provide a brief summary.

To fix this issue, it is convenient to first do a canonical transformation

$$I_{\rm ren}[\gamma_{tt},\phi,\pi^t] = I^{\rm IR}_{\rm 2D} - \int {\rm d}t\,\pi^t A_t\ , \tag{4.5.25}$$

which is a Legendre transform for the gauge field, and start from the variational problem

$$\delta I_{\rm ren} = \int {\rm d}t\left(\pi^{tt}\,\delta\gamma_{tt} + \pi_\phi\,\delta\phi - A_t^{\rm ren}\,\delta\pi^t\right)\ , \tag{4.5.26}$$

Here $A_t^{\rm ren}$ is identified as the conjugate variable to π^t and obeys

$$A_t^{\rm ren} = A_t \;-\; \frac{I^{\rm IR}_{\rm 2D}}{\delta\pi^t}\ . \tag{4.5.27}$$

[8] The "$\pm$" in (4.5.24) is due to selecting a sign as one uses (4.5.7) to evaluate the contribution to π^t from the rCS. The minus sign corresponds to $Q<0$, while the plus sign corresponds to $Q>0$.

Now, as one constructs the renormalised action $I^{\rm IR}_{\rm 2D}$, one should assure that from (4.5.27) we obtain $A^{\rm ren}_t = \nu_{\rm ir} + O(e^{-2r/\ell})$. Finally, since we want to have a Dirichlet valued problem for all fields, the last step is to do another Legendre transform

$$\hat{I}_{\rm ren} = I_{\rm ren} - \int {\rm d}t\, \pi^t A^{\rm ren}_t \ , \tag{4.5.28}$$

and look for finite responses of the effective action, i.e.

$$\delta \hat{I}_{\rm ren} = \int {\rm d}t \left(\pi^{tt}\, \delta\gamma_{tt} + \pi_\phi\, \delta\phi + \pi^t\, \delta A^{\rm ren}_t \right) \ , \tag{4.5.29}$$

where now our boundary conditions for all fields are

$$\delta\gamma_{tt} = -2\alpha_{\rm ir}\, e^{4r/\ell} \delta\alpha_{\rm ir} \ , \quad \delta e^{-2\phi} = e^{2r/\ell} \delta\lambda_{\rm ir} \ , \quad \delta A^{\rm ren}_t = \delta\nu_{\rm ir} \ . \tag{4.5.30}$$

In the following we will start our construction of counterterms immediately from (4.5.29), and not build $I_{\rm ren}$ or $I^{\rm IR}_{\rm 2D}$ explicitly; we refer to [254] for those intermediate steps which are easily adapted to the discussion here.

One-point functions

We now turn to building the boundary terms needed to make (4.5.29) a well defined variational problem. It is easier to first focus on the contributions from EMD, which resembles the analysis in [254] adopted to our setup. As in the UV analysis, the Gibbons-Hawking term guarantees a Dirichlet boundary problem

$$I^{\rm IR}_{\rm GH} = \frac{L}{4G_3} \int {\rm d}t\, \sqrt{-\gamma}\, e^{-\phi}\, K \ , \tag{4.5.31}$$

and the counterterm that renders the variation finite is

$$I_{\rm d1} = -\frac{L}{4G_3\ell} \int {\rm d}t\, \sqrt{-\gamma}\, e^{\phi_0}\, \mathcal{Y} + \frac{L}{8G_3\ell} \int {\rm d}t \sqrt{-\gamma}\, e^{3\phi_0}\, \mathcal{Y}^2 \ . \tag{4.5.32}$$

The on- shell variation of the EMD action combined with these terms gives

$$\begin{aligned} \delta \left(I_{\rm EMD} + I^{\rm IR}_{\rm GH} + I_{\rm d1} \right) =& \frac{L}{8G_3} \int {\rm d}t \sqrt{-\gamma} \left(\partial_r e^{-\phi} - \frac{1}{\ell}\, e^{\phi_0}\, \mathcal{Y} \right) \gamma^{tt} \delta\gamma_{tt} \\ & - \frac{L}{4G_3} \int {\rm d}t \sqrt{-\gamma} \left(K e^{-\phi} - \frac{2}{\ell}\, e^{-\phi_0} \right) \delta\phi - \frac{L}{4G_3} \int {\rm d}t\, Q\, \delta A^{\rm ren}_t \ . \end{aligned} \tag{4.5.33}$$

For the rCS action, we can start from (4.4.17): The combination $I_{\rm rCS} + I_{\rm c2}$ fixes Dirichlet boundary conditions. Replacing (4.5.8), (4.5.9), and (4.5.19) in (4.4.17),

and keeping terms consistent with (4.5.22), gives

$$\delta_{\gamma_{tt}}\left(I_{\rm rCS}+I_{\rm c2}\right)=-\frac{L}{16G_3\mu}\int {\rm d}t\sqrt{-\gamma_0}\,e^{3\phi_0}\,Q\,\partial_r\mathcal{Y}\,\gamma_0^{tt}\delta\gamma_{tt}\ , \tag{4.5.34}$$

and

$$\delta_{\phi}\left(I_{\rm rCS}+I_{\rm c2}\right)=\frac{L}{4G_3\mu}\int {\rm d}t\,e^{3\phi_0}\,Q\left(e^{-2\phi_0}\partial_r\sqrt{-\gamma_0}-\mathcal{Y}\,\partial_r\sqrt{-\gamma_0}-\frac{3}{2}\sqrt{-\gamma_0}\,\partial_r\mathcal{Y}\right)\delta\phi\ . \tag{4.5.35}$$

Contrarily to the on-shell values for the UV, where (4.4.17) led to finite contributions, the above terms are divergent as $r\to\infty$ for the IR values (4.5.6) and (4.5.15). Removing these IR divergences will lead to quantitative differences in our one-point functions as will be evident shortly. To cure the remaining divergences in (4.5.34)-(4.5.35) we will add the following counterterms

$$I_{\rm c3}=\frac{L}{4G_3\mu\ell}\int {\rm d}t\,\sqrt{-\gamma}\,e^{3\phi_0}\,Q\,\mathcal{Y}-\frac{3\,L}{8G_3\mu\ell}\int {\rm d}t\,\sqrt{-\gamma}\,e^{5\phi_0}\,Q\,\mathcal{Y}^2\ . \tag{4.5.36}$$

It is worth noting that these counterterms are very similar to those in (4.5.32) used for EMD. The reason for their similarity is due to the fact that we are working at first order in the perturbations, and these are the allowed combinations of $\mathcal{Y}$ that could cancel divergences induced by the irrelevant deformation.

Combining the contributions from (4.5.34)-(4.5.36), plus the contribution from $A_t^{\rm ren}$, we finally have

$$\begin{aligned}\delta\left(I_{\rm rCS}+I_{\rm c2}+I_{\rm c3}\right)=&-\frac{L}{16G_3\mu}\int {\rm d}t\,e^{3\phi_0}\,Q\,\sqrt{-\gamma_0}\left(\partial_r\mathcal{Y}-\frac{2}{\ell}\,\mathcal{Y}\right)\gamma_0^{tt}\delta\gamma_{tt}\\&-\frac{L}{4G_3\mu}\int {\rm d}t\,e^{3\phi_0}\,Q\left(\mathcal{Y}\,\partial_r\sqrt{-\gamma_0}+\frac{3}{2}\sqrt{-\gamma_0}\,\partial_r\mathcal{Y}-4\sqrt{-\gamma_0}\,\mathcal{Y}\right)\delta\phi\\&+\frac{L}{4G_3\mu}\int {\rm d}t\,e^{\phi_0}\,Q\left(\partial_r\sqrt{-\gamma_0}-\frac{2}{\ell}\sqrt{-\gamma_0}-\frac{2}{\ell}\sqrt{-\gamma_1}\right)\delta\phi\\&-\frac{L}{4G_3\mu}\int {\rm d}t\,e^{2\phi_0}\,Q^2\,\delta A_t^{\rm ren}\ .\end{aligned} \tag{4.5.37}$$

The renormalised one-point functions in the IR are given by[9]

$$\mathcal{T}_{\rm IR}\equiv\frac{2}{\alpha_{\rm ir}}\lim_{r\to\infty}\pi_t{}^t\ ,\quad \mathcal{O}_{\rm IR}\equiv-\frac{1}{\alpha_{\rm ir}}\lim_{r\to\infty}e^{2r/\ell}\pi_\phi\ ,\quad \mathcal{J}^t_{\rm IR}\equiv-\frac{1}{\alpha_{\rm ir}}\lim_{r\to\infty}\pi^t\ . \tag{4.5.38}$$

[9]Note that there is a small difference in the definition of $\mathcal{O}$ in the UV relative to the IR. This is simply because of the nature of our boundary fall-offs: in the UV we have $\delta\phi=\lambda^{-1}\delta\lambda$, while in the IR $\delta\phi=-\frac{1}{2}e^{2\phi_0}e^{2r/\ell}\delta\lambda_{\rm ir}$.

Explicitly, using (4.5.6) and (4.5.15) we obtain

$$\begin{aligned}
\mathcal{T}_{\rm IR} &= -\frac{L}{2G_3\ell}\, e^{\phi_0}\left(1-\frac{Q}{\mu}\, e^{2\phi_0}\right)\sigma_{\rm ir} = \frac{L\ell}{32G_3}\, e^{\phi_0}\left(1\pm\frac{1}{\mu\ell}\right)\frac{\mathfrak{q}(t)}{\lambda_{\rm ir}}\ ,\\
\mathcal{O}_{\rm IR} &= -\frac{L}{G_3\ell}\, e^{-\phi_0}\left(1-\frac{Q}{\mu}\, e^{2\phi_0}\right)\frac{\beta_{\rm ir}}{\alpha_{\rm ir}} = \frac{L\ell}{16G_3}\, e^{-\phi_0}\left(1\pm\frac{1}{\mu\ell}\right)\frac{1}{\lambda'_{\rm ir}}\partial_t\left(\frac{\mathfrak{q}(t)}{\lambda_{\rm ir}}\right)\ ,\\
\mathcal{J}^t_{\rm IR} &= \frac{L}{4G_3}\, Q\left(1+\frac{Q}{\mu}\, e^{2\phi_0}\right)\frac{1}{\alpha_{\rm ir}} = \frac{L}{4G_3}\, Q\left(1\mp\frac{1}{\mu\ell}\right)\frac{1}{\alpha_{\rm ir}}\ .
\end{aligned} \tag{4.5.39}$$

In the second equality we used (4.5.17) which gives the on-shell values of the one-point functions. We also used (4.5.7) which relates Q to $e^{-2\phi_0}$ up to a choice of sign for Q. From here we can deduced that the renormalised on-shell boundary action is

$$\hat{I}_{\rm ren} = \frac{L\ell}{32G_3}\left(1\pm\frac{1}{\mu\ell}\right)\int \mathrm{d}t\ e^{\phi_0}\,\frac{\alpha_{\rm ir}}{\lambda_{\rm ir}}\left[c_0-\left(\frac{\lambda'_{\rm ir}}{\alpha_{\rm ir}}\right)^2\right]+\frac{L}{4G_3}\left(1\mp\frac{1}{\mu\ell}\right)\int \mathrm{d}t\, Q\,\nu_{\rm ir}\ , \tag{4.5.40}$$

satisfying

$$\mathcal{T}_{\rm IR}=\frac{\delta I^{\rm IR}_{\rm 2D}}{\delta\alpha_{\rm ir}}\ ,\qquad \mathcal{O}_{\rm IR}=\frac{2}{\alpha_{\rm ir}}e^{-2\phi_0}\frac{\delta I^{\rm IR}_{\rm 2D}}{\delta\lambda_{\rm ir}}\ ,\qquad \mathcal{J}^t_{\rm IR}=\frac{1}{\alpha_{\rm ir}}\frac{\delta I^{\rm IR}_{\rm 2D}}{\delta\nu_{\rm ir}}\ . \tag{4.5.41}$$

From (4.5.39), our one-point functions obey

$$\partial_t\mathcal{T}_{\rm IR}-\frac{1}{2}\, e^{2\phi_0}\,\lambda'_{\rm ir}\,\mathcal{O}_{\rm IR}=0\ ,\qquad \partial_t\mathcal{J}^t_{\rm IR}+\mathcal{J}^t_{\rm IR}\,\partial_t\log\alpha_{\rm ir}=0\ , \tag{4.5.42}$$

and

$$\mathcal{T}_{\rm IR}+\frac{1}{2}\, e^{2\phi_0}\lambda_{\rm ir}\,\mathcal{O}_{\rm IR}=\frac{L\ell}{16G_3}\, e^{\phi_0}\left(1\pm\frac{1}{\mu\ell}\right)\frac{1}{\alpha_{\rm ir}}\partial_t\left(\frac{\lambda'_{\rm ir}}{\alpha_{\rm ir}}\right)\ . \tag{4.5.43}$$

4.6 Schwarzian effective action

In this last section we will provide an interpretation of the holographic renormalisation in the UV and IR in terms of the Schwarzian effective action. We will discuss the interpolation between these two fixed points and their role in describing the entropy of the near extremal BTZ black hole.

4.6.1 Effective action: IR

We will start by interpreting the results in Sec. 4.5, that are relevant for nAdS$_2$ holography. The renormalised on-shell boundary action found in (4.5.40) takes the form

$$\hat{I}_{\rm ren} = \frac{L\ell}{32G_3}\left(1+\frac{1}{\mu\ell}\right)\int \mathrm{d}t\; e^{\phi_0}\,\frac{\alpha_{\rm ir}}{\lambda_{\rm ir}}\left[c_0-\left(\frac{\lambda'_{\rm ir}}{\alpha_{\rm ir}}\right)^2\right]+\frac{L}{4G_3}\left(1-\frac{1}{\mu\ell}\right)\int \mathrm{d}t\, Q\,\nu_{\rm ir}\ , \tag{4.6.1}$$

where we selected $Q<0$; this is the correct choice as we compare to the conventions used for the BTZ black hole in Sec. 4.2.2.

To interpret the various pieces in this action, we will first venture into the asymptotic symmetries relevant to nAdS$_2$ holography. For simplicity we will set $\alpha_{\rm ir}=1$, and start by considering the empty AdS$_2$ background

$$ds^2 = \mathrm{d}r^2 - e^{4r/\ell}\mathrm{d}t^2\ , \qquad A = -Q\,e^{3\phi_0}\,e^{2r/\ell}\mathrm{d}t\ . \tag{4.6.2}$$

The set of diffeomorphisms that preserve the boundary metric and radial gauge are

$$\begin{aligned} t &\to f(t)+\frac{\ell^2}{8}\frac{f''(t)}{e^{4r/\ell}-\frac{\ell^2}{16}\frac{f''(t)^2}{f'(t)^2}}\ ,\\ e^{2r/\ell} &\to \frac{e^{-2r/\ell}}{f'(t)}\left(e^{4r/\ell}-\frac{\ell^2}{16}\frac{f''(t)^2}{f'(t)^2}\right)\ , \end{aligned} \tag{4.6.3}$$

where $f(t)$ labels reparametrizations of the boundary time. The gauge field transforms as well under this diffeomorphism, and to compensate for this, the diffeomorphism needs to be complemented by a gauge transformation [303, 304],

$$A_\mu \to A_\mu+\partial_\mu\Lambda\ , \qquad \Lambda = -\frac{Q\ell}{2}\,e^{3\phi_0}\,\log\left(\frac{4e^{2r/\ell}f'(t)-\ell f''(t)}{4e^{2r/\ell}f'(t)+\ell f''(t)}\right)\ , \tag{4.6.4}$$

designed to preserve $A_r=0$ and the asymptotic behaviour of the field. The resulting background is

$$\begin{aligned} ds^2 &= \mathrm{d}r^2-\left(e^{2r/\ell}+\frac{\ell^2}{8}\{f(t),t\}e^{-2r/\ell}\right)^2\mathrm{d}t^2\ ,\\ A &= -Q\,e^{3\phi_0}\left(e^{2r/\ell}-\frac{\ell^2}{8}\{f(t),t\}e^{-2r/\ell}\right)\mathrm{d}t\ , \end{aligned} \tag{4.6.5}$$

which clearly fits (4.5.6) with

$$\beta_{\rm ir} = \frac{\ell^2}{8}\{f(t),t\} \ , \qquad \{f(t),t\} = \left(\frac{f''}{f'}\right)' - \frac{1}{2}\left(\frac{f''}{f'}\right)^2 \ . \tag{4.6.6}$$

This makes explicit that $\beta_{\rm ir}$ is induced by a large diffeomorphism, and its value is the given by the Schwarzian derivative of $f(t)$. It is also instructive to revisit (4.5.17): Taking a derivative to remove c_0 from the first equation implies

$$\ell^2\lambda_{\rm ir}''' + 8\lambda_{\rm ir}\beta_{\rm ir}' + 16\beta_{\rm ir}\lambda_{\rm ir}' = 0 \ , \tag{4.6.7}$$

which via (4.6.6) becomes

$$\left(\frac{1}{f'}\left(\frac{(f'\lambda_{\rm ir})'}{f'}\right)'\right)' = 0 \ . \tag{4.6.8}$$

As expected from all other instances of nAdS_2 holography, the dynamics of the irrelevant deformation ignited by $\mathcal{Y}$ is related to the reparametrizations of boundary time.

The dynamics in (4.6.8) is elegantly encoded in $\hat{I}_{\rm ren}$, which can be seen as follows. From (4.5.17) can solve for c_0 substitute it in (4.6.9); this gives

$$\begin{aligned}
\hat{I}_{\rm ren} &= \frac{L\ell}{32G_3}\left(1+\frac{1}{\mu\ell}\right)\int {\rm d}t\, e^{\phi_0}\left(\frac{c_0}{\lambda_{\rm ir}} - \frac{\lambda_{\rm ir}'^2}{\lambda_{\rm ir}}\right) \\
&= \frac{L\ell}{32G_3}\left(1+\frac{1}{\mu\ell}\right)\int {\rm d}t\, e^{\phi_0}\left(\frac{16}{\ell^2}\lambda_{\rm ir}\beta_{\rm ir} + 2\lambda_{\rm ir}'' - 2\frac{\lambda_{\rm ir}'^2}{\lambda_{\rm ir}}\right) \\
&= \frac{L\ell}{16G_3}\left(1+\frac{1}{\mu\ell}\right)\int {\rm d}t\, e^{\phi_0}\left(\lambda_{\rm ir}\{f(t),t\} - \frac{\lambda_{\rm ir}'^2}{\lambda_{\rm ir}}\right) \ .
\end{aligned} \tag{4.6.9}$$

Recall that we have $\alpha_{\rm ir} = 1$, and we have also ignored $\nu_{\rm ir}$ since it is not important for this portion. In the second line we used (4.5.17), and in the last equality we ignored total derivatives and used (4.6.6). The variation of this last term with respect to $f(t)$ leads to (4.6.8): This is one of the renown features of nAdS_2 holography –the Schwarzian action captures the bulk dynamics of the irrelevant deformation [10].

Finally, it is useful to cast the coupling in (4.6.9) in terms of the CFT_2 central charges in Sec. 4.2.1; this gives

$$\frac{\ell}{16G_3}\left(1+\frac{1}{\mu\ell}\right) = \frac{c_L}{24} \ , \tag{4.6.10}$$

a clear indication that the left moving sector of the CFT$_2$ is controlling the nCFT$_1$.

4.6.2 Effective action: UV

In (4.4.19) we obtained the renormalised on-shell boundary action:

$$I_{\rm 2D}^{\rm UV} = -\frac{L}{8G_3}\ell\int {\rm d}t\,\left(\frac{\alpha}{\lambda}\left[m_0+2\frac{Q}{\mu\ell^2}\right]+\frac{\lambda'^2}{\alpha\lambda}+\frac{2\nu}{\ell}\left[Q+\frac{m_0}{2\mu}\right]\right)\,. \tag{4.6.11}$$

To make the Schwarzian action manifest in the UV we will take a slightly different route relative to the IR. In our derivations in the prior subsection we started by considering the set of diffeomorphisms (plus gauge transformations) that preserve the AdS$_2$ background; this allowed us to relate the irrelevant deformation $\lambda_{\rm ir}$ to the Schwarzian derivative. For the UV background in (4.4.6) we will instead inquire how the asymptotic background responds to Weyl transformations of the boundary fields, which is the strategy in [258].

A Weyl rescaling of the boundary parameters (4.4.6) corresponds to bulk diffeomorphisms that preserve the Fefferman-Graham gauge, i.e. a PBH transformation in the nomenclature of [258]. The response of the sources under this transformation is the expected one: We would have

$$\alpha\;\to\;\alpha\,e^{\sigma(t)}\;,\quad \lambda\;\to\;\lambda\,e^{\sigma(t)}\;,\quad \nu\;\to\;\nu\;, \tag{4.6.12}$$

where $\sigma(t)$ is an arbitrary function that rescales the boundary metric. In order to make explicit how to interpret this transformation as reparametrizations of the boundary time, we choose

$$\sigma(t)=\log\partial_t f(t)\;, \tag{4.6.13}$$

along the lines of the transformation in (4.6.3). For the choice $\alpha=\lambda=e^{\sigma(t)}=f'(t)$ the on-shell action, up to a total derivative, is

$$\begin{aligned} I_{\rm 2D}^{\rm UV} &= -\frac{L}{8G_3}\ell\int {\rm d}t\,\left(\frac{f''}{f'}\right)^2 \\ &= \frac{L}{4G_3}\ell\int {\rm d}t\,\{f(t),t\}\;. \end{aligned} \tag{4.6.14}$$

Here we ignored the terms proportional to Q and m_0 in (4.6.11), since they are unaffected by the Weyl rescaling. Therefore the manifestation of the Schwarzian derivative in this derivation comes as a responses of the system under Weyl transformations of the boundary metric. This is compatible with the CFT$_2$ interpretation of this term, where the coupling of (4.6.14) in terms of CFT$_2$ central charges

in Sec. 4.2.1 is

$$\frac{\ell}{4G_3} = \frac{c_L + c_R}{12} = \frac{c}{6} \ . \tag{4.6.15}$$

It is important to highlight that the overall coefficient of (4.6.14) is distinct from (4.6.9). This is already an indication that the origin of the Schwarzian term in the UV and IR is different. We will elaborate more on this point in the following.

4.6.3 Interpolation between UV and IR

Having done an independent analysis of the UV and IR backgrounds, we now proceed to compare them. In particular, we will illustrate how to obtain the deformed IR backgrounds as a decoupling limit of configurations in the UV.

To start let us consider static (time independent) configurations. In this case the UV backgrounds (4.4.4) and (4.4.3) become

$$\begin{aligned} e^{-2\phi} &= \lambda^2 e^{2r/\ell}\left(1 + \frac{\ell^2}{2\lambda^2} m_0 e^{-2r/\ell} + \frac{\ell^2}{16\lambda^4}\left(\ell^2 m_0^2 - 4Q^2\right) e^{-4r/\ell}\right) \ , \\ \sqrt{-\gamma} &= \alpha\lambda\left(e^{2r/\ell} - \frac{\ell^2}{16\lambda^4}\left(\ell^2 m_0^2 - 4Q^2\right) e^{-2r/\ell}\right) e^{\phi} \ , \\ A_t &= \frac{\ell\,\alpha}{\lambda}\, Q\, e^{2\phi} + \nu \ . \end{aligned} \tag{4.6.16}$$

To obtain the deformed AdS_2 background as a limit of this background, we redefine

$$\ell^2 m_0^2 = 4Q^2 + \epsilon^2 \ , \qquad e^{2r/\ell} \to \frac{\epsilon}{4}\, e^{2r/\ell} \ , \qquad t \to \frac{4}{\epsilon}\, t \ , \tag{4.6.17}$$

and take the limit $\epsilon \to 0$ while holding Q, λ and α fixed. The resulting background is the IR solution in Sec. 4.5.1, where we identify

$$\alpha_{\rm ir} = e^{\phi_0}\alpha\lambda \ , \qquad \lambda_{\rm ir} = \frac{\epsilon}{4}\,\lambda^2 \ , \qquad \nu_{\rm ir} = \frac{4}{\epsilon}\left(\nu - \frac{\alpha}{\lambda}\right) \ . \tag{4.6.18}$$

where $\ell|Q| = e^{-2\phi_0}$. If we restore time dependence in the UV background, the limit is still given by (4.6.17), and the relation between IR and UV quantities is unchanged. It is instructive to rewrite the relation for ν; we have

$$\nu = \frac{\epsilon}{4}\left(\nu_{\rm ir} + \frac{\alpha_{\rm ir}}{\lambda_{\rm ir}} e^{-\phi_0}\right) \ . \tag{4.6.19}$$

This relation indicates that gauge transformations in the UV affect time reparametrizations in the IR. The effect is that the gauge anomaly in the UV contributes to the conformal anomaly in the IR. In particular, for the dimensionally reduced 3D stress tensor in (4.4.28), replacing (4.6.17)-(4.6.18) in the renormalised action (4.4.31)

the Schwarzian effective action in (4.6.9). This illustrates that the conformal piece contained in (4.6.14) is modified as we flow to the IR.

4.6.4 Entropy of 2D black holes

In this last portion we will discuss the ties of the Wald entropy of 2D black holes, and its relation to the Schwarzian action. Comparisons with the entropy of BTZ follow as well.

For our purposes, a 2D black hole is a static solution with a zero in the metric component γ_{tt}. Let us start with the UV configurations, where all functions appearing in (4.4.2)-(4.4.5) will be considered to be constant, i.e., the solution in (4.6.16). The existence of a horizon in (4.6.16) requires $\ell|m_0| \geq 2|Q|$, and its location is

$$\gamma_{tt}(r = r_h) = 0 \quad \Rightarrow \quad e^{4r_h/\ell} = \frac{\ell^2}{16\lambda^4}(\ell^2 m_0^2 - 4Q^2) \ . \tag{4.6.20}$$

The temperature we will assign to the black hole is

$$T_{2D}^{\rm UV} = \partial_r \sqrt{-\gamma}|_{r_h} = \frac{4}{\ell}\alpha\lambda\, e^{2r_h/\ell}\, e^{\phi_h} \ , \tag{4.6.21}$$

where the value of the dilaton at the horizon is given by

$$e^{-2\phi_h} \equiv e^{-2\phi(r=r_h)} = \frac{\ell}{2}\left(\ell m_0 + \sqrt{\ell^2 m_0^2 - 4Q^2}\right) \ . \tag{4.6.22}$$

The Wald entropy $S_{\rm Wald}$, which for the 2D action (4.3.2) was derived in [42], in our notation takes the form

$$S_{\rm Wald} = \frac{\pi L}{2G_3}\left(e^{-\phi_h} + \frac{Q}{\mu}\, e^{\phi_h}\right) \ . \tag{4.6.23}$$

Note that by substituting (6.0.106) in (4.6.22) and (4.6.23) reproduces the entropy of the BTZ black hole in (4.2.18).

For the IR background, the logic is very similar, the values are just different. We will consider backgrounds (4.5.6)-(4.5.18) where all functions are constant. A black hole in this case requires $\beta_{\rm ir} < 0$; the location of the horizon is at

$$e^{4r_h/\ell} = -\beta_{\rm ir} \ , \tag{4.6.24}$$

which is the zero of γ_{tt} in (4.5.6) for static configurations. Note that we are

adopting $\alpha_{\rm ir} = 1$ to more easily compare with Sec. 4.6.1. The temperature is

$$T_{\rm 2D}^{\rm IR} = \partial_r \sqrt{-\gamma_0}|_{r_h} = \frac{4}{\ell}\sqrt{|\beta_{\rm ir}|}\ , \tag{4.6.25}$$

From (4.6.23), the entropy for this background is

$$S_{\rm Wald} = \frac{\pi L}{2G_3}\left(e^{-\phi_0}\left(1-\frac{1}{\mu\ell}\right)+\frac{1}{2}\,\mathcal{Y}_h\,e^{\phi_0}\left(1+\frac{1}{\mu\ell}\right)\right)+O(\mathcal{Y}_h^2)\ , \tag{4.6.26}$$

where we used (4.5.8) and only kept the first correction due to the irrelevant deformation. The value of $\mathcal{Y}$ at the horizon is

$$\mathcal{Y}_h = 2\lambda_{\rm ir}\sqrt{|\beta_{\rm ir}|} = \frac{\ell}{2}\lambda_{\rm ir} T_{\rm 2D}^{\rm IR}\ , \tag{4.6.27}$$

and so we can write

$$S_{\rm Wald} = \frac{\pi L}{2G_3}\left(e^{-\phi_0}\left(1-\frac{1}{\mu\ell}\right)+\frac{\ell}{4}\lambda_{\rm ir}\,e^{\phi_0}\left(1+\frac{1}{\mu\ell}\right)T_{\rm 2D}^{\rm IR}\right)+\dots\ , \tag{4.6.28}$$

where the dots indicate that this is an expansion around small values of $T_{\rm 2D}^{\rm IR}$. From here it is clear that the linear response in the temperature is captured by the IR effective action (4.6.9). In contrast the UV action (4.6.14), while it also contains a Schwarzian derivative, does not capture the corrections to the entropy away from extremality. And finally, using the relations in (6.0.113)-(6.0.114), we find perfect agreement with the near-extremal entropy of BTZ given by (4.2.24). This is all to reinforce that the Schwarzian effective action appearing in nAdS_2 holography of the BTZ should be interpreted as follows: It is the response of the left-moving sector of the CFT_2 as one deviates away from the zero temperature configuration [305–309].

5 Discussion

We can now summarise and discuss some future directions and more speculative remarks.

5.1 Toward a microscopic description of de Sitter space using matrix models

In chapter 2 we set up the various techniques to address matrix models and two-dimensional quantum gravity. We explained the conjectured duality along the particular cases of Hermitian matrix integrals and Hermitian matrix quantum mechanics. Former being conjecturally dual to Liouville theory coupled to the series $\mathcal{M}_{2,2m-1}$, $m \geq 2$ of minimal models, whereas the latter in the large N limit is conjectured to be dual to Liouville theory coupled to a timelike free boson. In chapter 3 we addressed a particular matrix integral known as multicritical matrix integrals. Multicritical matrix integrals are Hermitian matrix integrals with $(m-1)$, $m \geq 3$ real couplings. Upon tuning them to the multicritical point and taking the large N limit we recover Liouville theory coupled to $\mathcal{M}_{2,2m-1}$, $m \geq 3$. We explain this conjectured duality providing a one to one map between the couplings of the matrix integral and the primaries of the minimal model.

Genus one. In chapter 2 and 3 we have been discussing the relation between Hermitian matrix integrals and two-dimensional quantum gravity coupled to the non-unitary minimal model $\mathcal{M}_{2,2m-1}$. Our analysis thereby relied on the study of non-analytic behaviour of matrix integrals on the one hand and the structure of the partition function of two-dimensional quantum gravity coupled to one of the primary operators of $\mathcal{M}_{2,2m-1}$ on the other side. The natural question at hand is whether there are other observables which might give further evidence of the conjectured duality. As mentioned in the introduction to 3 one such approach uses correlation numbers. A different approach might be to understand the pre-factor of the non-analyticities in $\mathcal{F}_N^{(0)}(\boldsymbol{\alpha})$ (3.5.19). To overcome the redundancy in our

choice of deformation one further needs to build an ϵ independent quantity. One such expression could be the ratio of the free energy at genus zero and genus one. Using the technique of orthogonal polynomials in work in progress we obtained

$$\mathcal{F}_N^{(1)}(\boldsymbol{\alpha}) \sim \frac{2m-2}{24m}\frac{m}{1+r}\log\epsilon\ , \quad r=1,\dots,(m-1)\ . \tag{5.1.1}$$

As further mentioned at the end of 3 of particular importance is the identity operator, corresponding to the most fine tuned path in the matrix picture or equivalently $r=(m-1)$ in (5.1.1). Restricting to the identity operator for both genus zero as well as genus one a natural, ϵ independent, pure number can then be expressed as the ratio

$$\frac{\mathcal{F}_N^{(0)}(\boldsymbol{\alpha})}{\partial_\epsilon \mathcal{F}_N^{(1)}(\boldsymbol{\alpha})}\ . \tag{5.1.2}$$

Understanding this number from a matrix perspective and matching it to the continuum picture would lead to remarkable new evidence. A limit in which this number might reveal some structure and most importantly allow a connection to de Sitter space is the large m limit.

Large m limit. Following [20] we couple the identity operator of the minimal model to the Euclidean path integral on the topology of S^2 and fix the area

$$Z[\Lambda,\upsilon] = \int \frac{[D\varphi]}{\mathrm{vol}\,\mathrm{PSL}(2,\mathbb{C})}[D\Phi]\,[D\mathfrak{bc}]\,e^{-S_L[\varphi,\Lambda=0]-S_{\mathrm{CFT}}[\Phi]-S_{\mathrm{gh}}[\mathfrak{b},\mathfrak{c}]-\Lambda\int \mathrm{d}^2x\sqrt{\tilde{g}}\,e^{2b\varphi}} \times \delta\left(\int \mathrm{d}^2x\sqrt{\tilde{g}}\,e^{2b\varphi}-4\pi\upsilon\right)\ , \tag{5.1.3}$$

where υ is the area of the two-sphere and

$$S_L[\varphi,\Lambda] = \frac{1}{4\pi}\int \mathrm{d}x^2\sqrt{\tilde{g}}\left(\partial_\mu\varphi\partial^\nu\varphi + Q\varphi R + 4\pi\Lambda\, e^{2b\varphi}\right)\ , \tag{5.1.4}$$

is the Liouville action. Finally the fiducial metric is fixed to be the Fubini-Study metric

$$d\tilde{s}^2 = \tilde{g}_{z,\bar{z}}\mathrm{d}z\mathrm{d}\bar{z} = \upsilon\frac{4}{(1+z\bar{z})^2}\mathrm{d}z\mathrm{d}\bar{z}\ . \tag{5.1.5}$$

The large m limit is now equivalent to the limit of large negative central charge c_m or equivalently large positive Q. Whereas the υ and Λ dependency of this object has been studied in the literature the perturbative expansion of the above expression for large Q has not been discussed so far. The strategy is now threefold. i) Rewriting the delta function in its integral representation the partition function (5.1.3) can be expressed as

$$Z[\Lambda,\upsilon] = Z_{\rm CFT}[\Phi,\upsilon]\, Z_{\rm gh}[\mathfrak{b},\mathfrak{c},\upsilon]\upsilon^{-1}e^{-4\pi\upsilon\Lambda} \times \int_{\mathbb{R}}\frac{\mathrm{d}\alpha}{2\pi}\int\frac{[D\varphi]}{\mathrm{vol}\,\mathrm{PSL}(2,\mathbb{C})}\, e^{-\frac{\upsilon}{4\pi}\int \mathrm{d}\Omega\left(-\varphi\Delta\varphi+\frac{2}{\upsilon}Q\varphi\right)} \times e^{i\alpha\int\mathrm{d}\Omega\,(2b\varphi+\ldots)}\ , \quad (5.1.6)$$

where we furthermore evaluated the ghost and matter partition function on the round two-sphere of area υ. At the large Q saddle we find $\varphi_* = 0$ and $\alpha_* = -iQ/(4\pi b)$ and consequently the geometry and not only the topology of S^2. It now behooves to add fluctuations to both φ_* and α_* and to explore the large Q perturbative expansion of (5.1.6).

ii) Also primaries close to the identity primary allow a large m saddle point. It would be interesting to explore this saddle point in more detail in particular since in these cases the matter CFT and gravity theory no longer are independent of each other but interact and would therefore need a more refined treatment.

iii) Whereas in (5.1.3) we fix the topology to the round two-sphere also a genus zero surface should be sensitive to a large m saddle point solution. Understanding the saddle point expression on a torus would lead to the final ingredient to explore (5.1.2) from a continuum perspective.

Timelike Liouville. Timelike Liouville theory [148] switches the sign of the kinetic term

$$S_{tL}[\tilde{g},\varphi] = \frac{1}{4\pi}\int \mathrm{d}^2x\sqrt{\tilde{g}}\left(-\tilde{g}^{ij}\partial_i\varphi\partial_j\varphi - qR[\tilde{g}]\varphi + 4\pi\Lambda e^{2\beta\varphi}\right)\ , \quad (5.1.7)$$

where $\tilde{g}$ is the fiducial metric and Λ denotes the cosmological constant. The spinless primary operators of timelike Liouville $\mathcal{V}_\beta \equiv e^{2\beta\varphi}$ have conformal dimension

$$\Delta_\beta = \beta(q+\beta)\ . \quad (5.1.8)$$

Since to guarantee conformal invariance we need $(\Delta_\beta, \bar{\Delta}_\beta) = (1,1)$ this implies

$$q = \beta^{-1} - \beta\ . \quad (5.1.9)$$

Whereas spacelike Liouville (5.1.4) only allows for a semiclassical saddle upon restricting to a fixed area picture, timelike Liouville allows for a semiclassical S^2 saddle for large and positive c_m. The drawback of timelike Liouville theory of course is that no microscopic picture is known, it is completely unclear whether there exists a matrix model dual to this theory. Still it would be interesting to explore and compare the perturbative expansions around the semiclassical saddle in spacelike and timelike Liouville theory.

Lian-Zuckerman operators and non-unitary. The appearance of non-trivial

$\mathfrak{bc}$-ghost operators in the continuum theory remains underexplored from a matrix integral perspective. As the examples in chapter 2 show these operators are already present in the $\mathcal{M}_{3,2}$ model. This theory is conjecturally dual to the quartic matrix integral with only a single coupling. Both in chapter 2 and 3 we however seemed to have revealed all the non-analyticties this matrix integral has. Additionally since we only have one coupling we can only move along the real line and it remains an open question how to identify Lian-Zuckerman operators from a matrix perspective. One approach might be to complexify the couplings.

Since Lian-Zuckerman operators are build out of descendants of $\mathcal{M}_{2,2m-1}$ they could have negative norm. It would be interesting to understand the effect of this possible non-unitarity from both a continuum and a matrix integral perspective.

Fermionic matrix models. A different matrix model are fermionic quantum mechanical matrices (FMM). Instead of bosonic valued entries the entries of these matrix models are Grassmann valued [203]. For bosonic matrix models, the S-matrix introduced by Moore–Plesser–Ramgoolam is a natural observable which connects them — via the DOZZ formula — to c = 1 non-critical string theory. A similar observable for FMM is not known. Consequently, the gravity dual of FMM remains undiscovered. However, due to their fermionic structure FMM have a finite-dimensional Hilbert space. This finite-dimensional Hilbert space might also be realised in the worldsheet dual and FMM would therefore be another candidate theory to study de Sitter space.

5.2 Matrix integrals & black holes

The matrix integrals studied in chapter 3 of this paper naturally connect the two dualities studied in this thesis. The goal of this section is to explain this connection and propose some future directions.

Disk topology. In [33,186,188] Liouville theory was studied on the disk topology. Upon taking the semiclassical limit $b \to 0$ the Liouville action admits a saddle point solution for φ. From the perspective of the physical metric $g_{ij} = e^{2b\varphi}\tilde{g}_{ij}$ this can be interpreted as the hyperbolic metric on the Poincaré disk (the Euclidean AdS_2 black hole)

$$\mathrm{d}s^2 = \frac{1}{\pi b^2 \Lambda} \frac{1}{(1-\rho^2)^2} \left(\mathrm{d}\rho^2 + \rho^2 \mathrm{d}\theta^2\right) \ , \quad \rho \in [0,1) \ . \tag{5.2.1}$$

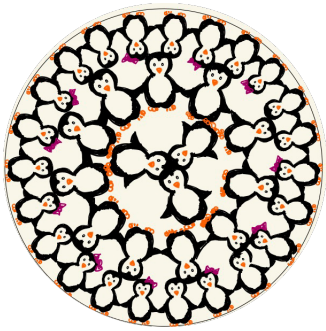

Figure 5.1: *Instead of studying Liouville theory on a sphere topology we can also study Liouville theory on a disk. The semiclassical saddle point is the hyperbolic metric.*

Since coupling $\mathcal{M}_{2m-1,2}$ to gravity implies $b = \sqrt{2/(2m-1)}$ (3.6.12) this semi-classical limit corresponds to a large m limit. It would be interesting to explore relations between this saddle and recent discussions on JT gravity and matrix integrals [149].

For Dirichlet boundary conditions φ diverges at the boundary of the disk and the relation to matrix integrals was studied in [189]. It would be interesting to generalise this to the multicritical case. For Neumann boundary conditions one needs to further add the boundary term

$$S_{\text{bdy}} = \int_{S^1} \mathrm{d}u\sqrt{h}\left(\frac{Q}{2\pi}K\varphi + \Lambda_B e^{b\varphi}\right) \ , \tag{5.2.2}$$

to the bulk action, where h is the induced metric on S^1 and K is the extrinsic curvature at the boundary. The comparison to the matrix integral uses either the resolvent $\mathrm{R}(z)$ or the loop operator W_ℓ [83]. The boundary cosmological constant Λ_B is connected to z. For multicritical matrix integrals $\mathrm{R}(z)$ is given by (3.2.15), W_ℓ is given by (3.2.16).

Double scaling limit in multicritical matrix integrals. In recent discussions on JT gravity the multicritical matrix integrals are considered in a full genus double scaling limit. This double scaling limit is captured by the string equation which, as we have seen in chapter 2, in case of multicritical matrix integrals can be expressed in terms of the Gelfand-Dikkii polynomials. In [149, 156] the double scaling limit has been taken along the generic path discussed in chapter 3. This path corresponds to turning on the minimal operator of $\mathcal{M}_{2,2m-1}$. It would be interesting to understand the effect of choosing a path leading to any of the other primaries of the minimal model.

5.3 Black holes & near-CFT$_1$

In chapter 4 we discussed the BTZ black hole embedded in TMG. This allowed us to discuss and contrast from a gravity perspective the role of the left and right moving central charge of the CFT$_2$ within the near-AdS$_2$/near-CFT$_1$ correspondence. In particular we observed that the near-CFT$_1$ resides in the left moving sector of the CFT$_2$.

near-CFT$_1$ $\subset$ CFT$_2$. It would be interesting to explore the role of the right moving central charge as well as to infer this behaviour from a CFT perspective. Maybe a possible approach to this could use the $c-$theorem [155].

Warped solutions. While all locally AdS$_3$ configurations are solutions of TMG, we can also find a different subset of solutions, known as warped solutions [272]. Warped solutions break the SL$(2,\mathbb{R})_L\times$ SL$(2,\mathbb{R})_R$ isometry group of AdS$_3$ down to SL$(2,\mathbb{R})_L$ $\times$ U(1) and appear in the near-horizon limit of a variety of black holes, including also the Kerr-black hole and hence these solutions bear relations to black holes observed in our own universe. It would be interesting to apply insights obtained from the nAdS$_2$/nCFT$_1$ duality to understand properties of warped solutions.

6 Appendices

R_n staircase

In this appendix we discuss a method to relate the R_n coefficients for the orthogonal polynomial problem to the h_n coefficients. Explicitly we demonstrate how to obtain the integral on the right hand side of (2.4.11) in a graphical way.

Obtaining all possible R_n leading to an expression proportional to h_n as outlined for the quartic potential in 2.4.2 can be tedious. For the case of an even degree polynomial there exists a graphical way of computing the R_n. Starting with a potential of degree $2p+2$ we have to combine powers of λ of degree less or equal to $2p+1$ with polynomials P_n and P_{n-1} in all possible ways to get two degree n polynomials. As a first step one identifies a certain level as the level $n-1$ (corresponding to the degree of P_{n-1}). Now we can perform exactly $p+1$ steps in an appropriate unit upwards – conveniently chosen along 45 degrees – followed by p steps downwards in a right angle with respect to the highest point. The final level corresponds to level n. Going downwards mimics the three term recurrence relation and for each step downwards from a level n to a level $n-1$ we get a factor R_n. In total there are $\binom{2p+1}{p}$ different possibilities to start at level $n-1$ and end up at level n. Each combination is a product of p R_n.

Non-planar contributions

In this appendix we will outline the calculations leading to non-planar contributions of the free energy.

More concretely we will calculate $\mathcal{F}^{(h)}(\alpha)$ (2.3.70) for $h = 2$, 3, and 4. Solving (2.4.20) for $s = 2, 3$, and $s = 4$ we find

$$r_4(x,\alpha) \quad = \quad \frac{\alpha^4 r_0(x,\alpha)\left(p_1(\alpha x) + \alpha r_0(x,\alpha)\right)}{(1+48\alpha x)^5}\,, \tag{6.0.1}$$

$$r_6(x,\alpha) = \frac{\alpha^6 r_0(x,\alpha)\left(p_1(\alpha x)+\alpha p_1(\alpha x) r_0(x,\alpha)\right)}{(1+48\alpha x)^{15/2}}\,, \tag{6.0.2}$$

$$r_8(x,\alpha) = \frac{\alpha^8 r_0(x,\alpha)\left(p_2(\alpha x)+\alpha p_1(\alpha x) r_0(x,\alpha)\right)}{(1+48\alpha x)^{10}}\,, \tag{6.0.3}$$

where $p_n(\alpha x)$ is a polynomial of degree n in αx. Introducing $\mathcal{R}_n(x,\alpha) \equiv r_n(\alpha,x)/r_0(x,\alpha)$ we find for $h=2$ and $h=3$

$$\mathcal{F}^{(2)}(\alpha) = -\int_0^1 \mathrm{d}x(1-x)\left[\mathcal{R}_4(x,\alpha)-\frac{1}{2}\mathcal{R}_2(x,\alpha)^2\right] - \frac{1}{12}\Big((1-x)\mathcal{R}_2(x,\alpha)\Big)^{(1)}\Big|_0^1 \tag{6.0.4}$$

$$+\frac{1}{720}\left((1-x)\log\frac{r_0(x,\alpha)}{x}\right)^{(3)}\Big|_0^1 + 1584\alpha^3$$

$$= \frac{\alpha\left(84\alpha+\left(3936\alpha^2-96\alpha-1\right)r_0(1,\alpha)+1\right)}{20(48\alpha+1)^{5/2}}$$

and

$$\mathcal{F}^{(3)}(\alpha) = -\int_0^1 (1-x)\left[\frac{1}{3}\mathcal{R}_2(x,\alpha)^3 - \mathcal{R}_2(x,\alpha)\mathcal{R}_4(x,\alpha)+\mathcal{R}_6(x,\alpha)\right] \tag{6.0.5}$$

$$-\frac{1}{12}\left((1-x)\left(\mathcal{R}_4(x,\alpha)-\frac{1}{2}\mathcal{R}_2(x,\alpha)^2\right)\right)^{(1)}\Big|_0^1 + \frac{1}{720}\Big((1-x)\mathcal{R}_2(x,\alpha)\Big)^{(3)}\Big|_0^1$$

$$-\frac{1}{30240}\left((1-x)\log\frac{r_0(x,\alpha)}{x}\right)^{(5)}\Big|_0^1 + \frac{25671168}{5}\alpha^5$$

$$= \frac{\alpha\, r_0(1,\alpha)\left(-954408960\alpha^5-61871616\alpha^4+1105920\alpha^3+23040\alpha^2+240\alpha+1\right)}{84(48\alpha+1)^{11/2}}$$

$$+\frac{\alpha\left(110932992\alpha^4-889920\alpha^3-20448\alpha^2-228\alpha-1\right)}{84(48\alpha+1)^{11/2}}\,.$$

$\mathcal{F}^{(4)}(\alpha)$ follows similarly. Near $\alpha_c = -1/48$ we therefore obtain $h=2$, 3, and 4 the following non-analytic behaviour

$$\lim_{\alpha\to\alpha_c} \mathcal{F}^{(h)}_{\text{n.a.}}(\alpha) = f_h(\alpha-\alpha_c)^{5\chi_h/4}\,, \qquad h\in\mathbb{N}\,, \tag{6.0.6}$$

providing further evidence for (2.3.78). The coefficients are given by

$$f_2 = -\frac{7}{13271040\sqrt{3}}\,, \qquad f_3 = -\frac{245}{10567230160896}\,, \qquad f_4 = -\frac{259553}{9953280}\,. \tag{6.0.7}$$

Additionally we have the small α expansion:

$$\begin{aligned}
\mathcal{F}^{(2)}(\alpha) &= 240\,\alpha^3 - 32112\,\alpha^4 + \frac{14501376}{5}\,\alpha^5 - 220174848\,\alpha^6 + 15138938880\,\alpha^7 + \mathcal{O}(\alpha^8)\ , \\
\mathcal{F}^{(3)}(\alpha) &= 483840\,\alpha^5 - 128130048\,\alpha^6 + \frac{139272044544}{7}\,\alpha^7 - 2366845194240\,\alpha^8 + \mathcal{O}(\alpha^9)\ , \\
\mathcal{F}^{(4)}(\alpha) &= 2767564800\,\alpha^7 + 257831155924992\,\alpha^9 - 1137924495360\,\alpha^8 + \mathcal{O}(\alpha^9)\ .
\end{aligned} \tag{6.0.8}$$

Wick contractions

In this appendix we provide a simple example for the type of Wick contractions used to get various results. We are interested in the following

$$\begin{aligned}
\langle \text{Fermi}|T_B\,\hat{n}(t_1,x_1)\hat{n}(t_2,x_2)|\text{Fermi}\rangle &= \Theta(t_1-t_2)\langle \text{Fermi}|\hat{n}(t_1,x_1)\hat{n}(t_2,x_2)|\,\text{Fermi}\rangle \\
&\quad + \Theta(t_2-t_1)\langle \text{Fermi}|\hat{n}(t_2,x_2)\hat{n}(t_1,x_1)|\text{Fermi}\rangle\ .
\end{aligned} \tag{6.0.9}$$

Using (2.6.27) and the number density operator (2.6.28) this can be expressed in Fourier space as

$$\begin{aligned}
&\langle \text{Fermi}|T_B\,\hat{n}(t_1,x_1)\hat{n}(t_2,x_2)|\text{Fermi}\rangle \\
&= \Big(\Theta(t_1-t_2)\int_{\mathbb{R}^4}\frac{\mathrm{d}\nu_1\mathrm{d}\nu_2\mathrm{d}\nu_3\mathrm{d}\nu_4}{(2\pi)^4}\,e^{i\nu_1 t_1 - i\nu_2 t_1 + i\nu_3 t_2 - i\nu_4 t_2}\psi_{\nu_1}(x_1)\psi^*_{\nu_2}(x_1)\psi_{\nu_3}(x_2)\psi^*_{\nu_4}(x_2) \\
&+ \Theta(t_2-t_1)\int_{\mathbb{R}^4}\frac{\mathrm{d}\nu_1\mathrm{d}\nu_2\mathrm{d}\nu_3\mathrm{d}\nu_4}{(2\pi)^4}\,e^{i\nu_1 t_2 - i\nu_2 t_2 + i\nu_3 t_1 - i\nu_4 t_1}\psi_{\nu_1}(x_2)\psi^*_{\nu_2}(x_2)\psi_{\nu_3}(x_1)\psi^*_{\nu_4}(x_1)\Big) \\
&\times \langle \text{Fermi}|a^\dagger_{\nu_1}a_{\nu_2}a^\dagger_{\nu_3}a_{\nu_4}|\text{Fermi}\rangle
\end{aligned} \tag{6.0.10}$$

where for notational convenience we suppress the parity index. When anti-commuting these operators we will use (2.6.25) and (2.6.26). We then obtain

$$\begin{aligned}
\langle \text{Fermi}|a^\dagger_{\nu_1}a_{\nu_2}a^\dagger_{\nu_3}a_{\nu_4}|\text{Fermi}\rangle &= (2\pi)^2\delta_{\nu_1\nu_2}\delta_{\nu_3\nu_4}\Theta(\nu_F-\nu_4)\Theta(\nu_F-\nu_2) \\
&\quad + (2\pi)^2\delta_{\nu_1\nu_4}\delta_{\nu_3\nu_2}\Theta(\nu_F-\nu_4)\Theta(\nu_3-\nu_F)\ ,
\end{aligned} \tag{6.0.11}$$

where we normalised the ground state such that $\langle \text{Fermi}|\text{Fermi}\rangle = 1$. The first term on the right hand side of the above expression corresponds to the contraction of $\Psi^\dagger(t_i,x_i)$ with $\Psi(t_i,x_i)$ and therefore does not contribute to the connected correlation function $\mathcal{Q}_c(\{t_i,x_i\})$. Dropping this term and combining (6.0.10) with (6.0.11) we obtain for the connected correlation function

$$\langle \text{Fermi}|T_B\,\hat{n}(t_1,x_1)\hat{n}(t_2,x_2)|\text{Fermi}\rangle_c =$$

$$\Theta(t_1-t_2)\int_{\nu_F}^{\infty}\frac{\mathrm{d}\nu}{2\pi}\,e^{-i\nu(t_1-t_2)}\psi^*_\nu(x_1)\psi_\nu(x_2)\int_{-\infty}^{\nu_F}\frac{\mathrm{d}\upsilon}{2\pi}\,e^{-i\upsilon(t_2-t_1)}\psi^*_\upsilon(x_2)\psi_\upsilon(x_1)$$
$$+\,\Theta(t_2-t_1)\int_{\nu_F}^{\infty}\frac{\mathrm{d}\nu}{2\pi}\,e^{-i\nu(t_2-t_1)}\psi^*_\nu(x_2)\psi_\nu(x_1)\int_{-\infty}^{\nu_F}\frac{\mathrm{d}\upsilon}{2\pi}\,e^{-i\upsilon(t_1-t_2)}\psi^*_\upsilon(x_1)\psi_\upsilon(x_2)$$
$$=S_F(t_1,x_1;t_2,x_2)S_F(t_2,x_2;t_1,x_1)\ , \quad (6.0.12)$$

where in the last line we used the definition of the Feynman propagator in (2.6.32).

Perturbative expansion of the reflection coefficient

To evaluate the S-matrix in section 2.7 we need the perturbative expansion of the reflection coefficient (2.7.5). More concretely we need the perturbative expansion of the combination $R_{\nu_F+a}R^*_{\nu_F+b}$. For the one-to-n scattering the parameters a and b are fixed by demanding one incoming and $n\geq 1$ outgoing waves. To obtain the perturbative expansion of the scattering amplitudes we will quotient out the phase $e^{-i(a-b)\log(-\nu_F)}$ in the expansion of $R_{\nu_F+a}R^*_{\nu_F+b}$. In other words we will evaluate the S-matrix elements using the expansion below on the right:

$$e^{i(a-b)\log(-\nu_F)}\,R_{\nu_F+a}R^*_{\nu_F+b}=1-\frac{i}{2\nu_F}(a^2-b^2)$$
$$-\frac{1}{24\nu_F^2}\left(3(a^2-b^2)^2-i(a(1+4a^2)-b(1+4b^2))\right)+\mathcal{O}\left(\nu_F^{-3}\right)\ , \quad (6.0.13)$$

with a and b fixed appropriately. We note that (6.0.13) can be expressed as follows

$$e^{i(a-b)\log(-\nu_F)}\,R_{\nu_F+a}R^*_{\nu_F+b}=1+\frac{i}{2\nu_F}\left(B_2(1/2-ia)-B_2(1/2+ib)\right)$$
$$+\frac{1}{6\nu_F^2}\left(\left(B_3(1/2-ia)+B_3(1/2+ib)\right)-\frac{3}{4}\left(B_2(1/2-ia)-B_2(1/2+ib)\right)^2\right)+\mathcal{O}\left(\nu_F^{-3}\right)\ , \quad (6.0.14)$$

where $B_k(x)$ are the Bernoulli polynomials and we used the expansion of the Gamma function in terms of the reflection coefficient which implies

$$R_{\nu_F+a}\,e^{i\nu_F(-1+\log(-\nu_F))}=e^{\sum_{n\geq 1}\frac{(-i)^{n+2}}{n(n+1)}\frac{B_{n+1}(1/2-ia)}{\nu_F^n}}\ . \quad (6.0.15)$$

We note that in (6.0.14) the power n of $1/\nu_F$ a particular Bernoulli polynomial is multiplied with is related to its degree by $\deg(B_k(x))\geq n$. Since now the k^{th}

Bernoulli polynomial is a polynomial of degree k we can use

$$\sum_{\Omega\in\{\omega_1,..,\omega_{n-1}\}} (-1)^{|\Omega|}\omega(\Omega)^k = 0 \ , \quad k < n-1 \ , \tag{6.0.16}$$

which in combination with (6.0.14) implies the leading order power of ν_F in the perturbative expansion of the S-matrix.

Further examples of scattering amplitudes

In this appendix we give some additional examples of scattering amplitudes.

One-to-four scattering. To obtain the one-to-four amplitude we start with

$$\mathcal{Q}\left(\{t_i,x_i\}\right) = \langle \text{Fermi}|\, T_B\, \hat{n}(t_1,x_1)\hat{n}(t_2,x_2)\hat{n}(t_3,x_3)\hat{n}(t_4,x_4)\hat{n}(t_5,x_5)\,|\text{Fermi}\rangle \ . \tag{6.0.17}$$

After performing Wick contractions we go to Fourier space and extract the scattering amplitude defined in (2.7.16) as in the previous examples. This leads to

$$S(\omega_1,\omega_2,\omega_3,\omega_4\,|\,\omega_5) \equiv e^{-i\omega_5\log(-\nu_F)} \sum_{\Omega\subseteq\{\omega_1,..,\,\omega_4\}} (-1)^{|\Omega|+1} \int_0^{\omega(\Omega)} \mathrm{d}\upsilon\, R^*_{\nu_F-\upsilon} R_{\nu_F-\upsilon-\omega_5} \ , \tag{6.0.18}$$

where the sum ranges over all subsets Ω of $\{\omega_1,..,\omega_4\}$, $|\Omega|$ is the number of elements in Ω, and $\omega(\Omega) = \sum_{\omega\in\Omega}\omega$. We note again that the additional minus sign arises because of the initial definition in (2.7.16). Inserting the expressions of the reflection coefficient (2.7.5) and its perturbative expansion (6.0.13) we obtain

$$\begin{aligned} S(\omega_1,\omega_2,\omega_3,\omega_4\,|\,\omega_5) = &-\frac{i}{\nu_F^3}\,\omega_1\omega_2\omega_3\omega_4\omega_5(\omega_5+i)(\omega_5+2i) + \frac{i}{24\nu_F^5}\,\omega_1\omega_2\omega_3\omega_4\omega_5 \\ &\times(\omega_5+i)(\omega_5+2i)(\omega_5+3i)(\omega_5+4i)\Big(\omega_1\,(\omega_1-i)+\omega_2\,(\omega_2-i) \\ &+\omega_3\,(\omega_3-i)+\omega_4\,(\omega_4-i)+1\Big) + \mathcal{O}\left(\nu_F^{-7}\right) \ . \end{aligned} \tag{6.0.19}$$

One-to-five scattering. To obtain the one-to-five amplitude we start with

$$\mathcal{Q}\left(\{t_i,x_i\}\right) = \langle \text{Fermi}|\, T\, \hat{n}(t_1,x_1)\hat{n}(t_2,x_2)\hat{n}(t_3,x_3)\hat{n}(t_4,x_4)\hat{n}(t_5,x_5)\hat{n}(t_6,x_6)\,|\text{Fermi}\rangle \ . \tag{6.0.20}$$

After performing Wick contractions we go to Fourier space and extract the scattering amplitude defined in (2.7.16) along the lines explained in the last examples.

This leads to

$$S(\omega_1,\omega_2,\omega_3,\omega_4,\omega_5\,|\,\omega_6) \equiv e^{-i\omega_6\log(-\nu_F)} \sum_{\Omega\subseteq\{\omega_1,..,\omega_5\}} (-1)^{|\Omega|+1} \int_0^{\omega(\Omega)} \mathrm{d}\upsilon\, R^*_{\nu_F-\upsilon} R_{\nu_F-\upsilon-\omega_6} \ . \tag{6.0.21}$$

Inserting the expressions of the reflection coefficient we obtain

$$\begin{aligned} S(\omega_1,\omega_2,\omega_3,\omega_4,\omega_5\,|\,\omega_6) &= \frac{1}{\nu_F^4}\,\omega_1\omega_2\omega_3\omega_4\omega_5\omega_6(\omega_6+i)(\omega_6+2i)(\omega_6+3i) \\ &- \frac{1}{24\nu_F^6}\,\omega_1\omega_2\omega_3\omega_4\omega_5\omega_6(\omega_6+i)(\omega_6+2i)(\omega_6+3i)(\omega_6+4i)(\omega_6+5i) \\ &\times \big(\omega_1\,(\omega_1-i)+\omega_2\,(\omega_2-i)+\omega_3\,(\omega_3-i)+\omega_4\,(\omega_4-i) \\ &\qquad +\omega_5\,(\omega_5-i)+1\big)+\mathcal{O}\left(\nu_F^{-8}\right) \ . \end{aligned} \tag{6.0.22}$$

One-to-six scattering. After performing Wick contractions we go to Fourier space and extract the scattering amplitude defined in (2.7.16) along the lines explained in the last examples. This leads to

$$S(\omega_1,\omega_2,\omega_3,\omega_4,\omega_5,\omega_6\,|\,\omega_7) \equiv e^{-i\omega_7\log(-\nu_F)} \sum_{\Omega\subseteq\{\omega_1,..,\omega_6\}} (-1)^{|\Omega|+1} \int_0^{\omega(\Omega)} \mathrm{d}\upsilon\, R^*_{\nu_F-\upsilon} R_{\nu_F-\upsilon-\omega_7} \ . \tag{6.0.23}$$

Inserting the expressions of the reflection coefficient we obtain

$$\begin{aligned} S(\omega_1,\dots,\omega_6\,|\,\omega_7) &= \frac{i}{\nu_F^5}\,\omega_1\omega_2\omega_3\omega_4\omega_5\omega_6\omega_7(\omega_7+i)(\omega_7+2i)(\omega_7+3i)(\omega_7+4i)+ \\ &- \frac{i}{24\nu_F^7}\,\omega_1\omega_2\omega_3\omega_4\omega_5\omega_6\omega_7(\omega_7+i)(\omega_7+2i)(\omega_7+3i)(\omega_7+4i)(\omega_7+5i)(\omega_7+6i) \\ &\times \big(\omega_1\,(\omega_1-i)+\omega_2\,(\omega_2-i)+\omega_3\,(\omega_3-i)+\omega_4\,(\omega_4-i)+\omega_5\,(\omega_5-i) \\ &\qquad +\omega_6\,(\omega_6-i)+1\big)+\mathcal{O}\left(\nu_F^{-9}\right) \ . \end{aligned} \tag{6.0.24}$$

Three-to-two scattering. We are looking for the term proportional to

$$e^{-i\omega_1 u_1 - i\omega_2 u_2 + i\omega_3 u_3 + i\omega_4 u_4 + i\omega_5 u_5}\,\delta(\omega_1+\omega_2+\omega_3+\omega_4+\omega_5)\,S(\omega_1,\omega_2\,|\,\omega_3,\omega_4,\omega_5) \ , \tag{6.0.25}$$

with ω_1,ω_2 outgoing and positive and $\omega_3,\omega_4,\omega_5$ incoming negative. Further we assume

$$\omega_2>\omega_1 \ , \quad \omega_5>\omega_4>\omega_3 \ , \quad \omega_2>-\omega_3-\omega_4 \ , \quad \omega_1<-\omega_4-\omega_5 \ , \tag{6.0.26}$$

which implies $\omega_2 = \max\{\omega_1, \omega_2, |\omega_3|, |\omega_4|, |\omega_5|\}$. We find

$$
\begin{aligned}
&S(\omega_1, \omega_2 \,|\, \omega_3, \omega_4, \omega_5) \\
&\equiv e^{-i(\omega_3+\omega_4+\omega_5)\log(-\nu_F)} \Bigg[\int_{\omega_4}^{\omega_1+\omega_4} \mathrm{d}\upsilon \, R^*_{\nu_F-\upsilon+\omega_4} R_{\nu_F-\upsilon} R^*_{\nu_F-\upsilon-\omega_2} R_{\nu_F-\upsilon+\omega_1+\omega_4} \\
&+ \int_{\omega_3}^{\omega_1+\omega_3} \mathrm{d}\upsilon \, R^*_{\nu_F-\upsilon+\omega_3} R_{\nu_F-\upsilon} R^*_{\nu_F-\upsilon-\omega_2} R_{\nu_F-\upsilon+\omega_1+\omega_3} - \int_{0}^{\omega_1} \mathrm{d}\upsilon \, R_{\nu_F-\upsilon+\omega_1} R^*_{\nu_F-\upsilon-\omega_2} \\
&+ \int_{\omega_5}^{\omega_1+\omega_5} \mathrm{d}\upsilon \, R^*_{\nu_F-\upsilon+\omega_5} R_{\nu_F-\upsilon} R^*_{\nu_F-\upsilon-\omega_2} R_{\nu_F-\upsilon+\omega_1+\omega_5} + \int_{0}^{\omega_1} \mathrm{d}\upsilon \, R_{\nu_F-\upsilon+\omega_1+\omega_2} R^*_{\nu_F-\upsilon} \\
&- \int_{\omega_4}^{\omega_1+\omega_4} \mathrm{d}\upsilon \, R^*_{\nu_F-\upsilon-\omega_2-\omega_5} R_{\nu_F-\upsilon+\omega_1+\omega_4} R^*_{\nu_F-\upsilon+\omega_4} R_{\nu_F-\upsilon-\omega_5} \\
&- \int_{\omega_3}^{\omega_1+\omega_3} \mathrm{d}\upsilon \, R^*_{\nu_F-\upsilon-\omega_2-\omega_4} R_{\nu_F-\upsilon+\omega_1+\omega_3} R^*_{\nu_F-\upsilon+\omega_3} R_{\nu_F-\upsilon-\omega_4} \\
&- \int_{\omega_5}^{\omega_1+\omega_5} \mathrm{d}\upsilon \, R^*_{\nu_F-\upsilon-\omega_2-\omega_3} R_{\nu_F-\upsilon+\omega_1+\omega_5} R^*_{\nu_F-\upsilon+\omega_5} R_{\nu_F-\upsilon-\omega_3} \Bigg] \\
&= -\frac{i}{\nu_F^3} \omega_1\omega_2\omega_3\omega_4\omega_5(\omega_2 - i)(\omega_2 - 2i) + \mathcal{O}(\nu_F^{-5}) \; . \qquad (6.0.27)
\end{aligned}
$$

Non-planar contribution

To compare to the log-divergence in (3.7.15) we need to go beyond the planar approximation of the large N limit of $\mathcal{F}_m(\boldsymbol{\alpha})$ (3.4.35). Whereas the planar contribution is obtained from a large N saddle point approximation, to find non-planar contributions one needs to make use of other techniques. We will use the method of orthogonal polynomials [80]. We will only provide minimalistic details, for a more detailed explanation of this method we refer for example to [63]. Two polynomials are said to be orthogonal with respect to a weight function $w(x)$ if they satisfy

$$
\mathrm{ortho}_a : \quad \int \mathrm{d}x \, w(x) \, p_n(x) p_m(x) = h_n \delta_{m,n} \qquad (6.0.28)
$$

In addition to (6.0.28), orthogonal polynomials satisfy the *three-term recurrence relation*

$$
\begin{aligned}
\mathrm{ortho}_b : \quad & x \, p_n(x) = A_n \, p_n(x) + S_n \, p_{n+1}(x) + R_n \, p_{n-1}(x) \qquad \text{for} \qquad n > 0 \; , \\
& x \, p_0(x) = A_0 \, p_0(x) + S_0 \, p_1(x) \; , \qquad (6.0.29)
\end{aligned}
$$

where A_n, S_n, and R_n are some real constants. Focusing on monic polynomials

$$P_n(\lambda) \equiv \lambda^n + \sum_{j=0}^{n-1} a_j \lambda^j \ , \qquad n = 0, \dots, N-1 \ , \tag{6.0.30}$$

we obtain [80]

$$\frac{1}{N^2}\mathcal{F}_m(\boldsymbol{\alpha}) = -\frac{1}{N}\log\frac{h_0(\boldsymbol{\alpha})}{h_0(\mathbf{0})} - \frac{1}{N}\sum_{n=1}^{N-1}\Big(1-\frac{n}{N}\Big)\log\frac{R_n(\boldsymbol{\alpha})}{R_n(\mathbf{0})} \ , \tag{6.0.31}$$

where we highlight the coupling dependency of h_n (6.0.28) and R_n (6.0.29) explicitly.

Example $m = 3$**.** Using (6.0.28) and (6.0.29) for $\omega(x) = e^{-NV_3(x,\boldsymbol{\alpha})}$ we obtain [63]

$$\begin{aligned}\frac{n}{N} = R_n(\boldsymbol{\alpha})\Big[1 &+ \alpha_2\left(R_{n+1}(\boldsymbol{\alpha}) + R_n(\boldsymbol{\alpha}) + R_{n-1}(\boldsymbol{\alpha})\right) \\ &+ \alpha_3\big(2R_{n+1}(\boldsymbol{\alpha}) + 2R_n(\boldsymbol{\alpha})R_{n-1}(\boldsymbol{\alpha}) + R_{n+1}(\boldsymbol{\alpha})R_{n-1}(\boldsymbol{\alpha}) + R_{n-1}(\boldsymbol{\alpha})R_{n-2}(\boldsymbol{\alpha}) \\ &+ R_n^2(\boldsymbol{\alpha}) + R_{n+1}^2(\boldsymbol{\alpha}) + R_{n-1}^2(\boldsymbol{\alpha}) + R_{n+1}(\boldsymbol{\alpha})R_{n+2}(\boldsymbol{\alpha})\big)\Big] \ .\end{aligned} \tag{6.0.32}$$

Let us now define the variables $\varepsilon \equiv 1/N$ and $x \equiv n\varepsilon$. In the large N limit, x is well approximated by a continuous parameter. In view of this, it is convenient to set $r(x, \boldsymbol{\alpha}) \equiv R_n(\boldsymbol{\alpha})$. We note that $r(x, \boldsymbol{\alpha})$ is also a function of N, but we suppress this dependence for notational simplicity. We can rewrite (6.0.32) as

$$\begin{aligned}x = r(x,\boldsymbol{\alpha}) + \alpha_2 r(x,\boldsymbol{\alpha})\left[r(x+\varepsilon,\boldsymbol{\alpha}) + r(x,\boldsymbol{\alpha}) + r(x-\varepsilon,\boldsymbol{\alpha})\right] + \alpha_3\Big[2r(x,\boldsymbol{\alpha})r(x+\epsilon,\boldsymbol{\alpha}) \\ + 2r(x,\boldsymbol{\alpha})r(x-\epsilon,\boldsymbol{\alpha}) + r(x+\epsilon,\boldsymbol{\alpha})r(x-\epsilon,\boldsymbol{\alpha}) + r(x-\epsilon,\boldsymbol{\alpha})r(x-2\epsilon,\boldsymbol{\alpha}) + r(x,\boldsymbol{\alpha})^2 \\ + r(x-\epsilon,\boldsymbol{\alpha})^2 + r(x+\epsilon,\boldsymbol{\alpha})^2 + r(x+\epsilon,\boldsymbol{\alpha})r(x+2\epsilon,\boldsymbol{\alpha})\Big] \ .\end{aligned} \tag{6.0.33}$$

It follows from (6.0.33) that $r(x, \boldsymbol{\alpha})$ is symmetric under $\varepsilon \leftrightarrow -\varepsilon$ and we can expand it in even powers of ε

$$r(x,\boldsymbol{\alpha}) = r_0(x,\boldsymbol{\alpha}) + \varepsilon^2\, r_2(x,\boldsymbol{\alpha}) + \varepsilon^4\, r_4(x,\boldsymbol{\alpha}) + \cdots \ . \tag{6.0.34}$$

To obtain the first non-planar contribution we only need $r_0(x, \boldsymbol{\alpha})$ and $r_2(x, \boldsymbol{\alpha})$ which we easily infer from (6.0.33) by comparing powers of ϵ.

An equation similar to (6.0.33) can be obtained for $m \geq 3$ upon choosing $\omega(x) = e^{-NV_m(x,\boldsymbol{\alpha})}$, $m \geq 4$ (6.0.28). Our final ingredient will be the Euler-Maclaurin

formula

$$\frac{1}{N}\sum_{n=1}^{N} f\left(\frac{n}{N}\right) = \int_0^1 \mathrm{d}x f(x) + \frac{1}{2N} f(x)\Big|_0^1 + \sum_{n=1}^{p-1} \frac{B_{2n}}{(2n)!}\frac{1}{N^{2n}} f(x)^{(2n-1)}\Big|_0^1 + \mathcal{R}_N \ . \tag{6.0.35}$$

In the above, $f(x)$ is a $2p$ times continuously differentiable function, $\mathcal{R}_N$ is a remainder term scaling as $\mathcal{O}(1/N^{2p+1})$, and the B_{2n} denote the Bernoulli numbers. Applying the Euler-Maclaurin formula to

$$f\left(x\right) = (1-x)\log\frac{r(x,\boldsymbol{\alpha})}{x} \ , \tag{6.0.36}$$

and expanding (6.0.31) in inverse powers of N, we find

$$\begin{aligned}\frac{1}{N^2}\mathcal{F}_m(\boldsymbol{\alpha}) = &-\int_0^1 \mathrm{d}x(1-x)\log\frac{r(x,\boldsymbol{\alpha})}{x} - \frac{1}{N}\log\frac{h_0(\boldsymbol{\alpha})}{h_0(0)} + \frac{1}{2N}\lim_{x\to 0}\log\frac{r(x,\boldsymbol{\alpha})}{x} \\ &- \frac{1}{12N^2}\left((1-x)\log\frac{r(x,\boldsymbol{\alpha})}{x}\right)^{(1)}\Bigg|_0^1\end{aligned} \tag{6.0.37}$$

up to order $\mathcal{O}(1/N^4)$ corrections. Expanding all three terms in (6.0.34) and evaluating $h_0(\boldsymbol{\alpha})$ for small $\boldsymbol{\alpha}$ we find up to powers of order $\mathcal{O}(1/N^2)$

$$\begin{aligned}\frac{1}{N^2}\mathcal{F}_m(\boldsymbol{\alpha}) = &-\int_0^1 \mathrm{d}x\,(1-x)\,\log\frac{r_0(x,\boldsymbol{\alpha})}{x} \\ &- \frac{1}{N^2}\left[\int_0^1 \mathrm{d}x\,(1-x)\,\frac{r_2(x,\boldsymbol{\alpha})}{r_0(x,\boldsymbol{\alpha})} + \frac{1}{12}\left[(1-x)\log\frac{r_0(x,\boldsymbol{\alpha})}{x}\right]^{(1)}\Bigg|_0^1 - \frac{3}{4}\alpha_2\right] \ .\end{aligned} \tag{6.0.38}$$

Note that we encounter an ambiguity in choosing $r_0(x,\boldsymbol{\alpha})$ since it is the solution of an m^{th} order polynomial. We pick the solution yielding the on-shell value (3.2.21) when evaluating the $\mathcal{O}(N^0)$ integral along $\gamma_\star^{(m)}$. Evaluating the second line in the above expression is in general difficult however to get the coefficient of the log-divergence we only care about the first integral. To further simplify our analysis we zoom into the multicritical point $\boldsymbol{\alpha}_c$ (3.2.13). The non-analytic behaviour of (6.0.38) occurring for $\boldsymbol{\alpha} = \boldsymbol{\alpha}_c$ close to the upper boundary, equals the non-analyticity observed upon considering small deformations away from the multicritical point only after evaluating the integral. We obtain for $m = 3$ and $m = 4$

$$\mathcal{F}^{(1)}_{3,\text{n.a.}}(\boldsymbol{\alpha_c}) = \frac{1}{18}\log\epsilon \ , \quad \mathcal{F}^{(1)}_{4,\text{n.a.}}(\boldsymbol{\alpha_c}) = \frac{1}{16}\log\epsilon \ , \quad \epsilon \ll 1 \ , \tag{6.0.39}$$

where the subscript indicates the leading non-analyticity. For general $m \geq 3$ we conjecture

$$\mathcal{F}^{(1)}_{m,\text{n.a.}}(\boldsymbol{\alpha_c}) = \frac{2m-2}{24(2m-1)} \log \epsilon \ , \quad \epsilon \ll 1 \ , \tag{6.0.40}$$

and the coefficient of the log agrees with the coefficient of the log of the torus partition function (3.7.15) of the continuum theory. For $m = 2$ and the generalisations thereof discussed in section 3.3.1 on the other side we obtain

$$\tilde{\mathcal{F}}^{(1)}_{m,\text{n.a.}}(\boldsymbol{\alpha_c}) = \frac{1}{24} \log \epsilon \ , \quad \epsilon \ll 1 \ . \tag{6.0.41}$$

As a final remark we note that $\mathcal{F}^{(1)}_m(4\alpha_2, \ldots, 2m\alpha_m)$ counts leading non-planar diagrams. More explicitly it counts diagrams whose vertices are emanating four or $2m$ edges and which can fit on a surface of genus one. As an example, a perturbative analysis of (6.0.38) using $r_0(x, \boldsymbol{\alpha})$ and $r_2(x, \boldsymbol{\alpha})$ for $m = 3$ easily reveals

$$\mathcal{F}^{(1)}_3(4\alpha_2, 6\alpha_3) = \alpha_2 + 10\alpha_3 - 30\alpha_2^2 - 2400\alpha_3^2 - 600\alpha_2\alpha_3 + \ldots \ . \tag{6.0.42}$$

Solutions of $\mathcal{N}_4(\boldsymbol{\alpha}) = 0$

In this section, we discuss the solutions of the normalisation condition (3.4.18) for the $m = 4$ case:

$$u^{(4)}_{1,\pm} = -\frac{2\alpha_3}{7\alpha_4} - S \pm \frac{1}{2}\sqrt{-4S^2 - 2p + \frac{q}{S}} \ , \quad u^{(4)}_{2,\pm} = -\frac{2\alpha_3}{7\alpha_4} + S \pm \frac{1}{2}\sqrt{-4S^2 - 2p - \frac{q}{S}} \ , \tag{6.0.43}$$

where

$$p \equiv \frac{24(14\alpha_2\alpha_4 - 5\alpha_3^2)}{245\alpha_4^2} \ , \quad q \equiv \frac{64(5\alpha_3^3 - 21\alpha_2\alpha_3\alpha_4 + 49\alpha_4^2)}{1715\alpha_4^3} \ . \tag{6.0.44}$$

In the above, we have defined

$$S \equiv \frac{1}{2}\sqrt{-\frac{2}{3}p - \frac{256}{105\alpha_4}\left(Q + \frac{\Delta_0}{Q}\right)} \ , \tag{6.0.45}$$

$$Q \equiv \sqrt[3]{\frac{\Delta_1 + \sqrt{\Delta_1^2 - 4\Delta_0^3}}{2}} \ , \tag{6.0.46}$$

$$\Delta_0 \equiv \frac{3}{256}(3\alpha_2^2 - 10(\alpha_3 + 14\alpha_4)) \ , \tag{6.0.47}$$

$$\Delta_1 \equiv -\frac{27}{4096}\left(2(\alpha_2^3 - 5\alpha_2\alpha_3 - 50\alpha_3^2) + 35\alpha_4(1 + 8\alpha_2)\right) \ , \tag{6.0.48}$$

$$D_4 \quad \equiv \quad -\frac{1}{27}\left(\Delta_1^2 - 4\Delta_0^3\right) \ . \tag{6.0.49}$$

Much of our interest lies in a solution of $\mathcal{N}_4(\boldsymbol{\alpha}) = 0$ that is regular in a small neighbourhood $\aleph_{\mathbf{0}}$ around the origin of coupling space $\boldsymbol{\alpha} = 0$. To analyse the problem, we can consider approaching $\boldsymbol{\alpha} = 0$ uniformly in all directions, and exploring the behaviour of the various solutions throughout $\aleph_{\mathbf{0}}$. An exhaustive analysis reveals that one must keep track of the various signs of $\boldsymbol{\alpha}$ and the special combination $(\alpha_3 + 14\alpha_4)$. The term $(\alpha_3 + 14\alpha_4)$ is already revealed in the form of Δ_0 and can be seen to carry through into the more involved building blocks such as Q and S. For instance, near $\aleph_{\mathbf{0}}$ we have

$$Q = \begin{cases} \frac{5^{2/3}}{8\times 7^{1/3}}\left(\frac{\alpha_3+14\alpha_4}{\alpha_4}\right)^{1/3} + \mathcal{O}(\alpha^{4/3}) \ , & \alpha_4 \geq 0 \ , \\ \frac{3\times 35^{1/3}}{16}\left(-\alpha_4\right)^{1/3} + \mathcal{O}(\alpha^{4/3}) \ , & \alpha_4 < 0 \ . \end{cases} \tag{6.0.50}$$

We find the following combination of solutions to be smooth near $\aleph_{\mathbf{0}}$

$$\begin{aligned} B_4(\boldsymbol{\alpha}) = u^{(4)}_{1,+}\left(\Theta_{+++} + \Theta_{-++} + \Theta^{+}_{--+} + \Theta^{+}_{+-+}\right) + \\ u^{(4)}_{2,-}\left(\Theta_{---} + \Theta_{++-} + \Theta_{-+-} + \Theta_{+--} + \Theta^{-}_{--+} + \Theta^{-}_{+-+}\right) \ , \end{aligned} \tag{6.0.51}$$

where we have introduced the notation

$$\Theta_{\rho_2\rho_3\rho_4} \quad \equiv \quad \Theta(\rho_2\alpha_2)\Theta(\rho_3\alpha_3)\Theta(\rho_4\alpha_4) \ , \tag{6.0.52}$$

$$\Theta^{\rho}_{\rho_2\rho_3\rho_4} \quad \equiv \quad \Theta(\rho_2\alpha_2)\Theta(\rho_3\alpha_3)\Theta(\rho_4\alpha_4)\Theta(\rho(\alpha_3 + 14\alpha_4)) \ . \tag{6.0.53}$$

Further properties of $\mathcal{N}_4(\boldsymbol{\alpha}) = 0$

The solutions (6.0.43) also reveal additional information. For instance, expanding the discriminant D_4 (6.0.49) at small α_2 and α_3, we identify $\alpha_4 = -27/8960$ as the special value $\tilde{\alpha}_{4,c}$ in (3.3.11). Similarly, expanding the discriminant D_4 at small α_3 and α_4, we identify $\alpha_2 = -1/12$ as the special value $\alpha^{(2)}_{2,c}$ in (3.2.13). Finally expanding for small α_2 and α_4 reveals $\alpha_3 = -2/135$ as the special value $\tilde{\alpha}_{3,c}$ (3.3.11). Near $(\alpha_2, \alpha_3, \alpha_4) = (0, 0, -27/8960)$, $(\alpha_2, \alpha_3, \alpha_4) = (0, -2/135, 0)$ as well as $(\alpha_2, \alpha_3, \alpha_4) = (-1/12, 0, 0)$, Δ_1 remains non-vanishing such that the non-analytic behaviour of the solutions $u^{(4)}$ is that of a **square root**. Expanding the discriminant D_4 near $\alpha_2 = -1/8$, reveals $\alpha_3 = 1/160$ as a special value, which we recognise as $\alpha^{(4)}_{3,c}$, one of the multicritical couplings (3.2.13). At $(\alpha_2, \alpha_3) = (-1/8, 1/160)$ we further have that $\Delta_1 = 0$, while D_4 goes as $(1 + 8960\alpha_4)^3$ revealing the third multicritical value $\alpha_4 = -1/8960$. Also, at $(\alpha_2, \alpha_3) = (-1/8, 1/160)$ we observe that Q in (6.0.46) goes as $(1 + 8960\alpha_4)^{1/2}$, and p in (6.0.44) goes as $(1 + 8960\alpha_4)$. Expanding away from the multicritical point reveals distinct non-

analytic behaviour in the solutions of $\mathcal{N}_4(\boldsymbol{\alpha}) = 0$. For instance, fixing $(\alpha_2, \alpha_3) = (-1/8, 1/160)$ and deviating slightly away from $\alpha_4 = -1/8960$, we uncover a **fourth root** non-analyticity.

Non-analyticities: normalisation condition

In this appendix we prove the following.

Claim. For

$$\boldsymbol{\alpha}^{\epsilon} \equiv \boldsymbol{\alpha}_c + \boldsymbol{s}\,\epsilon\ , \quad u = 4m + \tilde{x}\,\epsilon^{\frac{1}{m-r'}}\ , \quad \tilde{x} \in \mathbb{R}\ , \tag{6.0.54}$$

with $\boldsymbol{s}$ living on $\mathcal{H}_m^{(1)} \cup \mathcal{H}_m^{(2)} \ldots \cup \mathcal{H}_m^{(r')} = 0$, $r' = 1, \ldots m-2$, (3.5.15) the normalisation condition (3.2.11) reduces to (3.5.17)

$$\mathcal{N}_m^{(r')}(\boldsymbol{\alpha}^{\epsilon}) = \left[(-1)^m \frac{\tilde{x}^m}{(4m)^m} - \frac{\tilde{x}^{r'}}{4^{r'}} m^2\, \mathcal{H}_m^{(r'+1)}\right] \epsilon^{\frac{m}{m-r'}} + \mathcal{O}\left(\epsilon^{\frac{m+1}{m-r'}}\right)\ . \tag{6.0.55}$$

Proof. Plugging (3.5.16) with $\boldsymbol{s}$ constraint to live on the hypersurface $\mathcal{H}_m^{(1)} \cup \mathcal{H}_m^{(2)} \ldots \cup \mathcal{H}_m^{(r')} = 0$ into the normalisation condition (3.2.11) and expanding for small ϵ we obtain

$$\mathcal{N}_m^{(r')}(\boldsymbol{\alpha}^{\epsilon}) = (-1)^m \frac{\tilde{x}^m}{(4m)^m} \epsilon^{\frac{m}{m-r'}} - \sum_{n=2}^{m} \left(\frac{4^n}{2nB(n,1/2)} \sum_{\ell=0}^{n} \binom{n}{\ell} \left(\frac{\tilde{x}}{4m}\right)^{\ell} \epsilon^{\frac{\ell}{m-r'}+1} \right) m^n\, s_n\ . \tag{6.0.56}$$

We apply a recursive argument by showing that the sum multiplying the term $\tilde{x}^{k-1}$, $k \geq 3$, vanishes for $\boldsymbol{s}$ constraint to

$$\mathcal{H}_m^{(k-2)} \cup \mathcal{H}_m^{(k-1)} \cup \mathcal{H}_m^{(k)} = 0\ . \tag{6.0.57}$$

For $\ell = k-1$ we have (6.0.55)

$$\begin{aligned}
&\sum_{n=k-1}^{m} \frac{4^n}{2nB(n,1/2)} \binom{n}{k-1} m^n s_n = \frac{(4m)^{k-1}}{2(k-1)B(k-1,1/2)} s_{k-1} \\
&+ \sum_{n=k}^{m} \frac{4^n}{2nB(n,1/2)} \binom{n}{k-1} m^n s_n \\
&\overset{\mathcal{H}_m^{(k-2)}}{=} \sum_{n=k}^{m} \frac{4^n}{2nB(n,1/2)} \left(\binom{n}{k-1} - \binom{n-2}{k-3} \right) m^n s_n = \frac{(4m)^k}{kB(k,1/2)} s_k + \\
&+ \sum_{n=k+1}^{m} \frac{4^n}{2nB(n,1/2)} \left(\binom{n}{k-1} - \binom{n-2}{k-3} \right) m^n s_n
\end{aligned}$$

$$\overset{\mathcal{H}_m^{(k-1)}}{=} \sum_{n=k+1}^{m} \frac{4^n}{2nB(n,1/2)} \left(\binom{n}{k-1} - \binom{n-2}{k-3} - 2\binom{n-2}{k-2} \right) m^n s_n$$

$$= \sum_{n=k+1}^{m} \frac{4^n}{2nB(n,1/2)} \binom{n-2}{k-1} m^n s_n = \mathcal{H}_m^{(k)} \ . \tag{6.0.58}$$

A superscript over an equality sign means that we are using the condition $\boldsymbol{s} \in \mathcal{H}_m^{(j)}$. For $\ell = 1$ the sum already vanishes on $\mathcal{H}_m^{(1)} \cup \mathcal{H}_m^{(2)} = 0$. For $\ell = 0$ it vanishes on $\mathcal{H}_m^{(1)} = 0$. If the directions $\boldsymbol{s}$ now lives on

$$\bigcup_{j=1}^{r'} \mathcal{H}_m^{(j)} = 0 \ , \tag{6.0.59}$$

in (6.0.56) all terms of order $\mathcal{O}(\tilde{x}^k)$, $k < r'$ vanish and we obtain (6.0.55).

Non-analyticities: action

In this appendix we prove the following.

Claim. Along

$$\alpha^{\epsilon}_{n\neq p} = \alpha^{(m)}_{c,n\neq p} + s_{n\neq p}\,\epsilon \ , \quad \alpha^{\beta}_{p} = \alpha^{(m)}_{c,p} + s_p\,\epsilon + \tilde{s}\,\epsilon^{\frac{m}{m-r'}} \ , \quad u = 4m + \tilde{x}\,\epsilon^{\frac{1}{m-r'}} \ . \tag{6.0.60}$$

and using (3.5.19) we obtain

$$S_m^{(r')}[\rho_{\rm ext}^{(m)}(\lambda, \boldsymbol{\alpha}^{\epsilon})] = \mathcal{S}_m^{(r')}[\boldsymbol{s}, \epsilon, \epsilon^2]$$
$$- \frac{1}{2} H_m \left[(-1)^m \frac{\tilde{x}^m}{(4m)^m} - \frac{\tilde{x}^{r'}}{4^{r'}} m^2\, \mathcal{H}_m^{(r'+1)} - \frac{(4m)^p}{2pB(p,1/2)} \tilde{s} \right] \epsilon^{\frac{m}{m-r'}}$$
$$+ \frac{(4m)^p}{2p^2 B(p,1/2)} \frac{m!p!}{(m+p)!}\, \tilde{s}\, \epsilon^{\frac{m}{m-r'}} + \mathcal{O}\left(\epsilon^{\frac{m+1}{m-r'}}\right) \ , \tag{6.0.61}$$

where

$$\mathcal{S}_m^{(r')}[\boldsymbol{s}, \epsilon, \epsilon^2] \equiv S_c[\rho_{\rm ext}^{(m)}(\lambda, \boldsymbol{\alpha}_c)]$$
$$+ \epsilon \left(\sum_{n=2}^{m} \frac{(4m)^n}{4n^2 B(n,1/2)} s_n + \sum_{\substack{n=1 \\ k\geq 2}}^{m} \frac{(-1)^{n+1}}{4n(n+k)} \binom{m}{n} \frac{(4m)^k}{B(k,1/2)} s_k \right.$$
$$\left. + \sum_{\substack{k=1 \\ n\geq 2}}^{m} (-1)^{k+1} \frac{k}{4n^2(n+k)} \binom{m}{k} \frac{(4m)^n}{B(n,1/2)} s_n \right)$$

$$+\epsilon^2 \sum_{n,k=2}^{m} \frac{s_n}{4n^2 B(n,1/2)} \frac{s_k}{2(n+k)} \frac{(4m)^{n+k}}{B(k,1/2)} \tag{6.0.62}$$

evaluated on (3.5.14). The action $S_c[\rho_{\text{ext}}^{(m)}(\lambda, \boldsymbol{\alpha}_c)]$ at criticality was defined in (3.2.21).

Proof. To proof (6.0.61) we split the on-shell action (3.2.20) into pieces and write out the series expansion of the logarithm. This leads to

$$\begin{aligned} &S_m^{(k)}[\rho_{\text{ext}}(\lambda)] \\ &= \sum_{n=1}^{m} \frac{(2n)!}{4n} \alpha_n \, \omega_n^{(m)} + \sum_{n=1}^{m} \frac{\alpha_{n,c} u^n}{4n^2 B(n,1/2)} + \epsilon \sum_{n=2}^{m} \frac{s_n u^n}{4n^2 B(n,1/2)} - \sum_{\ell=1}^{\infty} \frac{(-1)^{\ell+1}}{2\ell} \frac{\tilde{x}^\ell}{(4m)^\ell} \epsilon^{\frac{\ell}{m-k}} , \end{aligned} \tag{6.0.63}$$

where (3.2.17)

$$\omega_n^{(m)}(\boldsymbol{\alpha}) \equiv \frac{1}{(n!)^2 4^n} \sum_{k=1}^{m} \frac{\alpha_k u^{n+k}}{2(n+k) B(k,1/2)} . \tag{6.0.64}$$

and $B(n,1/2)$ is the beta function

$$B(n,1/2) = \frac{4^n (n!)^2}{n(2n)!} . \tag{6.0.65}$$

1^{st} **term.** For the first term in the action (6.0.63) we find

$$\begin{aligned} \sum_{n=1}^{m} \frac{(2n)!}{4n} \alpha_n \, \omega_n^{(m)} &= \frac{1}{2}(H_{2m} - H_m) + \frac{(-1)^{m+1}}{2} \frac{\tilde{x}^m}{(4m)^m} H_m \, \epsilon^{\frac{m}{m-r'}} + \frac{1}{2} H_m \frac{m^2}{4^{r'}} \mathcal{H}_m^{(r'+1)} \\ &+ \sum_{n,k=1}^{m} \sum_{\ell>m}^{n+k} \frac{(-1)^{n+k} k}{2n(n+k)} \binom{m}{n} \binom{m}{k} \binom{n+k}{\ell} \frac{\tilde{x}^\ell}{(4m)^\ell} \epsilon^{\frac{\ell}{m-r'}} \\ &+ \sum_{n,k=2}^{m} \frac{s_n}{4n^2 B(n,1/2)} \frac{s_k}{2(n+k)} \frac{(4m)^{n+k}}{B(k,1/2)} \epsilon^2 + \mathcal{O}\left(\epsilon^{\frac{2m-r'-1}{m-r'}}\right) . \end{aligned} \tag{6.0.66}$$

where we used i1), i2), i3) (6.0.73) and c2) (6.0.74) and H_m is the m^{th} harmonic number. Additionally (6.0.66) contains a coupling and $\tilde{x}$ dependent part. Using (6.0.64) we obtain along (6.0.60)

$$\sum_{n,k=1}^{m} \sum_{\ell=0}^{n+k} \frac{\alpha_n}{4n^2 B(n,1/2)} \frac{\alpha_k}{2(n+k)} \frac{(4m)^{n+k}}{B(k,1/2)} \binom{n+k}{\ell} \frac{\tilde{x}^\ell}{(4m)^\ell} \epsilon^{\frac{\ell}{m-r'}}$$

$$
\begin{aligned}
&= \sum_{n,k=1}^{m} \frac{\alpha_n}{4n^2 B(n,1/2)} \frac{\alpha_k}{2(n+k)} \frac{(4m)^{n+k}}{B(k,1/2)} \\
&+ \sum_{n,k=1}^{m} \sum_{\ell=1}^{n+k} \frac{\alpha_n}{4n^2 B(n,1/2)} \frac{\alpha_k}{2(n+k)} \frac{(4m)^{n+k}}{B(k,1/2)} \binom{n+k}{\ell} \frac{\tilde{x}^\ell}{(4m)^\ell} \epsilon^{\frac{\ell}{m-r'}} \quad (6.0.67)
\end{aligned}
$$

where the case of the α's in both sums equal to their critical value we already treated in obtaining (6.0.66). For the other case using (3.2.13) we have

$$
\begin{aligned}
&\sum_{n,k=1}^{m} \sum_{\ell=1}^{n+k} \frac{1}{4n(n+k)} \left[(-1)^{n+1} \binom{m}{n} \frac{(4m)^k}{B(k,1/2)} s_k + (-1)^{k+1} \frac{k}{n} \binom{m}{k} \frac{(4m)^n}{B(n,1/2)} s_n \right] \\
&\times \binom{n+k}{\ell} \frac{\tilde{x}^\ell}{(4m)^\ell} \epsilon^{\frac{\ell}{m-r'}+1} \\
&+ \sum_{n,k=1}^{m} \frac{1}{4n(n+k)} \left[(-1)^{n+1} \binom{m}{n} \frac{(4m)^k}{B(k,1/2)} s_k + (-1)^{k+1} \frac{k}{n} \binom{m}{k} \frac{(4m)^n}{B(n,1/2)} s_n \right] \epsilon \\
&+ \sum_{n,k=2}^{m} \frac{s_n}{4n^2 B(n,1/2)} \frac{s_k}{2(n+k)} \frac{(4m)^{n+k}}{B(k,1/2)} \epsilon^2 \\
&+ \sum_{n,k=2}^{m} \sum_{\ell=1}^{n+k} \binom{n+k}{\ell} \frac{s_n}{4n^2 B(n,1/2)} \frac{s_k}{2(n+k)} \frac{(4m)^{n+k}}{B(k,1/2)} \frac{\tilde{x}^\ell}{(4m)^\ell} \epsilon^{\frac{\ell}{m-r'}+2} \, .
\end{aligned} \quad (6.0.68)
$$

Only the sums in the first line of (6.0.68) and the last sum could contribute to the leading non-analyticity in (6.0.61). We treat the sums independently. For the second sum in the second line we use that (6.0.74) vanishes for $\ell < m$ and the first non-vanishing term arises for $\ell = m$ proportional to $\epsilon^{(2m-r')/(m-r')}$. Since our leading non-analyticity grows us $\mathcal{O}(\epsilon^{m/(m-r')})$, $r' = 1, \ldots, m-2$ the former is subleading with respect to the non-analyticity we are after. For the first sum of the second line we show that for $\boldsymbol{s} \in \mathcal{H}_m^{(1)} \cup \mathcal{H}_m^{(2)} \ldots \cup \mathcal{H}_m^{(\ell)} = 0$ we have

$$
\sum_{n=1}^{m} \sum_{k=2}^{m} \frac{(-1)^{n+1}}{4n(n+k)} \binom{m}{n} \frac{(4m)^k}{B(k,1/2)} s_k \binom{n+k}{\ell} \frac{\tilde{x}^\ell}{(4m)^\ell} = \frac{1}{2} H_m \frac{m^2}{4^\ell} \mathcal{H}_m^{(\ell+1)} \, . \quad (6.0.69)
$$

We show (6.0.69) for $\ell = 1$ and $\ell = 2$, for general $\ell > 2$ the logic stays the same. For $\ell = r'$ it leads to the claimed result (6.0.61). For $\ell = 1$ we have

$$
\frac{1}{4m} \sum_{n=1}^{m} \sum_{k=2}^{m} \frac{1}{4n} \left[(-1)^{n+1} \binom{m}{n} \frac{(4m)^k}{B(k,1/2)} s_k \right] = \frac{1}{4m} \sum_{k>2} \sum_{n=1}^{m} \frac{1}{4n} (-1)^{n+1} \binom{m}{n} \frac{(4m)^k}{B(k,1/2)} s_k
$$

$$+\frac{1}{4m}\frac{(4m)^2}{B(2,1/2)}s_2\sum_{n=1}^{m}\frac{(-1)^{n+1}}{4n}\binom{m}{n}\overset{\mathcal{H}_m^{(1)}}{=}\frac{1}{2}H_m\frac{m^2}{4}\mathcal{H}_m^{(2)}\ . \tag{6.0.70}$$

For $\ell=2$ we have

$$\begin{aligned}
&\frac{1}{(4m)^2}\sum_{k=2}^{m}\sum_{n=1}^{m}\frac{(-1)^{n+1}}{4n(n+k)}\binom{m}{n}\frac{(4m)^k}{B(k,1/2)}\binom{n+k}{2}s_k\\
\overset{\mathcal{H}_m^{(1)}}{=}&\frac{1}{(4m)^2}\sum_{\substack{n=1\\k\geq 3}}^{m}\frac{(-1)^{n+1}}{4n}\binom{m}{n}\frac{(4m)^k}{B(k,1/2)}\left[\frac{1}{n+k}\binom{n+k}{2}-\frac{2}{k(n+2)}\binom{n+2}{2}\right]s_k\\
\overset{\mathcal{H}_m^{(2)}}{=}&\frac{1}{(4m)^2}\sum_{\substack{n=1\\k\geq 3}}^{m}\frac{(-1)^{n+1}}{4n}\binom{m}{n}\frac{(4m)^k}{B(k,1/2)}\left[\frac{1}{n+k}\binom{n+k}{2}-\frac{2}{k(n+2)}\binom{n+2}{2}\right.\\
&\left.-\frac{6(k-2)}{2k}\left(\frac{1}{n+3}\binom{n+3}{2}-\frac{2}{3(n+2)}\binom{n+2}{2}\right)\right]s_k\\
=&\frac{1}{(4m)^2}\sum_{\substack{n=1\\k\geq 3}}^{m}\frac{(-1)^{n+1}}{4n}\binom{m}{n}\frac{(4m)^k}{B(k,1/2)}\frac{1}{k}\binom{k-2}{2}s_k\\
=&\frac{1}{(4m)^2}\sum_{n=1}^{m}\frac{(-1)^{n+1}}{2n}\binom{m}{n}\sum_{k\geq 4}\frac{(4m)^k}{2kB(k,1/2)}\binom{k-2}{2}s_k=\frac{1}{2}H_m\frac{m^2}{4^2}\mathcal{H}_m^{(3)}.
\end{aligned} \tag{6.0.71}$$

Finally the last sum in (6.0.68). For any fixed ℓ it vanishes on $\mathcal{H}_m^{(1)}\cup\ldots\cup\mathcal{H}_m^{(\ell+1)}=0$. We start by showing this for $\ell=1$:

$$\begin{aligned}
&\sum_{n,k=2}^{m}\frac{s_n}{4n^2B(n,1/2)}\frac{s_k}{2(n+k)}\frac{(4m)^{n+k}}{B(k,1/2)}\binom{n+k}{1}=\frac{(4m)^2}{B(2,1/2)}s_2\sum_{n=2}^{m}\frac{(4m)^n s_n}{4n^2B(n,1/2)}\\
+&\sum_{k>2}\sum_{n=2}^{m}\frac{(4m)^n s_n}{4n^2B(n,1/2)}\frac{(4m)^k}{2B(k,1/2)}s_g=\sum_{k>2}\sum_{n=2}^{m}\frac{(4m)^n s_n}{4n^2B(n,1/2)}\frac{(4m)^k}{B(k,1/2)}\left(\frac{1}{2}-\frac{1}{k}\right)\\
=&\sum_{n=2}^{m}\frac{(4m)^n s_n}{4n^2B(n,1/2)}\sum_{k=3}^{m}\frac{(4m)^k}{2kB(k,1/2)}\binom{k-2}{1}s_k\ \propto\mathcal{H}_m^{(2)}\ .
\end{aligned} \tag{6.0.72}$$

Now for $\boldsymbol{s}\in\mathcal{H}_m^{(1)}\cup\mathcal{H}_m^{(2)}$ we obtain non-analyticity $\mathcal{O}\left(\epsilon^{m/(m-2)}\right)$, i.e. $k=2$. However from (6.0.68) we infer a leading contribution of order $\mathcal{O}\left(\epsilon^{(2m-3)/(m-2)}\right)$. For $m>3$ which is the only case in which $k=2$ is allowed the exponent is therefore bigger than $m/(m-2)$ and so we do not get a contribution violating $\mathcal{O}\left(\epsilon^{m/(m-2)}\right)$ as a leading non-analyticity. For $\ell>1$ the logic is the same.

Identities for harmonic numbers H_m.

$$\begin{aligned}
&\text{i1)}\quad \sum_{n,k=1}^{m} \frac{(-1)^{n+k}k}{2n(n+k)}\binom{m}{n}\binom{m}{k}\binom{n+k}{m} = \frac{(-1)^{m+1}}{2}H_m \ , \\
&\text{i2)}\quad \sum_{n=1}^{m} \frac{(-1)^{n+1}}{2n}\binom{m}{n} = \frac{1}{2}H_m \ , \\
&\text{i3)}\quad \sum_{n,k=1}^{m} \frac{(-1)^{n+k}k}{2n(n+k)}\binom{m}{n}\binom{m}{k} = \frac{1}{2}(H_{2m}-H_m) \ ,
\end{aligned} \tag{6.0.73}$$

Conjectures.

$$\begin{aligned}
&\text{c1)}\quad 0 = \sum_{n,k=1}^{m}\sum_{\ell=1}^{m-1} \frac{(-1)^{n+k}k}{2n(n+k)}\binom{m}{n}\binom{m}{k}\binom{n+k}{\ell}\frac{1}{(4m)^\ell} \ , \\
&\text{c2)}\quad 0 = \sum_{k=1}^{m}\sum_{n=2}^{m} \frac{(-1)^{k+1}}{4n(n+k)}\frac{k}{n}\binom{m}{k}\frac{(4m)^n}{B(n,1/2)}s_n\binom{n+k}{\ell}\frac{1}{(4m)^\ell}\Big|_{\ell=1,\dots m-1}
\end{aligned} \tag{6.0.74}$$

2^{nd} **term.** For the second term in (6.0.63) we start by rewriting the normalisation condition (3.2.11)

$$1 - \sum_{n=1}^{m} \frac{\alpha_{n,c}u^n}{2nB(n,1/2)} = (-1)^m(4m)^{-m}(u-4m)^m \ . \tag{6.0.75}$$

Dividing both sides by $2u$ and integrating with respect to u and $\eta > 0$ we have

$$\int_\eta^{u'} \mathrm{d}u \left(\frac{1}{2u} - \sum_{n=1}^{m} \frac{\alpha_{n,c}u^{n-1}}{4nB(n,1/2)}\right) = (-1)^m(4m)^{-m}\int_\eta^{u'} \mathrm{d}u\,\frac{(u-4m)^m}{2u} \ . \tag{6.0.76}$$

We then get

$$\begin{aligned}
\frac{1}{2}\log(u'/\eta) - \sum_{n=1}^{m} \frac{\alpha_{n,c}u'^n}{4n^2B(n,1/2)} &= \frac{1}{2}\int_\epsilon^{u'} \mathrm{d}u\frac{1}{u}\left(1-\frac{u}{4m}\right)^m = \frac{1}{2}\int_\epsilon^{u'} \mathrm{d}u\sum_{\ell=0}^{m}(-1)^\ell\binom{m}{\ell}\frac{u^{\ell-1}}{(4m)^\ell} \\
&= \sum_{\ell=1}^{m}\frac{(-1)^\ell}{2\ell}\binom{m}{\ell}\frac{u'^\ell}{(4m)^\ell} + \frac{1}{2}\log(u'/\eta) \ .
\end{aligned} \tag{6.0.77}$$

From this we conclude

$$\sum_{n=1}^{m}\frac{\alpha_{n,c}u^n}{4n^2B(n,1/2)}=\sum_{\ell=1}^{m}\frac{(-1)^{\ell+1}}{2\ell}\binom{m}{\ell}\frac{u^\ell}{(4m)^\ell}=\sum_{n=1}^{m}\frac{(-1)^{n+1}}{2n}\frac{\tilde{x}^n}{(4m)^n}\,\epsilon^{\frac{n}{m-k}}+\frac{1}{2}H_m\ . \tag{6.0.78}$$

The $\tilde{x}$ dependent term therefore exactly cancels the 4^{th} term in (6.0.63).

3^{rd} term. For the third term in the on-shell action (6.0.63) we find for $\boldsymbol{s}\in\mathcal{H}_m^{(1)}\cup\ldots\mathcal{H}_m^{(r')}$, following the same reasoning as in appendix 6

$$\epsilon\sum_{n=2}^{m}\frac{s_nu^n}{4n^2B(n,1/2)}=\epsilon\sum_{n=2}^{m}\frac{(4m)^n}{4n^2B(n,1/2)}s_n+\frac{\tilde{x}^{r'+1}}{(4m)^{r'+1}}\epsilon^{\frac{m+1}{m-r'}}\frac{m^{r'+2}}{2(k+1)}\mathcal{H}_m^{(r'+1)}\ . \tag{6.0.79}$$

Fine-tuning

We get the fine-tuning by realising that in the on-shell action (3.2.20) only the first and second term are affected to order $\mathcal{O}(\epsilon^{m/(m-r')})$ when fine-tuning α_p^β (6.0.60). Clearly the only contribution of the second term scaling as $\tilde{s}\,\epsilon^{m/(m-r')}$ is

$$\sum_{n=1}^{m}\frac{\alpha_nu^n}{4n^2B(n,1/2)}=\tilde{s}\frac{(4m)^p}{4p^2B(p,1/2)}\epsilon^{\frac{m}{m-r'}}+\mathcal{O}\left(\epsilon^{\frac{m}{m-r'}+1}\right)\ . \tag{6.0.80}$$

From the first term of the on-shell action (3.2.20) on the other side we get the contribution

$$\begin{aligned}
&\left(\frac{(2p)!}{4p}\frac{\tilde{s}}{(p!)^2 4^p}\sum_{n=1}^{m}\frac{\alpha_{n,c}}{2(n+p)}\frac{(4m)^{n+p}}{B(n,1/2)}+\tilde{s}\sum_{n=1}^{m}\frac{(2n)!}{4n(n!)^2}\frac{\alpha_{n,c}}{4^n}\frac{(4m)^{n+p}}{2(n+p)B(p,1/2)}\right)\epsilon^{\frac{m}{m-r'}}\\
=&\left(\frac{(2p)!}{4p}\frac{m^p}{(p!)^2}\tilde{s}\sum_{n=1}^{m}(-1)^{n+1}\binom{m}{n}\frac{n}{(n+p)}\right.\\
&\left.+\frac{(4m)^p}{B(p,1/2)}\tilde{s}\sum_{n=1}^{m}(-1)^{n+1}\binom{m}{n}\frac{1}{4n(n+p)B(n,1/2)}\right)\epsilon^{\frac{m}{m-r'}}\\
=&\left(\frac{(4m)^p}{4p^2B(p,1/2)}\frac{m!p!}{(m+p)!}+\frac{(4m)^p}{B(p,1/2)}\sum_{n=1}^{m}\binom{m}{n}\frac{(-1)^{n+1}}{4n(n+p)}\right)\tilde{s}\,\epsilon^{\frac{m}{m-r'}}\\
=&\left(\frac{(4m)^p}{2p^2B(p,1/2)}\frac{m!p!}{(m+p)!}-\frac{(4m)^p}{4p^2B(p,1/2)}\right)\tilde{s}\,\epsilon^{\frac{m}{m-r'}}+H_m\frac{(4m)^p}{4pB(p,1/2)}\tilde{s}\,\epsilon^{\frac{m}{m-r'}}\ .
\end{aligned} \tag{6.0.81}$$

Hypergeometric functions

We collect some useful properties about (regularised, generalised) hypergeometric functions. For $|z|<1$, $a_1,a_2,b_1\in\mathbb{C}$ the hypergeometric function is defined by the power series

$$ {}_2F_1\left(a_1,a_2;b_1;z\right)\equiv\sum_{n=0}^{\infty}\frac{(a_1)_n(a_2)_n}{(b_1)_n}\frac{z^n}{n!}\,,\quad (x)^n\equiv x(x+1)\cdots(x+n-1)=\frac{\Gamma(x+n)}{\Gamma(x)}\,. \tag{6.0.82}$$

In particular for $a_1=a_2=b_1=1$ we obtain the geometric series

$$ {}_2F_1\left(1,1;1;x\right)=\sum_{n=0}^{\infty}x^n\,. \tag{6.0.83}$$

For $a_1,\dots a_p,b_1,\dots b_q\in\mathbb{C}$ and $|z|<1$, (6.0.82) generalises to the generalised hypergeometric function

$$ {}_pF_q\left[\begin{matrix}a_1 & a_2 & \cdots & a_p\\ b_1 & b_2 & \cdots & b_q\end{matrix};z\right]\equiv\sum_{n=0}^{\infty}\frac{(a_1)_n\cdots(a_p)_n}{(b_1)_n\cdots(b_q)_n}\frac{z^n}{n!}\,. \tag{6.0.84}$$

Finally we define the regularised hypergeometric

$$ {}_p\tilde{F}_q\equiv\frac{1}{\Gamma(b_1)\cdots\Gamma(b_q)}\,{}_pF_q\left[\begin{matrix}a_1 & a_2 & \cdots & a_p\\ b_1 & b_2 & \cdots & b_q\end{matrix};z\right]\,. \tag{6.0.85}$$

Normalisation condition $m=3$**.** To prove the conjecture (3.4.11) we study

$$ u_\star^{(3)}(\alpha_2,\alpha_3)=4\sqrt{\pi}\sum_{k=0}^{\infty}\left(\frac{20\alpha_3}{3\alpha_2}\right)^k\frac{1}{\Gamma(2+k)}\,{}_3\tilde{F}_2\left(1,-k,1+k;\frac{1}{2}-\frac{k}{2},1-\frac{k}{2};\frac{9\alpha_2^2}{40\alpha_3}\right)\,, \tag{6.0.86}$$

along the path $\gamma_\star^{(3)}$ (3.4.7). We start on the right hand side.

$$ {}_3\tilde{F}_2\left(1,1-k,k;1-\frac{k}{2},\frac{3}{2}-\frac{k}{2};\frac{3}{4}\right)=\lim_{(\rho_1,\rho_2)\to 1}{}_3\tilde{F}_2\left(1,1-k,k;\rho_2-\frac{k}{2},\frac{3\rho_1}{2}-\frac{k}{2};\frac{3}{4}\right)\,. \tag{6.0.87}$$

Using the definition of the regularised hypergeometric function (6.0.85) we obtain

$$ \begin{aligned}{}_3\tilde{F}_2\left(1,1-k,k;\rho_2-\frac{k}{2},\frac{3\rho_1}{2}-\frac{k}{2};\frac{3}{4}\right)&=\frac{1}{\Gamma\left(\rho_2-\frac{k}{2}\right)\Gamma\left(\frac{3\rho_1}{2}-\frac{k}{2}\right)}\\ &\times\left(1+\sum_{\ell=1}^{k-1}(-1)^\ell\left(\frac{3}{4}\right)^\ell\frac{(k)^\ell(k-1)_\ell}{\prod_{n=0}^{\ell-1}\left(\frac{k}{2}-n-\frac{3\rho_1}{2}\right)\left(\frac{k}{2}-n-\rho_2\right)}\right)\,,\end{aligned} \tag{6.0.88}$$

where $(k)_\ell$ is the factorial

$$(k)_\ell \equiv \frac{\Gamma(k+1)}{\Gamma(k-\ell+1)} \ , \tag{6.0.89}$$

leading to

$$u_\star^{(3)}(\alpha_2,\alpha_3)\big|_{\gamma_\star^{(3)}} = 12\sum_{k=1}^{\infty}\frac{(-t)^{k-1}}{\Gamma(k+1)}\sum_{\ell=0}^{k-1}\frac{(-3)^\ell}{3^{2k-1}}\frac{\Gamma(k+\ell)}{\Gamma(k-\ell)\Gamma(2+2\ell-k)} \tag{6.0.90}$$

We are left to show for $k \geq 1$

$$-12\frac{(-1)^k}{\Gamma(k+1)}\sum_{\ell=0}^{k-1}(-3)^\ell\frac{\Gamma(k+\ell)}{3^{2k-1}\Gamma(k-\ell)\Gamma(2+2\ell-k)} = -12(-1)^k\binom{1/3}{k} \ . \tag{6.0.91}$$

By writing out the fractional binomial coefficient we obtain

$$-12(-1)^k\binom{1/3}{k} = -12(-1)^k\frac{\Gamma(4/3)}{\Gamma(k+1)\Gamma(4/3-k)} = -12\frac{(-1)^k}{3^k\Gamma(k+1)}\prod_{n=0}^{k-1}(1-3n) \ . \tag{6.0.92}$$

The last product we write in terms of stirling numbers $s_1(n,k)$ for the first kind. The Stirling numbers $s_1(n,k)$ enumerate $(-1)^{n-k}$ times the number of partitions of the symmetric group S_n with exactly k cycles. By definition, they are also the coefficients of the falling factorial

$$(x)_n \equiv x(x-1)(x-2)\cdots(x-n+1) = \sum_{k=0}^{n} s_1(n,k)x^k \ . \tag{6.0.93}$$

Applying this to the product in (6.0.92) with $x = 1/3$ we find

$$\begin{aligned}\prod_{n=0}^{k-1}(1-3n) &= (1-3)(1-3\times 2)(1-3\times 3)\cdots(1-3(k-1)) = \sum_{n=0}^{k+1}3^{k-n-1}\,s_1(k+1,n)\\ &= \sum_{n=0}^{k+1}3^n\,s_1(k+1,k+1-n) \ ,\end{aligned} \tag{6.0.94}$$

where in going to the last line we substituted $n \to k - n + 1$. We now define

$$L_k \equiv \sum_{n=0}^{k} 3^n s_1(k+1, k+1-n) \ , \quad R_k \equiv k! \sum_{n=0}^{k} 3^n \frac{(-1)^n}{3^k} \binom{n+k}{n} \binom{n}{k-n} \ . \tag{6.0.95}$$

We show that both expressions satisfy

$$L_k = (1-3k) L_{k-1} \ , \quad R_k = (1-3k) R_{k-1} \ , \quad k \geq 1 \ . \tag{6.0.96}$$

We start with L_k. Using the recursion relation for the Stirling numbers

$$s_1(k+1, n+1) = s_1(k, n) - k s_1(k, n+1) \ , \tag{6.0.97}$$

and $s_1(k, 0) = 0$ we find

$$\begin{aligned} L_k &\equiv \sum_{n=0}^{k} 3^n s_1(k+1, k+1-n) = \sum_{n=0}^{k} 3^n s_1(k, k-n) - k \sum_{n=0}^{k} 3^n s_1(k, k+1-n) \\ &= \sum_{n=0}^{k-1} 3^n s_1(k, k-n) + 3^k s_1(k, 0) - k \sum_{n=0}^{k} 3^n s_1(k, k+1-n) = (1-3k) L_{k-1} \ . \end{aligned} \tag{6.0.98}$$

We now show the same recursion equation for R_k. We have

$$R_k \equiv k! \sum_{n=0}^{k} 3^n \frac{(-1)^n}{3^k} \binom{n+k}{n} \binom{n}{k-n} = \frac{(-3)^k}{(-1/3)!} \left(-\frac{1}{3} + k\right)! = \frac{(-3)^k}{(-1/3)!} \Gamma\left(k + \frac{2}{3}\right) \tag{6.0.99}$$

which implies

$$R_{k-1} = -\frac{1}{3} \frac{(-3)^k}{(-1/3)!} \left(-\frac{4}{3} + k\right)! = -\frac{1}{3} \frac{(-3)^k}{(-1/3)!} \Gamma\left(-\frac{1}{3} + k\right) = \frac{1}{(1-3k)} R_k \ . \tag{6.0.100}$$

Since $L_0 = R_0$ and $L_1 = R_1$ so (6.0.96) completes the proof.

On-shell action $m = 3$. We now also rewrite the regularised hypergeometric appearing in (3.4.15). Following the same logic as for the normalisation condition

we have

$$ {}_3\tilde{F}_2\left(1,-k,k;\frac{1}{2}-\frac{k}{2},1-\frac{k}{2};\frac{3}{4}\right)=\sum_{n=1}^{k}(-1)^n\frac{3^n}{2^k\sqrt{\pi}}\frac{k\Gamma(k+n)}{\Gamma(1+2n-k)\Gamma(1-n+k)}\ , \tag{6.0.101} $$

and consequently we can write $\mathcal{F}^{(3)}(\alpha_2,\alpha_3)$ along $\gamma_\star^{(3)}$ as

$$ \mathcal{F}^{(3)}\left(\alpha_2,\alpha_3\right)\big|_{\gamma_\star^{(3)}}=-\sum_{k=1}^{\infty}\frac{(-1)^k}{3^{2k}\Gamma(k+3)}\sum_{\ell=0}^{k-1}\frac{(-3)^{\ell+1}\Gamma(k+\ell)}{\Gamma(k-\ell)\Gamma(3+2\ell-k)}(k+\ell)\,t^k\ . \tag{6.0.102} $$

Comparing to the normalisation condition (6.0.91) we thus indeed obtain the scaling $\sim k^{-\mathbf{10/3}}$.

BTZ as a 2D black hole

Here we briefly review how to view the BTZ black hole in terms of the 2D variables used in the main portions of the draft. First it is useful to cast the black hole in the Fefferman-Graham gauge (4.2.5): Using

$$ \rho^2=\rho_+^2\cosh^2(\eta/\ell-\eta_0/\ell)-\rho_-^2\sinh^2(\eta/\ell-\eta_0/\ell)\ ,\qquad e^{2\eta_0/\ell}\equiv\frac{\rho_+^2-\rho_-^2}{4\ell^2}\ , \tag{6.0.103} $$

in (4.2.14) gives

$$ \begin{aligned} ds_3^2=&\,\mathrm{d}\eta^2+e^{2\eta/\ell}(-\mathrm{d}t^2+\ell^2\mathrm{d}\varphi^2)+\frac{\left(\rho_+-\rho_-\right)^2}{4\ell^2}\left(\mathrm{d}t+\ell\mathrm{d}\varphi\right)^2\\ &+\frac{\left(\rho_++\rho_-\right)^2}{4\ell^2}\left(\mathrm{d}t-\ell\mathrm{d}\varphi\right)^2+\frac{\left(\rho_+^2-\rho_-^2\right)^2}{16\ell^4}e^{-2\eta/\ell}(-\mathrm{d}t^2+\ell^2\mathrm{d}\varphi^2)\ , \end{aligned} \tag{6.0.104} $$

From here we can relate the values of the 2D variables used in Sec. 4.4.1 that lead to the BTZ solution. In relation to (4.3.1) and (4.4.1), we have $\eta=r$, $\varphi=z/\ell$, and $L=\ell$. From (4.2.5) and (4.4.24) we have

$$ \alpha=1\ ,\quad \lambda=1\ ,\quad \nu=0\ , \tag{6.0.105} $$

since $g_{ij}^{(0)}=\eta_{ij}$, and using (4.4.25) gives

$$ \ell^2 m_0=\frac{\rho_+^2+\rho_-^2}{\ell^2}=8G_3\,m\ , $$

$$\ell^2 Q = -\frac{\rho_+\rho_-}{\ell} = -4G_3\, j \ , \tag{6.0.106}$$

where m and j are defined in (4.2.15). For $\rho_- > 0$, as we chose in Sec. 4.2.2, then $Q < 0$.

It is also instructive to map the near horizon geometry of near-extremal BTZ in terms of the variables used in Sec. 4.5.1 for the IR deformations. Using the coordinate system in (6.0.104), the decoupling limit to capture the near horizon is as follows. We first define the near-extremal black hole as

$$\rho_\pm = \rho_0 \pm \delta + O(\delta^2) \ . \tag{6.0.107}$$

Extremality is at $\delta = 0$, and near extremality corresponds to small values of δ. This deviation away from extremality will increase the mass and temperature as described in Sec. 4.2.2. In particular from (4.2.20) we have

$$T = \frac{2\delta}{\pi\ell^2} + O(\delta^2) \ . \tag{6.0.108}$$

The dependence on δ of $\rho_\pm$ is determined by requiring that the angular momentum is fixed for small values of δ. In the coordinate system used here, the horizon is at

$$e^{2\eta_h/\ell} = e^{2\eta_0/\ell} = \frac{\rho_0}{\ell^2}\,\delta + O(\delta^2) \tag{6.0.109}$$

and hence at extremality corresponds to $\eta \to -\infty$. The near horizon region is therefore reached via rescaling our coordinates as

$$\eta \to \eta + \eta_0 \ , \quad t \to \frac{\ell t}{\delta} \ , \quad \varphi \to \varphi + \frac{t}{\delta} \tag{6.0.110}$$

and take the limit $\delta \to 0$ in (6.0.104). The resulting geometry is

$$ds_3^2 \underset{\delta\to 0}{\longrightarrow} \mathrm{d}\eta^2 - \gamma^{nh}_{tt}\mathrm{d}t^2 + r_0^2\left(\mathrm{d}\varphi + A^{nh}_t \mathrm{d}t\right)^2 + O(\delta) \ , \tag{6.0.111}$$

where

$$\gamma^{nh}_{tt} = -(e^{2\rho/\ell} - e^{-2\rho/\ell})^2 \ , \quad A^{nh}_t = -\frac{1}{r_0}(e^{2\rho/\ell} + e^{-2\rho/\ell}) \ . \tag{6.0.112}$$

This solution perfectly agrees with the IR fixed point (4.5.6), where we can identify

$$\alpha_{\rm ir} = -\beta_{\rm ir} = 1 \ , \quad e^{-2\phi_0} = \frac{r_0^2}{\ell^2} \ , \quad Q = -\frac{r_0^2}{\ell^3} \ . \tag{6.0.113}$$

The first correction in δ can also be matched with the irrelevant deformation

(4.5.8). We find

$$\mathcal{Y}_{nh} = r_0\delta\left(e^{2\rho/\ell} + e^{-2\rho/\ell}\right) . \tag{6.0.114}$$

And from here we identify $\lambda_{\text{ir}} = \sigma_{\text{ir}} = r_0\delta$.

Bibliography

Introduction

[1] B. P. Abbott *et al.* [LIGO Scientific and Virgo], "GWTC-1: A Gravitational-Wave Transient Catalog of Compact Binary Mergers Observed by LIGO and Virgo during the First and Second Observing Runs," Phys. Rev. X **9**, no.3, 031040 (2019) doi:10.1103/PhysRevX.9.031040 [arXiv:1811.12907 [astro-ph.HE]].

[2] T. Venumadhav, B. Zackay, J. Roulet, L. Dai and M. Zaldarriaga, "New binary black hole mergers in the second observing run of Advanced LIGO and Advanced Virgo," Phys. Rev. D **101**, no.8, 083030 (2020) doi:10.1103/PhysRevD.101.083030 [arXiv:1904.07214 [astro-ph.HE]].

[3] A. H. Nitz, T. Dent, G. S. Davies, S. Kumar, C. D. Capano, I. Harry, S. Mozzon, L. Nuttall, A. Lundgren and M. Tápai, Astrophys. J. **891**, 123 doi:10.3847/1538-4357/ab733f [arXiv:1910.05331 [astro-ph.HE]].

[4] W. de Sitter, "On the relativity of inertia. Remarks concerning Einstein's latest hypothesis" KNAW, Proceedings, 19 II, 1917, Amsterdam, 1917, pp. 1217-1225

[5] G. W. Gibbons and S. W. Hawking, "Cosmological Event Horizons, Thermodynamics, and Particle Creation," Phys. Rev. D **15**, 2738 (1977). doi:10.1103/PhysRevD.15.2738

[6] J. D. Bekenstein, "Black Holes and Entropy," doi:10.1142/9789811203961_0023

[7] S. W. Hawking, "Particle Creation by Black Holes," Commun. Math. Phys. **43**, 199-220 (1975) [erratum: Commun. Math. Phys. **46**, 206 (1976)] doi:10.1007/BF02345020

[8] A. M. Polyakov, "Quantum Geometry of Bosonic Strings," Phys. Lett. **103B**,

207 (1981). doi:10.1016/0370-2693(81)90743-7

[9] A. Almheiri and J. Polchinski, "Models of AdS_2 backreaction and holography," JHEP **11**, 014 (2015) doi:10.1007/JHEP11(2015)014 [arXiv:1402.6334 [hep-th]].

[10] J. Maldacena, D. Stanford and Z. Yang, "Conformal symmetry and its breaking in two dimensional Nearly Anti-de-Sitter space," PTEP **2016**, no.12, 12C104 (2016) doi:10.1093/ptep/ptw124 [arXiv:1606.01857 [hep-th]].

[11] A. Sen, "Entropy Function and AdS(2) / CFT(1) Correspondence," JHEP **11**, 075 (2008) doi:10.1088/1126-6708/2008/11/075 [arXiv:0805.0095 [hep-th]].

[12] A. Sen, "Quantum Entropy Function from AdS(2)/CFT(1) Correspondence," Int. J. Mod. Phys. A **24**, 4225-4244 (2009) doi:10.1142/S0217751X09045893 [arXiv:0809.3304 [hep-th]].

[13] A. Strominger, "AdS(2) quantum gravity and string theory," JHEP **01**, 007 (1999) doi:10.1088/1126-6708/1999/01/007 [arXiv:hep-th/9809027 [hep-th]].

[14] J. M. Maldacena, J. Michelson and A. Strominger, "Anti-de Sitter fragmentation," JHEP **02**, 011 (1999) doi:10.1088/1126-6708/1999/02/011 [arXiv:hep-th/9812073 [hep-th]].

[15] V. A. Kazakov, "The Appearance of Matter Fields from Quantum Fluctuations of 2D Gravity," Mod. Phys. Lett. A **4**, 2125 (1989). doi:10.1142/S0217732389002392

[16] M. Staudacher, "The Yang-lee Edge Singularity on a Dynamical Planar Random Surface," Nucl. Phys. B **336**, 349 (1990). doi:10.1016/0550-3213(90)90432-D

[17] T. Banks, B. Fiol and A. Morisse, "Towards a quantum theory of de Sitter space," JHEP **0612** (2006) 004 doi:10.1088/1126-6708/2006/12/004 [hep-th/0609062];

[18] M. K. Parikh and E. P. Verlinde, "De Sitter holography with a finite number of states," JHEP **0501** (2005) 054 doi:10.1088/1126-6708/2005/01/054 [hep-th/0410227];

[19] X. Dong, B. Horn, E. Silverstein and G. Torroba, Class. Quant. Grav. **27**, 245020 (2010) doi:10.1088/0264-9381/27/24/245020 [arXiv:1005.5403 [hep-th]].

[20] A. B. Zamolodchikov, "On The Entropy Of Random Surfaces," Phys. Lett. **117B**, 87 (1982). doi:10.1016/0370-2693(82)90879-6

[21] Wigner, E. Characteristic vectors of bordered matrices with infinite dimensions. Ann. of Math. v.62 (1955) no.3, 548-564; Wigner, E. Characteristic vectors of bordered matrices of infinite dimensions II. Ann. of Math. v.65 (1957) no.2, 203-207; Wigner, E. On the distribution of the roots of certain symmetric matrices. Ann. of Math. v.67 (1958) no.2, 325-326

[22] Wigner, E. Random Matrices in Physics. SIAM Reviews v.9 (1967) No. 1, 1-23

[23] F. J. Dyson, "The Threefold Way. Algebraic Structure of Symmetry Groups and Ensembles in Quantum Mechanics," J. Math. Phys. **3**, 6 (1962). doi:10.1063/1.1703863; F. J. Dyson, "Statistical theory of the energy levels of complex systems. I," J. Math. Phys. **3**, 140 (1962). doi:10.1063/1.1703773

[24] G. 't Hooft, "A Planar Diagram Theory for Strong Interactions," Nucl. Phys. B **72**, 461 (1974). doi:10.1016/0550-3213(74)90154-0

[25] E. Brezin, C. Itzykson, G. Parisi and J. B. Zuber, "Planar Diagrams," Commun. Math. Phys. **59**, 35 (1978). doi:10.1007/BF01614153

[26] M. L. Mehta, "A Method of Integration Over Matrix Variables," Commun. Math. Phys. **79**, 327 (1981). doi:10.1007/BF01208498

[27] A. M. Polyakov, A. A. Belavin and A. B. Zamolodchikov, "Infinite Conformal Symmetry of Critical Fluctuations in Two-Dimensions," J. Statist. Phys. **34**, 763 (1984). doi:10.1007/BF01009438

[28] D. Friedan, Z. A. Qiu and S. H. Shenker, "Conformal Invariance And Critical Exponents In Two-dimensions," Preprint - FRIEDAN, D. (86,REC.AUG.) 3p

[29] J. Distler and H. Kawai, "Conformal Field Theory and 2D Quantum Gravity," Nucl. Phys. B **321**, 509 (1989). doi:10.1016/0550-3213(89)90354-4

[30] F. David, "Conformal Field Theories Coupled to 2D Gravity in the Conformal Gauge," Mod. Phys. Lett. A **3**, 1651 (1988). doi:10.1142/S0217732388001975

[31] G. W. Moore, "Double scaled field theory at c = 1," Nucl. Phys. B **368**, 557 (1992). doi:10.1016/0550-3213(92)90214-V

[32] G. W. Moore, M. R. Plesser and S. Ramgoolam, "Exact S matrix for 2-D string theory," Nucl. Phys. B **377**, 143 (1992) doi:10.1016/0550-3213(92)90020-C [hep-th/9111035].

[33] N. Seiberg, "Notes on quantum Liouville theory and quantum gravity," Prog. Theor. Phys. Suppl. **102**, 319 (1990). doi:10.1143/PTPS.102.319

[34] H. Dorn and H. J. Otto, "Two and three point functions in Liouville the-

ory," Nucl. Phys. B **429**, 375 (1994) doi:10.1016/0550-3213(94)00352-1 [hep-th/9403141].

[35] J. Teschner, "Liouville theory revisited," Class. Quant. Grav. **18**, R153 (2001) doi:10.1088/0264-9381/18/23/201 [hep-th/0104158].

[36] A. B. Zamolodchikov and A. B. Zamolodchikov, "Structure constants and conformal bootstrap in Liouville field theory," Nucl. Phys. B **477**, 577 (1996) doi:10.1016/0550-3213(96)00351-3 [hep-th/9506136].

[37] A. B. Zamolodchikov, "Three-point function in the minimal Liouville gravity," Theor. Math. Phys. **142**, 183 (2005) doi:10.1007/s11232-005-0003-3 [hep-th/0505063].

[38] B. Balthazar, V. A. Rodriguez and X. Yin, "The $c = 1$ string theory S-matrix revisited," JHEP **1904**, 145 (2019) doi:10.1007/JHEP04(2019)145 [arXiv:1705.07151 [hep-th]].

[39] M. Banados, C. Teitelboim and J. Zanelli, "The Black hole in three-dimensional space-time," Phys. Rev. Lett. **69**, 1849-1851 (1992) doi:10.1103/PhysRevLett.69.1849 [arXiv:hep-th/9204099 [hep-th]].

[40] A. Almheiri and B. Kang, "Conformal Symmetry Breaking and Thermodynamics of Near-Extremal Black Holes," JHEP **10**, 052 (2016) doi:10.1007/JHEP10(2016)052 [arXiv:1606.04108 [hep-th]].

[41] J. D. Brown and M. Henneaux, "Central Charges in the Canonical Realization of Asymptotic Symmetries: An Example from Three-Dimensional Gravity," Commun. Math. Phys. **104**, 207-226 (1986) doi:10.1007/BF01211590

[42] B. Sahoo and A. Sen, JHEP **07**, 008 (2006) doi:10.1088/1126-6708/2006/07/008 [arXiv:hep-th/0601228 [hep-th]].

[43] G. Guralnik, A. Iorio, R. Jackiw and S. Y. Pi, Annals Phys. **308**, 222-236 (2003) doi:10.1016/S0003-4916(03)00142-8 [arXiv:hep-th/0305117 [hep-th]].

[44] S. Deser, R. Jackiw and S. Templeton, Annals Phys. **140**, 372-411 (1982) [erratum: Annals Phys. **185**, 406 (1988)] doi:10.1016/0003-4916(82)90164-6

[45] S. Deser, R. Jackiw and S. Templeton, Phys. Rev. Lett. **48**, 975-978 (1982) doi:10.1103/PhysRevLett.48.975

[46] S. Deser and X. Xiang, Phys. Lett. B **263**, 39-43 (1991) doi:10.1016/0370-2693(91)91704-Y

[47] J. M. Maldacena, "The Large N limit of superconformal field theories and supergravity," Int. J. Theor. Phys. **38** (1999) 1113 [Adv. Theor. Math. Phys.

2 (1998) 231] doi:10.1023/A:1026654312961, 10.4310/ATMP.1998.v2.n2.a1 [hep-th/9711200].

Matrix models & two-dimensional quantum gravity

A. History & Philosophy

[48] N. Bohr, "Neutron Capture and Nuclear Constitution," Nature **137**, 344 (1936). doi:10.1038/137344a0

[49] M. L. Mehta, "On the statistical properties of the level-spacings in nuclear spectra, " Nuclear Phys. 18, 395 (1960); M. L. Mehta and M. Gaudin, "On the density of eigenvalues of a random matrix," Nuclear Phys. 18, 420 (1960); , Nucl. Phys. ; M. Gaudin, "On the distribution of the roots of certain symmetric matrices," Nuclear Phys. 25, 447 (1961)., Nucl. Phys.

[50] T. Regge, "General Relativity Without Coordinates," Nuovo Cim. **19**, 558 (1961). doi:10.1007/BF02733251

[51] Berry Michael Victor, Tabor M. and Ziman John Michael "Level clustering in the regular spectrum," 356 Proc. R. Soc. Lond. A http://doi.org/10.1098/rspa.1977.0140

[52] O. Bohigas, M. J. Giannoni and C. Schmit, "Characterization of chaotic quantum spectra and universality of level fluctuation laws," Phys. Rev. Lett. **52**, 1 (1984). doi:10.1103/PhysRevLett.52.1

[53] C. G. Callan, Jr., E. J. Martinec, M. J. Perry and D. Friedan, "Strings in Background Fields," Nucl. Phys. B **262**, 593 (1985). doi:10.1016/0550-3213(85)90506-1; J. Scherk and J. H. Schwarz, "Dual Models for Non-hadrons," Nucl. Phys. B **81**, 118-144 (1974) doi:10.1016/0550-3213(74)90010-8; T. Yoneya, "Connection of Dual Models to Electrodynamics and Gravidynamics," Prog. Theor. Phys. **51**, 1907-1920 (1974) doi:10.1143/PTP.51.1907

[54] J. Ambjørn, B. Durhuus and J. Frohlich, "Diseases of Triangulated Random Surface Models, and Possible Cures," Nucl. Phys. B **257**, 433 (1985). doi:10.1016/0550-3213(85)90356-6; J. Ambjørn, B. Durhuus, J. Frohlich and P. Orland, "The Appearance of Critical Dimensions in Regulated String Theories," Nucl. Phys. B **270**, 457 (1986). doi:10.1016/0550-3213(86)90563-8

[55] F. David, "A Model of Random Surfaces with Nontrivial Critical Behavior," Nucl. Phys. B **257**, 543 (1985). doi:10.1016/0550-3213(85)90363-3; A. Billoire and F. David, "Scaling Properties of Randomly Triangulated Planar Random Surfaces: A Numerical Study," Nucl. Phys. B **275**, 617 (1986). doi:10.1016/0550-3213(86)90577-8

[56] V. A. Kazakov, A. A. Migdal and I. K. Kostov, "Critical Properties of Randomly Triangulated Planar Random Surfaces," Phys. Lett. **157B**, 295 (1985). doi:10.1016/0370-2693(85)90669-0; V. Kazakov, "Bilocal Regularization of Models of Random Surfaces," Phys. Lett. B **150**, 282-284 (1985) doi:10.1016/0370-2693(85)91011-1

[57] D. V. Boulatov, V. A. Kazakov, I. K. Kostov and A. A. Migdal, "Analytical and Numerical Study of the Model of Dynamically Triangulated Random Surfaces," Nucl. Phys. B **275**, 641 (1986). doi:10.1016/0550-3213(86)90578-X

[58] M. Mezard, G. Parisi, and M. A. Virasoro. Spin Glass Theory and Beyond. vol. 9, Lecture Notes in Physics, (World Scientific, 1987) Google books. 9971501155

[59] E. Witten, "Two-dimensional gravity and intersection theory on moduli space," Surveys Diff. Geom. **1**, 243 (1991). doi:10.4310/SDG.1990.v1.n1.a5

[60] M. Kontsevich, "Intersection theory on the moduli space of curves and the matrix Airy function," Commun. Math. Phys. **147**, 1 (1992). doi:10.1007/BF02099526

[61] M. Mirzakhani, "Simple geodesics and Weil-Petersson volumes of moduli spaces of bordered Riemann surfaces," Invent. Math. **167**, no. 1, 179 (2006). doi:10.1007/s00222-006-0013-2

[62] B. Eynard and N. Orantin, "Invariants of algebraic curves and topological expansion," Commun. Num. Theor. Phys. **1**, 347 (2007) doi:10.4310/CNTP.2007.v1.n2.a4 [math-ph/0702045].

B. Reviews on matrix models and related topics

[63] D. Anninos and B. Mühlmann, "Notes on Matrix Models," J. Stat. Mech. **2008**, 083109 (2020) doi:10.1088/1742-5468/aba499 [arXiv:2004.01171 [hep-th]].

[64] M.L.Mehta, "Random Matrices (Revised and Enlarged Second Edition)", Academic Press, 1991, isbn: 978-0-12-488051-1, doi: 10.1016/B978-0-12-488051-1.50004-4

[65] I. R. Klebanov, "String theory in two-dimensions," In *Trieste 1991, Proceedings, String theory and quantum gravity '91* 30-101 and Princeton Univ. - PUPT-1271 (91/07,rec.Oct.) 72 p [hep-th/9108019].

[66] P. H. Ginsparg and G. W. Moore, "Lectures on 2-D gravity and 2-D string theory," Yale Univ. New Haven - YCTP-P23-92 (92,rec.Apr.93) 197 p. Los Alamos Nat. Lab. - LA-UR-92-3479 (92,rec.Apr.93) 197 p. e: LANL hep-

th/9304011 [hep-th/9304011].

[67] J. Polchinski, "What is string theory?," hep-th/9411028.

[68] P. Di Francesco, P. H. Ginsparg and J. Zinn-Justin, "2-D Gravity and random matrices," Phys. Rept. **254**, 1 (1995) doi:10.1016/0370-1573(94)00084-G [hep-th/9306153].

[69] Polchinski, J. (1998). String Theory. Vol. 1: An Introduction to the Bosonic String. (Cambridge Monographs on Mathematical Physics). Cambridge: Cambridge University Press. doi:10.1017/CBO9780511816079

[70] W. Taylor, "M(atrix) Theory: Matrix Quantum Mechanics as a Fundamental Theory," Rev. Mod. Phys. **73**, 419 (2001) doi:10.1103/RevModPhys.73.419 [hep-th/0101126].

[71] G. 't Hooft, "Large N," doi:10.1142/97898127769140001 hep-th/0204069.

[72] S. Alexandrov, "Matrix quantum mechanics and two-dimensional string theory in nontrivial backgrounds," hep-th/0311273.

[73] Y. Nakayama, "Liouville field theory: A Decade after the revolution," Int. J. Mod. Phys. A **19**, 2771 (2004) doi:10.1142/S0217751X04019500 [hep-th/0402009].

[74] M. Marino, "Les Houches lectures on matrix models and topological strings," hep-th/0410165.

[75] E. J. Martinec, "Matrix models and 2D string theory," hep-th/0410136.

[76] M. Marino, "Lectures on non-perturbative effects in large N gauge theories, matrix models and strings," Fortsch. Phys. **62**, 455 (2014) doi:10.1002/prop.201400005 [arXiv:1206.6272 [hep-th]].

[77] B. Eynard, T. Kimura and S. Ribault, "Random matrices," arXiv:1510.04430 [math-ph].

C. Large N matrices

[78] G. 't Hooft, "A Two-Dimensional Model for Mesons," Nucl. Phys. B **75**, 461 (1974). doi:10.1016/0550-3213(74)90088-1

[79] D. Bessis, "A New Method in the Combinatorics of the Topological Expansion," Commun. Math. Phys. **69**, 147 (1979). doi:10.1007/BF01221445

[80] D. Bessis, C. Itzykson and J. B. Zuber, "Quantum field theory techniques in graphical enumeration," Adv. Appl. Math. **1**, 109 (1980). doi:10.1016/0196-8858(80)90008-1

[81] L. G. Yaffe, "Large n Limits as Classical Mechanics," Rev. Mod. Phys. **54**, 407 (1982). doi:10.1103/RevModPhys.54.407

[82] J. Ambjørn, T. Budd and Y. Makeenko, "Generalized multicritical one-matrix models," Nucl. Phys. B **913**, 357 (2016) doi:10.1016/j.nuclphysb.2016.09.013 [arXiv:1604.04522 [hep-th]].

i) Loop equations

[83] A. M. Polyakov, Nucl. Phys. B **164**, 171-188 (1980) doi:10.1016/0550-3213(80)90507-6

[84] Dyson-Schwinger equations approach to the large-N limit: Model systems and string representation of Yang-Mills theory, Wadia, Spenta R., Phys. Rev. D, 1981 doi: 10.1103/PhysRevD.24.970,

[85] A. A. Migdal, "Loop Equations and 1/N Expansion," Phys. Rept. **102**, 199 (1983). doi:10.1016/0370-1573(83)90076-5

[86] J. Ambjørn and Y. M. Makeenko, "Properties of Loop Equations for the Hermitean Matrix Model and for Two-dimensional Quantum Gravity," Mod. Phys. Lett. A **5**, 1753 (1990). doi:10.1142/S0217732390001992

[87] V. Kazakov, "A Simple Solvable Model of Quantum Field Theory of Open Strings," Phys. Lett. B **237**, 212-215 (1990) doi:10.1016/0370-2693(90)91431-A

[88] I. K. Kostov, "Exactly Solvable Field Theory of $D = 0$ Closed and Open Strings," Phys. Lett. B **238**, 181 (1990). doi:10.1016/0370-2693(90)91717-P

[89] R. Dijkgraaf, H. L. Verlinde and E. P. Verlinde, "Loop equations and Virasoro constraints in nonperturbative 2-D quantum gravity," Nucl. Phys. B **348**, 435 (1991). doi:10.1016/0550-3213(91)90199-8

[90] E. J. Martinec, "On the origin of integrability in matrix models," Commun. Math. Phys. **138**, 437 (1991). doi:10.1007/BF02102036

[91] J. Ambjørn, L. Chekhov, C. F. Kristjansen and Y. Makeenko, "Matrix model calculations beyond the spherical limit," Nucl. Phys. B **404**, 127 (1993) Erratum: [Nucl. Phys. B **449**, 681 (1995)] doi:10.1016/0550-3213(93)90476-6, 10.1016/0550-3213(95)00391-5 [hep-th/9302014].

[92] M. Staudacher, "Combinatorial solution of the two matrix model," Phys. Lett. B **305**, 332 (1993) doi:10.1016/0370-2693(93)91063-S [hep-th/9301038].

[93] H. W. Lin, "Bootstraps to Strings: Solving Random Matrix Models with Positivity," arXiv:2002.08387 [hep-th].

D. Non-perturbative effects

[94] I. M. Gelfand and L. A. Dikii, "Asymptotic behavior of the resolvent of Sturm-Liouville equations and the algebra of the Korteweg-De Vries equations," Russ. Math. Surveys **30**, no. 5, 77 (1975) [Usp. Mat. Nauk **30**, no. 5, 67 (1975)]. doi:10.1070/RM1975v030n05ABEH001522

[95] T. Banks, M. R. Douglas, N. Seiberg and S. H. Shenker, "Microscopic and Macroscopic Loops in Nonperturbative Two-dimensional Gravity," Phys. Lett. B **238**, 279 (1990). doi:10.1016/0370-2693(90)91736-U

[96] D. J. Gross and A. A. Migdal, "A Nonperturbative Treatment of Two-dimensional Quantum Gravity," Nucl. Phys. B **340**, 333 (1990). doi:10.1016/0550-3213(90)90450-R

[97] S. H. Shenker, 1990 "The Strength of nonperturbative effects in string theory," In *Brezin, E. (ed.), Wadia, S.R. (ed.): The large N expansion in quantum field theory and statistical physics* 809-819

[98] A. Jevicki and T. Yoneya, "Action Principle for Strings in Less Than One-dimension," Mod. Phys. Lett. A **5**, 1615 (1990). doi:10.1142/S0217732390001840

[99] P. H. Ginsparg, M. Goulian, M. R. Plesser and J. Zinn-Justin, "(p, q) STRING ACTIONS," Nucl. Phys. B **342**, 539 (1990). doi:10.1016/0550-3213(90)90326-9

[100] P. H. Ginsparg and J. Zinn-Justin, "Large order behavior of nonperturbative gravity," Phys. Lett. B **255**, 189 (1991). doi:10.1016/0370-2693(91)90234-H

[101] B. Eynard and J. Zinn-Justin, "Large order behavior of 2-D gravity coupled to d $<$ 1 matter," Phys. Lett. B **302**, 396 (1993) doi:10.1016/0370-2693(93)90416-F [hep-th/9301004].

i) Single matrix model

[102] M. R. Douglas and S. H. Shenker, "Strings in Less Than One-Dimension," Nucl. Phys. B **335**, 635 (1990). doi:10.1016/0550-3213(90)90522-F

[103] D. J. Gross and A. A. Migdal, "Nonperturbative Two-Dimensional Quantum Gravity," Phys. Rev. Lett. **64**, 127 (1990). doi:10.1103/PhysRevLett.64.127

[104] E. Brezin and V. A. Kazakov, "Exactly Solvable Field Theories of Closed Strings," Phys. Lett. B **236**, 144 (1990). doi:10.1016/0370-2693(90)90818-Q

[105] F. David, "Loop Equations and Nonperturbative Effects in Two-dimensional Quantum Gravity," Mod. Phys. Lett. A **5**, 1019 (1990). doi:10.1142/S0217732390001141

[106] F. David, "Nonperturbative effects in matrix models and vacua of two-dimensional gravity," Phys. Lett. B **302**, 403 (1993) doi:10.1016/0370-2693(93)90417-G [hep-th/9212106].

[107] A.A. Kapaev, "Quasi-linear Stokes phenomenon for the Painlevé first equation", 2004

[108] C. M. Bender and J. Komijani, "Painlevé Transcendents and PT-Symmetric Hamiltonians," J. Phys. A **48**, no. 47, 475202 (2015) doi:10.1088/1751-8113/48/47/475202 [arXiv:1502.04089 [math-ph]].

ii) Two matrix model

[109] D. J. Gross and A. A. Migdal, "Nonperturbative Solution of the Ising Model on a Random Surface," Phys. Rev. Lett. **64**, 717 (1990). doi:10.1103/PhysRevLett.64.717

[110] E. Brezin, M. R. Douglas, V. Kazakov and S. H. Shenker, "The Ising Model Coupled to 2-D Gravity: A Nonperturbative Analysis," Phys. Lett. B **237**, 43 (1990). doi:10.1016/0370-2693(90)90458-I

[111] M. R. Douglas, "Strings in Less Than One-dimension and the Generalized K^-D^-V Hierarchies," Phys. Lett. B **238**, 176 (1990). doi:10.1016/0370-2693(90)91716-O

[112] C. Crnkovic, P. H. Ginsparg and G. W. Moore, "The Ising Model, the Yang-Lee Edge Singularity, and 2D Quantum Gravity," Phys. Lett. B **237**, 196 (1990). doi:10.1016/0370-2693(90)91428-E

iii) Eigenvalues & instantons

[113] M. Hanada, M. Hayakawa, N. Ishibashi, H. Kawai, T. Kuroki, Y. Matsuo and T. Tada, "Loops versus matrices: The Nonperturbative aspects of noncritical string," Prog. Theor. Phys. **112**, 131 (2004) doi:10.1143/PTP.112.131 [hep-th/0405076].

[114] H. Kawai, T. Kuroki and Y. Matsuo, "Universality of nonperturbative effect in type 0 string theory," Nucl. Phys. B **711**, 253 (2005) doi:10.1016/j.nuclphysb.2005.01.002 [hep-th/0412004].

[115] N. Ishibashi and A. Yamaguchi, "On the chemical potential of D-instantons in c=0 noncritical string theory," JHEP **0506**, 082 (2005) doi:10.1088/1126-6708/2005/06/082 [hep-th/0503199].

[116] A. Sato and A. Tsuchiya, "ZZ brane amplitudes from matrix models," JHEP **0502**, 032 (2005) doi:10.1088/1126-6708/2005/02/032 [hep-th/0412201].

E. Two large N matrices

[117] M. A. Bershadsky and A. A. Migdal, "Ising Model of a Randomly Triangulated Random Surface as a Definition of Fermionic String Theory," Phys. Lett. B **174**, 393 (1986). doi:10.1016/0370-2693(86)91023-3

[118] V. A. Kazakov, "Ising model on a dynamical planar random lattice: Exact solution," Phys. Lett. A **119**, 140 (1986). doi:10.1016/0375-9601(86)90433-0

[119] D. V. Boulatov and V. A. Kazakov, "The Ising Model on Random Planar Lattice: The Structure of Phase Transition and the Exact Critical Exponents," Phys. Lett. B **186**, 379 (1987). doi:10.1016/0370-2693(87)90312-1

[120] T. Tada, "(q,p) critical point from two matrix models," Phys. Lett. B **259**, 442 (1991). doi:10.1016/0370-2693(91)91654-E

[121] M. R. Douglas and M. Li, "Free variables and the two matrix model," Phys. Lett. B **348**, 360 (1995) doi:10.1016/0370-2693(95)00176-L [hep-th/9412203].

[122] P. Zinn-Justin and J. B. Zuber, "On some integrals over the U(N) unitary group and their large N limit," J. Phys. A **36**, 3173 (2003) doi:10.1088/0305-4470/36/12/318 [math-ph/0209019].

F. Matrix quantum mechanics

[123] V. Kazakov and A. A. Migdal, "Recent Progress in the Theory of Noncritical Strings," Nucl. Phys. B **311**, 171 (1988) doi:10.1016/0550-3213(88)90146-0

[124] E. Brezin, V. A. Kazakov and A. B. Zamolodchikov, "Scaling Violation in a Field Theory of Closed Strings in One Physical Dimension," Nucl. Phys. B **338**, 673 (1990). doi:10.1016/0550-3213(90)90647-V

[125] G. Parisi, "On the One-dimensional Discretized String," Phys. Lett. B **238**, 209-212 (1990) doi:10.1016/0370-2693(90)91722-N

[126] D. J. Gross and N. Miljkovic, "A Nonperturbative Solution of $D = 1$ String Theory," Phys. Lett. B **238**, 217 (1990). doi:10.1016/0370-2693(90)91724-P

[127] P. H. Ginsparg and J. Zinn-Justin, "2-d GRAVITY + 1-d MATTER," Phys. Lett. B **240**, 333 (1990). doi:10.1016/0370-2693(90)91108-N

[128] S. R. Das and A. Jevicki, "String Field Theory and Physical Interpretation of $D = 1$ Strings," Mod. Phys. Lett. A **5**, 1639 (1990). doi:10.1142/S0217732390001888

[129] D. J. Gross and I. R. Klebanov, "Fermionic string field theory of c = 1 two-dimensional quantum gravity," Nucl. Phys. B **352**, 671 (1991). doi:10.1016/0550-3213(91)90103-5

[130] A. M. Sengupta and S. R. Wadia, Int. J. Mod. Phys. A **6**, 1961-1984 (1991) doi:10.1142/S0217751X91000988

[131] E. Brezin, "Two-dimensional quantum gravity," 1990, Conf. Proc. C **900802V1** [Conf. Proc. C **900802V1**, C900802V1:262].

[132] D. Boulatov and V. Kazakov, "One-dimensional string theory with vortices as the upside down matrix oscillator," Int. J. Mod. Phys. A **8**, 809 (1993) doi:10.1142/S0217751X9300031X [hep-th/0012228].

[133] J. Polchinski, "Effective field theory and the Fermi surface," In *Boulder 1992, Proceedings, Recent directions in particle theory* 235-274, and Calif. Univ. Santa Barbara - NSF-ITP-92-132 (92,rec.Nov.) 39 p. (220633) Texas Univ. Austin - UTTG-92-20 (92,rec.Nov.) 39 p [hep-th/9210046].

[134] T. Takayanagi and N. Toumbas, "A Matrix model dual of type 0B string theory in two-dimensions," JHEP **0307**, 064 (2003) doi:10.1088/1126-6708/2003/07/064 [hep-th/0307083].

[135] M. R. Douglas, I. R. Klebanov, D. Kutasov, J. M. Maldacena, E. J. Martinec and N. Seiberg, 2003 "A New hat for the c=1 matrix model," In *Shifman, M. (ed.) et al.: From fields to strings, vol. 3* 1758-1827 [hep-th/0307195].

[136] R. Dijkgraaf, G. W. Moore and R. Plesser, "The Partition function of 2-D string theory," Nucl. Phys. B **394**, 356 (1993) doi:10.1016/0550-3213(93)90019-L [hep-th/9208031].

[137] J. McGreevy and H. L. Verlinde, "Strings from tachyons: The c=1 matrix reloaded," JHEP **0312**, 054 (2003) doi:10.1088/1126-6708/2003/12/054 [hep-th/0304224].

[138] J. M. Maldacena, "Long strings in two dimensional string theory and non-singlets in the matrix model," JHEP **0509**, 078 (2005) [Int. J. Geom. Meth. Mod. Phys. **3**, 1 (2006)] doi:10.1088/1126-6708/2005/09/078, 10.1142/S0219887806001053 [hep-th/0503112].

[139] , Hamiltonian group actions and dynamical systems of calogero type, David Kazhdan and Bertram Kostant and Shlomo Sternberg, 1978

[140] A. P. Polychronakos, J. Phys. A **39**, 12793 (2006) doi:10.1088/0305-4470/39/41/S07 [hep-th/0607033].

i) $c = 1$ scattering

[141] G. Mandal, A. M. Sengupta and S. R. Wadia, "Interactions and scattering in d = 1 string theory," Mod. Phys. Lett. A **6**, 1465 (1991). doi:10.1142/S0217732391001585

[142] J. Polchinski, "Classical limit of (1+1)-dimensional string theory," Nucl. Phys. B **362**, 125 (1991). doi:10.1016/0550-3213(91)90559-G

G. 2d quantum gravity and Liouville theory

[143] V. G. Knizhnik, A. M. Polyakov and A. B. Zamolodchikov, "Fractal Structure of 2D Quantum Gravity," Mod. Phys. Lett. A **3**, 819 (1988). doi:10.1142/S0217732388000982

[144] J. Polchinski, "Critical Behavior of Random Surfaces in One-dimension," Nucl. Phys. B **346**, 253 (1990). doi:10.1016/0550-3213(90)90280-Q

[145] K. Krasnov, "Holography and Riemann surfaces," Adv. Theor. Math. Phys. **4**, 929 (2000) doi:10.4310/ATMP.2000.v4.n4.a5 [hep-th/0005106].

[146] A. Zamolodchikov, "Scaling Lee-Yang model on a sphere. 1. Partition function," JHEP **0207**, 029 (2002) doi:10.1088/1126-6708/2002/07/029 [hep-th/0109078].

[147] A. B. Zamolodchikov, "Perturbed conformal field theory on fluctuating sphere," 2005, hep-th/0508044.

[148] D. Harlow, J. Maltz and E. Witten, "Analytic Continuation of Liouville Theory," JHEP **1112**, 071 (2011) doi:10.1007/JHEP12(2011)071 [arXiv:1108.4417 [hep-th]].

[149] P. Saad, S. H. Shenker and D. Stanford, [arXiv:1903.11115 [hep-th]].

[150] D. Anninos, T. Anous, P. de Lange and G. Konstantinidis, "Conformal quivers and melting molecules," JHEP **1503**, 066 (2015) doi:10.1007/JHEP03(2015)066 [arXiv:1310.7929 [hep-th]].

[151] F. Benini, K. Hristov and A. Zaffaroni, "Black hole microstates in AdS_4 from supersymmetric localization," JHEP **1605** (2016) 054 doi:10.1007/JHEP05(2016)054 [arXiv:1511.04085 [hep-th]].

[152] A. Cabo-Bizet and S. Murthy, "Supersymmetric phases of 4d $N = 4$ SYM at large N," arXiv:1909.09597 [hep-th].

[153] D. Anninos, T. Anous and F. Denef, "Disordered Quivers and Cold Horizons," JHEP **1612**, 071 (2016) doi:10.1007/JHEP12(2016)071 [arXiv:1603.00453 [hep-th]].

i) Correlation functions in Liouville theory

[154] J. Liu and J. Polchinski, "Renormalization of the Mobius Volume," Phys. Lett. B **203**, 39 (1988). doi:10.1016/0370-2693(88)91566-3

[155] A. B. Zamolodchikov, "Irreversibility of the Flux of the Renormalization Group in a 2D Field Theory," JETP Lett. **43**, 730-732 (1986)

[156] C. V. Johnson, Phys. Rev. D **101**, no.10, 106023 (2020) doi:10.1103/PhysRevD.101.106023 [arXiv:1912.03637 [hep-th]].

[157] C. Holzhey, F. Larsen and F. Wilczek, "Geometric and renormalized entropy in conformal field theory," Nucl. Phys. B **424**, 443 (1994) doi:10.1016/0550-3213(94)90402-2 [hep-th/9403108].

[158] P. Calabrese and J. L. Cardy, "Entanglement entropy and quantum field theory," J. Stat. Mech. **0406**, P06002 (2004) doi:10.1088/1742-5468/2004/06/P06002 [hep-th/0405152].

[159] H. Casini, M. Huerta and R. C. Myers, "Towards a derivation of holographic entanglement entropy," JHEP **1105**, 036 (2011) doi:10.1007/JHEP05(2011)036 [arXiv:1102.0440 [hep-th]].

ii) Minimal Liouville Theory

[160] N. Seiberg and D. Shih, "Minimal string theory," Comptes Rendus Physique **6**, 165 (2005) doi:10.1016/j.crhy.2004.12.007 [hep-th/0409306].

[161] A. Belavin and A. Zamolodchikov, "Polyakov's string: Twenty five years after. Proceedings," 2005 hep-th/0510214.

[162] A. A. Belavin and A. B. Zamolodchikov, "Integrals over moduli spaces, ground ring, and four-point function in minimal Liouville gravity," Theor. Math. Phys. **147**, 729 (2006) [Teor. Mat. Fiz. **147**, 339 (2006)]. doi:10.1007/s11232-006-0075-8

[163] G. W. Moore, N. Seiberg and M. Staudacher, "From loops to states in 2-D quantum gravity," Nucl. Phys. B **362**, 665-709 (1991) doi:10.1016/0550-3213(91)90548-C

[164] G. W. Moore and N. Seiberg, "From loops to fields in 2-D quantum gravity," Int. J. Mod. Phys. A **7**, 2601-2634 (1992) doi:10.1142/S0217751X92001174

[165] A. A. Belavin and V. A. Belavin, "Frobenius manifolds, Integrable Hierarchies and Minimal Liouville Gravity," JHEP **09**, 151 (2014) doi:10.1007/JHEP09(2014)151 [arXiv:1406.6661 [hep-th]].

[166] A. A. Belavin and A. B. Zamolodchikov, "On Correlation Numbers in 2D Minimal Gravity and Matrix Models," J. Phys. A **42**, 304004 (2009) doi:10.1088/1751-8113/42/30/304004 [arXiv:0811.0450 [hep-th]].

[167] A. Belavin and C. Rim, "Bulk one-point function on disk in one-matrix

model," Phys. Lett. B **687**, 264 (2010) doi:10.1016/j.physletb.2010.03.020 [arXiv:1001.4356 [hep-th]].

[168] V. Belavin, "Torus Amplitudes in Minimal Liouville Gravity and Matrix Models," Phys. Lett. B **698**, 86 (2011) doi:10.1016/j.physletb.2011.03.003 [arXiv:1010.5508 [hep-th]].

[169] V. Belavin and Y. Rud, J. Phys. A **48**, no. 18, 18FT01 (2015) doi:10.1088/1751-8113/48/18/18FT01 [arXiv:1502.05575 [hep-th]].

iii) Minimal models

[170] A. Rocha-Caridi, in "Vertex Operators in Mathematics and Physics" Proceedings of a Conference November 10–17, 1983 Editors: Lepowsky, J., Mandelstam, S., Singer, I.M. (Eds.

[171] J. L. Cardy, "Conformal Invariance and the Yang-lee Edge Singularity in Two-dimensions," Phys. Rev. Lett. **54**, 1354-1356 (1985) doi:10.1103/PhysRevLett.54.1354

[172] L. Alvarez-Gaume, G. Sierra and C. Gomez, "Topics in conformal field theory," CERN-TH-5540-89.

[173] P. di Francesco, P. Mathieu, D. Sénéchal, "Conformal field theory," Springer Science+ Business Media, LLC, 1997

[174] L. P. Kadanoff, "Scaling laws for Ising models near T(c)," Physics Physique Fizika **2**, 263-272 (1966) doi:10.1103/PhysicsPhysiqueFizika.2.263

[175] Yang, C. N. , Lee, T. D. "Statistical Theory of Equations of State and Phase Transitions. I. Theory of Condensation," Phys. Rev.,87, ssue = 3, 404–409pg, 1952, doi = 10.1103/PhysRev.87.404

[176] G. von Gehlen, "NonHermitian tricriticality in the Blume-Capel model with imaginary field," [arXiv:hep-th/9402143 [hep-th]].

[177] M. Blume, "Theory of the First-Order Magnetic Phase Change in UO_2," Phys. Rev. 141, issue 2, pages: 517-524, 1966 doi = 10.1103/PhysRev.141.517; H.W. Capel, "On the possibility of first-order phase transitions in Ising systems of triplet ions with zero-field splitting", Physica 32, number 5, pages: 966-988, 1966 doi = 10.1016/0031-8914(66)90027-9

[178] C. Itzykson, H. Saleur and J. B. Zuber, "Conformal Invariance of Nonunitary Two-dimensional Models," Europhys. Lett. **2**, 91 (1986) doi:10.1209/0295-5075/2/2/004

iv) Scattering from the continuum

[179] D. J. Gross and I. R. Klebanov, "S = 1 for c = 1," Nucl. Phys. B **359**, 3 (1991). doi:10.1016/0550-3213(91)90291-5

[180] J. de Boer, A. Sinkovics, E. P. Verlinde and J. T. Yee, "String interactions in c = 1 matrix model," JHEP **0403**, 023 (2004) doi:10.1088/1126-6708/2004/03/023 [hep-th/0312135].

[181] B. Balthazar, V. A. Rodriguez and X. Yin, "Long String Scattering in c = 1 String Theory," JHEP **1901**, 173 (2019) doi:10.1007/JHEP01(2019)173 [arXiv:1810.07233 [hep-th]].

[182] H. Erbin, J. Maldacena and D. Skliros, "Two-Point String Amplitudes," JHEP **1907**, 139 (2019) doi:10.1007/JHEP07(2019)139 [arXiv:1906.06051 [hep-th]].

H. Non-perturbative effects in Liouville

[183] E. Witten, "On string theory and black holes," Phys. Rev. D **44**, 314 (1991). doi:10.1103/PhysRevD.44.314

[184] G. Mandal, A. M. Sengupta and S. R. Wadia, "Classical solutions of two-dimensional string theory," Mod. Phys. Lett. A **6**, 1685 (1991). doi:10.1142/S0217732391001822

[185] M. Fukuma and S. Yahikozawa, "Comments on D instantons in $c < 1$ strings," Phys. Lett. B **460**, 71 (1999) doi:10.1016/S0370-2693(99)00744-3 [hep-th/9902169].

[186] V. Fateev, A. B. Zamolodchikov and A. B. Zamolodchikov, "Boundary Liouville field theory. 1. Boundary state and boundary two point function," 2000, hep-th/0001012.

[187] J. Teschner, "Remarks on Liouville theory with boundary," PoS tmr **2000**, 041 (2000) doi:10.22323/1.006.0041 [hep-th/0009138].

[188] A. B. Zamolodchikov and A. B. Zamolodchikov, (2001) , "Liouville field theory on a pseudosphere," hep-th/0101152.

[189] S. Y. Alexandrov, V. A. Kazakov and D. Kutasov, "Nonperturbative effects in matrix models and D-branes," JHEP **0309**, 057 (2003) doi:10.1088/1126-6708/2003/09/057 [hep-th/0306177].

[190] I. R. Klebanov, J. M. Maldacena and N. Seiberg, "D-brane decay in two-dimensional string theory," JHEP **0307**, 045 (2003) doi:10.1088/1126-6708/2003/07/045 [hep-th/0305159].

[191] E. J. Martinec, "The Annular report on noncritical string theory," 2003, hep-th/0305148.

[192] V. Kazakov, I. K. Kostov and D. Kutasov, "A Matrix model for the two-dimensional black hole," Nucl. Phys. B **622**, 141 (2002) doi:10.1016/S0550-3213(01)00606-X [hep-th/0101011].

[193] A. Sen, "Rolling tachyon," JHEP **04**, 048 (2002) doi:10.1088/1126-6708/2002/04/048 [arXiv:hep-th/0203211 [hep-th]].

[194] N. Seiberg and D. Shih, "Branes, rings and matrix models in minimal (super)string theory," JHEP **0402**, 021 (2004) doi:10.1088/1126-6708/2004/02/021 [hep-th/0312170].

[195] D. Kutasov, K. Okuyama, J. w. Park, N. Seiberg and D. Shih, "Annulus amplitudes and ZZ branes in minimal string theory," JHEP **0408**, 026 (2004) doi:10.1088/1126-6708/2004/08/026 [hep-th/0406030].

[196] A. Sato and A. Tsuchiya, "ZZ brane amplitudes from matrix models," JHEP **0502**, 032 (2005) doi:10.1088/1126-6708/2005/02/032 [hep-th/0412201].

[197] A. B. Zamolodchikov and A. B. Zamolodchikov, "Decay of Metastable Vacuum in Liouville Gravity," Conf. Proc. C **060726**, 1223 (2006) [hep-th/0608196].

[198] D. Gaiotto, "Long strings condensation and FZZT branes," hep-th/0503215.

[199] P. Betzios and O. Papadoulaki, "FZZT branes and non-singlets of Matrix Quantum Mechanics," arXiv:1711.04369 [hep-th].

[200] B. Balthazar, V. A. Rodriguez and X. Yin, "ZZ Instantons and the Non-Perturbative Dual of c = 1 String Theory," arXiv:1907.07688 [hep-th].

[201] B. Balthazar, V. A. Rodriguez and X. Yin, "Multi-Instanton Calculus in c = 1 String Theory," arXiv:1912.07170 [hep-th].

[202] A. Sen, "Divergent to Complex Amplitudes in Two Dimensional String Theory," arXiv:2003.12076 [hep-th].

N. Finiteness, a Hilbert space & Cosmology?

[203] D. Anninos and G. A. Silva, "Solvable Quantum Grassmann Matrices," J. Stat. Mech. **1704**, no.4, 043102 (2017) doi:10.1088/1742-5468/aa668f [arXiv:1612.03795 [hep-th]].

[204] Y. Chen, V. Gorbenko and J. Maldacena, "Bra-ket wormholes in gravitationally prepared states," [arXiv:2007.16091 [hep-th]].

[205] J. B. Hartle and S. W. Hawking, "Wave Function of the Universe," Phys. Rev. D **28**, 2960 (1983) [Adv. Ser. Astrophys. Cosmol. **3**, 174 (1987)]. doi:10.1103/PhysRevD.28.2960

[206] S. R. Coleman, "Why There Is Nothing Rather Than Something: A Theory of the Cosmological Constant," Nucl. Phys. B **310**, 643 (1988). doi:10.1016/0550-3213(88)90097-1

[207] S. B. Giddings and A. Strominger, "Baby Universes, Third Quantization and the Cosmological Constant," Nucl. Phys. B **321**, 481 (1989). doi:10.1016/0550-3213(89)90353-2

[208] M. Li, "Matrix model for de Sitter," JHEP **0204**, 005 (2002) [AIP Conf. Proc. **607**, no. 1, 146 (2002)] doi:10.1063/1.1454368, 10.1088/1126-6708/2002/04/005 [hep-th/0106184].

[209] E. Silverstein, "(A)dS backgrounds from asymmetric orientifolds," Clay Mat. Proc. **1**, 179 (2002) [hep-th/0106209].

[210] A. Strominger, "Inflation and the dS / CFT correspondence," JHEP **0111**, 049 (2001) doi:10.1088/1126-6708/2001/11/049 [hep-th/0110087].

[211] S. Kachru, R. Kallosh, A. D. Linde and S. P. Trivedi, "De Sitter vacua in string theory," Phys. Rev. D **68**, 046005 (2003) doi:10.1103/PhysRevD.68.046005 [hep-th/0301240].

[212] N. Goheer, M. Kleban and L. Susskind, "The Trouble with de Sitter space," JHEP **07**, 056 (2003) doi:10.1088/1126-6708/2003/07/056 [arXiv:hep-th/0212209 [hep-th]]; M. K. Parikh and E. P. Verlinde, "De Sitter holography with a finite number of states," JHEP **0501** (2005) 054 doi:10.1088/1126-6708/2005/01/054 [hep-th/0410227]; T. Banks, B. Fiol and A. Morisse, "Towards a quantum theory of de Sitter space," JHEP **0612** (2006) 004 doi:10.1088/1126-6708/2006/12/004 [hep-th/0609062]; X. Dong, B. Horn, E. Silverstein and G. Torroba, "Micromanaging de Sitter holography," Class. Quant. Grav. **27** (2010) 245020 doi:10.1088/0264-9381/27/24/245020 [arXiv:1005.5403 [hep-th]]; D. Anninos, S. A. Hartnoll and D. M. Hofman, "Static Patch Solipsism: Conformal Symmetry of the de Sitter Worldline," Class. Quant. Grav. **29**, 075002 (2012) doi:10.1088/0264-9381/29/7/075002 [arXiv:1109.4942 [hep-th]]; S. Leuven, E. Verlinde and M. Visser, "Towards non-AdS Holography via the Long String Phenomenon," JHEP **06**, 097 (2018) doi:10.1007/JHEP06(2018)097 [arXiv:1801.02589 [hep-th]]; H. Geng, S. Grieninger and A. Karch, "Entropy, Entanglement and Swampland Bounds in DS/dS," JHEP **06**, 105 (2019) doi:10.1007/JHEP06(2019)105 [arXiv:1904.02170 [hep-th]]; A. Lewkowycz, J. Liu, E. Silverstein and G. Tor-

roba, "$T\bar{T}$ and EE, with implications for (A)dS subregion encodings," [arXiv:1909.13808 [hep-th]].

[213] A. M. Polyakov, "De Sitter space and eternity," Nucl. Phys. B **797**, 199 (2008) doi:10.1016/j.nuclphysb.2008.01.002 [arXiv:0709.2899 [hep-th]].

[214] M. Spradlin, A. Strominger and A. Volovich, "Les Houches lectures on de Sitter space," hep-th/0110007; D. Anninos, "De Sitter Musings," Int. J. Mod. Phys. A **27**, 1230013 (2012) doi:10.1142/S0217751X1230013X [arXiv:1205.3855 [hep-th]].

[215] T. Bautista and A. Dabholkar, "Quantum Cosmology Near Two Dimensions," Phys. Rev. D **94**, no. 4, 044017 (2016) doi:10.1103/PhysRevD.94.044017 [arXiv:1511.07450 [hep-th]].

[216] P. Betzios, U. Gürsoy and O. Papadoulaki, "Matrix Quantum Mechanics on $S^1/\mathbb{Z}_2$," Nucl. Phys. B **928**, 356 (2018) doi:10.1016/j.nuclphysb.2018.01.019 [arXiv:1612.04792 [hep-th]].

[217] P. Betzios and O. Papadoulaki, "Liouville theory and Matrix models A Wheeler DeWitt perspective," [arXiv:2004.00002 [hep-th]].

[218] F. Denef, "TASI lectures on complex structures," doi:10.1142/9789814350525 0007 arXiv:1104.0254 [hep-th].

[219] D. Anninos and F. Denef, "Cosmic Clustering," JHEP **1606**, 181 (2016) doi:10.1007/JHEP06(2016)181 [arXiv:1111.6061 [hep-th]].

[220] D. Anninos, F. Denef, R. Monten and Z. Sun, "Higher Spin de Sitter Hilbert Space," JHEP **1910**, 071 (2019) doi:10.1007/JHEP10(2019)071 [arXiv:1711.10037 [hep-th]].

[221] D. Anninos and D. M. Hofman, "Infrared Realization of dS_2 in AdS_2," Class. Quant. Grav. **35**, no. 8, 085003 (2018) doi:10.1088/1361-6382/aab143 [arXiv:1703.04622 [hep-th]].

[222] D. Anninos, D. A. Galante and D. M. Hofman, "De Sitter Horizons & Holographic Liquids," JHEP **1907**, 038 (2019) doi:10.1007/JHEP07(2019)038 [arXiv:1811.08153 [hep-th]].

[223] D. J. Gross, J. Kruthoff, A. Rolph and E. Shaghoulian, "$T\overline{T}$ in AdS_2 and Quantum Mechanics," arXiv:1907.04873 [hep-th].

[224] D. J. Gross, J. Kruthoff, A. Rolph and E. Shaghoulian, "Hamiltonian deformations in quantum mechanics, $T\bar{T}$, and SYK," arXiv:1912.06132 [hep-th].

[225] J. Maldacena, G. J. Turiaci and Z. Yang, "Two dimensional Nearly de Sitter

gravity," arXiv:1904.01911 [hep-th].

[226] J. Cotler, K. Jensen and A. Maloney, "Low-dimensional de Sitter quantum gravity," arXiv:1905.03780 [hep-th].

[227] J. Cotler and K. Jensen, "Emergent unitarity in de Sitter from matrix integrals," arXiv:1911.12358 [hep-th].

[228] M. Bershadsky and I. R. Klebanov, "Genus one path integral in two-dimensional quantum gravity," Phys. Rev. Lett. **65**, 3088-3091 (1990) doi:10.1103/PhysRevLett.65.3088; M. Bershadsky and I. R. Klebanov, "Partition functions and physical states in two-dimensional quantum gravity and supergravity," Nucl. Phys. B **360**, 559-585 (1991) doi:10.1016/0550-3213(91)90416-U

[229] D. Kutasov and N. Seiberg, "Number of degrees of freedom, density of states and tachyons in string theory and CFT," Nucl. Phys. B **358**, 600-618 (1991) doi:10.1016/0550-3213(91)90426-X

[230] B. H. Lian and G. J. Zuckerman, "New selection rules and physical states in 2-D gravity: Conformal gauge," Phys. Lett. B **254**, 417-423 (1991) doi:10.1016/0370-2693(91)91177-W

[231] C. Imbimbo, S. Mahapatra and S. Mukhi, "Construction of physical states of nontrivial ghost number in c < 1 string theory," Nucl. Phys. B **375**, 399-420 (1992) doi:10.1016/0550-3213(92)90038-D

[232] P. Bouwknegt, J. G. McCarthy and K. Pilch, "Fock space resolutions of the Virasoro highest weight modules with c <= 1," Lett. Math. Phys. **23**, 193-204 (1991) doi:10.1007/BF01885497 [arXiv:hep-th/9108023 [hep-th]].

[233] D. Kutasov, E. J. Martinec and N. Seiberg, "Ground rings and their modules in 2-D gravity with c <= 1 matter," Phys. Lett. B **276**, 437-444 (1992) doi:10.1016/0370-2693(92)91664-U [arXiv:hep-th/9111048 [hep-th]].

[234] T. Eguchi and H. Kawai, "Number of Random Surfaces on the Lattice and the Large N Gauge Theory," Phys. Lett. B **110**, 143-147 (1982) doi:10.1016/0370-2693(82)91023-1

[235] C. Itzykson and J. B. Zuber, "Two-Dimensional Conformal Invariant Theories on a Torus," Nucl. Phys. B **275**, 580-616 (1986) doi:10.1016/0550-3213(86)90576-6

[236] J. Teschner, "On the Liouville three point function," Phys. Lett. B **363**, 65-70 (1995) doi:10.1016/0370-2693(95)01200-A [arXiv:hep-th/9507109 [hep-th]].

[237] B. S. DeWitt, "Quantum Theory of Gravity. 1. The Canonical Theory," Phys. Rev. **160**, 1113-1148 (1967) doi:10.1103/PhysRev.160.1113; B. S. DeWitt, "Quantum Theory of Gravity. 2. The Manifestly Covariant Theory," Phys. Rev. **162**, 1195-1239 (1967) doi:10.1103/PhysRev.162.1195

Black hole holography

[238] A. Sen, "Black Hole Entropy Function, Attractors and Precision Counting of Microstates," Gen. Rel. Grav. **40**, 2249-2431 (2008) doi:10.1007/s10714-008-0626-4 [arXiv:0708.1270 [hep-th]].

[239] I. Mandal and A. Sen, "Black Hole Microstate Counting and its Macroscopic Counterpart," Nucl. Phys. B Proc. Suppl. **216**, 147-168 (2011) doi:10.1088/0264-9381/27/21/214003 [arXiv:1008.3801 [hep-th]].

[240] A. Sen, "Microscopic and Macroscopic Entropy of Extremal Black Holes in String Theory," Gen. Rel. Grav. **46**, 1711 (2014) doi:10.1007/s10714-014-1711-5 [arXiv:1402.0109 [hep-th]].

[241] R. Jackiw, "Lower Dimensional Gravity," Nucl. Phys. B **252**, 343-356 (1985) doi:10.1016/0550-3213(85)90448-1

[242] C. Teitelboim, "Gravitation and Hamiltonian Structure in Two Space-Time Dimensions," Phys. Lett. B **126**, 41-45 (1983) doi:10.1016/0370-2693(83)90012-6

[243]

[243] D. Grumiller, J. Salzer and D. Vassilevich, "AdS_2 holography is (non-)trivial for (non-)constant dilaton," JHEP **12**, 015 (2015) doi:10.1007/JHEP12(2015)015 [arXiv:1509.08486 [hep-th]].

[244] D. Grumiller, R. McNees, J. Salzer, C. Valcárcel and D. Vassilevich, "Menagerie of AdS_2 boundary conditions," JHEP **10**, 203 (2017) doi:10.1007/JHEP10(2017)203 [arXiv:1708.08471 [hep-th]].

[245] G. Sárosi, PoS **Modave2017**, 001 (2018) doi:10.22323/1.323.0001 [arXiv:1711.08482 [hep-th]].

[246] K. Jensen, "Chaos in AdS_2 Holography," Phys. Rev. Lett. **117**, no.11, 111601 (2016) doi:10.1103/PhysRevLett.117.111601 [arXiv:1605.06098 [hep-th]].

[247] J. Engelsöy, T. G. Mertens and H. Verlinde, "An investigation of AdS_2 backreaction and holography," JHEP **07**, 139 (2016) doi:10.1007/JHEP07(2016)139 [arXiv:1606.03438 [hep-th]].

[248] P. Nayak, A. Shukla, R. M. Soni, S. P. Trivedi and V. Vishal, "On the Dynamics of Near-Extremal Black Holes," JHEP **09**, 048 (2018) doi:10.1007/JHEP09(2018)048 [arXiv:1802.09547 [hep-th]].

[249] U. Moitra, S. P. Trivedi and V. Vishal, JHEP **07**, 055 (2019) doi:10.1007/JHEP07(2019)055 [arXiv:1808.08239 [hep-th]].

[250] U. Moitra, S. K. Sake, S. P. Trivedi and V. Vishal, JHEP **11**, 047 (2019) doi:10.1007/JHEP11(2019)047 [arXiv:1905.10378 [hep-th]].

[251] D. Anninos, T. Anous and R. T. D'Agnolo, JHEP **12**, 095 (2017) doi:10.1007/JHEP12(2017)095 [arXiv:1707.03380 [hep-th]].

[252] K. S. Kolekar and K. Narayan, Phys. Rev. D **98**, no.4, 046012 (2018) doi:10.1103/PhysRevD.98.046012 [arXiv:1803.06827 [hep-th]].

[253] F. Larsen, JHEP **04**, 055 (2019) doi:10.1007/JHEP04(2019)055 [arXiv:1806.06330 [hep-th]].

[254] A. Castro, F. Larsen and I. Papadimitriou, JHEP **10**, 042 (2018) doi:10.1007/JHEP10(2018)042 [arXiv:1807.06988 [hep-th]].

[255] J. Hong, F. Larsen and J. T. Liu, JHEP **10**, 260 (2019) doi:10.1007/JHEP10(2019)260 [arXiv:1907.08862 [hep-th]].

[256] A. Castro and V. Godet, SciPost Phys. **8**, no.6, 089 (2020) doi:10.21468/SciPostPhys.8.6.089 [arXiv:1906.09083 [hep-th]].

[257] M. Banados, M. Henneaux, C. Teitelboim and J. Zanelli, Phys. Rev. D **48**, 1506-1525 (1993) [erratum: Phys. Rev. D **88**, 069902 (2013)] doi:10.1103/PhysRevD.48.1506 [arXiv:gr-qc/9302012 [gr-qc]].

[258] M. Cvetič and I. Papadimitriou, JHEP **12**, 008 (2016) [erratum: JHEP **01**, 120 (2017)] doi:10.1007/JHEP12(2016)008 [arXiv:1608.07018 [hep-th]].

[259] A. Gaikwad, L. K. Joshi, G. Mandal and S. R. Wadia, JHEP **02**, 033 (2020) doi:10.1007/JHEP02(2020)033 [arXiv:1802.07746 [hep-th]].

[260] S. R. Das, A. Jevicki and K. Suzuki, JHEP **09**, 017 (2017) doi:10.1007/JHEP09(2017)017 [arXiv:1704.07208 [hep-th]].

[261] M. Taylor, JHEP **01**, 010 (2018) doi:10.1007/JHEP01(2018)010 [arXiv:1706.07812 [hep-th]].

[262] R. R. Poojary, JHEP **03**, 048 (2020) doi:10.1007/JHEP03(2020)048 [arXiv:1812.10073 [hep-th]].

[263] G. Turiaci and H. Verlinde, JHEP **10**, 167 (2017) doi:10.1007/JHEP10(2017)167 [arXiv:1701.00528 [hep-th]].

[264] G. Mandal, P. Nayak and S. R. Wadia, JHEP **11**, 046 (2017) doi:10.1007/JHEP11(2017)046 [arXiv:1702.04266 [hep-th]].

[265] T. G. Mertens, G. J. Turiaci and H. L. Verlinde, JHEP **08**, 136 (2017) doi:10.1007/JHEP08(2017)136 [arXiv:1705.08408 [hep-th]].

[266] P. Kraus and F. Larsen, JHEP **01**, 022 (2006) doi:10.1088/1126-6708/2006/01/022 [arXiv:hep-th/0508218 [hep-th]].

[267] D. Grumiller and W. Kummer, Annals Phys. **308**, 211-221 (2003) doi:10.1016/S0003-4916(03)00138-6 [arXiv:hep-th/0306036 [hep-th]].

[268] Y. S. Myung, Y. W. Kim and Y. J. Park, JHEP **06**, 043 (2009) doi:10.1088/1126-6708/2009/06/043 [arXiv:0901.2141 [hep-th]].

[269] M. Alishahiha, R. Fareghbal and A. E. Mosaffa, JHEP **01**, 069 (2009) doi:10.1088/1126-6708/2009/01/069 [arXiv:0812.0453 [hep-th]].

[270] K. A. Moussa, G. Clement and C. Leygnac, Class. Quant. Grav. **20**, L277-L283 (2003) doi:10.1088/0264-9381/20/24/L01 [arXiv:gr-qc/0303042 [gr-qc]].

[271] A. Bouchareb and G. Clement, Class. Quant. Grav. **24**, 5581-5594 (2007) doi:10.1088/0264-9381/24/22/018 [arXiv:0706.0263 [gr-qc]].

[272] D. Anninos, W. Li, M. Padi, W. Song and A. Strominger, JHEP **03**, 130 (2009) doi:10.1088/1126-6708/2009/03/130 [arXiv:0807.3040 [hep-th]].

[273] S. Carlip, JHEP **10**, 078 (2008) doi:10.1088/1126-6708/2008/10/078 [arXiv:0807.4152 [hep-th]].

[274] B. Chen and J. Long, JHEP **12**, 114 (2011) doi:10.1007/JHEP12(2011)114 [arXiv:1110.5113 [hep-th]].

[275] Y. Nutku, Class. Quant. Grav. **10**, 2657-2661 (1993) doi:10.1088/0264-9381/10/12/022

[276] M. Gurses, Gen. Rel. Grav. **42**, 1413 (2010) doi:10.1007/s10714-009-0914-7 [arXiv:0812.2576 [gr-qc]].

[277] D. D. K. Chow, C. N. Pope and E. Sezgin, Class. Quant. Grav. **27**, 105001 (2010) doi:10.1088/0264-9381/27/10/105001 [arXiv:0906.3559 [hep-th]].

[278] D. Anninos, JHEP **02**, 046 (2010) doi:10.1007/JHEP02(2010)046 [arXiv:0906.1819 [hep-th]].

[279] G. Compere and S. Detournay, Class. Quant. Grav. **26**, 012001 (2009) [erratum: Class. Quant. Grav. **26**, 139801 (2009)] doi:10.1088/0264-9381/26/1/012001 [arXiv:0808.1911 [hep-th]].

[280] S. El-Showk and M. Guica, JHEP **12**, 009 (2012) doi:10.1007/JHEP12(2012)009 [arXiv:1108.6091 [hep-th]].

[281] W. Song and A. Strominger, JHEP **05**, 120 (2012) doi:10.1007/JHEP05(2012)120 [arXiv:1109.0544 [hep-th]].

[282] M. Guica, JHEP **12**, 084 (2012) doi:10.1007/JHEP12(2012)084 [arXiv:1111.6978 [hep-th]].

[283] S. Detournay, T. Hartman and D. M. Hofman, Phys. Rev. D **86**, 124018 (2012) doi:10.1103/PhysRevD.86.124018 [arXiv:1210.0539 [hep-th]].

[284] S. Deser and B. Tekin, Class. Quant. Grav. **19**, L97-L100 (2002) doi:10.1088/0264-9381/19/11/101 [arXiv:hep-th/0203273 [hep-th]].

[285] S. N. Solodukhin, JHEP **07**, 003 (2006) doi:10.1088/1126-6708/2006/07/003 [arXiv:hep-th/0512216 [hep-th]].

[286] W. Li, W. Song and A. Strominger, JHEP **04**, 082 (2008) doi:10.1088/1126-6708/2008/04/082 [arXiv:0801.4566 [hep-th]].

[287] K. Hotta, Y. Hyakutake, T. Kubota and H. Tanida, JHEP **07**, 066 (2008) doi:10.1088/1126-6708/2008/07/066 [arXiv:0805.2005 [hep-th]].

[288] K. Skenderis, M. Taylor and B. C. van Rees, JHEP **09**, 045 (2009) doi:10.1088/1126-6708/2009/09/045 [arXiv:0906.4926 [hep-th]].

[289] W. Li, W. Song and A. Strominger, [arXiv:0805.3101 [hep-th]].

[290] D. Grumiller and N. Johansson, JHEP **07**, 134 (2008) doi:10.1088/1126-6708/2008/07/134 [arXiv:0805.2610 [hep-th]].

[291] A. Maloney, W. Song and A. Strominger, Phys. Rev. D **81**, 064007 (2010) doi:10.1103/PhysRevD.81.064007 [arXiv:0903.4573 [hep-th]].

[292] V. Balasubramanian and P. Kraus, Commun. Math. Phys. **208**, 413-428 (1999) doi:10.1007/s002200050764 [arXiv:hep-th/9902121 [hep-th]].

[293] S. de Haro, S. N. Solodukhin and K. Skenderis, Commun. Math. Phys. **217**, 595-622 (2001) doi:10.1007/s002200100381 [arXiv:hep-th/0002230 [hep-th]].

[294] K. Skenderis, Class. Quant. Grav. **19**, 5849-5876 (2002) doi:10.1088/0264-9381/19/22/306 [arXiv:hep-th/0209067 [hep-th]].

[295] S. N. Solodukhin, Phys. Rev. D **74**, 024015 (2006) doi:10.1103/PhysRevD.74.024015 [arXiv:hep-th/0509148 [hep-th]].

[296] H. Saida and J. Soda, Phys. Lett. B **471**, 358-366 (2000) doi:10.1016/S0370-2693(99)01405-7 [arXiv:gr-qc/9909061 [gr-qc]].

[297] P. Kraus and F. Larsen, JHEP **09**, 034 (2005) doi:10.1088/1126-6708/2005/09/034 [arXiv:hep-th/0506176 [hep-th]].

[298] Y. Tachikawa, Class. Quant. Grav. **24**, 737-744 (2007) doi:10.1088/0264-9381/24/3/014 [arXiv:hep-th/0611141 [hep-th]].

[299] S. Detournay, Phys. Rev. Lett. **109**, 031101 (2012) doi:10.1103/PhysRevLett.109.031101 [arXiv:1204.6088 [hep-th]].

[300] I. Papadimitriou, "Holographic renormalization as a canonical transformation," JHEP **11**, 014 (2010) doi:10.1007/JHEP11(2010)014 [arXiv:1007.4592 [hep-th]].

[301] H. Elvang and M. Hadjiantonis, JHEP **06**, 046 (2016) doi:10.1007/JHEP06(2016)046 [arXiv:1603.04485 [hep-th]].

[302] M. Gürses, Class. Quant. Grav. **11**, no.10, 2585 (1994) doi:10.1088/0264-9381/11/10/017

[303] T. Hartman and A. Strominger, JHEP **04**, 026 (2009) doi:10.1088/1126-6708/2009/04/026 [arXiv:0803.3621 [hep-th]].

[304] A. Castro, D. Grumiller, F. Larsen and R. McNees, JHEP **11**, 052 (2008) doi:10.1088/1126-6708/2008/11/052 [arXiv:0809.4264 [hep-th]].

[305] C. G. Callan and J. M. Maldacena, Nucl. Phys. B **472**, 591-610 (1996) doi:10.1016/0550-3213(96)00225-8 [arXiv:hep-th/9602043 [hep-th]].

[306] G. T. Horowitz and A. Strominger, Phys. Rev. Lett. **77**, 2368-2371 (1996) doi:10.1103/PhysRevLett.77.2368 [arXiv:hep-th/9602051 [hep-th]].

[307] F. Larsen, Phys. Rev. D **56**, 1005-1008 (1997) doi:10.1103/PhysRevD.56.1005 [arXiv:hep-th/9702153 [hep-th]].

[308] V. Balasubramanian, A. Naqvi and J. Simon, JHEP **08**, 023 (2004) doi:10.1088/1126-6708/2004/08/023 [arXiv:hep-th/0311237 [hep-th]].

[309] V. Balasubramanian, J. de Boer, M. M. Sheikh-Jabbari and J. Simon, JHEP **02**, 017 (2010) doi:10.1007/JHEP02(2010)017 [arXiv:0906.3272 [hep-th]].

Samenvatting

Dit proefschrift behandelt laagdimensionale dualiteiten, beschouwd als werkbare modellen waarmee men tweedimensionale De Sitter-ruimte en zwarte gaten kan bestuderen. De eerste twee hoofdstukken geven een samenvatting van een nieuwe constructie die een brug kan slaan van De Sitter-ruimte naar de vermoedelijke dualiteit tussen matrixmodellen en tweedimensionale kwantumzwaartekracht. Dit zou een volgende stap vormen richting een beter begrip van het universum op microscopische schaal. In het laatste hoofdstuk behandelen we fundamentele vraagstukken over de microscopische beschrijving van zwarte gaten, door middel van een laagdimensionale dualiteit die bekend staat als de "vlakbij-AdS_2/vlakbij-CFT_1 correspondentie".

We leven in een tijdperk waarin nauwkeurige astronomische instrumenten ons in staat stellen om meer te weten te komen over het universum waarin wij ons bevinden. Observaties van de kosmische achtergrondstraling en de explosies van vergelegen witte dwergsterren (type Ia supernova's) wijzen erop dat ons universum zich naar een stadium beweegt van versnelde uitdijing, aangedreven door een zeer kleine positieve kosmologische constante. In de afgelopen jaren heeft men met behulp van de LIGO- en Virgo-detectoren de zwaartekrachtsgolven kunnen waarnemen die uitgezonden zijn door verscheidene binaire zwarte gaten, wat aanvullend bewijs heeft geleverd voor het het bestaan van deze zwarte gaten.

Een maximaal symmetrische ruimtetijd met positieve kosmologische constante wordt ook een De Sitter-ruimte genoemd. Door toedoen van de versnelde uitdijing kan een waarnemer in een De Sitter-ruimte slechts tot op een eindige afstand zien en wordt deze omgeven door een waarnemingshorizon. De waarnemingshorizon markeert ook de grens van het zwarte gat, waar de ontsnappingssnelheid groter wordt dan de lichtsnelheid. Zowel de horizon van De Sitter-ruimte als de horizon van een zwart gat hebben een eindige oppervlakte, en vermoedelijk is er tevens een eindige entropie geassocieerd met deze horizons.

De eindigheid van deze entropieën hebben mij ertoe geleid om modellen met een

eindig aantal vrijheidsgraden te gebruiken om een microscopische beschrijving van De Sitter-ruimte en zwarte gaten te geven. Deze modellen worden gerealiseerd als laagdimensionale dualiteiten. Een dualiteit is een vertaalslag tussen twee theorieën, die de ene theorie op de ander afbeeldt en vice versa. Afhankelijk van het exacte probleem wat we willen bestuderen, kunnen we besluiten welke van de twee formalismen het meest bruikbaar is. In een laagdimensionale dualiteit bevinden de twee duale theorieën zich in een ruimtetijddimensie lager dan vier.

In de komende twee alinea's geven we een inkijk in de twee dualiteiten waar we ons in dit proefschrift voornamelijk op richten.

Matrixmodellen en tweedimensionale kwantumzwaartekracht. Om een microscopische beschrijving te geven van ons uitdijende universum proberen we een verband te leggen tussen De Sitter-ruimte en matrixmodellen. Hoewel er zeer weinig bekend is over De Sitter-ruimte op kwantumniveau, vormen matrixmodellen nauwkeurig uitgewerkte instrumenten binnen de theoretische natuurkunde. Er bestaan vermoedens dat onder bepaalde omstandigheden — zoals wanneer de afmetingen van de matrix zeer groot worden — enkele eigenschappen van een matrixmodel duaal zijn aan observabelen van een specifiek model van tweedimensionale kwantumzwaartekracht, gekoppeld aan materievelden. Dit model staat bekend als de Liouville-theorie. Een cruciaal aspect van de Liouville-theorie geplaatst op de topologie van een twee-bol (met aanvullende voorwaarden, zoals een grote negatieve centrale lading en een beperking op de totale oppervlakte), is dat deze een semi-klassieke De Sitter-benadering toelaat. Deze tweedimensionale De Sitter-ruimte lijkt op de hogerdimensionale De Sitter-theorie die onze ruimtetijd beschrijft, en beide modellen delen bepaalde belangrijke eigenschappen. Matrixmodellen zouden daarom een ultraviolet-voltooiing kunnen vormen van een De Sitter-kwantumzwaartekrachttheorie, en mogelijk meer inzicht kunnen bieden in een microscopische beschrijving van ons universum.

Zwarte gaten. Zwarte gaten zijn oplossingen van de Einsteinvergelijkingen uit de algemene relativiteitstheorie, met een krommingssingulariteit in het centrum en een waarnemingshorizon daarbuiten. Een verrassend aspect van zwarte gaten is dat ze bepaalde thermodynamische eigenschappen hebben, gelijkend op statistische systemen. Hoewel er een uitgebreide theorie over zwarte gaten bestaat, blijven er voorlopig vele vraagstukken bestaan over de AdS_2-geometrie in de buurt van de horizon van een vlakbij-extremaal zwart gat. Een voorbeeld van dergelijke vraagstukken is het feit dat de temperatuur van een extremaal zwart gat gelijk is aan nul, terwijl de entropie van de horizon eindig (en groter dan nul) is, zelfs in het extremale geval. De aanpak die men gebruikt om een microscopische beschrijving van deze entropie te geven, maakt gebruik van de zogenaamde (vlakbij-)AdS_2/(vlakbij)-CFT_1-correspondentie. Deze corresponden-

tie koppelt een theorie van tweedimensionale zwaartekracht met negatieve kromming (AdS_2) aan een eendimensionale hoekgetrouwe kwantummechanische theorie (CFT_1) die gesitueerd is op de rand van de AdS_2-ruimtetijd. Het voorvoegsel "vlakbij" verwijst naar een gebied in de buurt van het zuivere AdS_2/CFT_1-regime. Zoals uitgelegd in het eerstvolgende hoofdstuk, laat een zuivere AdS_2-achtergrond slechts configuraties in de grondtoestand toe. Vlakbij-AdS_2 is een kleine afwijking hiervan, die nog steeds in verbinding staat met AdS_2, maar toch excitaties toelaat met eindige energie groter dan nul. Een belangrijke toelichting hierbij is dat de theorie op de rand in de vlakbij-AdS_2/vlakbij-CFT_1-correspondentie een hoekgetrouwe kwantummechanische theorie is in plaats van een kwantumveldentheorie, en dat de dualiteit daardoor slechts een eindig aantal vrijheidsgraden bevat.

Dankwoord

I would like to thank my supervisor Alejandra Castro. Working with you helped me grow as a physicist, but also as a person. During our projects I learned a lot and your feedback on talks and presentations was very useful for me. I am grateful that you also allowed me to find my own path.

Additionally I would like to thank Dio Anninos. Dio, you have been mentor and collaborator, but first and foremost friend for me. The last almost four years have been an exciting and fun journey through the land of penguins, matrix models and de Sitter space. Your enthusiasm when talking about physics is contagious and inspiring. The last almost one and a half years however have also been very difficult. Discussing physics with you though, our projects, checking ArXiv together, as well as chatting during plant walks have made the corona-isolation easier for me. I truly hope that this is just the beginning of a wonderfully adventurous collaboration and friendship.

I would also like to thank my collaborators Alex and Christoph, from whom I learnt a lot. Moreover I would like to thank the other PhD students, in particular Antonio, Carlos, Greg, Evita, Ankit, Jeremy and Dora as well as the other postdocs and faculties. In particular Carlos and Toni, I will miss your Tortilla in Montreal Carlos as well as some al dente pasta, Toni! A particular thanks goes to Austin for illuminating me on N- and M-dashes and his support during my postdoc application. Even though we have not seen much of each other over the last two years, you all have made the String group a welcoming and fun environment. Damian, we met in Amsterdam but I got to know you better only after you moved to London. I would like to thank you for always welcoming me warmly when I was visiting London, I still owe you muffins... maybe along with the bbq!

A particular thanks goes to Lars and Joren. Thanks Lars for helping me out with LaTeX issues. Joren, thank you so much for translating my summary.

Amsterdam without Corona is also an amazing place to go out and have fun, enjoy

concerts, operas and ballets. Eleftheria, Maria, Eric and Greg I really hope that there will be a time when we can do that again. These were wonderful evenings gave me a lot of strength and made this path much easier. Maria and Eleftheria, our weekend in Lisbon I will hardly forget, it was so much fun! There is of course not just Amsterdam, we also had the Delta-ITP meetings and schools. I would like to thank Joren, Huibert and Killian for fun times in Dalfsen and Greg, Antonio and Eric for some unforgettable moments in Brazil.

I also had the opportunity to go to Jerusalem for a Winter school in my second year. Shreya, you were the greatest roommate I could have imagined. I will never forget jumping off a tram together, or getting lost in Jerusalem together. Our zoom movie club is one of the funniest things for me during the current times. I don't think someone will ever again watch Harry Potter forward and backward with me.

When I arrived in Amsterdam I immediately fell in love with this city and in particular the biking. Lorenzo, the bike tours with you and knowing that there was also always a chair at your dinner table free for me has made some weekends and evenings a lot of fun.

Jesko, Moji, Jocelyne and Philipp we stayed friends from my Zurich times. Jesko, I would like to thank you for fun weekend trips. Moji, you had an open ear whenever I needed it. Jocelyne, I know I can always count on you and Philipp, for one of the best holidays I ever had. Looking forward to some nice beach days!

This thesis would not have been possible without the unconditional support of my mom. I would therefore like to dedicate this thesis to her. For always being there for me and always believing in me. Hon di volle fescht lieb mama. Danke, dass du olm fir mi do bisch wenn i di brauch!